

Technische Universität München

Lehrstuhl für Ernährungsphysiologie

**Murine one-carbon metabolism in non-alcoholic fatty liver  
disease**

Christoph Dahlhoff

Vollständiger Abdruck der von der Fakultät Wissenschaftszentrum Weihenstephan für Ernährung, Landnutzung und Umwelt der Technischen Universität München zur Erlangung des akademischen Grades eines

Doktors der Naturwissenschaften

genehmigten Dissertation.

Vorsitzender: Univ.-Prof. Dr. D. Haller

Prüfer der Dissertation:

1. Univ.-Prof. Dr. H. Daniel
2. Univ.-Prof. Dr. M. Klingenspor

Die Dissertation wurde am 26.07.2012 bei der Technischen Universität München eingereicht und durch die Fakultät Wissenschaftszentrum Weihenstephan für Ernährung, Landnutzung und Umwelt am 07.12.2012 angenommen.

## Table of contents

<i>Table of contents</i> .....	<b>II</b>
<i>List of figures</i> .....	<b>VI</b>
<i>List of tables</i> .....	<b>XIV</b>
<i>List of abbreviations</i> .....	<b>XVIII</b>
<b>1 Introduction</b> .....	<b>1</b>
1.1 <i>Non-alcoholic fatty liver disease</i> .....	2
1.1.1 <i>Pathogenesis of non-alcoholic fatty liver disease</i> .....	2
1.1.2 <i>Animal models of non-alcoholic fatty liver disease</i> .....	5
1.2 <i>Hepatic one-carbon metabolism</i> .....	6
1.2.1 <i>Metabolic regulation</i> .....	9
1.2.2 <i>Genetic disease associations</i> .....	10
1.2.3 <i>Nutritional methyl-group deficiency</i> .....	11
1.2.4 <i>Nutritional methyl-group supplementation</i> .....	11
1.3 <i>C1-metabolism and hepatic phosphatidylcholine biosynthesis and lipid homeostasis</i> .....	12
1.3.1 <i>The CDP-choline pathway</i> .....	13
1.3.2 <i>The PE methylation pathway</i> .....	14
1.4 <i>Epigenetics</i> .....	15
1.5 <i>Aim of the thesis</i> .....	18
<b>2 Material and Methods</b> .....	<b>19</b>
2.1 <i>Animals and sample collection</i> .....	19
2.1.1 <i>High-fat feeding trial</i> .....	19
2.1.2 <i>Effects of methyl-group supplementation during high-fat feeding trial</i> .....	19
2.2 <i>Cell culture</i> .....	22
2.3 <i>Intraperitoneal glucose tolerance test</i> .....	23
2.4 <i>Insulin ELISA</i> .....	23
2.5 <i>Histology</i> .....	23
2.6 <i>Metabolite analysis</i> .....	24
2.6.1 <i>Amino acids and amino acid derivatives</i> .....	24
2.6.2 <i>Acyl-carnitines, phosphatidylcholines, lysophosphatidylcholines sphingolipids and biogenic amines</i> .....	25
2.6.3 <i>Triacylglycerol, non-esterified fatty acids, total phospholipids and choline</i> .....	26
2.7 <i>RNA isolation</i> .....	26

2.8	<i>Agarose gel electrophoresis</i> .....	27
2.9	<i>Quantitative real-time PCR</i> .....	28
2.10	<i>Protein extraction and Western blot analysis</i> .....	31
2.11	<i>DNA isolation</i> .....	32
2.12	<i>Luminometric methylation assay</i> .....	32
2.13	<i>Methylation-sensitive quantitative PCR</i> .....	33
2.14	<i>Bisulfite genomic pyrosequencing</i> .....	35
2.14.1	<i>Bisulfite conversion</i> .....	35
2.14.2	<i>Pyrosequencing</i> .....	35
2.15	<i>Statistical analysis</i> .....	38
<b>3</b>	<b><i>Results</i></b> .....	<b>39</b>
3.1	<i>Influence of DIO induced NAFLD on phospholipid homeostasis and C1 metabolism</i> .....	39
3.1.1	<i>Gene expression of the hepatic transsulfuration and sarcosine pathways in C1 metabolism is altered in DIO mice</i> .....	39
3.1.2	<i>Hepatic protein levels of BHMT are increased and CBS level are decreased in DIO mice</i> .....	41
3.1.3	<i>Amino acid profiling reveals homeostasis in the methionine cycle, reflects increased BHMT mediated homocysteine remethylation and supports a repression of the transsulfuration pathway</i> .....	41
3.1.4	<i>PPAR<math>\alpha</math> activity is increased in DIO mice and is implicated in the repression of the transsulfuration pathway</i> .....	44
3.2	<i>Influence of HF diet on epigenetic gene regulation and on global and gene-specific DNA methylation</i> .....	46
3.2.1	<i>De novo DNA methyltransferase gene expression is reduced in HF mice</i> .....	46
3.2.2	<i>Hepatic global DNA methylation is unaffected by a HF diet</i> .....	46
3.2.3	<i>DNA methylation status of CpG-islands in the Cbs and PPAR<math>\alpha</math> gene promoter and CBS intragenic region is unchanged in liver tissue of HF mice</i> ..	47
3.3	<i>Influence of dietary methyl-group supplementation on the progression of NAFLD in DIO mice</i> .....	50
3.3.1	<i>Methyl-group supplementation does not affect body weight development, hyperglycemia, hyperinsulinemia and glucose tolerance</i> .....	53
3.3.2	<i>Amino acid analyses reveal a specific plasma and liver metabolic-profile in methyl-group supplemented mice</i> .....	55
3.3.3	<i>Hepatic C1-metabolism gene and protein expression are affected by methyl-group supplementation in DIO mice</i> .....	61
3.3.4	<i>Hepatic steatosis and hepatic free fatty acids are reduced while free fatty acids in blood plasma are unaffected in methyl-group supplemented DIO mice</i> .....	62
3.3.5	<i>Reduced Fasn mRNA expression and increased PPAR<math>\alpha</math> activity and AMPK<math>\alpha</math> phosphorylation state suggests a reduced de novo lipogenesis and increased <math>\beta</math>-oxidation in methyl-group supplemented DIO mice</i> .....	65

3.3.6	<i>Methyl-group supplementation leads to reduced hepatic acyl-carnitine concentrations in CMS and HFMS mice, supporting improved <math>\beta</math>-oxidation in methyl-group supplemented mice</i>	68
3.3.7	<i>Analysis of hepatic phospholipid signature reveals no significant influence of methyl-group supplementation, but an increase of specific phospholipids by HF diets</i>	70
<b>4</b>	<b>Discussion</b>	<b>74</b>
4.1	<i>High-fat diet induced NAFLD in phospholipid homeostasis and regulation of C1-metabolism</i>	74
4.1.1	<i>The influence of HF diet on NAFLD and the hepatic C1-metabolism</i>	75
4.1.2	<i>Regulation of the Hcy branch-point in HF diet-dependent NAFLD</i>	75
4.1.3	<i>Homeostasis of the hepatic methionine cycle in DIO mice</i>	76
4.1.4	<i>Choline availability in DIO mice</i>	76
4.1.5	<i>Transcriptional regulation of the Hcy branch-point in the C1-metabolism</i>	77
4.1.6	<i>HF diet and NAFLD effects on the hepatic C1-metabolism associated with the synthesis of taurine, glutathione, ophthalmic acid and sulfate</i>	78
4.2	<i>DIO induced NAFLD in nuclear epigenetic processes</i>	80
4.2.1	<i>Hepatic DNA methylation in HF diet induced NAFLD</i>	80
4.3	<i>Methyl-group supplementation and the effects on progression of DIO induced NAFLD</i>	81
4.3.1	<i>Obesity related changes in basal clinical parameters in DIO mice</i>	81
4.3.2	<i>Influence of methyl-group supplementation on changes in basal clinical parameters</i>	82
4.3.3	<i>Specific blood plasma metabolite profile in methyl-group supplemented mice</i>	82
4.3.4	<i>Specific hepatic metabolite profile in methyl-group supplemented mice</i>	84
4.3.5	<i>Influence of methyl-group supplementation on the Hcy branch-point of the C1-metabolism</i>	86
4.3.6	<i>Progression of NAFLD in methyl-group supplemented mice</i>	87
4.3.7	<i>Possible causes of the alleviation of NAFLD progression in methyl-group supplemented mice</i>	88
4.3.8	<i>Hepatic phospholipid synthesis in HF diet induced NAFLD and methyl-group supplementation</i>	91
4.4	<i>Concluding remarks and perspectives</i>	92
<b>5</b>	<b>Summary</b>	<b>94</b>
<b>6</b>	<b>References</b>	<b>96</b>
<b>7</b>	<b>Appendix</b>	<b>112</b>
7.1	<i>qRT-PCR</i>	112
7.2	<i>Metabolites</i>	117
7.3	<i>Methylation-sensitive qPCR</i>	122
7.4	<i>Food intake</i>	123

---

*7.5 Chemicals* ..... 126

*Acknowledgements*..... 127

*Curriculum Vitae* ..... 129

## List of figures

- Figure 1.** Pathways implicated in hepatic lipid homeostasis are depicted. Lipid homeostasis is maintained by equilibration of fatty acid uptake, de novo lipogenesis, fatty acid oxidation and VLDL dependent triacylglycerol export to peripheral tissues. Imbalance in these processes lead to hepatic triacylglycerol deposition. Abbreviations: FA, Free fatty acids; HDL, High density lipoprotein particle; HSL, Hormone sensitive lipase; IDL, Intermediary density lipoprotein particle; LDL, Low density lipoprotein particle; LPL, Lipoprotein lipase; NEFA, Non-esterified fatty acids; SI, Small intestine; TG, Triacylglycerol; VLDL, Very low density lipoprotein particle. .... 1
- Figure 2.** Hepatic one-carbon metabolism with the subpathways methionine cycle, folate cycle, sarcosine pathway and transsulfuration pathway is depicted. Reaction enzymes: 1, Methionine adenosyltransferase; 2, SAM dependent methyltransferase; 3, S-adenosylhomocysteine hydrolase; 4, Choline oxidase and betaine aldehyde dehydrogenase; 5, Betaine-homocysteine methyltransferase; 6, Dimethylglycine dehydrogenase; 7, Sarcosine dehydrogenase or Pipecolic acid oxidase; 8, Glycine methyltransferase; 9, Methionine synthase; 10, Serine hydroxymethyltransferase 1 or 2; 11, 5,10-methylenetetrahydrofolate reductase; 12, Cystathionine  $\beta$ -synthase; 13, Cystathionase; 14, Cysteine dioxygenase 1; 15, Glutamate oxaloacetate transaminase 1; 16, Cysteine sulfinic acid decarboxylase; 17, Gutamate-cysteine ligase; 18, Glutathione synthetase. Abbreviations: ATP, Adenosine triphosphate; AMP, Adenosine monophosphate; DHF, Dihydrofolate; DMG, Dimethylglycine; dTMP, Deoxythymidine monophosphate; dUMP, Deoxyuridine monophosphate; Glu; L-glutamate; Gly, Glycine; GSH, Glutathione; Hcy, L-homocysteine; Methylene-THF, Methylene-tetrahydrofolate; 5-Methyl-THF, 5-Methyl-tetrahydrofolate; Met, L-methionine; PC, Phosphatidylcholine; PE, Phosphatidylethanolamine; SAH, S-adenosyl-homocysteine; SAM, S-adenosyl-methionine; Ser, L-serine; THF, Tetrahydrofolate. .... 8
- Figure 3.** Hepatic polyamine synthesis and methionine salvage with the subpathway methionine cycle is depicted. Reaction enzymes: 1, Methionine adenosyltransferase; 2, SAM-dependent methyltransferase; 3, S-adenosylhomocysteine hydrolase; 4, Choline oxidase; 5, Betaine-homocysteine methyltransferase; 6, Methionine synthase; 7, S-adenosylmethionine decarboxylase; 8, Spermidine synthase; 9, Spermine synthase; 10, Ornithine decarboxylase; 11, Ornithine carbamoyltransferase; 12, Argininosuccinate synthase; 13, Argininosuccinate lyase; 14, Arginase; 15, Nitric-oxide synthase. Abbreviations: dcSAM, decarboxylated S-adenosyl-methionine; MTA, methylthioadenosine; THF, tetrahydrofolate..... 9
- Figure 4.** The CDP-choline pathway is the principal cellular phosphatidylcholine biosynthesis pathway (modified from (106)). Biosynthesis is dependent on activation of cellular free choline and synthesis of diacylglycerol. The rate limiting step is the CTP:phosphocholine cytidyltransferase mediated CDP-choline synthesis. Abbreviations: CK, choline kinase; CPT, CDP-

- choline:1,2-diacylglycerol choline-phosphotransferase; CT, CTP:phosphocholine cytidyltransferase; CMP, Cytidine monophosphate; CTP, Cytidine triphosphates; PPAP, Phosphatidic acid phosphatase; PP<sub>i</sub>, Pyrophosphate. .... 13*
- Figure 5.** *Hepatic de novo PC biosynthesis via the PE methylation pathway is presented. Three sequential methylation steps of phosphatidylethanolamine lead to the synthesis of phosphatidylcholine. Methyl-group source is S-adenosyl-methionine. Abbreviations: FA, fatty acid; PEMT, Phosphatidylethanolamine methyltransferase; SAH, S-adenosyl-homocysteine; SAM, S-adenosyl-methionine. .... 15*
- Figure 6.** *The pivotal epigenetic modifications of DNA (DNA methylation) (A) and histones (histone modifications) (B) is depicted (136). The diversity of signals can lead to activation or repression of gene function also depending on chromatin conformation. Abbreviations: Dnmt, DNA methyltransferase; dMTase, DNA demethylase; H2A, Histone 2A, H2B, Histone 2B; H3, Histone 3; H4, Histone 4; SAH, S-adenosyl-homocysteine; SAM, S-adenosyl-methionine. .... 17*
- Figure 7.** *Experimental design of the methyl-group supplementation feeding trial is depicted. Open and grey boxes represent C and HF dietary feeding and open lined and grey lined boxes represent CMS and HFMS dietary feeding. C and HF mice sacrificed after eight weeks are defined as 8W and C, CMS, HF and HFMS mice sacrificed after twelve weeks are defined as 12W. .... 20*
- Figure 8.** *Image of DNA ladders applied upon agarose gel electrophoresis. Nucleotide sizes are depicted at the site. .... 28*
- Figure 9.** *Global DNA methylation can be analyzed by restriction digestion of genomic DNA with the isoschizomers MspI and HpaII. The enzymatic activity of the methylation-sensitive restriction enzyme HpaII is blocked by CpG methylation. .... 33*
- Figure 10.** *Cytosine residues of DNA are chemical modified by sodium bisulfite conversion for specific quantification of CpG-site methylation. Methylated cytosine residues are very slowly affected from the chemical deamination process. .... 35*
- Figure 11.** *Image of the principal mechanism of pyrosequencing is presented. Nucleotide incorporation leads to pyrophosphate release which is used by ATP sulfurylase to synthesize ATP. Subsequently, ATP is consumed by luciferase and results in luminescence. Emitted light is detected by the CCD camera and converted into a pyrogram. Unincorporated nucleotides are degraded by apyrase (152). .... 36*
- Figure 12.** *Hepatic mRNA expression of genes encoding enzymes in C1-metabolism in mice on C and HF diets. Data are presented for A the methionine cycle, B the folate cycle, C sarcosine pathway, and D transsulfuration pathway as mean ± SEM (n = 5-6). Open and grey columns represent data from control and HF (DIO) animals. Asterisk indicates statistical significance (p < 0.05). Abbreviations: Ahcy, S-adenosylhomocysteine hydrolase; Bhmt, Betaine-homocysteine methyltransferase; Bhmt2, Betaine-homocysteine methyltransferase 2; Cbs, Cystathionine β-synthase; Chdh, Choline dehydrogenase; Csad, Cysteine sulfinic acid decarboxylase; Cth, Cystathionase; Dmgdh, Dimethylglycine dehydrogenase precursor; Gclc, Glutamate-cysteine ligase catalytic subunit; Gnmt, Glycine N-methyltransferase; Got1, Glutamate oxaloacetate transaminase 1; Gss,*

- Glutathione synthetase; Mat1a, Methionine adenosyltransferase I alpha; Mat2a, Methionine adenosyltransferase II alpha; Mthfr, 5,10-methylenetetrahydrofolate reductase; Mtr, 5-methyltetrahydrofolate-homocysteine methyltransferase; Pemt, Phosphatidylethanolamine N-methyltransferase; Shmt1, Serine hydroxymethyltransferase 1; Shmt2, Serine hydroxymethyltransferase 2.* ..... 40
- Figure 13.** Influence of DIO on hepatic BHMT and CBS protein expression after twelve weeks of dietary treatment. Data are presented as mean  $\pm$  SEM ( $n = 6$ ). Open and grey columns represent data from C and HF animals. Asterisk indicates statistical significance ( $p < 0.05$ ). Abbreviations: *Bhmt*, Betaine-homocysteine methyltransferase; *Cbs*, Cystathionine  $\beta$ -synthase; *H3*, Histone H3. .... 41
- Figure 14.** Impact of HF diet feeding on selected hepatic metabolites after twelve weeks of dietary treatment. Data are presented as box and whisker plot ( $n = 9-11$ ). Open and grey boxes represent data from C and HF animals. Asterisk indicates statistical significance ( $p < 0.05$ ). Abbreviations: *Abu*, L- $\alpha$ -amino-n-butyrate; *Cit*, L-citrulline; *Gln*, L-glutamine; *Hyp*, Hydroxyproline; *Met*, L-methionine; *Orn*, L-ornithine; *Tau*, Taurine. .... 42
- Figure 15.** Analysis of hepatic SAM, SAH, [SAM] / [SAH] ratio, Hcy and cystathionine in hepatic tissues of C and HF fed mice. Data are presented as box and whisker plot ( $n = 5-6$ ). Open and grey boxes represent data from C and HF animals. Asterisk indicates statistical significance ( $p < 0.05$ ). Abbreviations: *Cth*, Cystathionine; *Hcy*, L-homocysteine; *SAH*, S-adenosyl-homocysteine; *SAM*, S-adenosyl-methionine. .... 43
- Figure 16.** The impact of DIO on the choline level in liver tissues of mice fed a C or HF diet. Data are presented as box and whisker plot ( $n = 6$ ). Open and grey boxes represent data from C and HF animals. Asterisk indicates statistical significance ( $p < 0.05$ ). .... 44
- Figure 17.** Analysis of the effect of WY14,643 on PPAR $\alpha$ -dependent gene expression of *Bhmt* and *Cbs* in Fao rat hepatoma cells. Prior to the stimulation, cells were preincubated in DMEM (5.56 mM glucose) supplemented with 0.5 % bovine serum albumin for 48 h followed by stimulation with 25  $\mu$ M, 50  $\mu$ M and 100  $\mu$ M WY14,643. Data are presented as mean  $\pm$  SEM ( $n = 4$ ). Asterisk indicates statistical significance ( $p < 0.05$ ). Abbreviations: *Bhmt*, Betaine-homocysteine methyltransferase; *Cbs*, Cystathionine  $\beta$ -synthase; *Cpt1a*, Carnitine palmitoyltransferase 1a. .... 45
- Figure 18.** Analysis of PPAR $\alpha$  and PPAR $\alpha$  target gene expression in liver of C and HF mice reflecting PPAR $\alpha$  activity. Open and grey columns represent data from C and HF animals. Data are presented as mean  $\pm$  SEM ( $n = 5-6$ ). Asterisk indicates statistical significance ( $p < 0.05$ ). Abbreviations: *Acox1*, Acyl-coenzyme A oxidase 1; *Cpt1a*, Carnitine palmitoyltransferase 1a; *PPAR $\alpha$* , Peroxisome proliferator activated receptor  $\alpha$ ; *Ucp2*, Uncoupling protein 2. .... 45
- Figure 19.** Influence of HF diet treatment on hepatic DNA methyltransferase gene expression. Data are presented as mean  $\pm$  SEM ( $n = 5-6$ ). Open and grey columns represent data from C and HF animals. Asterisk indicates statistical significance ( $p < 0.05$ ). Abbreviations: *Dnmt1*, DNA methyltransferase 1; *Dnmt3a*, DNA methyltransferase 3a; *Dnmt3b*, DNA methyltransferase 3b. .... 46



- Figure 20.** Analysis of hepatic global DNA methylation in liver tissue of mice fed C and HF diets. DNA methylation was calculated from the (HpaII / MspI) ratio. Data are presented as mean  $\pm$  SEM ( $n = 6$ ). Open and grey columns represent data from C and HF animals. Asterisk indicates statistical significance ( $p < 0.05$ ). ..... 47
- Figure 21.** Genomic structure of the mouse Cbs gene and experimental design of Cbs DNA methylation analysis. **Top:** Filled black boxes represent exons interspaced by introns and black arrow indicates transcription start site (ENSMUST00000067801). Filled grey boxes represent Cbs CpG-islands and open boxes mark the investigated regions. **Bottom:** Investigated regions and positions of informative restriction sites are depicted. Abbreviations: Cbs I7, Cystathionine  $\beta$ -synthase intragenic CpG-island region 7; Cbs P1, Cystathionine  $\beta$ -synthase promoter CpG-island region 1; Cbs P2, Cystathionine  $\beta$ -synthase promoter CpG-island region 2; chr17, chromosome 17. .... 48
- Figure 22.** Quantitative analysis of CpG restriction sites in promoter and intragenic Cbs CpG-islands in liver tissues of C and HF mice. Data are shown for the restriction enzymes AciI and HpaII in the mentioned regions. Data are presented as mean  $\pm$  SEM ( $n = 6$ ). Open and grey columns represent data from C and HF animals. Asterisk indicates statistical significance ( $p < 0.05$ ). Abbreviations: Cbs I7, Cystathionine  $\beta$ -synthase intragenic CpG-island region 7; Cbs P1, Cystathionine  $\beta$ -synthase promoter CpG-island region 1; Cbs P2, Cystathionine  $\beta$ -synthase promoter CpG-island region 2; chr17, chromosome 17; n.d., no detection. .... 48
- Figure 23.** Effects of a HF diet on Cbs promoter CpG-island DNA methylation assessed by bisulfite genomic pyrosequencing. **Left:** Experimental design is depicted. Filled black box represents exon 1 and black arrow indicates transcription start site (ENSMUST00000067801). Filled grey box represent Cbs promoter CpG-islands and open box present the investigated nucleotide sequence. **Right:** Quantification of Cbs promoter CpG methylation (forward and reverse strand). Data are presented as mean  $\pm$  SEM ( $n = 5-6$ ). Open and grey columns represent data from C and HF animals. Asterisk indicates statistical significance ( $p < 0.05$ ). Abbreviations: chr17, chromosome 17; fwd, forward; rev, reverse. .... 49
- Figure 24.** Influence of HF diet on PPAR $\alpha$  promoter CpG-island DNA methylation in C and HF mice by bisulfite genomic pyrosequencing. **Left:** Experimental design is depicted. Filled black box represents exon 1 and black arrow indicates transcription start site (ENSMUST00000109422). Filled grey box represent Cbs promoter CpG-islands and open box present the investigated nucleotide sequence. **Right:** Quantification of PPAR $\alpha$  promoter CpG methylation (forward strand). Data are presented as mean  $\pm$  SEM ( $n = 5-6$ ). Open and grey columns represent data from C and HF animals. Asterisk indicates statistical significance ( $p < 0.05$ ). Abbreviations: chr15, chromosome 15. .... 50
- Figure 25.** Body weight development of animals in C and HF groups during eight weeks before the methyl-group supplementation phase. Data are presented as mean  $\pm$  SEM ( $n = 8-9$ ). Asterisk indicates statistical significance ( $p < 0.05$ ). .... 51

- Figure 26.** Intraperitoneal glucose tolerance test of C and HF mice after seven weeks of C or HF diet treatment is depicted. Data are presented as mean  $\pm$  SEM ( $n = 5$ ). Asterisk indicates statistical significance ( $p < 0.05$ ). ..... 52
- Figure 27.** Body weight development in mice receiving the C, CMS, HF and HFMS diets for four weeks after the eight weeks pre-treatment. Mice are treated in total for twelve weeks. Data are presented as mean  $\pm$  SEM ( $n = 8-9$ ). Asterisk indicates statistical significance of HF and HFMS mice compared to C and CMS mice ( $p < 0.05$ ). ..... 53
- Figure 28.** Intraperitoneal glucose tolerance test performed in mice receiving the C, CMS, HF and HFMS diets for four weeks. Data are presented as mean  $\pm$  SEM ( $n = 8-9$ ). Asterisk indicates statistical significance between C and HF mice (time point 30 min) and between C and HF and CMS and HF mice (time point 60 min) ( $p < 0.05$ ). ..... 55
- Figure 29.** Analyses of plasma from animals receiving the C, CMS, HF and HFMS for four weeks. Data are presented as box and whisker plot ( $n = 8-9$ ). Open and grey boxes represent data from C and HF animals and open lined and grey lined boxes represent data from CMS and HFMS animals. Different subscript letters indicate statistical significance ( $p < 0.05$ ). Abbreviations: 3MHis, 3-methyl-histidine; Aad, L- $\alpha$ -amino adipic acid; Asn, L-asparagine; Cit, L-citrulline; Gly, Glycine; Met, L-methionine; Orn, L-ornithine; Sar, Sarcosine; Ser, L-serine. .... 56
- Figure 30.** Analysis of plasma tHcy in animals on C and HF diets (8W) ( $n = 5$ ) and C, CMS, HF and HFMS diets (12W). Data are presented as box and whisker plot. Open and grey boxes represent data from C and HF animals and open lined and grey lined boxes represent data from CMS and HFMS animals. Different subscript letters indicate statistical significance ( $p < 0.05$ ). ..... 57
- Figure 31.** Analysis of liver tissue from animals receiving the C, CMS, HF and HFMS for four weeks. Data are presented as box and whisker plot ( $n = 8-9$ ). Open and grey boxes represent data from C and HF animals and open lined and grey lined boxes represent data from CMS and HFMS animals. Different subscript letters indicate statistical significance ( $p < 0.05$ ). Abbreviations: Abu, L- $\alpha$ -amino-n-butyrate;  $\beta$ Ala,  $\beta$ -alanine;  $\beta$ Aib, D,L- $\beta$ -aminoisobutyrate; Asn, L-asparagine; Asp, L-aspartate, Cit, L-citrulline; EtN, Ethanolamine; Gly, Glycine; Hyp, Hydroxyproline; Ile, L-isoleucine; Leu, L-leucine; Lys, L-lysine; Orn, L-ornithine; Phe, L-phenylalanine; Sar, Sarcosine; Ser, L-serine; Tau, Taurine; Thr, L-threonine; Trp, L-tryptophane; Tyr, L-tyrosine; Val, L-valine. .... 58
- Figure 32.** Analysis of SAM, SAH, [SAM] / [SAH] ratio, Hcy and cystathionine in the liver of C and HF (8W) mice ( $n = 4-5$ ) and C, CMS, HF and HFMS mice ( $n = 7-9$ ) is depicted. Data are presented as box and whisker plot. Open and grey boxes represent data from C and HF animals and open lined and grey lined boxes represent data from CMS and HFMS animals. Different subscript letters indicate statistical significance ( $p < 0.05$ ). Abbreviations: Cth, Cystathionine; Hcy, Homocysteine; SAH, S-adenosyl-homocysteine; SAM, S-adenosyl-methionine. .... 60
- Figure 33.** Hepatic Bhmt and Cbs mRNA expression levels in liver of C (8W) and HF mice at week eight ( $n = 5$ ) and C, CMS, HF and HFMS mice at week twelve ( $n = 8-9$ ). Data are presented as mean  $\pm$  SEM. Open and grey columns represent data from C and HF animals and open lined and grey

- lined columns represent data from CMS and HFMS animals. Different subscript letters indicate statistical significance ( $p < 0.05$ ). Abbreviations: Bhmt, Betaine-homocysteine methyltransferase; Cbs, Cystathionine  $\beta$ -synthase. .... 61
- Figure 34.** Effect of eight weeks (left,  $n = 5$ ) and additional four weeks of dietary treatment (right,  $n = 8-9$ ) on hepatic BHMT and CBS protein expression levels. Data are presented as mean  $\pm$  SEM. Open and grey columns represent data from C and HF animals and open lined and grey lined columns represent data from CMS and HFMS animals. Different subscript letters indicate statistical significance ( $p < 0.05$ ). Abbreviations: Bhmt, Betaine-homocysteine methyltransferase; Cbs, Cystathionine  $\beta$ -synthase. .... 62
- Figure 35.** Plasma non-esterified fatty acids in C, CMS, HF and HFMS mice after eight weeks ( $n = 5$ ) and twelve weeks ( $n = 8-9$ ) of dietary treatment. Open and grey boxes represent data from C and HF animals and open lined and grey lined boxes represent data from CMS and HFMS animals. Data are presented as box and whisker plot. Different subscript letters indicate statistical significance ( $p < 0.05$ ). Abbreviations: NEFA, non-esterified fatty acids; TG, triacylglycerol. .... 63
- Figure 36.** Hepatic triacylglycerol, non-esterified fatty acids and total phospholipids in C, CMS, HF and HFMS mice after eight weeks (8W) ( $n = 5$ ) and twelve weeks (12W) ( $n = 8-9$ ) of dietary treatment. Open and grey boxes represent data from C and HF animals and open lined and grey lined boxes represent data from CMS and HFMS animals. Data are presented as box and whisker plot. Different subscript letters indicate statistical significance ( $p < 0.05$ ). Abbreviations: NEFA, non-esterified fatty acids; tPL, total phospholipids; TG, triacylglycerol. .... 64
- Figure 37.** Representative histological analysis of livers from C, CMS, HF and HFMS mice after eight weeks and additional four weeks in cryosection with oilred O staining. Scale bar indicates 20  $\mu$ m. Magnification, 400x. .... 65
- Figure 38.** Effects of diets on gene and protein expression of marker enzymes implicated in de novo lipogenesis. In **A**, Srebp1c and Fasn mRNA levels and in **B** activation of SREBP1 (aSREBP1) are depicted. Data are presented as mean  $\pm$  SEM ( $n = 8-9$ ). Open and grey columns represent data from C and HF animals and open lined and grey lined columns represent data from CMS and HFMS animals. Different subscript letters indicate statistical significance ( $p < 0.05$ ). Abbreviations: aSrebp1, soluble activated Srebp1; Fasn, Fatty acid synthase. .... 66
- Figure 39.** Hepatic mRNA expression levels of Cpt1a gene in C, CMS, HF and HFMS mice after 12 weeks ( $n = 8-9$ ). Data are presented as mean  $\pm$  SEM. Open and grey columns represent data from C and HF animals and open lined and grey lined columns represent data from CMS and HFMS animals. Different subscript letters indicate statistical significance ( $p < 0.05$ ). Abbreviations: Cpt1a, Carnitine palmitoyltransferase 1a. .... 67
- Figure 40.** Effect of four weeks dietary methyl-group supplementation on hepatic AMPK $\alpha$  expression and phosphorylation state. Data are presented as mean  $\pm$  SEM ( $n = 7-9$ ). Open and grey columns represent data from C and HF animals and open lined and grey lined columns represent data from CMS and HFMS animals. Different subscript letters indicate statistical significance ( $p < 0.05$ ). Abbreviations: AMPK $\alpha$ , AMP-activated protein

- kinase  $\alpha$ ; P-AMPK $\alpha$ , Phosphorylated AMP-activated protein kinase  $\alpha$  (Thr172). ..... 68
- Figure 41.** Analysis of selected hepatic carnitine and acyl-carnitine concentrations in liver tissues from C, CMS, HF and HFMS mice after four weeks of dietary methyl-group supplementation. Data are presented as box and whisker plot ( $n = 8-9$ ). Open and grey boxes represent data from C and HF animals and open lined and grey lined boxes represent data from CMS and HFMS animals. Different subscript letters indicate statistical significance ( $p < 0.05$ ). Abbreviations: C0, DL-carnitine; C10, Decanoyl-L-carnitine; C10:1 Decenoyl-L-carnitine; C12, Dodecanoyl-L-carnitine; C12:1, Dodecenoyl-L-carnitine; C14, Tetradecanoyl-L-carnitine; C14:1-OH, Hydroxytetradecenoyl-L-carnitine; C16, Hexadecanoyl-L-carnitine; C16-OH, Hydroxyhexadecenoyl-L-carnitine; C16:1, Hexadecenoyl-L-carnitine; C16:1-OH, Hydroxyhexadecenoyl-L-carnitine; C16:2-OH, Hydroxyhexadecadienyl-L-carnitine; C18, Octadecanoyl-L-carnitine; C18:1, Octadecenoyl-L-carnitine; C18:1-OH, Hydroxyoctadecenoyl-L-carnitine; C18:2, Octadecadienyl-L-carnitine; C2, Acetyl-L-carnitine; C3, Propionyl-L-carnitine; C3-DC / C4-OH, Malonyl-L-carnitine / Hydroxybutyryl-L-carnitine; C3-OH, Hydroxypropionyl-L-carnitine; C4, Butyryl-L-carnitine; C4:1, Butenyl-L-carnitine; C5, Valeryl-L-carnitine; C5-DC / C6-OH, Glutaryl-L-carnitine / Hydroxyhexanoyl-L-carnitine; C5-M-DC, Methylglutaryl-L-carnitine; C5-OH / C3-DC-M, Methylmalonyl-L-carnitine / Hydroxyvaleryl-L-carnitine; C5:1-DC, Glutaconyl-L-carnitine; C6 / C4:1-DC, Fumaryl-L-carnitine / Hexanoyl-L-carnitine; C7-DC, Pimelyl-L-carnitine; C8, Octanoyl-L-carnitine; C9, Nonanyl-L-carnitine. .... 69
- Figure 42.** Restriction map of informative restriction sites for MS-qPCR in the normalisation region on chromosome 18. No *AciI* or *HpaII* restriction sites can be detected. .... 122
- Figure 43.** *Zrsr1* CpG-island restriction map of informative restriction sites for MS-qPCR. **Top:** Filled black box represents the first exon and black arrow indicates transcription start site (ENSMUST00000049506). Filled grey box represents *Zrsr1* CpG-island and open box mark the investigated region. **Down:** Investigated regions and position of informative restriction sites are depicted. Abbreviations: *Zrsr1*, Zinc finger (CCCH type), RNA binding motif and serine/arginine rich 1. .... 122
- Figure 44.** Quantitative analysis of CpG restriction sites in promoter *Zrsr1* CpG-island in liver and testis of C57BL/6N mouse. Data are shown for the restriction enzymes *AciI* in the previously mentioned region. Data are presented as mean  $\pm$  SEM ( $n = 1$ ). Open and black bar represents liver and testis. Abbreviations: *Zrsr1*, Zinc finger (CCCH type), RNA binding motif and serine/arginine rich 1. .... 123
- Figure 45.** Food intake of C, HF group during the first eight weeks of dietary treatment is depicted. Data are presented as mean  $\pm$  SEM ( $n = 8-9$ ). Asterisk indicates statistical significance ( $p < 0.05$ ). .... 124
- Figure 46.** Cumulative food intake of C, CMS, HF and HFMS group during the last four weeks of the twelve weeks of dietary treatment is depicted. Vertical line indicates start of therapeutic intervention by methyl-group supplementation in CMS and HFMS mice. Data are presented as mean  $\pm$  SEM ( $n = 8-9$ ).

---

*Asterisk indicates statistical significance of C and HF, C and HFMS, CMS and HF, CMS and HFMS groups at the depicted time points ( $p < 0.05$ ). ..... 125*

## List of tables

<b>Table 1.</b> Composition of experimental diets. Nutrient composition is expressed as [g / kg], except it is delineated differently. ....	21
<b>Table 2.</b> DNA-sequences of mouse primers used for determination of gene expression.....	29
<b>Table 3.</b> DNA-sequences of rat primers used for gene expression analysis in rat hepatoma cells (Fao). ....	31
<b>Table 4.</b> DNA-sequences for MS-qPCR primers used for local DNA methylation analysis. * primer DNA-sequences are derived from Oakes et al (149).....	34
<b>Table 5.</b> List of primer sequences used for quantification of individual CpG-site DNA methylation analysis by bisulfite genomic pyrosequencing. Fst, forward genomic DNA strand; rst, reverse genomic DNA strand; B, biotinylation. ....	37
<b>Table 6.</b> Basal parameters of C and HF C57BL/6N male mice after eight weeks dietary treatment. Data are presented as mean $\pm$ SEM (n = 5). Different subscript letters indicate statistical significance (p < 0.05). VAT was calculated by summing up the weight of epididymal, perirenal and mesenteric adipose tissue. Abbreviations: AUC, area under the curve; ipGTT, intraperitoneal glucose tolerance test; VAT, visceral adipose tissue. ...	52
<b>Table 7.</b> Basal phenotypic parameters of mice fed the C, CMS, HF and HFMS diets for four weeks. Data are presented as mean $\pm$ SEM (n = 8-9). Different subscript letters indicates statistical significance (p < 0.05).VAT was calculated by summing up the weight of epididymal, perirenal and mesenteric adipose tissue. Abbreviations: AUC, area under the curve; ipGTT, intraperitoneal glucose tolerance test; VAT, visceral adipose tissue. ...	54
<b>Table 8.</b> Concentrations of PC, lyso-PC, hydroxyl- and sphingomyelin metabolites in liver tissues of mice fed C, CMS, HF and HFMS diets for four weeks. Data are presented as mean $\pm$ SEM (n = 8-9). Bold numbers and different subscript letters indicate statistical significance (p < 0.05). Abbreviations: PC aa, Phosphatidylcholine diacyl; PC ae, Phosphatidylcholine acyl-alkyl; SM (OH), Hydroxysphingomyeline; SM, Sphingomyeline.....	71
<b>Table 9.</b> Analysis of HF diet induced NAFLD on hepatic gene expression. C <sub>q</sub> -values of invariant house keeping genes are listed for C and HF group. Abbreviations: Actb, $\beta$ -Actin; Gapdh, Glyceraldehyde-3-phosphate dehydrogenase; Hpvt, Hypoxanthine guanine phosphoribosyl transferase.....	112
<b>Table 10.</b> Analysis of HF diet induced NAFLD on hepatic gene expression. C <sub>q</sub> -values of genes operating in the methionine cycle are listed for C and HF group. Abbreviations: Ahcy, S-adenosylhomocysteine hydrolase; Mat1a, Methionine adenosyltransferase I alpha; Mat2a, Methionine adenosyltransferase II alpha; Pemt, Phosphatidylethanolamine N-methyltransferase. ....	112
<b>Table 11.</b> Analysis of HF diet induced NAFLD on hepatic gene expression. C <sub>q</sub> -values of genes operating in the folate cycle are listed for C and HF group. Abbreviations: Mthfr, 5,10-methylenetetrahydrofolate reductase; Mtr, 5-methyltetrahydrofolate-homocysteine methyltransferase; Shmt1, Serine hydroxymethyltransferase 1; Shmt2, Serine hydroxymethyltransferase 2.....	113

- Table 12.** Analysis of HF diet induced NAFLD on hepatic gene expression.  $C_q$ -values of genes operating in the sarcosine pathway are listed for C and HF group. Abbreviations: *Bhmt*, Betaine-homocysteine methyltransferase; *Bhmt2*, Betaine-homocysteine methyltransferase 2; *Chdh*, Choline dehydrogenase; *Dmgdh*, Dimethylglycine dehydrogenase precursor; *Gnmt*, Glycine N-methyltransferase..... 113
- Table 13.** Analysis of HF diet induced NAFLD on hepatic gene expression.  $C_q$ -values of genes operating in the transsulfuration pathway are listed for C and HF group. Abbreviations: *Cbs*, Cystathionine  $\beta$ -synthase; *Csad*, Cysteine sulfinic acid decarboxylase; *Cth*, Cystathionase; *Gclc*, Glutamate-cysteine ligase catalytic subunit; *Got1*, Glutamate oxaloacetate transaminase 1; *Gss*, Glutathione synthetase..... 114
- Table 14.** Analysis of HF diet induced NAFLD on hepatic gene expression.  $C_q$ -values of PPAR $\alpha$  and PPAR $\alpha$  target genes are listed for C and HF group. Abbreviations: *Acox1*, Acyl-coenzyme A oxidase 1; *Cpt1a*, Carnitine palmitoyltransferase 1a; *Ppara*, Peroxisome proliferator activated receptor  $\alpha$ ; *Ucp2*, Uncoupling protein 2..... 114
- Table 15.** Analysis of HF diet induced NAFLD on hepatic gene expression.  $C_q$ -values of DNA methyltransferase genes are listed for C and HF group. Abbreviations: *Dnmt1*, DNA methyltransferase 1; *Dnmt3a*, DNA methyltransferase 3a; *Dnmt3b*, DNA methyltransferase 3b..... 115
- Table 16.** Influence of WY14,643 mediated PPAR $\alpha$  activation on gene expression of invariant housekeeping gene (*Gus*), PPAR $\alpha$  target gene (*Cpt1a*) and genes operating in the C1-metabolism (*Cbs*, *Bhmt*) in rat hepatoma FAO cells.  $C_q$ -values are listed for 0 – 100  $\mu$ M WY14,643 treatment for 24 h. Abbreviations: *Bhmt*, Betaine-homocysteine methyltransferase; *Cbs*, Cystathionine  $\beta$ -synthase; *Cpt1a*, Carnitine palmitoyltransferase 1a; *Gus*,  $\beta$ -Glucuronidase..... 115
- Table 17.** Analysis of hepatic gene expression in animals of the methyl-group supplementation feeding trial.  $C_q$ -values of invariant housekeeping genes (*Gapdh*, *Hprt*), genes operating in the C1-metabolism (*Bhmt*, *Cbs*), genes implicated in DNL (*Srebp1c*, *Fasn*) as well as  $C_q$ -values of a PPAR $\alpha$  target gene (*Cpt1a*) are listed for C, CMS, HF and HFMS mice. Abbreviations: *Bhmt*, Betaine-homocysteine methyltransferase; *Cbs*, Cystathionine  $\beta$ -synthase; *Cpt1a*, Carnitine palmitoyltransferase 1a; *Fasn*, Fatty acid synthase; *Gapdh*, Glyceraldehyde-3-phosphate dehydrogenase; *Hprt*, Hypoxanthine guanine phosphoribosyl transferase; *Srebp1c*, Sterol regulatory element binding transcription factor 1c..... 116
- Table 18.** Effect of dietary HF treatment on hepatic metabolite level is listed. Data are presented as mean  $\pm$  SEM [ $\mu$ mol/g protein] ( $n = 9-11$ ). Bold numbers indicate statistical significance ( $P < 0.05$ ). Abbreviations: 1MHis, 1-methyl-L-histidine; Aad, L- $\alpha$ -amino adipic acid; Abu, L- $\alpha$ -amino-n-butyrate; Ala, L-alanine; Asn, L-asparagine; Asp, L-asparic acid; bAib, D,L- $\beta$ -aminoisobutyrate; Cit, L-citrulline; Cth, Cystathionine; EtN, Ethanolamine; GABA,  $\gamma$ -amino-n-butyrate; Gln, L-glutamine; Glu, L-glutamate; Gly, Glycine; His, L-histidine; Hyp, Hydroxyproline; Ile, L-isoleucine; Leu, L-leucine; Lys, L-lysine; Met, L-methionine; Orn, L-ornithine; PEtN, O-phosphoethanolamine; Phe, L-phenylalanine; Pro, L-proline; Sar, Sarcosine; Ser, L-serine; Tau, Taurine; Thr, L-threonine; Trp, L-tryptophane; Tyr, L-tyrosine; Val, L-valine..... 117

- Table 19.** Analysis of C, CMS, HF and HFMS blood plasma metabolite level after four weeks of dietary methyl-group supplementation is listed. Data are presented as mean  $\pm$  SEM ( $n = 8-9$ ). Bold numbers indicate statistical significance ( $p < 0.05$ ). Abbreviations: 3MHis, 3-methyl-L-histidine; Aad, L- $\alpha$ -aminoadipic acid; Abu, L- $\alpha$ -amino-n-butyrate; Ala, L-alanine; Arg, L-arginine; Asn, L-asparagine; Asp, L-asparic acid; Cit, L-citrulline; Cys, L-cystine; EtN, Ethanolamine; Gln, L-glutamine; Glu, L-glutamate; Gly, Glycine; His, L-histidine; Hyp, Hydroxyproline; Ile, L-isoleucine; Leu, L-leucine; Lys, L-lysine; Met, L-methionine; Orn, L-ornithine; PEtN, O-phosphoethanolamine; Phe, L-phenylalanine; Pro, L-proline; Sar, Sarcosine; Ser, L-serine; Tau, Taurine; Thr, L-threonine; Trp, L-tryptophane; Tyr, L-tyrosine; Val, L-valine. .... 118
- Table 20.** Analysis of C, CMS, HF and HFMS liver tissue for selected hepatic metabolite level after four weeks of dietary methyl-group supplementation is listed. Data are presented as mean  $\pm$  SEM [ $\mu\text{mol/g protein}$ ] ( $n = 8-9$ ). Bold numbers indicate statistical significance ( $p < 0.05$ ). Abbreviations: 1MHis, 1-methyl-L-histidine; Aad, L- $\alpha$ -aminoadipic acid; Abu, L- $\alpha$ -amino-n-butyrate; Ala, L-alanine; Asn, L-asparagine; Asp, L-asparic acid; bAib, D,L- $\beta$ -aminoisobutyrate; bAla,  $\beta$ -alanine; Cit, L-citrulline; Cth, Cystathionine; EtN, Ethanolamine; GABA,  $\gamma$ -amino-n-butyrate; Gln, L-glutamine; Glu, L-glutamate; Gly, Glycine; His, L-histidine; Hyp, Hydroxyproline; Ile, L-isoleucine; Leu, L-leucine; Lys, L-lysine; Met, L-methionine; Orn, L-ornithine; PEtN, O-phosphoethanolamine; Phe, L-phenylalanine; Pro, L-proline; Sar, Sarcosine; Ser, L-serine; Tau, Taurine; Thr, L-threonine; Trp, L-tryptophane; Tyr, L-tyrosine; Val, L-valine. .... 119
- Table 21.** Analysis of C, CMS, HF and HFMS liver tissue for hepatic biogenic amine concentrations after four weeks of dietary methyl-group supplementation is listed. Data are presented as mean  $\pm$  SEM [ $\mu\text{mol/mg tissue}$ ] ( $n = 8-9$ ). Bold numbers and different subscript letters indicate statistical significance ( $p < 0.05$ ), - indicates below detection limit. Abbreviations: ADMA, asymmetric dimethylarginine; Ac-Orn, acetylorntithine; DOPA, dihydroxy-phenylalanine; Met-SO, methioninesulfoxide; Nitro-Tyr, nitrotyrosine; OH-Pro, Hydroxyproline; PEA, phenylethylamine; SDMA, symmetric dimethylarginine; alpha-AAA,  $\alpha$ -aminoadipic acid; total DMA, total dimethylarginine. .... 120
- Table 22.** Analysis of C, CMS, HF and HFMS liver tissue for hepatic acyl-carnitine concentrations after four weeks of dietary methyl-group supplementation is listed. Data are presented as mean  $\pm$  SEM [ $\mu\text{mol/mg tissue}$ ] ( $n = 8-9$ ). Bold numbers indicate statistical significance ( $p < 0.05$ ). Abbreviations: C0, DL-carnitine; C10, Decanoyl-L-carnitine; C10:1 Decenoyl-L-carnitine; C10:2, Decadienyl-L-carnitine; C12, Dodecanoyl-L-carnitine; C12-DC, Dodecanedioyl-L-carnitine; C12:1, Dodecenoyl-L-carnitine; C14, Tetradecanoyl-L-carnitine; C14:1, Tetradecenoyl-L-carnitine; C14:1-OH, Hydroxytetradecenoyl-L-carnitine; C14:2, Tetradecadienyl-L-carnitine; C14:2-OH, Hydroxytetradecadienyl-L-carnitine; C16, Hexadecanoyl-L-carnitine; C16-OH, Hydroxyhexadecanoyl-L-carnitine; c16:1, Hexadecenoyl-L-carnitine; C16:1-OH, Hydroxyhexadecenoyl-L-carnitine; C16:2, Hexadecadienyl-L-carnitine; C16:2-OH, Hydroxyhexadecadienyl-L-carnitine; C18, Octadecanoyl-L-carnitine; C18:1, Octadecenoyl-L-carnitine; C18:1-OH, Hydroxyoctadecenoyl-L-carnitine; C18:2, Octadecadienyl-L-carnitine; C2, Acetyl-L-carnitine; C3, Propionyl-L-



*carnitine; C3-DC / C4-OH, Malonyl-L-carnitine / Hydroxybutyryl-L-carnitine; C3-OH, C3:1, Propenyl-L-carnitine; Hydroxypropionyl-L-carnitine; C4, Butyryl-L-carnitine; C4:1, Butenyl-L-carnitine; C5, Valeryl-L-carnitine; C5-DC / C6-OH, Glutaryl-L-carnitine / Hydroxyhexanoyl-L-carnitine; C5-M-DC, Methylglutaryl-L-carnitine; C5-OH / C3-DC-M, Methylmalonyl-L-carnitine / Hydroxyvaleryl-L-carnitine; C5:1, Tiglyl-L-carnitine; C5:1-DC, Glutaconyl-L-carnitine; C6 / C4:1-DC, Fumaryl-L-carnitine / Hexanoyl-L-carnitine; C6:1, Hexenoyl-L-carnitine; C7-DC, Pimelyl-L-carnitine; C8, Octanoyl-L-carnitine; C9, Nonayl-L-carnitine ..... 120*

- Table 23.** *Effect of HF diet feeding on nutrient and energy intake of C and HF mice of the first feeding trial. Data are presented as mean  $\pm$  SEM (n = 9-11). Bold numbers and asterisk indicates statistical significance (p < 0.05). ..... 123*
- Table 24.** *Effect of HF diet feeding on nutrient and energy intake of C and HF mice of the methyl-group supplementation feeding trial after eight weeks. Data are presented as mean  $\pm$  SEM (n = 8-9). Bold numbers and asterisk indicates statistical significance (p < 0.05). ..... 124*
- Table 25.** *Effect of HF diet feeding on nutrient and energy intake of C, CMS, HF and HFMS mice of the methyl-group supplementation feeding trial after twelve weeks. Data are presented as mean  $\pm$  SEM (n = 8-9). Bold numbers and different subscript letters indicate statistical significance (p < 0.05). ..... 125*

## List of abbreviations

[SAM]/[SAH]	SAM to SAH concentration
3MHis	3-methyl-histidine
5-Methyl-THF	5-Methyl-tetrahydrofolate
Aad	L- $\alpha$ -aminoadipic acid
Abu	L- $\alpha$ -amino-n-butyrate
ACC	Acetyl-CoA carboxylase
ACC2	Acetyl-CoA carboxylase 2
Acox1	Acyl-coenzyme A oxidase 1
ACTB	$\beta$ -Actin
Adipokines	Adipocyte specific proteins
AHCY	SAH Hydrolase
AMP	Adenosine monophosphate
AMPK	AMP-activated protein kinase
Asn	L-asparagine
Asp	L-aspartate
aSrebp1	soluble activated Srebp1
ATP	Adenosine triphosphate
AUC	Area under the curve
bcDNA	Bisulfite converted DNA
BHMT	Betaine-homocysteine methyltransferase
Bhmt2	Betaine-homocysteine methyltransferase 2
C	Control
C0	DL-carnitine
C10	Decanoyl-L-carnitine
C10:1	Decenoyl-L-carnitine
C12	Dodecanoyl-L-carnitine
C12:1	Dodecenoyl-L-carnitine
C14	Tetradecanoyl-L-carnitine
C14:1-OH	Hydroxytetradecenoyl-L-carnitine
C16	Hexadecanoyl-L-carnitine
C16:1	Hexadecenoyl-L-carnitine
C16:1-OH	Hydroxyhexadecenoyl-L-carnitine
C16:2-OH	Hydroxyhexadecadienyl-L-carnitine
C16-OH	Hydroxyhexadecanoyl-L-carnitine
C18	Octadecanoyl-L-carnitine
C18:1	Octadecenoyl-L-carnitine
C18:1-OH	Hydroxyoctadecenoyl-L-carnitine
C18:2	Octadecadienyl-L-carnitine
C1-metabolism	One-carbon metabolism
C2	Acetyl-L-carnitine
C3	Propionyl-L-carnitine
C3-DC / C4-OH	Malonyl-L-carnitine / Hydroxybutyryl-L-carnitine
C3-OH	Hydroxypropionyl-L-carnitine
C4	Butyryl-L-carnitine
C4:1	Butenyl-L-carnitine
C5	Valeryl-L-carnitine
C5:1-DC	Glutaconyl-L-carnitine
C5-DC / C6-OH	Glutaryl-L-carnitine / Hydroxyhexanoyl-L-carnitine
C5-M-DC	Methylglutaryl-L-carnitine
C5-OH / C3-DC-M	Methylmalonyl-L-carnitine / Hydroxyvaleryl-L-carnitine
C6 / C4:1-DC	Fumaryl-L-carnitine / Hexanoyl-L-carnitine

---

C7-DC	Pimelyl-L-carnitine
C8	Octanoyl-L-carnitine
C9	Nonanyl-L-carnitine
CACT	Carnitine-acylcarnitine translocase
CBS	Cystathionine $\beta$ -synthase
Cbs I7	Cystathionine $\beta$ -synthase intragenic CpG-island region 7
Cbs P1	Cystathionine $\beta$ -synthase promoter CpG-island region 1
Cbs P2	Cystathionine $\beta$ -synthase promoter CpG-island region 2
Chdh	Choline dehydrogenase
chr15	chromosome 15
chr17	chromosome 17
Cit	L-citrulline
CK	choline kinase
CMP	Cytidine monophosphate
CMS	Control methyl-group supplemented
CPT	CDP-choline:1,2-diacylglycerol cholinephosphotransferase
CPT-1	Carnitine palmitoyltransferase
C <sub>q</sub>	Threshold cycle
Csad	Cysteine sulfinic acid decarboxylase
CT	CTP:phosphocholine cytidyltransferase
Cth	Cystathionine
CTP	Cytidine triphosphate
dcSAM	decarboxylated s-adenosyl-methionine
DHF	Dihydrofolate
DIO	Diet induced obesity
DMG	Dimethylglycine
Dmgdh	Dimethylglycine dehydrogenase precursor
dMTase	DNA demethylase
DNA	Deoxyribonucleic acid
DNL	<i>De novo</i> lipogenesis
DNMT	DNA methyltransferase
Dnmt1	DNA methyltransferase 1
Dnmt3a	DNA methyltransferase 3a
Dnmt3b	DNA methyltransferase 3b
dTMP	Deoxythymidine monophosphate
dUMP	Deoxyuridine monophosphate
EDTA	Ethylene diaminetetraacetic acid
ER	Endoplasmatic reticulum
EtN	Ethanolamine
FA	Free fatty acid
FASN	Fatty acid synthase
FIA	Flow injection analysis
FoxO1	Forkhead box O1
Fst	Forward genomic DNA strand
fwd	forward
GAMT	Guanidinoacetate methyltransferase
GAPDH	Glyceraldehyde-3-phosphate dehydrogenase
Gclc	Glutamate-cysteine ligase catalytic subunit
Gln	L-glutamine
Glu	L-glutamate
Gly	Glycine
Gnmt	Glycine N-methyltransferase
Got1	Glutamate oxaloacetate transaminase 1
GSH	Glutathione
Gss	Glutathione synthetase
GUS	$\beta$ -Glucuronidase

---

H2A	Histone 2A
H2B	Histone 2B
H3	Histone 3
H4	Histone 4
Hcy	Homocysteine
HDL	High density lipoprotein
HF	High-fat
HFMS	High-fat methyl-group supplemented
HPRT	Hypoxanthine guanine phosphoribosyltransferase
HSL	Hormone sensitive lipase
Hyp	Hydroxyproline
IDL	Intermediary density lipoprotein
Ile	L-isoleucine
ipGTT	Intraperitoneal glucose tolerance test
K <sub>m</sub>	Michaelis constant
KOH	Potassium hydroxide
LCT $\alpha^{-/-}$	Liver specific CTP:phosphocholine cytidyltransferase $\alpha$ knock out
LDL	Low density lipoprotein
Leu	L-leucine
LINE	Long interspersed nuclear elements
LPL	Lipoprotein lipase
LTR IAP	Long terminal repeat intracisternal A particle
Lys	L-lysine
MAT	Methionine adenosyltransferase
Mat1a	Methionine adenosyltransferase I alpha
Mat2a	Methionine adenosyltransferase II alpha
MCD	Methionine choline deficient
MDR2	Multidrug resistance protein 2
Met	L-methionine
Methylene-THF	Methylene-tetrahydrofolate
MS	Mass spectrometry
MS-qPCR	Methylation-sensitive quantitative polymerase chain reaction
MTA	Methylthioadenosine
Mthfr	5,10-methylenetetrahydrofolate reductase
MTR	Methionine synthase
n.d.	no detection
NaCl	Sodium chloride
NAFLD	Non-alcoholic fatty liver disease
NEFA	Non-esterified fatty acids
Orn	L-ornithine
PC	Phosphatidylcholine
PC aa	Phosphatidylcholine diacyl
PC ae	Phosphatidylcholine acyl-alkyl
PE	Phosphatidylethanolamine
PEMT	Phosphatidylethanolamine methyltransferase
PGC-1 $\alpha$	Peroxisome proliferative activated receptor $\gamma$ coactivator 1 $\alpha$
Phe	L-phenylalanine
PI(3)-kinase	Phosphoinositid-3-kinase
PL	Phospholipid
PPAP	Phosphatidic acid phosphatase
PPAR $\alpha$	Peroxisome proliferator activated receptor $\alpha$
PP <sub>i</sub>	Pyrophosphate
qRT-PCR	Quantitative real-time polymerase chain reaction
rev	reverse
RNA	Ribonucleic acid

---

ROI	Region of interest
ROS	Reactive oxygen species
rst	Reverse genomic DNA strand
SAH	S-adenosyl-homocysteine
SAM	S-adenosyl-methionine
SAMDC	S-adenosyl-methionine decarboxylase
Sar	Sarcosine
SCD	Stearoyl-CoA desaturase
SDS	Sodium dodecyl sulfate
Ser	L-serine
Shmt1	Serine hydroxymethyltransferase 1
Shmt2	Serine hydroxymethyltransferase 2
SI	Small intestine
SM	Sphingomyeline
SM (OH)	Hydroxysphingomyeline
SREBP-1c	Sterol regulatory element binding protein 1c
Tau	Taurine
TBS	Tris buffered saline
TBS-T	Tris buffered saline-Tween 20
TF	Transcription factor
TG	Triacylglycerol
tHcy	total homocysteine
THF	Tetrahydrofolate
Thr	L-threonine
TML	Trimethyllysine
tPL	total phospholipid
TRIS	Tris(hydroxymethyl)-aminomethan
Trp	L-tryptophane
Tyr	L-tyrosine
Ucp2	Uncoupling protein 2
Val	L-valine
VAT	Visceral adipose tissue
VLDL	Very low density lipoprotein
$\beta$ Aib	D,L- $\beta$ -aminoisobutyrate
$\beta$ Ala	$\beta$ -alanine

## 1 Introduction

The liver is a visceral organ of prime importance in metabolic homeostasis. It can store carbohydrates as glycogen and utilizes glycerol as well as amino acids for gluconeogenesis and converts the ammonia into urea for excretion. With phase I and phase two enzymes it also is of prime importance in xenobiotic detoxification. It is a central organ in lipid metabolism by production of bile acids for enabling dietary lipid absorption, it synthesizes fat from a carbohydrate excess and secretes VLDL for lipid distribution to peripheral tissues. Mechanistically different pathways are implicated in the hepatic lipid homeostasis (**Figure 1**) that cover *de novo* lipacidogenesis and fatty acid  $\beta$ -oxidation, lipoprotein uptake and release and storage of triacylglycerol (TG). Imbalances in these processes can result in enhanced TG accumulation and fatty liver disease (1).

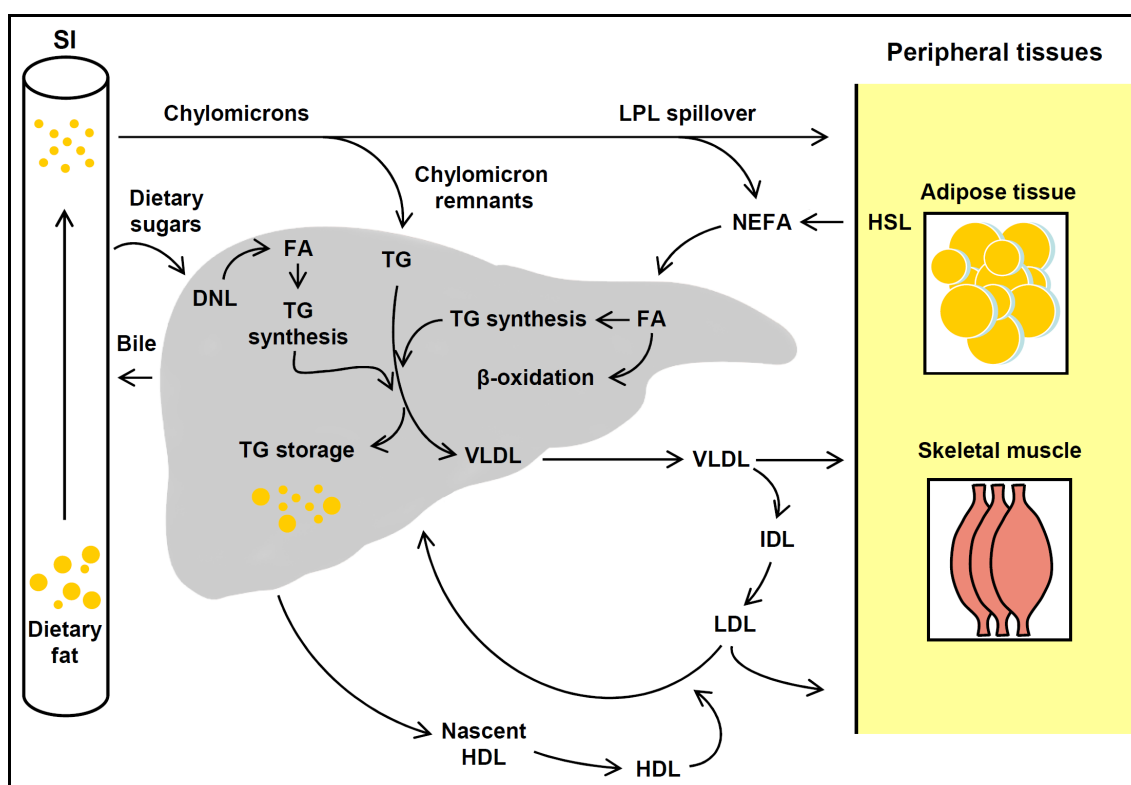


**Figure 1.** Pathways implicated in hepatic lipid homeostasis are depicted. Lipid homeostasis is maintained by equilibration of fatty acid uptake, *de novo* lipogenesis, fatty acid oxidation and VLDL dependent triacylglycerol export to peripheral tissues. Imbalance in these processes lead to hepatic triacylglycerol deposition. Abbreviations: FA, Free fatty acids; HDL, High density lipoprotein particle; HSL, Hormone sensitive lipase; IDL, Intermediary density lipoprotein particle; LDL, Low density lipoprotein particle; LPL, Lipoprotein lipase; NEFA, Non-esterified fatty acids; SI, Small intestine; TG, Triacylglycerol; VLDL, Very low density lipoprotein particle.

## 1.1 Non-alcoholic fatty liver disease

Non-alcoholic fatty liver disease (NAFLD) is a generic term describing an incremental lipid metabolic dysfunction of the liver that can induce a wide range of alterations starting with TG accumulation (steatosis), fibrosis and inflammation (steatohepatitis) that can progress to end-stage liver diseases like cirrhosis and hepatocellular cancer (2). NAFLD was first described by Westwater and Fainer as obesity associated fatty liver disease (3). The pathological similarities to alcohol induced liver injury was described by Adler and Schaffner (4) and Ludwig *et al.* defined the impairments as non-alcoholic steatohepatitis in the year 1980 (5, 6). NAFLD is known to be the phenotypical manifestation of the metabolic syndrome in the liver and is therefore associated with conditions like obesity, type 2 diabetes mellitus and hyperlipidemia which influence the prevalence of developing NAFLD (7). 33 % of NAFLD patients have the entire characteristic of the metabolic syndrome and nearly 90 % have one particular feature of the syndrome (8). The overall prevalence of NAFLD ranges from 20 % to 30 % in the western population which can increase to 75-100 % in obese people (8) and is increasingly diagnosed in childhood also predominantly in association with obesity (9, 10). This reveals that NAFLD is highly associated with obesity and the rising prevalence of obesity and type 2 diabetes leads to an increase in hepatic steatosis (11). The development of non-alcoholic steatohepatitis (NASH) is observed in 10-20 % of steatotic patients and only less than 5 % of NASH patients progress to cirrhosis (10) while 70-80 % of cancers occur in cirrhotic livers (12). NAFLD can be distinguished in primary and secondary disease depending on etiological impacts. Obesity or the metabolic syndrome is one of the principal causes of hepatic steatosis and can be defined as primary NAFLD while secondary NAFLD occurs due to infections, medications, parenteral feeding and rare metabolic and congenital diseases (13, 14). Hepatic TG accumulation and fatty liver disease can therefore have different origins and different modulators (7).

### 1.1.1 Pathogenesis of non-alcoholic fatty liver disease

The pathogenesis of NAFLD starts with the development of hepatic steatosis that is often explained by an imbalance of free fatty acid (non-esterified fatty acids, NEFA) uptake from the blood, TG synthesis (*de novo* lipogenesis, DNL), fatty acid oxidation and TG export via very low density lipoprotein (VLDL) particles to peripheral fat stores (adipose tissue) as shown in **Figure 1** (1). Collectively, it reflects a disturbance of fatty acid homeostasis and results in hepatic fatty acid storage as TG. In the following the major mechanisms underlying hepatic lipid homeostasis and NAFLD etiology will be highlighted.

The visceral adipose tissue plays an important role in the regulation of the hepatic uptake of free fatty acids from blood plasma. Circulating NEFA are released from adipose tissues by lipolysis and are used as energy substrates predominantly in muscle and liver. Adipocytes also secrete adipocyte specific proteins (adipokines) like adiponectin or leptin, the inflammatory chemokine tumor necrosis factor- $\alpha$  (TNF- $\alpha$ ), interleukins and angiogenic molecules in an endocrine and paracrine mode (14). In obesity, the increase in TNF- $\alpha$  is implicated in the development of insulin resistance which increases lipolysis in adipose tissue due to reduced insulin suppression of the hormone sensitive lipase (8). This leads to an increased release of free fatty acids and also of TNF- $\alpha$  into circulation. Systemic TNF- $\alpha$  can enhance the expression of fatty acid translocases in hepatocytes resulting in an increased hepatic fatty acid uptake from the circulation (15) and thus TNF- $\alpha$  contributes to the development of NAFLD.

In liver, the conversion of a glucose excess into fatty acids is accomplished via *de novo* fatty acid synthesis. Glucose utilization in the glycolytic chain leads to pyruvate that enters the Krebs cycle in mitochondria (11). Synthesized citrate is shuttled back into the cytosol and is converted to oxaloacetate and acetyl-CoA via ATP citrate lyase (11). The next involves the carboxylation of acetyl-CoA to malonyl-CoA by acetyl-CoA carboxylase (ACC). Malonyl-CoA is used by fatty acid synthase (FASN) for the synthesis of palmitic acid (C16:0) which can be elongated to stearic acid (C18:0) and desaturated to oleic acid (C18:1) by long-chain fatty acyl elongases and stearoyl-CoA desaturase (SCD) (11). In case of energy excess (glucose excess) cytosolic citrate (precursor of acetyl-CoA) accumulates and leads to allosteric activation of ACC leading to enhanced malonyl-CoA synthesis used by FASN for long-chain fatty acid synthesis (16), whereas the system is controlled by feedback inhibition of FASN by acyl-CoA (17). Insulin dependent activation of DNL is mediated by increasing transcription of the gene encoding the membrane bound transcription factor (TF) sterol regulatory element-binding protein 1c (SREBP-1c) via phosphoinositid-3-kinase (PI(3)-kinase) dependent pathways (18-22). Activation of SREBP-1c to promote DNL first leads to migration of the premature TF from the endoplasmatic reticulum (ER) to the Golgi apparatus, which is followed by proteolytical processing of the precursor to the soluble mature form (aSREBP-1c). The mature form translocates into the nucleus and regulates expression of lipogenic enzymes like FASN, ACC and SCD (23-25). The molecular mechanism how insulin enhances SREBP-1c processing is undefined, although there is some evidence of an indirect insulin action (24). The influence of SREBP-1c expression on DNL and hepatic steatosis is for example shown in a transgenic mouse model (26).

Obesity leads to the development of peripheral and hepatic insulin resistance which induces an increase in plasma glucose level and promotes a hyperinsulinemia. Despite reduced insulin sensitivity, insulin is able to stimulate SREBP-1c transcription and thereby induces DNL (27). Paradoxically, insulin induced SREBP-1c expression



coexists with disturbed suppression of gluconeogenesis during insulin resistance, which has been related to different regulations of insulin receptor substrate-1 and -2 and to FoxO1 (gluconeogenesis regulating TF) -mediated AKT-phosphorylation mimicking PI(3) kinase dependent pathway activation and restoring induction of SREBP1c expression (24). Dysregulation of DNL during particular features of the metabolic syndrome results in increased hepatic fatty acid synthesis and is implicated in the induction of NAFLD which has been shown in rodent models of diabetes and obesity (27-29).

For hepatic fatty acid oxidation the three main pathways mitochondrial, peroxisomal  $\beta$ -oxidation and microsomal  $\omega$ -oxidation are important for oxidative lipid disposal. Mitochondrial  $\beta$ -oxidation is the dominant oxidative pathway (11) whereby the rate limiting step is the transfer of activated fatty acids to the carrier carnitine for mitochondrial import of fatty acids via carnitine-acyl-carnitine transporter on the inner mitochondrial membrane. The acylation of carnitine is catalyzed by carnitine palmitoyltransferase 1 (CPT-1) on the outer mitochondrial membrane (8). In the state of energy excess, obesity or type 2 diabetes enhanced DNL increases the level of malonyl-CoA, which is a potent inhibitor of CPT-1. Furthermore, SREBP-1c activates the isoform acetyl-Coenzyme A carboxylase (ACC2) that synthesizes malonyl-CoA directly at the mitochondrial membrane (23, 30). This interconnection of DNL and mitochondrial  $\beta$ -oxidation reduces fatty acid oxidation and contributes to the pathogenesis of NAFLD due to an increased DNL. In addition to this regulatory mechanism a counterbalance exists by the activation of AMP-activated protein kinase (AMPK), leading to activation of the catabolic pathway. A low energy state reflected by increased cellular AMP levels activates AMPK (31), which phosphorylates ACC2 and reduces malonyl-CoA synthesis (32). Furthermore, activated AMPK reduces SREBP-1c expression by yet undefined mechanisms (11). The expression of key enzymes in the mitochondrial and peroxisomal  $\beta$ -oxidation is regulated by the pivotal TF peroxisome proliferator activated receptor  $\alpha$  (PPAR $\alpha$ ) (33). PPAR $\alpha$  is activated by free fatty acids, synthetic fibrates and as very recently shown by the phosphatidylcholine (PC) 1-palmitoyl-2-oleoyl-sn-glycerol-3-phosphocholine as an endogenous PPAR $\alpha$  ligand (33, 34). The activity of the TF also modulates the cellular oxidative free fatty acid disposal.

To prevent hepatic lipotoxicity, cellular free fatty acids are esterified into TG via TG synthesis pathway. Synthesized TG is either stored in the liver leading to hepatic steatosis or exported to peripheral tissues via VLDL export (**Figure 1**). The assembly and secretion of VLDL particles is catalyzed by microsomal triglyceride transfer protein (MTP) and is dependent on the expression of the lipoprotein ApoB 100 and the availability of PC (1, 35). The activity of MTP is important for prevention of hepatic TG deposition (36, 37). In NASH patients, the VLDL trafficking is possibly impaired due to an altered ApoB 100 synthesis (38).

Beyond hepatic steatosis, further progression of NAFLD pathogenesis can be described by the two-hit model first proposed by Day and James in 1998 (39). The first hit relates to hepatic TG deposition which is the prerequisite for a second hit. Proposed secondary hits are cytokines, mitochondrial dysfunction and lipid peroxidation (8) which promote the development of NASH. Mitochondrial dysfunction may associate with an increase in reactive oxygen species (ROS) levels and results from insulin resistance and increased hepatic free fatty acids (8). In addition, enhanced free fatty acid levels increase peroxisomal  $\beta$ -oxidation and microsomal  $\omega$ -oxidation resulting also in increased ROS production. Increased ROS levels can deplete the cellular redox-equivalent glutathione (GSH) leading to enhanced lipid peroxidation of polyunsaturated fatty acids, DNA and protein damage, inflammation by proinflammatory cytokines, fibrosis by stellate cell activation and cell injury (11) that can progress to chronic liver diseases like cirrhosis and carcinomas.

### 1.1.2 Animal models of non-alcoholic fatty liver disease

In general, the previously described etiology of NAFLD and progression from hepatic steatosis to NASH, cirrhosis and cancers is only poorly understood. For a better understanding of the disease initiation and progression a number of genetic and dietary animal models have been developed. Genetic models like leptin signaling deficient (*ob/ob*, *db/db*, *fa/fa*) or melanocortin deficient (*KK-Ay/a*) mice develop hepatic steatosis, obesity and insulin resistance and their etiology is mediated by hyperphagia (40). Genetic models are important to study NAFLD, but dietary induced NAFLD models resemble more the human condition because only a minority of human patients exhibit NAFLD due to genetic defects (40). A frequently used dietary NAFLD model is feeding a methionine and choline deficient diet (MCD). Pathophysiologic features are intrahepatic lipid accumulation from increased fatty acid uptake, decreased VLDL secretion, VLDL assembly and  $\beta$ -oxidation (41), oxidative stress, inflammation, fibrosis and also increased cell injury and death compared to other NAFLD models (42) while the pathology seems to be reversible (43). Most of the deleterious effects can also be observed by a methionine deficient diet, whereas a choline deficiency is mainly responsible for steatosis (44). The disadvantage of this dietary model is that the disease is induced by an nutritional deficiency and only the liver is affected while the human disease is highly associated with the features of the metabolic syndrome. A second nutritional model is the diet induced obesity (DIO) with the majority of energy in the diet derived from fat. This high-fat (HF) diet model is sufficient to induce obesity, insulin resistance, dyslipidemia and hepatic steatosis resembling more closely the pathophysiology of human NAFLD (40, 45). DIO mice do not develop the same severity of NAFLD compared to genetic or MCD models, but here the adipose tissue is also influencing the liver. HF diet induced NAFLD therefore mimics the NAFLD state

as part of the metabolic syndrome with the link between the fat deposits in white adipose tissue depots and NAFLD.

## 1.2 Hepatic one-carbon metabolism

The sulfur amino acids are central to one-carbon metabolism (C1-metabolism) a metabolic pathway with pivotal importance in the liver. C1-metabolism is implicated in the synthesis of various biological substances, regulates enzyme activities and cellular redox capacity and is important in nuclear processes like cellular differentiation, genome integrity, imprinting and gene regulation. Due to these diverse functions the pathway is associated with many pathological conditions like cancer development, cardiovascular disease, neurodegenerative diseases, birth defects and fatty liver diseases (46-49). In general, the C1-metabolism can be divided into the four different sub-pathways of the methionine cycle, folate cycle, sarcosine pathway and transsulfuration pathway (**Figure 2**). In addition, C1-metabolism is connected to polyamine synthesis and the methionine salvage pathway (**Figure 3**). The prime biological function of C1-metabolism is to provide the cell with activated methyl-groups for transmethylation of a large variety of molecules (proteins, RNA, DNA, phospholipids), maintaining methionine homeostasis and regulating the synthesis of cysteine, thymine and polyamines. The C1-metabolism is present in almost all mammalian tissues, but some sub-pathways are exclusively expressed in the liver.

The central sub-pathway is represented by the methionine cycle which maintains the homeostasis of the essential amino acid methionine and synthesizes the activated methyl-group donor S-adenosyl-methionine (SAM). The activation of methionine is an ATP-dependent process catalyzed by methionine adenosyltransferases (MAT). The adult liver primarily contains the intermediate  $K_m$  isoform MATI, and the high  $K_m$  isoenzyme MATIII, originating from the gene *Mat1a* (50). The third MAT isoform is the low  $K_m$  isoform MATII encoded by the gene *Mat2a*. It is mainly expressed in extrahepatic and fetal liver tissue, but also to a lower extent in the adult liver (50, 51). Synthesized SAM is the universal methyl-group donor in the cell and consumed in over 100 SAM-dependent transmethylation reactions (52). Interestingly, evidence exists indicating a rapidly exchanging SAM-pool in the cytosol and a less active mitochondrial pool (51, 53) which is likely maintained by a mitochondrial SAM-carrier (54). Although various methyl-group depending enzymes exist, the glycine methyltransferase (GNMT), guanidinoacetate methyltransferase (GAMT) and phosphatidylethanolamine methyltransferase (PEMT) quantitatively contribute most to the SAM-dependent transmethylation flux (50). The transfer of the methyl-group to its acceptor leads to the formation of S-adenosyl-homocysteine (SAH), a potent inhibitor of SAM-dependent methyltransferases. Subsequent hydrolysis of SAH leads to

homocysteine (Hcy) via the SAH hydrolase (AHCY). The reversible reaction thermodynamically favors the synthesis of SAH (55) and therefore the physiological reaction *in vivo* proceeds only, if Hcy and adenosine are constantly metabolized (51). Hcy is a non-proteinogenic amino acid that has been identified as an independent risk factor for cardiovascular disease and myocardial infarction (56, 57) and an increase of 2.5  $\mu\text{M}$  in the circulation is expected to increase the risk about 10 % (52). Hcy is the branching point of the methionine cycle (**Figure 2**) and can be either remethylated to preserve methionine i) via betaine-homocysteine methyltransferase (BHMT) in the sarcosine pathway or ii) via methionine synthase (MTR) (cobalamine-dependent) in the folate cycle or it can be irreversible degraded by cystathionine  $\beta$ -synthase (CBS) and cystathionase (Cth) (pyridoxal phosphate-dependent) in the transsulfuration pathway. The regeneration of methionine is dependent on the oxidation of choline to betaine in the sarcosine pathway or on the methyl-group transfer from 5-methyl tetrahydrofolate in the folate cycle. A genetic polymorphism (C677T) of the enzyme 5,10-methylenetetrahydrofolate reductase (MTHFR) implicated in the synthesis of 5-methyl tetrahydrofolate reduces its activity and has been associated with hyperhomocysteinemia in humans (58-60). Furthermore, inhibition of BHMT increases plasma total Hcy concentration in mice (61). Hcy that enters the transsulfuration pathway not only influences Hcy homeostasis, but also provides the sulfur containing amino acid L-cysteine, which can be ultimately transformed into the cellular redox equivalent glutathione, the osmolyte taurine or into sulfate (50). Degradation of Hcy by the transsulfuration pathway is essential for Hcy homeostasis because ablation of the pathway induces hyperhomocysteinemia as shown in CBS knock out (*Cbs*<sup>-/-</sup>) mice (62, 63). This indicates that all routes for Hcy collectively maintain Hcy homeostasis by the adjacent pathways folate cycle, sarcosine pathway and transsulfuration pathway by preventing hyperhomocysteinemia. Due to its Hcy degrading function, the transsulfuration pathway controls the abundance of the carrier or backbone (Hcy) for methyl-group carriage in the methionine cycle and indirectly influences the concentration of the essential amino acid L-methionine. The folate cycle and sarcosine pathway provide new labile methyl-groups for L-methionine regeneration from L-serine via 5,10-methylenetetrahydrofolate (folate cycle) or choline over betaine (sarcosine pathway) in C1-metabolism, while alternatively 5,10-methylenetetrahydrofolate or choline can be used for deoxythymidine monophosphate (dTMP) synthesis (50) or phosphatidylcholine and acetylcholine synthesis (64).

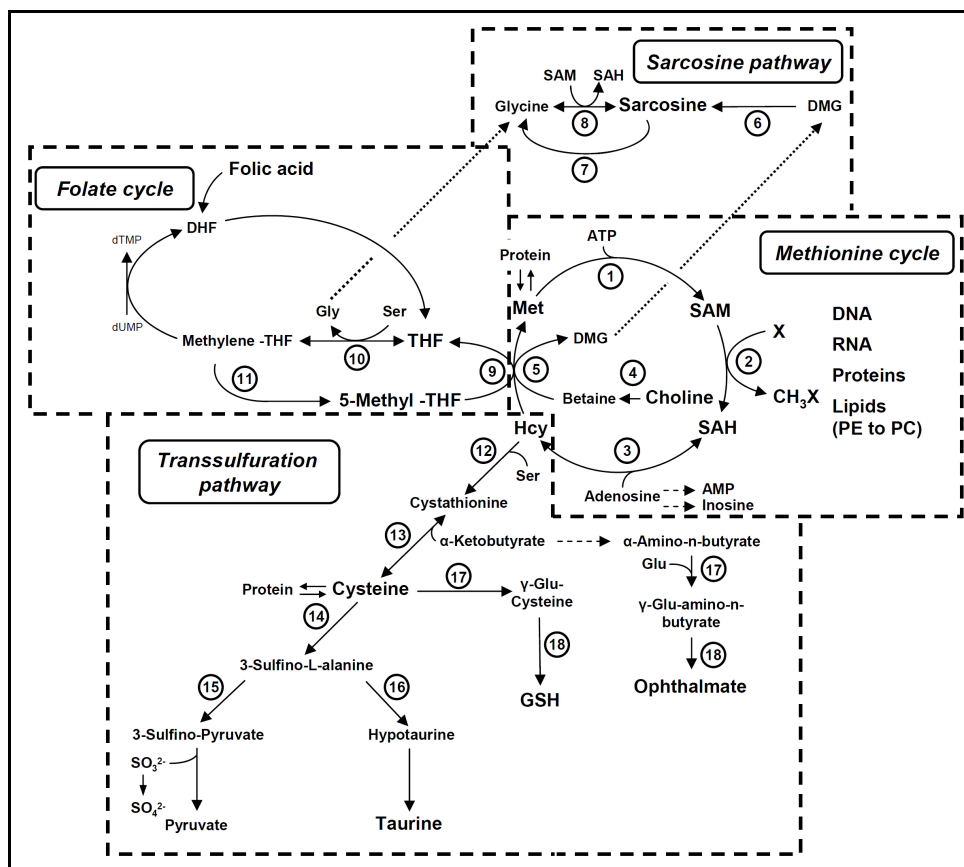


**Figure 2.** Hepatic one-carbon metabolism with the subpathways methionine cycle, folate cycle, sarcosine pathway and transsulfuration pathway is depicted. Reaction enzymes: 1, Methionine adenosyltransferase; 2, SAM dependent methyltransferase; 3, S-adenosylhomocysteine hydrolase; 4, Choline oxidase and betaine aldehyde dehydrogenase; 5, Betaine-homocysteine methyltransferase; 6, Dimethylglycine dehydrogenase; 7, Sarcosine dehydrogenase or Pipecolic acid oxidase; 8, Glycine methyltransferase; 9, Methionine synthase; 10, Serine hydroxymethyltransferase 1 or 2; 11, 5,10-methylenetetrahydrofolate reductase; 12, Cystathionine  $\beta$ -synthase; 13, Cystathionase; 14, Cysteine dioxygenase 1; 15, Glutamate oxaloacetate transaminase 1; 16, Cysteine sulfinic acid decarboxylase; 17, Gutamate-cysteine ligase; 18, Glutathione synthetase. Abbreviations: ATP, Adenosine triphosphate; AMP, Adenosine monophosphate; DHF, Dihydrofolate; DMG, Dimethylglycine; dTMP, Deoxythymidine monophosphate; dUMP, Deoxyuridine monophosphate; Glu; L-glutamate; Gly, Glycine; GSH, Glutathione; Hcy, L-homocysteine; Methylene-THF, Methylene-tetrahydrofolate; 5-Methyl-THF, 5-Methyl-tetrahydrofolate; Met, L-methionine; PC, Phosphatidylcholine; PE, Phosphatidylethanolamine; SAH, S-adenosyl-homocysteine; SAM, S-adenosyl-methionine; Ser, L-serine; THF, Tetrahydrofolate.

In addition to maintaining methionine and Hcy homeostasis and providing the synthesis of activated methyl-groups, L-cysteine, glutathione, taurine and sulphate the hepatic C1-metabolism is also implicated in polyamine biosynthesis (especially spermidine and spermine synthesis) via SAM decarboxylation (**Figure 3**). Biogenic polyamines are characterized by terminal amino groups that are interrupted by varying amounts of additional amino groups. These compounds are implicated in cell growth regulation and interact with and modulate the function of DNA, nucleotide triphosphates, proteins and

especially RNA (65). Decarboxylation of SAM via S-adenosyl-methionine decarboxylase (SAMDC) is a rate limiting step in polyamine biosynthesis and the crucial role of this mechanism is disclosed by the lethality of SAMDC knock out mice (65). Synthesis of spermidine or spermine from decarboxylated SAM (dcSAM) results in methylthioadenosine (MTA) a by-product of polyamine biosynthesis which is used to regenerate L-methionine in the methionine salvage pathway (50, 66). In general, dcSAM provides an amino group in the polyamine synthesis, while the sulphur and the methyl-group are recycled from MTA to L-methionine in the methionine salvage pathway.

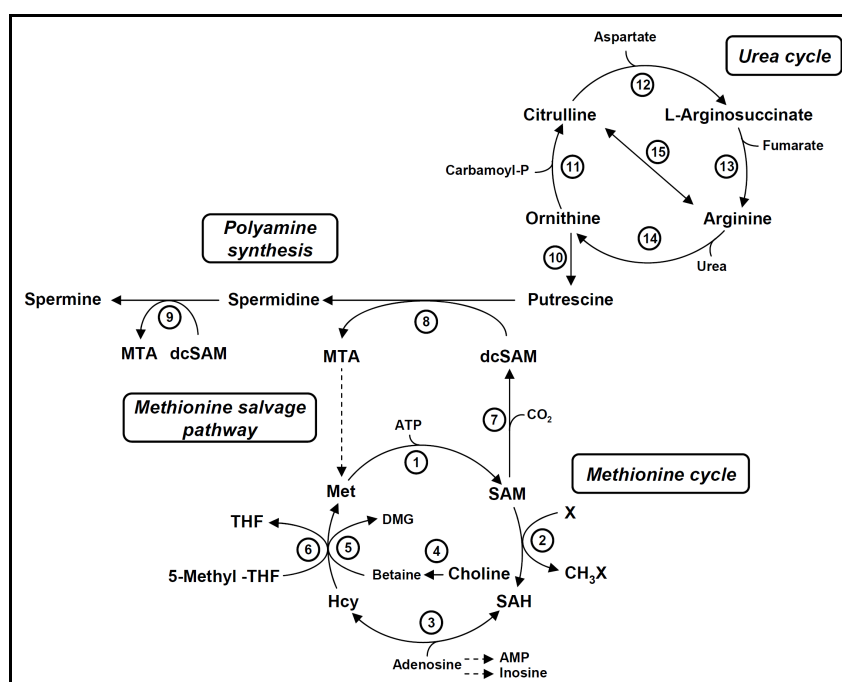


**Figure 3.** Hepatic polyamine synthesis and methionine salvage with the subpathway methionine cycle is depicted. Reaction enzymes: 1, Methionine adenosyltransferase; 2, SAM-dependent methyltransferase; 3, S-adenosylhomocysteine hydrolase; 4, Choline oxidase; 5, Betaine-homocysteine methyltransferase; 6, Methionine synthase; 7, S-adenosylmethionine decarboxylase; 8, Spermidine synthase; 9, Spermine synthase; 10, Ornithine decarboxylase; 11, Ornithine carbamoyltransferase; 12, Argininosuccinate synthase; 13, Argininosuccinate lyase; 14, Arginase; 15, Nitric-oxide synthase. Abbreviations: dcSAM, decarboxylated S-adenosyl-methionine; MTA, methylthioadenosine; THF, tetrahydrofolate

### 1.2.1 Metabolic regulation

Metabolic regulation of the C1-metabolism is based on L-methionine and Hcy homeostasis maintained by the kinetic properties of enzymes with intracellular SAM and SAH as cardinal gauges. SAM differentially regulates its own synthesis by inhibitory or activating influences on the different MAT isoforms. SAM inhibits the activity of MATII (67) while it allosterically increases the activity of MATIII (68, 69),

which in addition is activated by methionine. Furthermore increased SAM levels allosterically inhibit the enzyme MTHFR (70) reducing 5-methyl tetrahydrofolate synthesis which is an inhibitor of GNMT (67, 71). The SAM-dependent GNMT methylates the non-essential substrate glycine to generate the non-toxic product sarcosine via consumption of SAM. In addition SAM allosterically activates GNMT (72), whereas GNMT is less sensitive to SAH inhibition (71). Thus, increased SAM levels induce directly and indirectly SAM catabolism by synthesis of the metabolic non-active compound sarcosine, which constitutes a spillover mechanism for methyl-groups. Recently, Sreekumar *et al.* identified a potential role of sarcosine in prostate cancer progression (73). Regarding the metabolic regulation of the C1-metabolism SAM allosterically activates CBS (74) leading to increased transsulfuration of Hcy, the basic backbone of the methyl-group carrier methionine, mediating its catabolism. SAH limits its own synthesis by inhibiting almost all SAM-dependent methyltransferases and also activates CBS (67, 75). It inhibits Hcy remethylation by MTR and BHMT and inhibits SAM mediated MTHFR inhibition (67). Due to the inhibitory function of SAH on SAM-dependent methyltransferases and the catabolic function of SAM, the ratio of intracellular SAM to SAH concentration ( $[SAM] / [SAH]$ ) is used as an index for cellular transmethylation potential. Therefore a decreased  $[SAM] / [SAH]$  ratio seems to correlate with compromised transmethylation reactions (76).

### 1.2.2 Genetic disease associations

The importance of the C1-metabolism in maintaining liver physiology and lipid metabolism is often associated with homeostasis of the methionine cycle, especially derived from SAM and SAH regulations. Disturbances in the cycle often lead to steatosis, cirrhosis or hepatic cancers as derived from mouse models lacking distinct enzymes of the cycle. For example, MATI and MATIII deficiency (*Mat1a*<sup>-/-</sup> mice) leads to reduced hepatic SAM levels, despite an increased expression of *Mat2a* gene encoding the MATIII isoform. These mice are more prone to develop NAFLD in response to a MCD diet or spontaneously develop steatohepatitis (77). Furthermore, *Gnmt*<sup>-/-</sup> mice show elevated SAM levels with a ~100-fold increased  $[SAM] / [SAH]$  ratio (78) and develop hepatic steatosis and cancers (79). This demonstrates the crucial role of SAM and the homeostatic function of GNMT in hepatic lipid metabolism. Varela-Rey *et al.* showed that nutritional nicotinamide normalizes the hepatic SAM content in *Gnmt*<sup>-/-</sup> mice and prevented hepatosteatosis, likely due to the consumption of SAM by nicotinamide methyltransferase (80). Derived from *Mthfr*<sup>-/-</sup> mice, MTHFR deficiency not only leads to decreased hepatic levels of 5-methyl tetrahydrofolate, SAM and increased levels of SAH, the knock-out mice also develop severe liver steatosis (81-83). In general, the mouse models with enzyme deficiencies reveal as well the close interconnection of C1-metabolism with hepatic lipid metabolism.

### 1.2.3 Nutritional methyl-group deficiency

Like the genetic models dietary methyl-group deficiency can induce similar changes. For example, folate or vitamin B<sub>12</sub> (cobalamine) deficiencies lead to increased plasma Hcy levels in rats, while in folate-deficient rats an inverse correlation between intracellular SAM and plasma Hcy concentration could be observed (84, 85). It seems plausible that the etiology here is based on a diminished SAM synthesis. This is suggested by the administration of the methionine-analog ethionine that re-established the coordination of the C1-metabolism sub-pathways (84). Nutritional deficiency of vitamin B<sub>6</sub> was found not to influence plasma Hcy levels (86), but an oral methionine load, under vitamin B<sub>6</sub> restriction, elevated plasma Hcy levels accompanied by increased SAM concentrations in the liver (87). In addition to vitamin deficiencies, hepatic disorders can also be observed by amino acid deficiencies as reported for the MCD mouse model of NAFLD (see 1.1.2). This model is primarily based on deficiency of the methyl-group containing compounds methionine and choline and induces steatohepatitis. In general, a nutritional deficiency of C1-metabolism substrates leads to hyperhomocysteinemia and NAFLD, but it is also implicated in disturbances of epigenetic processes that require methyl-groups (see 1.4, detailed explanation). SAM is the pivotal methyl-group donor for DNA and histone methylation, which are important in chromatin organization, genome integrity and gene expression regulation. The mechanism is based on the methylation of cytosine (DNA) or on the methylation of lysine or arginine residues of histone tails by nuclear methyltransferases. A methionine and folate deficiency seems to alter the expression of DNA methylation machinery (e.g. DNA methyltransferases and methyl-CpG binding proteins) in rats and is associated with induction of hepatic cancers (88). The latter is a sequential process with accumulation of genetic alterations and aberrant DNA methylation that activates oncogenes and suppresses tumor suppressor genes (12). As an end-stage liver disease following a NAFLD state, nuclear methylation processes are implicated in its pathogenesis. Interestingly, Pogribny *et al.* identified a mechanistic link between nuclear methylation and the development of NAFLD in mice on a MCD diet (89), supporting the participation of aberrant genomic methylation in these processes.

### 1.2.4 Nutritional methyl-group supplementation

One strategy to prevent or attenuate liver diseases which are associated with hepatic steatosis is the dietary supplementation with lipotropic compounds to the C1-metabolism. One of the first reports on the ameliorating effect of the lipotropes choline and betaine on hepatic fat infiltration was published in 1964 by Ball (90). In 2009, Kwon *et al.* provided evidence of alleviating hepatic steatosis in rats on a liquid HF diet supplemented with betaine (91). Improvements of the disease state by methyl-group supplementation could also be observed in the related alcoholic fatty liver disease.



Betaine also reduced the alcohol induced hepatic TG deposition in a dose dependent manner and decreased adjacent hyperhomocysteinemia (92). Furthermore, lipotrope supplementation influences the formation of hepatic inclusion bodies. Mallory-Denk body called protein aggregates can be observed in alcoholic and non-alcoholic steatohepatitis and hepatocellular neoplasms (93). SAM and betaine administration attenuated the formation of Mallory bodies in drug primed mice by influencing nuclear epigenetic processes (94-96). This suggests that dietary methyl-group supplementation not only attenuates hepatic metabolic disturbances but also influence epigenetic mechanisms and gene regulation. This impact on epigenetic mechanisms is further supported by maternal methyl-group supplementation in mice and its consequences on fetal development in genetic hyperphagic obese mice, the Agouti  $A^{vy}/a$  mouse model. Supplementation could reverse the mutant hair color phenotype and prevent obesity development by DNA methylation in the offspring (97, 98). Methyl-group supplementation was based here on increased dietary supply of choline, betaine, folic acid, vitamin B<sub>12</sub>, L-methionine and zinc (97).

These examples show that in addition to methyl-group deficiencies, dietary methyl-group supplementation also affects hepatic lipid metabolism and nuclear epigenetic processes.

### **1.3 C1-metabolism and hepatic phosphatidylcholine biosynthesis and lipid homeostasis**

Phospholipids are amphiphilic compounds which constitute the major component of biomembranes and are therefore essential for membrane integrity of all living cells. Major mammalian phospholipids are phosphatidylcholine (PC), phosphatidylethanolamine (PE), phosphatidylserine and sphingomyelin. Interestingly, no uniform distribution of particular phospholipid classes can be observed. In the plasma membrane a specific enrichment of PC in the outer leaflet and PE in the inner leaflet can be detected (99). The outer leaflet phospholipid PC is of prime importance for processes like hepatic VLDL secretion (35). PC is also secreted into bile via the multi drug-resistance protein 2 (MDR2) in the hepatic canalicular membrane (1) and is used for high density lipoprotein formation in blood plasma (64). Biliary PC participates in the assembly of micelles in the intestinal lumen (100) to enable intestinal fat absorption. Around 95 % of the biliary PC is reabsorbed in the intestine but surprisingly, only 40 % of secreted PC returns to the liver via the enterohepatic circulation (64). The biliary phospholipid secretion was estimated to account to the total hepatic content of phospholipids secreted within 24 h (1). This would reflect a ~60 % loss of hepatic PC within 24 h and would likely result in a hepatic PC deficiency. The pathways that compensate this PC loss and maintain hepatic PC homeostasis are the CDP-choline and

PEMT routes. Disturbances in both pathways result in NASH and lethal liver impairment in rodents, which can be partially rescued by preventing biliary PC secretion in a MDR2 deficiency (101).

### 1.3.1 The CDP-choline pathway

The CDP-choline pathway is a ubiquitous PC biosynthesis route, synthesizing ~70 % of hepatic PC (102) at the ER. This pathway synthesizes PC from CDP-choline and diacylglycerol (DAG) (**Figure 4**). The phosphorylation of dietary choline is the initial step, followed by the conversion to CDP-choline via CTP:phosphocholine cytidyltransferase (CT). CT catalyzes the rate limiting step of the pathway (103) and is tightly regulated by translocation from a soluble inactive form to a membrane-bound active form (104). Induction of translocation is induced by a decreased PC pool or increased fatty acid or DAG levels. The final transfer of the activated CDP-choline to DAG is mediated by CDP-choline:1,2-diacylglycerol choline-phosphotransferase (CPT). The importance of the CDP-choline pathway and choline can be demonstrated by nutritional choline deficiency in rats. The removal results in hepatic steatosis, an increase of PE and a decrease of PC levels (105).

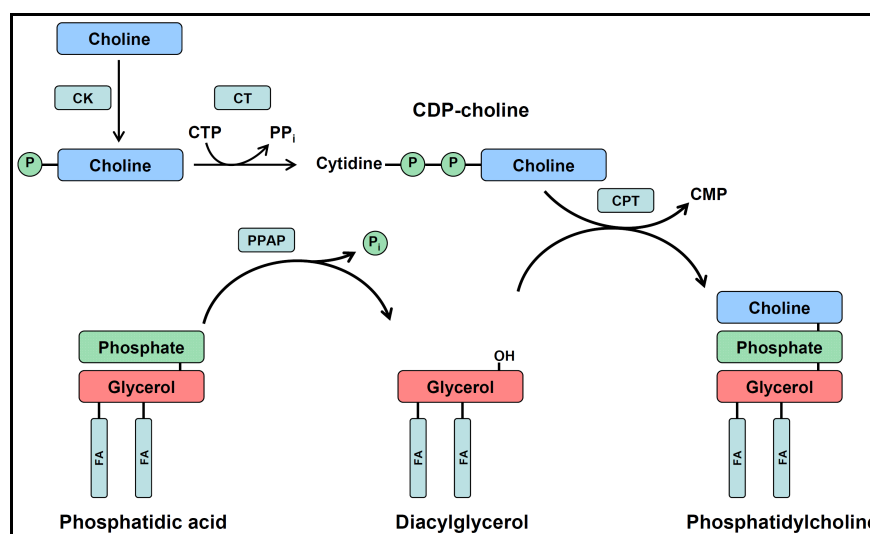


**Figure 4.** The CDP-choline pathway is the principal cellular phosphatidylcholine biosynthesis pathway (modified from (106)). Biosynthesis is dependent on activation of cellular free choline and synthesis of diacylglycerol. The rate limiting step is the CTP:phosphocholine cytidyltransferase mediated CDP-choline synthesis. Abbreviations: CK, choline kinase; CPT, CDP-choline:1,2-diacylglycerol choline-phosphotransferase; CT, CTP:phosphocholine cytidyltransferase; CMP, Cytidine monophosphate; CTP, Cytidine triphosphates; PPAP, Phosphatidic acid phosphatase; PP<sub>i</sub>, Pyrophosphate.

### 1.3.2 The PE methylation pathway

In addition to the CDP-choline pathway, the liver exclusively possesses a second intrinsic pathway to synthesize PC. This pathway is based on the membrane associated methylation of PE catalyzed by the enzyme PEMT. Three sequential methylation steps by PEMT result in the synthesis of PC (**Figure 5**). The donor of the methyl-group is SAM as the activated form of methionine. Although a certain redundancy in the two hepatic PC biosynthesis pathways may appear, DeLong *et al.* revealed a profound distinction between both pathways (107). PC derived from the CDP-choline pathway mainly comprise saturated medium-chain length fatty acids (e.g. C16:0 / C18:0), while the PE methylation pathway synthesizes more long-chain polyunsaturated PC species (e.g. C18:0 / C20:4) with a higher diversity (107). The main synthesis of PEMT derived PC has been attributed to the ER (PEMT1-activity), but a second localization of enzyme activity (PEMT2) has been discovered in an ER associated mitochondria membrane fraction (108, 109), while both isoforms of PEMT are encoded by a single gene (110). The PE methylation pathway synthesizes quantitatively ~30 % of hepatic PC (102), whereas during choline deficiency an increased PEMT activity due to elevation of PE substrate levels can be observed (111, 112). That the PE levels affect PEMT activity leads to the suggestion that PEMT is directly involved in the maintenance of membrane integrity (asymmetrical PC and PE distribution) by maintaining a certain PC / PE ratio. This is supported by studies in PEMT-deficient (*Pemt*<sup>-/-</sup>) mice. This deletion of PEMT does not result in any phenotypical difference in mice when fed a chow diet. Animals have normal liver morphology, bile secretion and composition (113-115). Restricting *de novo* PC biosynthesis by feeding a choline deficient diet in these mice however leads to a rapid development of steatosis, steatohepatitis and liver failure in 3 days (116). This is accompanied by the reduction of hepatic PC and PC / PE ratio (101, 116). The phenotype could be rescued by elimination of biliary secretion in *Pemt*<sup>-/-</sup> / *Mdr2*<sup>-/-</sup> double knock-out mice. Surprisingly, these mice also developed steatosis and possessed reduced hepatic PC levels, but the ratio of PC to PE was partially preserved in these animals (101). This suggests that the PC / PE membrane phospholipid ratio influences membrane integrity and cellular liver damage, whereby the ratio is maintained via the PE methylation pathway. Interestingly, in NASH patients a significantly reduction of the PC / PE ratio was observed (101), and a polymorphism in the PEMT gene, resulting in altered PEMT activities, has also been associated with the susceptibility for NAFLD (117). Further analysis of lipoprotein metabolism in *Pemt*<sup>-/-</sup> mice revealed a reduced secretion of VLDL in cultured hepatocytes derived from *Pemt*<sup>-/-</sup> mice (118) and diminished VLDL plasma levels in animals when fed a HF / high cholesterol diet (119). The *Pemt* deletion also attenuated atherosclerosis in LDL receptor knock-out mice (120). Although chow-fed *Pemt*<sup>-/-</sup> animals did not display altered bile secretion, the role of the PE methylation pathway in biliary PC secretion is supported by the localization

of the PEMT pathway to the apical canalicular membrane of hepatocytes (121). Noga and Vance reported in addition an enhanced biliary secretion of PC derived from PEMT in mice fed a HF / high cholesterol diet (122).

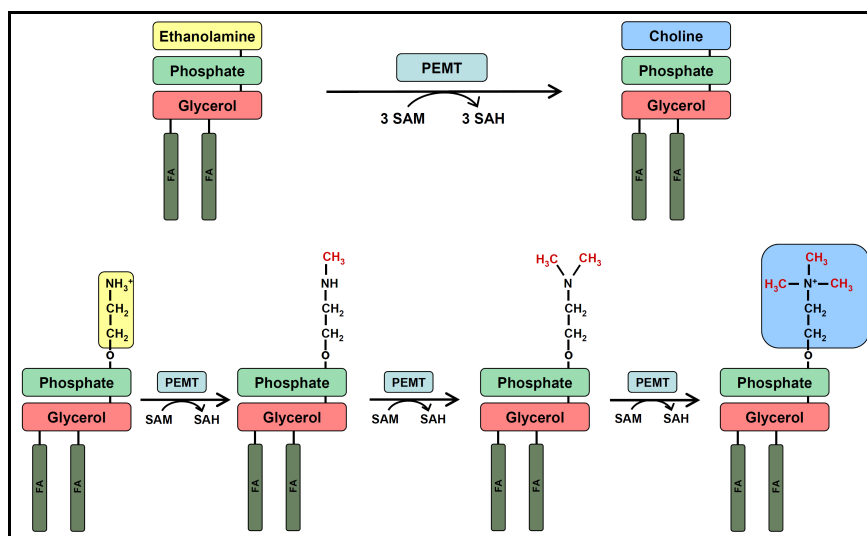


**Figure 5.** Hepatic *de novo* PC biosynthesis via the PE methylation pathway is presented. Three sequential methylation steps of phosphatidylethanolamine lead to the synthesis of phosphatidylcholine. Methyl-group source is S-adenosyl-methionine. Abbreviations: FA, fatty acid; PEMT, Phosphatidylethanolamine methyltransferase; SAH, S-adenosyl-homocysteine; SAM, S-adenosyl-methionine.

The prime importance of PEMT dependent PC synthesis in hepatic methyl-group homeostasis is reflected by PE methylation as one of the largest methyl-group consuming reactions in the liver and its significant contribution to Hcy production (76). This was evidenced in *Pemt*<sup>-/-</sup> mice, which display plasma Hcy levels of around 50 % of those in wild type mice (123) and in CDP-choline pathway deficient (*Cta*<sup>-/-</sup>) mice displaying 20-40 % elevated Hcy plasma levels (124). These data support a causal link between C1-metabolism, PC biosynthesis and NAFLD. Both hepatic PC biosynthesis pathways have important functions in hepatic and whole body lipid and lipoprotein metabolism and disturbances in these pathways result in NAFLD.

## 1.4 Epigenetics

Epigenetics describes the study of mitotical and meiotical heritable changes in gene function (gene expression) without alteration of the underlying DNA sequence and reflects a link between environment, genotype and phenotype. Nuclear epigenetic mechanisms are implicated in gene regulation, cell identity, cell differentiation, X-chromosome inactivation, genome integrity, chromatin organization, transposable element repression and transgenerational genomic imprinting. Epigenetic dysregulation is associated with cancer development (125) and expected to be involved in programming of adult diseases (126, 127). One of the general principles is based on the

regulation of chromatin organization and gene accessibility to the transcriptional machinery. Chromatin can be described as nuclear DNA-protein complex important for nuclear DNA organization. The DNA is wrapped around nucleosomes that can be arranged to higher order structures leading to chromatin condensation and compaction. Nucleosomes are constructed of an octamere of the four different histone proteins H2A, H2B, H3 and H4 (128). The chromatin state in the nucleus participates in the regulation of gene function via DNA accessibility (129). A euchromatic state describes open chromatin accessible for the transcriptional machinery while a heterochromatic state is more condensed and leads to silencing of gene functions. Thus cell type specific hetero- and euchromatic states establish and maintain cellular differentiation resulting in cell type specific transcriptional programs (130). The molecular basis of epigenetics is based on DNA methylation, posttranslational histone modification, chromatin remodeling, histone variants and RNA interference which influence nuclear genome organization and gene accessibility (128, 131-133).

DNA methylation is a prime mechanism in gene silencing and repression collaborating with chromatin associated proteins to establish a silent chromatin state (134). In mammals the molecular basis is the methylation of cytosine residues at position 5 exclusively on CG dinucleotides (CpG). Almost 80 % of globally distributed CpG dinucleotides are methylated (134) while a significant proportion of methylated CpGs is associated with repetitive elements in the genome (132). A non-random distribution of CpG motifs in the genome is reflected by CpG clustering called CpG-islands. CpG islands are defined by a (G+C)-content of at least 50 % and with a ratio of observed to expected CpG frequency of at least 0.6 (135). In humans, 60 % of identified CpG-islands are associated with gene promoters (132). In contrast to the overall CpG-site methylation, CpG-islands remain primarily unmethylated while a subset is methylated in differentiated somatic tissues (132, 134). DNA methyltransferases (Dnmts) are the enzymes that catalyze the transfer of an activated methyl-group from SAM to the specific CpG cytosine residue of the DNA (**Figure 6A**). Dnmt1 is a maintenance methyltransferase which methylates the newly synthesized DNA strand during semiconservative DNA replication. Dnmt3a and 3b are *de novo* methyltransferases introducing *de novo* DNA methylation at specific genomic loci (12). Enzymes for active DNA demethylation remain elusive, although evidence exists for active genome-wide demethylation of the paternal genome in the first stages of embryo development. Aberrant genomic DNA methylation patterns are associated with NAFLD (89) and cancer development and specifically DNA hypermethylation of tumor suppressor genes and global DNA hypomethylation has been characterized (12). Silencing of tumor suppressor genes occurs in pathways like cell cycle regulation, apoptosis, DNA repair or cell adhesion, leading to the induction or progression of carcinogenesis and DNA hypomethylation can affect genome integrity (12).

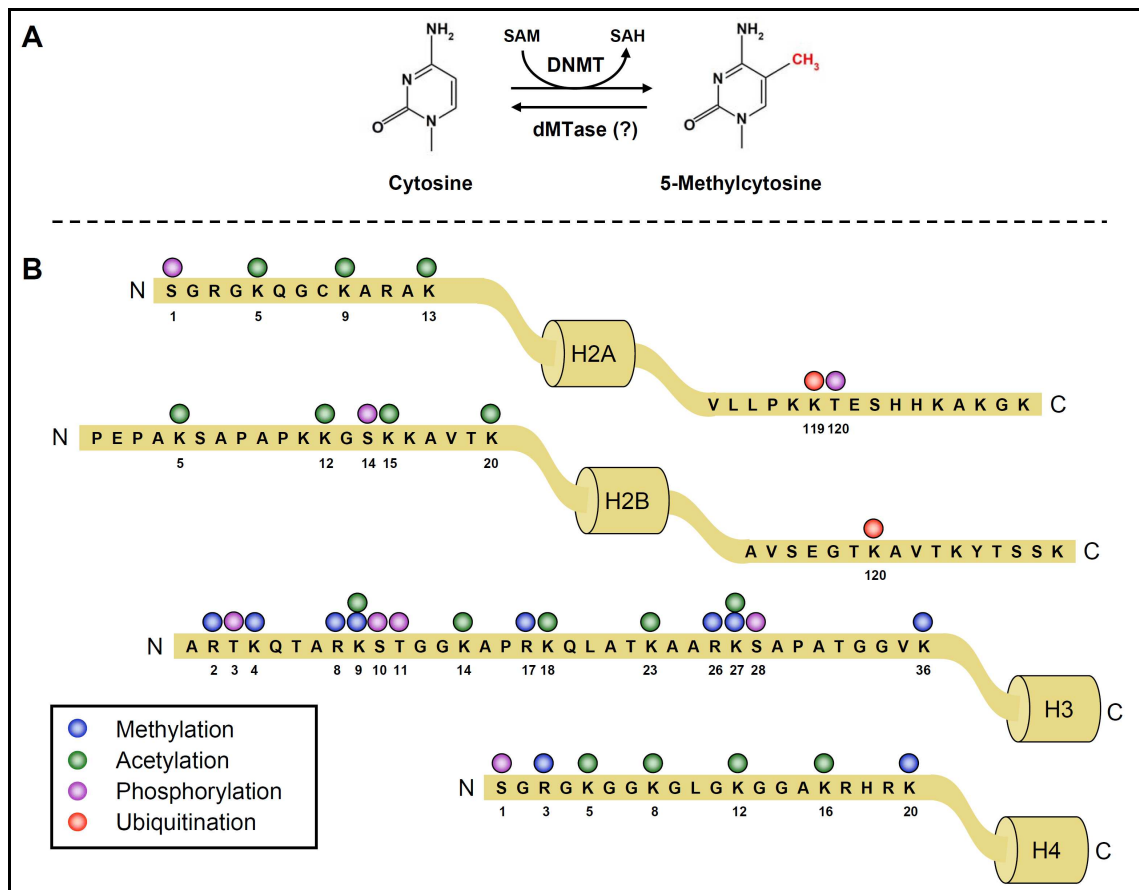


**Figure 6.** The pivotal epigenetic modifications of DNA (DNA methylation) (A) and histones (histone modifications) (B) is depicted (136). The diversity of signals can lead to activation or repression of gene function also depending on chromatin conformation. Abbreviations: Dnmt, DNA methyltransferase; dMTase, DNA demethylase; H2A, Histone 2A, H2B, Histone 2B; H3, Histone 3; H4, Histone 4; SAH, S-adenosyl-homocysteine; SAM, S-adenosyl-methionine.

A second important epigenetic mechanism is based on posttranslational modification of histone tails. Modifications like methylation, acetylation, phosphorylation, ubiquitination and sumoylation can be found primarily on N-terminal histone tails (**Figure 6B**). The meaning of the signal is dependent on the kind of modification, the modified amino acid and position in the histone tail and can activate or repress gene function. Targets of modification are the four amino acids lysine, arginine, serine and threonine, whereby in case of lysine and arginine methylation the modification can range from mono-, di- until trimethyl-lysine and comprise mono- and dimethyl-arginine. The substrate for the transmethylation by histone methyltransferases is again SAM. In case of lysine the amino acid position in the histone tail determines if lysine methylation has an activating or repressive function. On histone 3 methylation of lysine at the position 4 is associated with gene expression (H3K4me3) while at position 9 leads to an repressive signal (H3K9me3) (132). The diversity of histone tail modifications and their corresponding signals mediated by molecular readers led to a

histone code model (137). In addition to aberrant DNA methylation, histone modifications also influence cancer development by affecting chromatin conformation (12).

Epigenetic mechanisms are involved in maintaining genome integrity, cellular differentiation and gene function and labile methyl-groups are important in mediating and maintaining these functions. Alterations in these processes can lead to malignancies in somatic tissues and can program inherited traits leading to adult disease.

## 1.5 Aim of the thesis

Non-alcoholic fatty liver disease (NAFLD) reflects a lipid metabolic dysfunction of the liver that is generally associated with obesity and the metabolic syndrome in humans. Animal models such as diet induced obesity (DIO) in mice using HF diets try to simulate the human condition. HF DIO models however are artificial as the amount of fat provided in the diet to cause NAFLD is beyond that consumed by humans in which the metabolic syndrome and NAFLD is mainly caused by low energy expenditure and high caloric intake and not necessarily by the fat. For high dietary fat absorption and lipid transport as in the HF DIO models provision of hepatic phosphatidylcholine (PC) is essential and dependent on *de novo* biosynthesis. PC biosynthesis involves expenditure of activated methyl-groups provided by the one-carbon (C1) metabolism in the phosphatidylethanolamine methyltransferase (PEMT) pathway, which constitutes the causal link between lipid and C1-metabolism. Different metabolic or genetic disturbances of the C1-metabolism result in NAFLD and it is known that dietary methyl-group supplementation attenuates NAFLD. In animal models with HF diets the influence on hepatic PC homeostasis and C1-metabolism has not been carefully investigated and the underlying molecular mechanisms on how a HF diet induces NAFLD and how a surplus of methyl-groups can prevent or reduce NAFLD development are largely unknown.

Therefore the overall aim of this thesis was to elucidate the metabolic and molecular interactions between lipid and C1-metabolism and to study the impact on nuclear epigenetic processes. Different animal studies have been carried out followed by analysis of the hepatic PC profiles, C1-metabolism gene and protein expression, metabolite levels and DIO mouse model without or with supplementation of methyl-donors. Furthermore, the influence of a HF diet and NAFLD on hepatic nuclear epigenetic processes in mice was studied by assessing DNA methyltransferase (Dnmt) gene expression and analyzing local (gene specific) and global genomic DNA methylation.

## 2 Material and Methods

### 2.1 Animals and sample collection

For the experimental trials eight-week old C57BL/6NCrl mice (Charles River Laboratories) were maintained in 12 h light/dark cycles with unlimited access to food and water. Before dietary intervention animals were fed standard laboratory chow (Ssniff GmbH, cat. no. E1534) for two weeks. The performed feeding trials were conducted according to the German guidelines of animal care and approved by the state ethics committee. The composition of all experimental diets is shown in **Table 1**.

#### 2.1.1 High-fat feeding trial

For analysis of the influence of NAFLD on C1-metabolism, livers from a previously described feeding trial were used (138, 139). Briefly, the ten-week old C57BL/6NCrl mice were divided into control (C) and HF group with mean similar body weight. The experimental C group was fed a carbohydrate / starch rich diet, comprising 4.2 % (w / w) fat (Ssniff GmbH, cat. no. E15000-04) and the HF group animals were fed a HF diet, comprising 34 % (w / w) fat (Ssniff GmbH, cat. no. E15741-34, **Table 1**) for 12 weeks with unlimited access to food and water. During the trial fresh food was provided weekly to mice and body weight development, food and water intake rates were recorded weekly. At the end of the feeding trial, mice in a non-fasting state were anesthetized using isoflurane (Baxter) and blood was drawn from the retro-orbital sinus. Animals were killed by cervical dislocation and liver samples were collected, weighed, snap-frozen in liquid nitrogen and stored by -80 °C.

#### 2.1.2 Effects of methyl-group supplementation during high-fat feeding trial

The scheme with the experimental design for this feeding trial is shown in **Figure 7**. Prior to the methyl-group supplementation C57BL/6NCrl mice were fed HF and C diet as described under 2.1 and 2.1.1 for eight weeks to induce obesity and NAFLD (8W). After eight weeks of C and HF feeding blood was drawn from 5 animals (8W) in non-fasting state from the retro-orbital sinus as described before. Afterwards, these animals were killed by cervical dislocation and tissue samples were collected as described before (see 2.1.1). In addition to the previous described methodology, visceral adipose tissues (epididymal, perirenal and mesenteric adipose tissue depot) were collected, weighed, snap-frozen in liquid nitrogen and stored by -80 °C.



The four weeks methyl-supplementation experiment (12W) started with the remaining C and HF animals. C animals were divided into a control (C) and control methyl-group supplemented (CMS) group and remaining HF animals were divided into HF and HF methyl-group supplemented (HFMS) group with mean similar body weight, respectively. The eighteen-week old mice of the C and HF group were further fed the experimental C and HF diet for four weeks as described before. The CMS and HFMS diets contained for methyl-groups the following additional constituents: 15 g/kg choline chloride, 15 g/kg betaine, 7.5 g/kg methionine, 15 mg/kg folic acid, 1.5 mg/kg vitamin B<sub>12</sub> and 150 mg/kg ZnSO<sub>4</sub> (**Table 1**) and were supplied for four weeks (97). At the end of the trial, mice in non-fasting states were anesthetized using isoflurane and blood was drawn from the retro-orbital sinus as described before. The animals were killed by cervical dislocation and liver and visceral adipose tissue (epididymal, perirenal and mesenteric adipose tissue depots) samples were collected, weighed, snap-frozen in liquid nitrogen and stored by -80 °C.

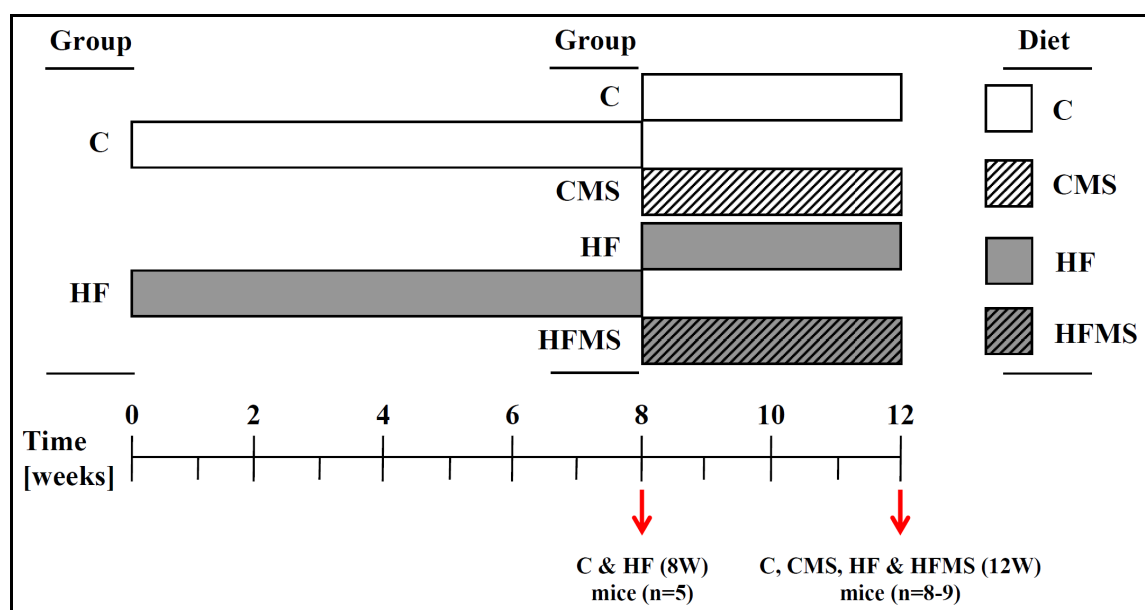


**Figure 7.** Experimental design of the methyl-group supplementation feeding trial is depicted. Open and grey boxes represent C and HF dietary feeding and open lined and grey lined boxes represent CMS and HFMS dietary feeding. C and HF mice sacrificed after eight weeks are defined as 8W and C, CMS, HF and HFMS mice sacrificed after twelve weeks are defined as 12W.

**Table 1.** Composition of experimental diets. Nutrient composition is expressed as [g / kg], except it is delineated differently.

	<b>C</b>	<b>CMS</b>	<b>HF</b>	<b>HFMS</b>
<b>Dry matter</b>	952	952	971	971
<b>Crude protein</b>	208	208	241	241
<b>Crude fat</b>	42	42	340	340
<b>Butter fat</b>	-	-	-	-
<b>Beef tallow</b>	-	-	310	310
<b>Soybean oil</b>	40	40	30	30
<b>Coconut fat</b>	-	-	-	-
<b>Cocoa butter</b>	-	-	-	-
<b>Crude fiber</b>	50	50	60	60
<b>Crude ash</b>	56	56	61	61
<b>Starch</b>	468	468	22	22
<b>Sugar/dextrine</b>	108	108	224	224
<b>N-free extracts</b>	594	594	270	270
<b>GE [MJ/kg]</b>	18	18	25.2	25.2
<b>ME [MJ/kg]</b>	15	15	21.4	21.4
<b>% carbohydrate</b>	66	66	21	21
<b>% protein</b>	23	23	19	19
<b>% fat</b>	11	11	60	60
<i>Amino acids</i>				
<b>Lysine</b>	17.1	17.1	19.8	19.8
<b>Methionine</b>	7.3	14.8	8.3	15.8
<b>Cystine</b>	0.9	0.9	4.6	4.6
<b>Met+Cys</b>	8.2	15.7	12.8	20.3
<b>Threonine</b>	9.3	9.3	10.7	10.7
<b>Tryptophan</b>	2.7	2.7	3.1	3.1
<b>Arginine</b>	7.6	7.6	8.8	8.8
<b>Histidine</b>	6.6	6.6	7.6	7.6
<b>Valine</b>	14.2	14.2	16.4	16.4
<b>Isoleucine</b>	10.9	10.9	12.5	12.5
<b>Leucine</b>	20.5	20.5	23.6	23.6
<b>Phenylalanine</b>	11.1	11.1	12.9	12.9
<b>Phe+Tyr</b>	22.2	22.2	25.7	25.7
<b>Glycine</b>	4.3	4.3	5.0	5.0
<b>Glutamic acid</b>	46.9	46.9	54.1	54.1
<b>Aspartic acid</b>	15.5	15.5	17.9	17.9
<b>Proline</b>	23.9	23.9	27.6	27.6
<b>Alanine</b>	6.8	6.8	7.9	7.9
<b>Serine</b>	12.4	12.4	14.3	14.3
<i>Vitamins</i>				
<b>Vitamin A</b>	15000 IU	15000 IU	15000 IU	15000 IU
<b>Vitamin D3</b>	1500 IU	1500 IU	1500 IU	1500 IU
<b>Vitamin E</b>	150 mg/kg	150 mg/kg	150 mg/kg	150 mg/kg

<b>Vitamin K (as menadione)</b>	20mg/kg	20mg/kg	20mg/kg	20mg/kg
<b>Vitamin C</b>	30 mg/kg	30 mg/kg	30 mg/kg	30 mg/kg
<b>Thiamin (B1)</b>	16 mg/kg	16 mg/kg	16 mg/kg	16 mg/kg
<b>Riboflavin (B2)</b>	16 mg/kg	16 mg/kg	16 mg/kg	16 mg/kg
<b>Pyridoxine (B6)</b>	18 mg/kg	18 mg/kg	18 mg/kg	18 mg/kg
<b>Cobalamin (B12)</b>	30 µg/kg	1530 µg/kg	30 µg/kg	1530 µg/kg
<b>Nicotinic acid</b>	49 mg/kg	49 mg/kg	45 mg/kg	45 mg/kg
<b>Pantothenic acid</b>	56 mg/kg	56 mg/kg	55 mg/kg	55 mg/kg
<b>Folic acid</b>	19 mg/kg	34 mg/kg	19 mg/kg	34 mg/kg
<b>Biotin</b>	310 µg/kg	310 µg/kg	310 µg/kg	310 µg/kg
<b>Choline chloride</b>	1.04 g/kg	16.04 g/kg	2.3 g/kg	17.3 g/kg
<b>Inositol</b>	80 mg/kg	80 mg/kg	80 mg/kg	80 mg/kg
<b>Betaine</b>	-	15 g/kg	-	15 g/kg
<b><i>Trace elements</i></b>				
<b>Iron</b>	166 mg/kg	166 mg/kg	139 mg/kg	139 mg/kg
<b>Manganese</b>	98 mg/kg	98 mg/kg	82 mg/kg	82 mg/kg
<b>Zinc</b>	65 mg/kg	65 mg/kg	56 mg/kg	56 mg/kg
<b>Zinc sulfate</b>	-	150 mg/kg	-	150 mg/kg
<b>Copper</b>	14 mg/kg	14 mg/kg	12 mg/kg	12 mg/kg
<b>Iodine</b>	1.2 mg/kg	1.2 mg/kg	0.97 mg/kg	0.97 mg/kg
<b>Selenium</b>	0.14 mg/kg	0.14 mg/kg	0.13 mg/kg	0.13 mg/kg
<b>Cobalt</b>	0.15 mg/kg	0.15 mg/kg	0.13 mg/kg	0.13 mg/kg
<b><i>Fatty acids [% in diet]</i></b>				
<b>C12:0</b>	-		0.03	
<b>C14:0</b>	0.02		1.03	
<b>C16:0</b>	0.45		8.06	
<b>C17:0</b>	-		0.38	
<b>C18:0</b>	0.19		5.61	
<b>C20:0</b>	0.02		0.04	
<b>C16:1</b>	0.02		0.78	
<b>C18:1</b>	1.07		12.13	
<b>C20:1</b>	-		0.01	
<b>C18:2</b>	2.12		2.37	
<b>C18:3</b>	0.26		0.33	
<b>C20:4</b>	-		0.07	

## 2.2 Cell culture

Fao rat hepatoma cells were grown in Dulbecco's Modified Eagle Medium (DMEM 25 mM glucose, Invitrogen) supplemented with 10 % fetal calf serum (PAA), 100 U / ml penicillin and 100 µg / ml streptomycin (PAA) in a humidified atmosphere at 95 % air and 5 % CO<sub>2</sub> and 37 °C. For experiments, Fao cells (2.1x10<sup>5</sup> cells / well) were seeded on 12 well plates and two days before stimulation, cells were adapted to DMEM (5.56mM glucose, Invitrogen) supplemented with 0.5 % bovine serum albumin

(Sigma-Aldrich). Cells were stimulated at 80 % confluence with WY14,643 (Sigma-Aldrich) from a stock solution in DMSO / PBS (50:50 (vol / vol)) for 24 h respectively. Non-stimulated control cells were treated with DMSO / PBS (50:50 (vol / vol)). At the end of the experiment cells were harvested in Trizol reagent (Invitrogen).

### 2.3 Intraperitoneal glucose tolerance test

After seven and eleven weeks of feeding, glucose tolerance was assessed in C and HF (7 weeks, n = 5) or C, CMS, HF and HFMS (11 weeks, n = 8-9) mice by intraperitoneal glucose tolerance test (ipGTT). Mice were deprived from food for 6 hours and per intraperitoneal injection a 20 % glucose solution (2 g / kg of body weight; B.Braun Melsungen AG) was administered. Blood glucose concentration was measured from the tail vein 0, 15, 30, 60 and 120 min after injection using the Accu-Check blood glucose meter (Roche Diagnostics). Blood glucose levels were first normalized to time point 0 min respectively and analyzed by calculation of the area under the curve (AUC) using Prism4 software (GraphPad Software).

### 2.4 Insulin ELISA

Plasma insulin levels were determined from mice in a non-fasting state by using an Ultra Sensitive Mouse Insulin ELISA Kit (Crystal Chem Inc.) according to the manufacturer's instructions. Intra-assay variation was generally < 10 %. Standard curve calculation was performed by Prism4 software using 4-parameter logistic fit model (sigmoidal dose-response (variable slope)).

### 2.5 Histology

For analysis of hepatic TG accumulation, liver cryosections (5  $\mu$ m) were fixed in 10 % formalin for 1 h, rinsed three times in water, equilibrated in 60 % isopropanol and stained for 1 h in 0.3 % Oilred O (Sigma-Aldrich) staining solution. Sections were again rinsed in 60 % isopropanol, counterstained by hematoxylin (Medit) for 1 min and rinsed in water. Stained sections were mounted in Aquatex<sup>®</sup> (Merck). Light microscopic analysis was performed by using the Leica DMI 4000 B light microscope and the Leica DFC 490 camera (Leica Microsystems).

## 2.6 Metabolite analysis

### 2.6.1 Amino acids and amino acid derivatives

Amino acids and amino acid derivatives were determined in blood plasma or liver samples. 40  $\mu$ l plasma from mice in a non-fasting state was used to determine the concentrations of metabolites following the iTRAQ-labeling method using the AA45 / 32 Starter Kit (Applied Biosystems). Liver tissue was ground in liquid nitrogen and 100 mg of the homogenates were dissolved in 150  $\mu$ l H<sub>2</sub>O / MeOH (50:50; vol / vol), vortexed and centrifuged. 40  $\mu$ l of the supernatant was used to determine the metabolite concentrations following also the iTRAQ-labeling method. Samples were treated according to the manufacturer's instructions and analyzed by mass spectrometry (MS) via LC-MS / MS (3200QTRAP LC / MS / MS, Applied Biosystems). Spectra were processed using the Analyst® 1.5 Software. For data normalization of liver metabolites, protein concentrations of liver homogenates were determined using the Bradford assay (Biorad) with BSA as standard.

The HPLC-MS / MS detection of hepatic SAM and SAH levels was performed using a Waters 2795 alliance HT, coupled to a Quattro Micro API tandem mass spectrometer (Waters Corporation) according to the previously described methodology, with minor modifications (140). Addition of double or triple amount ( $\mu$ l / mg tissue) of 1 M acetic acid buffer (pH 7.4) to each tissue sample was followed by homogenization in a Micro-Dismembrator U (Sartoris AG) by 2000 rpm for 5 min and centrifuged at 12000 g for 10 min. 25  $\mu$ l of the supernatant was added to 375  $\mu$ l of 20 mM ammonium acetate buffer (pH 7.4), stocked with 40  $\mu$ l of internal standard and analyzed by HPLC-MS / MS.

Plasma total Hcy (tHcy) levels were determined using the Homocysteine HPLC Kit (Immundiagnostik AG) and the Agilent 1100 Series HPLC System (Agilent Technologies) with fluorescence detector according to the manufacturer's instructions. Firstly, to 50  $\mu$ l plasma, control and calibrator samples, the internal standard, reduction and derivatization solution was added followed by reduction and derivatization for 10 min at 60 °C for determination of tHcy (tHcy, reduced Hcy). Higher molecular substances were removed by precipitation (at 2-8 °C for 5 min) and centrifugation (at 10000 g for 5 min) and 20  $\mu$ l of the supernatant was injected into the HPLC system. Separation followed an isocratic method at 30 °C with a reverse phased column. Chromatogram was recorded by fluorescence detection (Excitation 385 nm / Emission 515 nm) and integration of peak areas of internal standard and plasma samples was used for concentration determination.

Liver Hcy and cystathionine concentrations were analyzed by HPLC-MS / MS using a Hewlett Packard GCMS (5973 Mass selective detector / 6890 series GC system)

according to the previously described methodology with minor modifications (141). Preparation of tissue samples was performed by addition of the five-fold amount ( $\mu\text{l} / \text{mg}$  tissue) of 0.1 M perchloric acid buffer (pH 7.4) followed by homogenization in a Micro-Dismembrator U and centrifugation at 12000 g for 10 min. The supernatant was neutralized with 23  $\mu\text{l}$  1 M  $\text{K}_3\text{PO}_4$  and stored for final preparation described by Stabler *et al.* (141). Prior to analysis, the anion exchange resin was washed by an equivalent amount of 1 N HCL and methanol followed by 3 h drying at 60 °C. 100 mg of the prepared resin was again washed with 1 ml methanol and 3.3 ml  $\text{H}_2\text{O}$  in a chromatography-column. To 250  $\mu\text{l}$  of previously prepared supernatant 1 ml  $\text{H}_2\text{O}$ , 20  $\mu\text{l}$  of 8.27  $\mu\text{M}$  cystathionine-D4 and 15  $\mu\text{l}$  of 392  $\mu\text{M}$  homocystine-D4 internal standards were added and incubated at 42 °C for 30 min to allow homocystine reduction. The sample mixture was transferred to the chromatography-column and washed three times with 3 ml  $\text{H}_2\text{O}$  and once by 3 ml methanol. The sample was eluted by 0.4 N acetic acid in methanol and dried at 45 °C for 3 h. Further derivation of the sample was performed by 20  $\mu\text{l}$  acetonitril and 10  $\mu\text{l}$  MTBDSFA and analyzed by GC-MS / MS measurement.

### **2.6.2 Acyl-carnitines, phosphatidylcholines, lysophosphatidylcholines sphingolipids and biogenic amines**

Acyl-carnitine, phosphatidylcholine, lysophosphatidylcholine, sphingolipid and biogenic amine subclass quantifications were performed according to the Biocrates methodology for plasma using the Absolute IDQ<sup>TM</sup> Kit p180 (Biocrates Life Sciences AG) with modifications for tissue analysis (142). Prior analysis, analytes were extracted from 60 mg frozen ground liver tissue by incubation in MeOH for 10 min at 4°C using a 1 / 15 extraction ratio. Samples were centrifuged (4 °C, 14000 g, 10 min) and dried by evaporation of methanol in a vacuum centrifuge (SpeedVac SPDIIIIV, Thermo Savant) by applying 1 mbar pressure. According to weight of tissue samples the pellets were dissolved in 5 % phenylisothiocyanat (PITC) derivatization reagent (v / v) to extract analytes (120  $\mu\text{l}$  for 60 mg tissue). The PITC derivatization reagent for biogenic amines contained 150  $\mu\text{l}$  PITC (5 %) diluted in mixture of LC-MS water / EtOH / Pyridine, 950  $\mu\text{l}$  each. 20  $\mu\text{l}$  PITC reagent was used to transfer a sample aliquot of 10 mg tissue extract to a Biocrates 96-well microfilter plate on which the internal standard for biogenic amines has been added before. Lipid and acyl-carnitine standards were previously loaded by the manufacturers on the microfilter plate. Sample derivatization was performed by shaking and stopped by drying the plate. By applying 300  $\mu\text{l}$  methanol and 30 min shaking derivatives were eluted from the microfilters into a 96-deep well plate. For lipid analysis, samples were diluted 1:30 for flow injection analysis (FIA) using FIA coupled MS (AB SCIEX, QTRAP5500). Analysis of biogenic amines was performed by diluting samples 1:10 and quantified by LC-MS / MS measurement. Peak control for LC-MS / MS analysis was done by using the Analyst software v1.5.1

(AB SCIEX) and data were analyzed with MetIQ software v1.2.2 (Biocrates Life Sciences AG). Slightly differing sample weights were mathematically corrected after Biocrates MetIQ quantification. The MetIQ software expects an exact sample amount of 10 µl / mg tissue. Data normalization of liver lipid and biogenic amines was performed using wet tissue weight.

### **2.6.3 Triacylglycerol, non-esterified fatty acids, total phospholipids and choline**

For analysis of TG, NEFA and total phospholipid (PL), liver tissues were ground in liquid nitrogen and 35-70 mg tissue were dissolved in 300 µl 0.9 % NaCl. Samples were incubated by shaking at room temperature for 10 min and centrifuged at 10000 g for 10 min. Hepatic NEFA and total PL were determined from the supernatant using the commercial enzymatic colorimetric kits NEFA-HR(2) (NEFA, Wako Chemicals GmbH) and Phospholipid C (PL, Wako Chemicals GmbH) according to the manufacturer's instructions. For determination of plasma NEFA 10 µl of lithium heparin blood plasma samples from non-fasted animals were analyzed using also the commercial enzymatic colorimetric kit NEFA-HR(2) according to the manufacturer's instructions.

For analysis of hepatic TG level alkaline hydrolytic glycerin extraction was applied. The supernatants were incubated at 70 °C for 30 min in alcoholic KOH and 1 ml 0.15 M magnesium sulfate was added. Samples were centrifuged at 13000 g for 10 min and the isolated glycerin in the supernatant was determined by the commercial enzymatic colorimetric kit Triglycerides liquicolor<sup>mono</sup> (Human GmbH) according to the manufacturer's instruction. For data normalization of liver TG, NEFA and total PL levels, protein determination from the NaCl supernatant was performed using the Bradford assay (Biorad) with BSA as standard.

The hepatic free choline concentration was determined using a commercial enzymatic fluorimetric kit, following the manufacturer's instructions (Choline / Acetylcholine Quantification Kit, Biocat GmbH). Choline was extracted from 20 mg of ground liver tissue using the provided choline assay buffer. Protein concentrations for data normalization were performed by BCA protein determination (Thermo Scientific) using BSA as standard.

## **2.7 RNA isolation**

Isolation of total RNA was performed using Trizol reagent and the RNeasy Mini Kit (Qiagen GmbH). 50 mg liver tissue was homogenized in 1 ml Trizol reagent using the ART-MICCRA D-8 (ART moderne Labortechnik) homogenizer. Fa0 rat hepatoma cells were lysed in 0.5 ml Trizol reagent by a syringe (26 Gauge). 1 vol of chloroform was added to the homogenate, vortexed and after 5 min at room temperature the homogenate

was centrifuged at 16200 g for 15 min. RNA was precipitated from the aqueous phase by addition of 96 % ethanol and transferred to a RNeasy Mini Kit spin column. Total RNA was further isolated according to the RNeasy Mini Kit instructions (Qiagen GmbH). During the isolation residual DNA was digested using RNase-Free DNase Set (Qiagen GmbH). Concentration of eluted RNA was measured on a NanoDrop ND-1000 UV-Vis spectrophotometer and for liver samples RNA integrity was assessed with the 2100 Bioanalyzer (Agilent Technologies) using the RNA 6000 Nano Chip Kit (Agilent Technologies) according to the manufacturer's instructions. Integrity of isolated Fao RNA was determined by agarose gel electrophoresis.

## 2.8 Agarose gel electrophoresis

Separation of DNA or RNA was performed by agarose gel electrophoresis in a horizontal separation chamber (UniEquip GmbH). Depending on expected nucleotide size DNA or RNA was separated in 0.8-2.0 % agarose gel applying 120 mV using a tris-boric acid ethylenediaminetetraacetic acid (EDTA) TBE separation buffer (89 mM Tris base, 89 mM boric acid and 2 mM EDTA). Samples were loaded on the gel using orange G loading dye (4 % sucrose and 0.02 % orange G). Separated nucleotides were visualized by ethidium bromide staining ( $3 \times 10^{-3}$  %, Carl Roth) and UV excitation using the Gel iX imager system (INTAS, Science Imaging Instruments GmbH). For size reference the GeneRuler™ 50 bp DNA Ladder (Fermentas) or the 1 kb DNA Ladder (Invitrogen, **Figure 8**) was used.



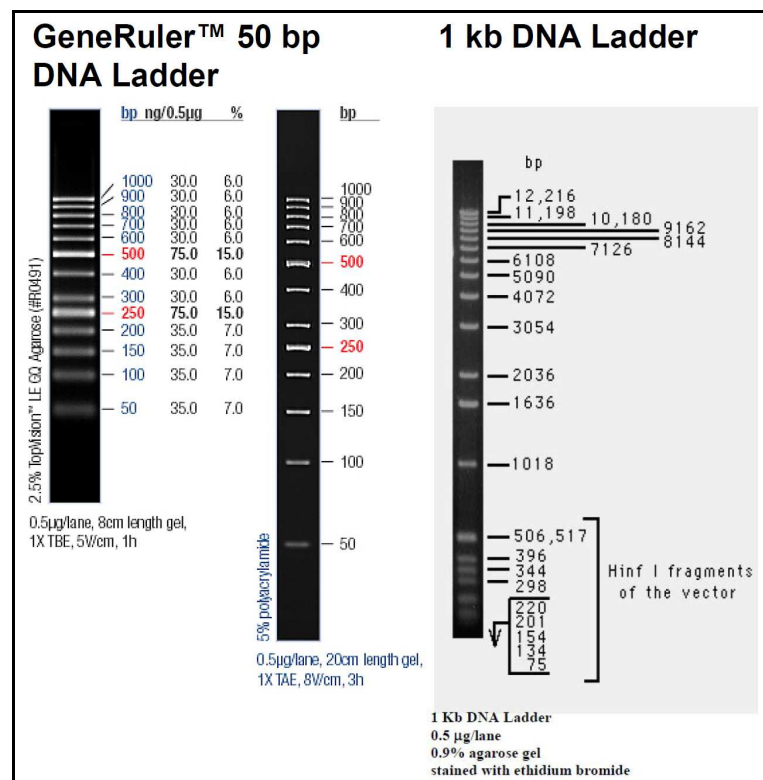


**Figure 8.** Image of DNA ladders applied upon agarose gel electrophoresis. Nucleotide sizes are depicted at the site.

## 2.9 Quantitative real-time PCR

Gene expression was determined by using relative quantitative real-time PCR (qRT-PCR) and the DNA intercalating fluorescence dye SYBR Green I. Principal mechanism is the real-time measurement of DNA template amplification by transcript-specific primers and SYBR Green I intercalation mediated fluorescence (143). For relative gene expression measurement, the threshold cycle ( $C_q$ ) in the exponential phase of the amplification curve was determined. For each liver RNA sample, 10 ng of isolated total RNA was used for qRT-PCR using the QuantiTect® SYBR Green RT-PCR kit (Qiagen GmbH, Hilden, Germany) and a Mastercycler ep realplex apparatus (Eppendorf, Hamburg, Germany) following the manufacturer's instructions. Gene sequences were obtained from the database Ensembl (<http://www.ensembl.org/>). Oligonucleotide primers were designed to flank introns on genomic DNA to prevent amplification of DNA and were analyzed using BLAST analysis (<http://blast.ncbi.nlm.nih.gov/Blast.cgi>). Furthermore, primers were tested for specificity with qRT-PCR followed by melting curve analysis and visualization on a 2% agarose gel, to obtain optimal annealing conditions. The following thermal cycling conditions were used: at 50 °C for 30 min (cDNA synthesis), at 95 °C for 15 min (reverse transcriptase enzyme inactivation), 40 cycles at 95 °C for 15 s, 61 °C for 30 s

and 72 °C for 30 s respectively, followed by melting curve analysis (1.75 °C/min).  $C_q$ -values were retrieved from the realplex 2.0 software (Eppendorf) and relative quantification was performed by  $2^{-\Delta\Delta C_q}$  method using the geometric mean of the housekeeping genes glyceraldehyde-3-phosphate dehydrogenase (Gapdh),  $\beta$ -Actin (Actb) and hypoxanthine guanine phosphoribosyl transferase (Hprt) or the geometric mean of Gapdh and Hprt (12W) to normalize the data (144, 145). For analysis of gene expression in Fao rat hepatoma cells minor modifications were applied. 50 ng of Fao total RNA was used for qRT-PCR and gene expression normalization was performed with the invariant gene  $\beta$ -glucuronidase (Gus). Oligonucleotide primer sequences are listed in **Table 2** and **Table 3**.

**Table 2.** DNA-sequences of mouse primers used for determination of gene expression.

Symbol	Gene name	Forward primer (5'-3')	Reverse primer (5'-3')
<b>Acox1</b>	Acyl-coenzyme A oxidase 1	CCAATCATGCGATAGT CCTGGC	CTTCAGGTAGCCATTAT CCATCTC
<b>Actb</b>	Actin, beta	CCACTGCCGCATCCTC TTCC	GCCACAGGATTCCATAC CCAAGA
<b>Ahcy</b>	S-adenosylhomocysteine hydrolase	CAGCTTCTGTCAGGCA TCCG	AACTTGCTCTTGGTGAC AGAATCG
<b>Bhmt</b>	Betaine-homocysteine methyltransferase	GGAGGCTGCGCGGTTG AAA	CTAGTGGCAACTCGGG GTTCC
<b>Bhmt2</b>	Betaine-homocysteine methyltransferase 2	CAT CCA AGT GCA GTT CGT CAA CT	TGC ATT CAC AGC TTC CCA CTT G
<b>Cbs</b>	Cystathionine $\beta$ -synthase	CACAGTGCTGACCAAA TCCCCC	CACACTTGGCCAAGAG CTCAC
<b>Chdh</b>	Choline dehydrogenase	CACGTCAGGCTGGCTA CCC	GCAAGTAGGCGCAGGC TG
<b>Cpt1a</b>	Carnitine palmitoyltransferase 1a	GTCCCAGCTGTCAAAG ATACCG	ATGGCGTAGTAGTTGCT GTAAACC
<b>Csad</b>	Cysteine sulfinic acid decarboxylase	GAGGACCTGGAGAGG CAGATC	CAAACATCGGCAATTGC ATCCAG
<b>Cth</b>	Cystathionase	GCTAGAGGCAGCGATT ACACC	GCAGACATGAAGGTGT TATCTACAACC
<b>Dmgdh</b>	Dimethylglycine dehydrogenase precursor	GGCACGCAGCAGGTTT AACAAC	GGAATCCCACCACCTGT CCGG
<b>Dnmt1</b>	DNA methyltransferase 1	GGAAGGCTACCTGGCT AAAGTCAAG	GGGTGTCACTGTCCGAC TTGC

<b>Dnmt3a</b>	DNA methyltransferase 3A	TGGAGAATGGCTGCTG TGTGAC	CACTCATCCCGTTTCCG TTTG
<b>Dnmt3b</b>	DNA methyltransferase 3B	AGTGACCAGTCCTCAG ACACGAAG	ATCAGAGCCATTCCCAT CATCTAC
<b>Fasn</b>	Fatty acid synthase	ATGAAGCTGGGCATGC TCA	CCGGCATTGAGAATCGT GGC
<b>Gapdh</b>	Glyceraldehyde-3-phosphate dehydrogenase	CCTGGAGAAACCTGCC AAGTATG	GAGTGGGAGTTGCTGTT GAAGTC
<b>Gclc</b>	Glutamate-cysteine ligase, catalytic subunit	AGCATCAGGCTCTCTG CACC	TTCTCCTCTCCGATGCC GG
<b>Gnmt</b>	Glycine N-methyltransferase	GCCAGACTGCAAAGGT GACCA	GTCGTAATGTCCTTGGT CAGGTCA
<b>Got1</b>	Glutamate oxaloacetate transaminase 1, soluble	GAGCTGTGCTTCTCGC CTAG	TCCCAGGTTGGTGATGA TACGTAG
<b>Gss</b>	Glutathione synthetase	CCTATGCTGTGCAGAT GGACTTC	CAAAGAGACGGGCAGT ATAGTCG
<b>Hprt</b>	Hypoxanthine guanine phosphoribosyl transferase	GTCGTGATTAGCGATG ATGAACC	GTCTTTCAGTCCTGTCC ATAATCAG
<b>Mat1a</b>	Methionine adenosyltransferase I, alpha	GTGGCCTGTGAGACAG TGTGC	TGCTCTCACCAACCCGC TGG
<b>Mat2a</b>	Methionine adenosyltransferase II, alpha	AAGTGGCTTGTGAAAC TGTTGCT	CTTGGGCAATATCTGGT GACTGTTG
<b>Mthfr</b>	5,10- methylenetetrahydrofolate reductase	GACATCTGTGTGGCAG GTTACCC	CTGAAGAAGGTGCTGG CCTC
<b>Mtr</b>	5-methyltetrahydrofolate- homocysteine methyltransferase	GCTGGTGGACTACATT GACTGGA	TTCTGGCTTCTTCACCT ACTGC
<b>Pemt</b>	Phosphatidylethanolamine N- methyltransferase	CTGGAATGTGGTAGCG AGATGG	CAGTGGGAGCGGAGGA TGTTTC
<b>Ppara</b>	Peroxisome proliferator activated receptor $\alpha$	CCAGTACTTAGGAAGC TGTTCCG	TATTCGACACTCGATGT TCAGGG
<b>Shmt1</b>	Serine hydroxymethyltransferase 1 (soluble)	CTGCGGAAGATTGCGG ATGAT	GTCTTGGGATCCACACT GCGC
<b>Shmt2</b>	Serine hydroxymethyltransferase 2 (mitochondrial)	CCTATGCCCGCCTCAT TGACT	TTCCGGTAGAAGATGA GCCCTG
<b>Srebp1c</b>	Sterol regulatory element binding transcription factor 1c	ATGGATTGCACATTTG AAGACATG	AGAGGAGGCCAGAGAA GCAG

<b>Ucp2</b>	Uncoupling protein 2	GCAGATCCAAGGGGA GAGTCAA	CCGGCGACCAGCCCATT G
-------------	----------------------	----------------------------	------------------------

**Table 3.** DNA-sequences of rat primers used for gene expression analysis in rat hepatoma cells (Fao).

<b>Symbol</b>	<b>Primer name</b>	<b>Forward primer (5'-3')</b>	<b>Reverse primer (5'-3')</b>
<b>Bhmt</b>	Betaine-homocysteine methyltransferase	AGGCTGCGGTGGAGCAC C	AGATATCTTCTCTGCCA CGTAGTTC
<b>Cbs</b>	Cystathionine $\beta$ -synthase	CGTAGGAGTGGCATGGC GAC	TTCCCGTCGCACTGCTG C
<b>Cpt1a</b>	Carnitine palmitoyltransferase 1a	GAGCCGCAGCACCAAGA TC	TCTTCCTTCATCAGTGG CCTCAC
<b>Gus</b>	$\beta$ -glucuronidase	GCATGAGCATCCAGCCT ACC	GAACTTGCTCTTTGTGA CAGCC

## 2.10 Protein extraction and Western blot analysis

Quantification of protein expression was performed by Western blot analysis (146). For hepatic protein extraction, 50 to 100 mg tissue were homogenized in radio-immuno precipitation buffer (RIPA: 150 mM NaCl, 50 mM Tris, 1 mM EDTA, 1% Nonidet-P40, 0.2% SDS, 0.25% sodium deoxycholate) including 1% protease inhibitor cocktail and 1% phosphatase inhibitor cocktail II (Sigma) using the Ultrathurax followed by centrifugation at 2000 g for 2 min. The supernatant was analyzed by BCA protein determination (Thermo Scientific) using BSA as standard. Western immunoblot analysis was performed by denaturing liver protein extract at 95 °C for 5 min in Laemmli sample buffer (310 mM Tris, pH 6.8, 5% SDS, 12.5% glycerol, 2.5 mM EDTA, 50 mM dithiothreitol and 0.01% bromophenol blue). 30-60  $\mu$ g of samples were loaded on a 10 or 15% SDS-polyacrylamide gel and separated in a separation buffer (250 mM Tris, 2 M glycine, 1% SDS, pH 8.3) at 120 V for 3 h. Protein-transfer to a nitrocellulose membrane (Whatman GmbH) was performed using the semidry Transblot B44 (Biometra) and the transfer buffer system containing anode buffer I (300 mM Tris, 20% methanol), anode buffer II (25 mM Tris, 20% methanol) and cathode buffer (25 mM Tris, 25 mM  $\epsilon$ -amino-n-caproic acid, 20% methanol), to which 235 mA were applied for 30 min. Membranes were blocked in 2% ECL advance blocking reagent (GE Healthcare) dissolved in TBS (20 mM Tris, 140 mM NaCl, pH 7.6) for 1 h

followed by incubation with the corresponding primary antibody at 1:1000 to 1:20000 dilutions in TBS-T (20 mM Tris, 140 mM NaCl, 0.1 % Tween 20, pH 7.6) at 4 °C overnight. The following antibodies were used: goat anti-bhmt (Novus Biologicals), rabbit anti-srebp1 (detects activated form of srebp1; Novus Biologicals), rabbit anti-cbs (Aviva Systems Biology), rabbit anti-ampk $\alpha$ , rabbit anti-phospho-ampk $\alpha$  (Thr172), rabbit anti- $\beta$ -actin and rabbit anti-histone H3 (all Cell Signaling). After several washing steps with TBS-T, membranes were exposed to corresponding secondary donkey anti-goat or goat anti-rabbit antibody conjugated with IRDye 800 (Li-cor) at 1:10000 to 1:50000 dilutions in TBS-T at room temperature for 1 h. Signal detection was performed with the Odyssey infrared imaging system (Li-cor). Quantification of fluorescence intensity was determined by using the Odyssey Application Software 3.0 (Li-cor) and average background method (top / bottom) for calculation of integrated intensity. Histone H3 and  $\beta$ -Actin were used for normalization of protein abundance.

### 2.11 DNA isolation

Genomic DNA was extracted from liver using the DNeasy Blood & Tissue Kit (Qiagen) according to the manufacturer's instruction with minor modifications. Briefly, 20-30 mg tissue was digested by proteinase K overnight and incubated with 800  $\mu$ g RNaseA for 2 min. 200  $\mu$ l AL buffer and 1 vol choloform was added to the lysate, vortexed and centrifuged at 15000 g for 15 min. DNA was isolated from the aqueous phase by precipitation with  $\frac{1}{2}$  vol 96 % ethanol and using the DNeasy Blood & Tissue Kit spin column according to the manufacturer's protocol. Concentration of isolated DNA was determined on a NanoDrop ND-1000 UV-Vis spectrophotometer (NanoDrop Technologies) and integrity was determined by agarose gel electrophoresis.

### 2.12 Luminometric methylation assay

Global DNA methylation was quantified using a luminometric methylation assay according to the previously described methodology with minor modifications (147, 148). Basic mechanism is the digestion of genomic DNA with the restriction isoschizomers *HpaII* and *MspI*. Both endonucleases recognize the DNA sequence CCGG, whereby *HpaII* enzymatic activity is blocked by cytosine methylation in the CpG motif (methylation-sensitivity) of the recognition site (**Figure 9**). *MspI* activity is independent of CpG methylation. Digested recognition sites can be elongated by pyrosequencing (2.14.2) which converts nucleotide incorporation into a light signal that is proportional to the restriction gaps.

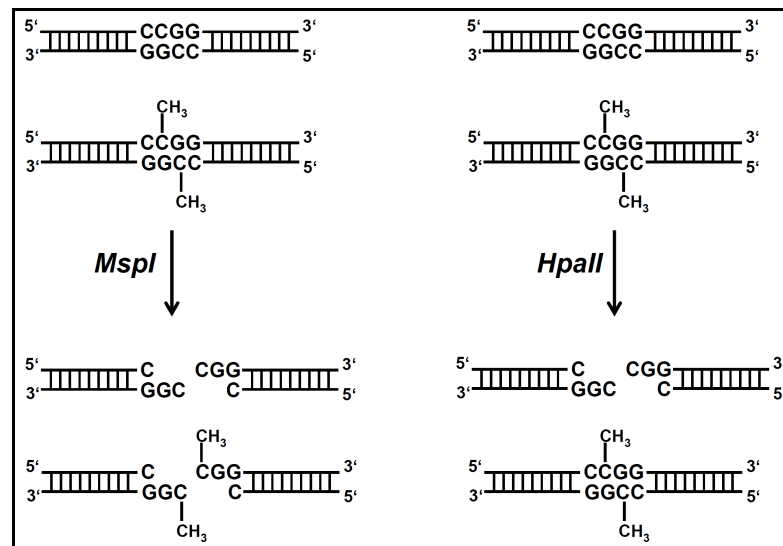


**Figure 9.** Global DNA methylation can be analyzed by restriction digestion of genomic DNA with the isoschizomers *MspI* and *HpaII*. The enzymatic activity of the methylation-sensitive restriction enzyme *HpaII* is blocked by CpG methylation.

1  $\mu$ g genomic DNA was cleaved with the FastDigest<sup>®</sup> restriction enzymes *HpaII* + *EcoRI* or *MspI* + *EcoRI* (Fermentas) in two separate reactions. The digestions of genomic DNA by the methylation sensitive *HpaII* (CCGG) and methylation insensitive *MspI* (CCGG) isoschizomers in combination with *EcoRI* (GAATTC) were performed in a 96-well format at 37 °C for 15 min. Digested restriction sites were elongated by pyrosequencing using a PSQ96<sup>™</sup> MA system (Biotage AB). Peak luminometric heights were calculated with the PSQ96<sup>™</sup> MA Software (Biotage AB). The *HpaII* / *EcoRI* and *MspI* / *EcoRI* ratios were calculated as (dGTP + dCTP) / dTTP for the respective reactions. DNA methylation was calculated from the *HpaII* / *MspI* ratio, whereby a ratio of 1 indicates 0 % methylation and a ratio approaching 0 corresponds to 100 % DNA methylation at the investigated sites.

### 2.13 Methylation-sensitive quantitative PCR

Local genomic DNA methylation of CpG-sites was quantified using methylation-sensitive quantitative PCR (MS-qPCR) according to the previously described methodology, with minor modifications (149, 150). Principal mechanism is the enrichment of methylated genomic DNA by methylation-sensitive restriction enzymes (**Figure 9**). Enrichment of a methylated target sequence can be quantified by qPCR and specific primers.

Before restriction enzyme digestion genomic DNA was incubated at 56 °C for 1 h. For each digestion 1  $\mu$ g DNA was incubated either without enzyme (sham) or with the methylation-sensitive FastDigest<sup>®</sup> restriction enzymes *AcI* or *HpaII* (Fermentas) in a T3000 Thermocycler (Biometra) at 37 °C for 5 h, followed by heat inactivation at 65 °C

for 20 min. CpG-island identification was performed by Methyl Primer Express 1.0 software<sup>®</sup> (Applied Biosystems) using the criteria defined by Gardiner-Garden and Frommer (135). For CpG restriction site DNA methylation analysis 5 ng of digested genomic DNA was amplified using the QuantiTect<sup>®</sup> SYBR Green PCR Kit (Qiagen) on a Mastercycler ep realplex apparatus (Eppendorf) with CpG-island specific primer pairs flanking informative restriction sites (**Figure 21, Table 4**) (*AciI*, CCGC / GCGG; *HpaII*, CCGG). The thermal cycling conditions were as follows: at 95 °C for 15 min, 40 cycles at 95 °C for 15 s, 56 °C for 30 s and 72 °C for 30 s respectively, followed by melting curve analysis (1.75 °C / min). For normalization, an internal control region on chromosome 18 was amplified using a primer pair flanking no informative restriction site (**Figure 42, Table 4**).  $C_q$ -values were retrieved from the realplex 2.0 software (Eppendorf). For restriction site specific CpG-DNA methylation, the  $C_q$  of digested DNA was subtracted from the  $C_q$  of sham DNA ( $\Delta C_q$ ) for the region of interest (ROI) and for the control region (chromosome 18). Calculation of restriction site DNA methylation was performed with the modified equation  $100 * 2^{-\Delta C_q \text{ ROI} - \Delta C_q \text{ control}}$  (149, 150). Performance of the method was controlled by analyzing the imprinted region of *Zrsr1* in liver and testis from a male C57BL6/N mouse (**Figure 43, Figure 44**).

**Table 4.** DNA-sequences for MS-qPCR primers used for local DNA methylation analysis. \* primer DNA-sequences are derived from Oakes *et al* (149).

Symbol	Primer name	Forward primer (5'-3')	Reverse primer (5'-3')
<b>Chr18*</b>	Chromosome 18	GCAATCAGGCTTGTAGC AGTT	CATATGCACCATGTGTC TTGG
<b>Cbs P1</b>	Cystathionine $\beta$ -synthase promoter region 1	GGTGAGTGGGAGGCCGT TCT	TGGAGAGCACGCTCGGA C
<b>Cbs P2</b>	Cystathionine $\beta$ -synthase promoter region 2	GTCCGAGCGTGCTCTCCA	TTAGCGAGCTGCGCGTC
<b>Cbs I7</b>	Cystathionine $\beta$ -synthase intragenic region (exon 7)	GCTGCTTACTGTAGGACT TGTTG	GCACCGTCACACTGCTG C
<b>Zrsr1*</b>	Zinc finger (CCCH type), RNA binding motif and serine/arginine rich 1	GGCCGTACCACAGATAA CCA	GCGCAGTTATCCGTCTA TCCA

## 2.14 Bisulfite genomic pyrosequencing

For specific quantification of individual CpG-site methylation chemical bisulfite conversion of genomic DNA followed by PCR based DNA amplification and pyrosequencing was applied.

### 2.14.1 Bisulfite conversion

The principal mechanism of bisulfite conversion is based on sodium bisulfite mediated deamination of cytosine to uracil (**Figure 10**) (151). Biological modified 5-methylcytosine residues are more slowly affected by the deamination process and therefore the treatment converts DNA methylation into a linear sequence information (151).

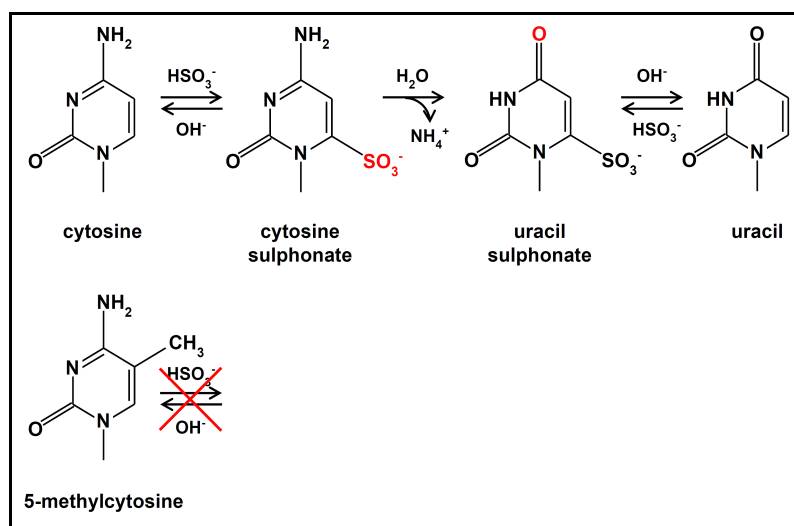


**Figure 10.** Cytosine residues of DNA are chemical modified by sodium bisulfite conversion for specific quantification of CpG-site methylation. Methylated cytosine residues are very slowly affected from the chemical deamination process.

Bisulfite conversion of genomic DNA was performed using 500 ng genomic DNA and the EZ DNA Methylation-Gold Kit (Zymo Research) according to the manufacturer's instructions. Eluted bisulfite converted DNA (bcDNA) was quantified on a NanoDrop ND-1000 UV-Vis spectrophotometer.

### 2.14.2 Pyrosequencing

For quantification of global or local DNA methylation pyrosequencing was applied (152, 153). General principle is based on the DNA sequencing by strand synthesis (single strand DNA template) and nucleotide incorporation based pyrophosphate release that can be used for chemiluminescent energy conversion by a cascade of enzymes (**Figure 11**). Emitted luminometric light is proportional to the amount of nucleotides



incorporated and pyrosequencing can be used for quantification of global or local DNA methylation.

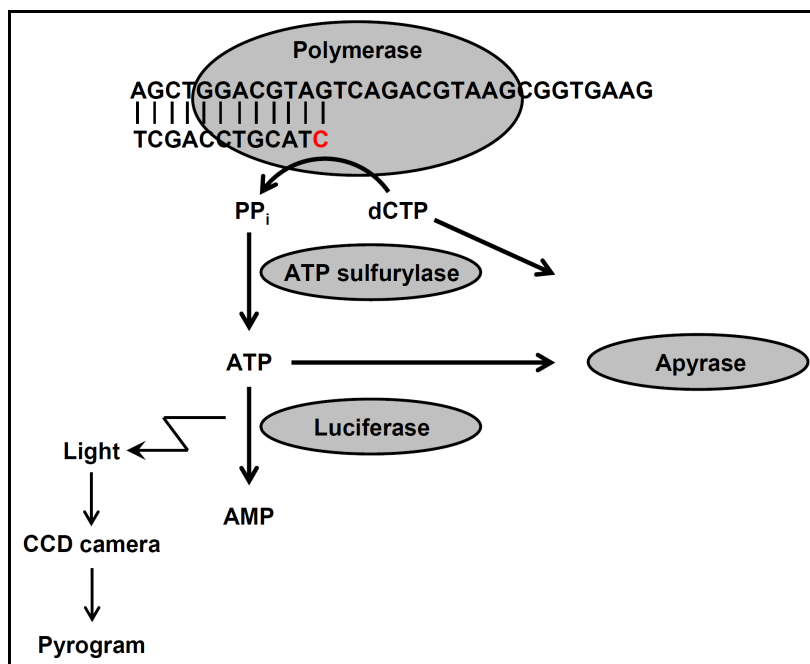


**Figure 11.** Image of the principal mechanism of pyrosequencing is presented. Nucleotide incorporation leads to pyrophosphate release which is used by ATP sulfurylase to synthesize ATP. Subsequently, ATP is consumed by luciferase and results in luminescence. Emitted light is detected by the CCD camera and converted into a pyrogram. Unincorporated nucleotides are degraded by apyrase (152).

Prior to analyses of local DNA methylation specific primers were designed on *in silico* bcDNA with the PyroMark Assay Design Software 2.0 (Qiagen). To prevent primer bias newly designed primers were evaluated by methylation sensitive high resolution melt using serial dilutions of 0 % and 100 % methylated liver DNA as template. Amplification of bcDNA template was performed as described below. 0 % and 100 % methylated DNA was obtained by using the REPLI-g Mini KIT (Qiagen) for whole genome amplification and by using the M.SssI CpG Methylase (Zymo Research) according to the manufacturer's instructions.

For quantification of individual CpG-site methylation, 35 ng of eluted bcDNA was amplified on a Rotor-gene Q using the EpiTect HRM PCR Kit with specific primer pairs (**Table 5**) according to the manufacturer's instructions. The following thermal cycling conditions were used: at 95 °C for 5 min, followed by 50 cycles at 95 °C for 10 s, at 58 °C for 30 s and at 72 °C for 30 s, respectively. Specificity of amplification was controlled by high resolution melting curve analysis with 0.05 °C/2 s increments. The specific PCR products were separated on 2 % agarose gel, excised and extracted using the Wizard SV Gel and PCR clean-Up System (Promega) according to the manufacturer's instructions. For subsequent pyrosequencing the biotinylated strand was

isolated from the PCR product by immobilization on streptavidin-sepharose beads (GE Healthcare) and subsequent denaturing of PCR product. The biotinylated strand was released into annealing buffer containing the specific sequencing primer (**Table 5**). Determination of local genomic DNA methylation was performed on a PyroMark Q24 System (Qiagen) and all pyrosequencing reagents (Qiagen) were prepared according to the manufacturer's instructions. Calculation of individual CpG-site methylation was performed by the PyroMark Q24 Software (Qiagen).

**Table 5.** List of primer sequences used for quantification of individual CpG-site DNA methylation analysis by bisulfite genomic pyrosequencing. Fst, forward genomic DNA strand; rst, reverse genomic DNA strand; B, biotinylation.

Symbol	Primer name	Forward primer (5'-3')	Reverse primer (5'-3')
<b>Cbs fst</b>	Cbs forward strand	AGGTTGTGTAGTAAGGT ATAGATTTTTGGGTATA G	<b>B-</b> CTCTCCACCCCACTCT AACTC
<b>Cbs fst seq</b>	Cbs forward strand sequencing primer	GGTATAGATTTGGGGTT TT	
<b>Cbs rst</b>	Cbs reverse strand	TTTTATAGAGGGGTGTTT GTTTGTTTTGGGAGTTG	<b>B-</b> ACTAACCCAAACCTCTC AAACCAATTACTT
<b>Cbs rst seq</b>	Cbs reverse strand sequencing primer	TTGTTTTGGGAGTTGT	
<b>PPAR<math>\alpha</math> fst</b>	PPAR $\alpha$ forward strand	AGGGGGAGGAGTTTTAG GGGAGTTAT	<b>B-</b> CCCTCCAACCCCTAAAC ACCTAAAACCTACT
<b>PPAR<math>\alpha</math> fst seq</b>	PPAR $\alpha$ forward strand sequencing primer	GGGATTTAGTAGGGGA	

### 2.15 Statistical analysis

Results are presented as mean  $\pm$  SEM. Statistical analyses were performed using Prism 4.01 software (GraphPad Software). For analysis of HF feeding trial and eight weeks C and HF treated animals (8W) in the preliminary experiment of the HF methyl-group supplementation feeding trial, data were tested using Student's t-test. In case of inhomogeneous variances, data were analyzed using Student's t-test with Welch's correction. Data from four weeks treated animals of HF methyl-group supplementation feeding trial (12W) and *in vitro* analysis in FAO cells were analyzed by one-way ANOVA followed by Tukey's Multiple Comparison Test. In case of unequal variances data were transformed logarithmic. In addition, outliers were detected by using Grubb's test and excluded from statistical data analysis. Analysis of body weight development, food intake and glucose tolerance data were performed with SigmaStat 3.5 (Systat Software, Inc.) using the two-way ANOVA with repeated measure and the Holm-Sidak method. Differences in liver PC subclasses and liver amino acid concentrations were tested using the R software package (154). The p-values were adjusted for multiple testing using the *p.adjust* function within the R-library *limma* and the Benjamini-Hochberg method (155). For all tests, the bilateral alpha risk was  $\alpha = 0.05$ .

## 3 Results

### 3.1 Influence of DIO induced NAFLD on phospholipid homeostasis and C1 metabolism

The HF DIO mouse model that leads to NAFLD is linked to the development of obesity, hyperglycemia and hyperinsulinemia (40, 45). For assessing NAFLD effects on hepatic C1 and phospholipid homeostasis, C57BL/6N male mice were fed a HF diet for 12 weeks as described by Desmarchelier *et al.* (138, 139). In this study, analysis of basal parameter revealed increased terminal body weight, liver weight, blood glucose and blood insulin level and increased AUC during the glucose tolerance test (138, 139). The induction of NAFLD was reflected by increased hepatic TG accumulation and associated with reduced total PL levels (138, 139), which was accompanied by differences in energy and food intake resulting also in differences of lipotrope and cofactor intake in obese mice (see 7.4, **Table 23**). These data suggested that the dietary treatment induced obesity, hyperglycemia, hyperinsulinemia, reduced insulin sensitivity and NAFLD in mice fed a HF diet.

The processing of the high dietary fat intake is a challenge for the organism. Hepatic PL and especially PC are important for intestinal fat absorption (biliary PC) and in hepatic TG export by VLDL-particles (see 1.3). To assess whether DIO induced NAFLD is associated with altered PC levels in livers of DIO mice, a PC subclass signature was obtained by mass spectrometry (139). HF diet feeding led to a significant increase in PC subclasses, especially an increase in long-chain polyunsaturated PC concentrations (PC.aa.38:4, PC.ae.38:4, PC.ae.40:5, PC.ae.40:6), which are most likely associated with the PE methylation pathway (139).

#### 3.1.1 Gene expression of the hepatic transsulfuration and sarcosine pathways in C1 metabolism is altered in DIO mice

To investigate whether the metabolic differences observed for long-chain polyunsaturated PC concentrations of the PE methylation pathway in HF DIO mice influence the hepatic C1-metabolism, gene expression of major enzymes operating in the C1-metabolism was determined by qRT-PCR. As shown in **Figure 12A & B**, gene expression of the methionine cycle or the folate cycle key enzymes, implicated in SAM synthesis or folate dependent Hcy remethylation, was not affected by the dietary treatment except for serine hydroxymethyltransferase 1 (Shmt1) which was marginally increased in DIO mice by  $30.7 \pm 12.0$  % ( $p = 0.075$ ) without reaching significance. In contrast, analysis of the sarcosine pathway revealed in DIO mice an increased gene

expression of choline dehydrogenase (Chdh) by  $32.0 \pm 5.3\%$  ( $p = 0.017$ ), betaine-homocysteine methyltransferase (Bhmt) by  $107.3 \pm 17.4\%$ ; ( $p = 0.001$ ) and dimethylglycine dehydrogenase precursor (Dmgdh) by  $43.3 \pm 10.6\%$  ( $p = 0.017$ ) as shown in **Figure 12C**. In the transsulfuration pathway, a marginal decrease in gene expression of cystathionine  $\beta$ -synthase (Cbs) ( $66.3 \pm 2.7\%$  of control ( $p = 0.078$ ) and glutamate oxaloacetate transaminase 1 (Got1) ( $48.7 \pm 7.0\%$  of control;  $p = 0.064$ ) without reaching significance was observed. Cysteine sulfinic acid decarboxylase (Csad) increased by  $112.5 \pm 38.9\%$  ( $p = 0.038$ ) and glutathione synthetase (Gss) by  $22.4 \pm 5.9\%$  ( $p = 0.032$ ) as shown in **Figure 12D**.

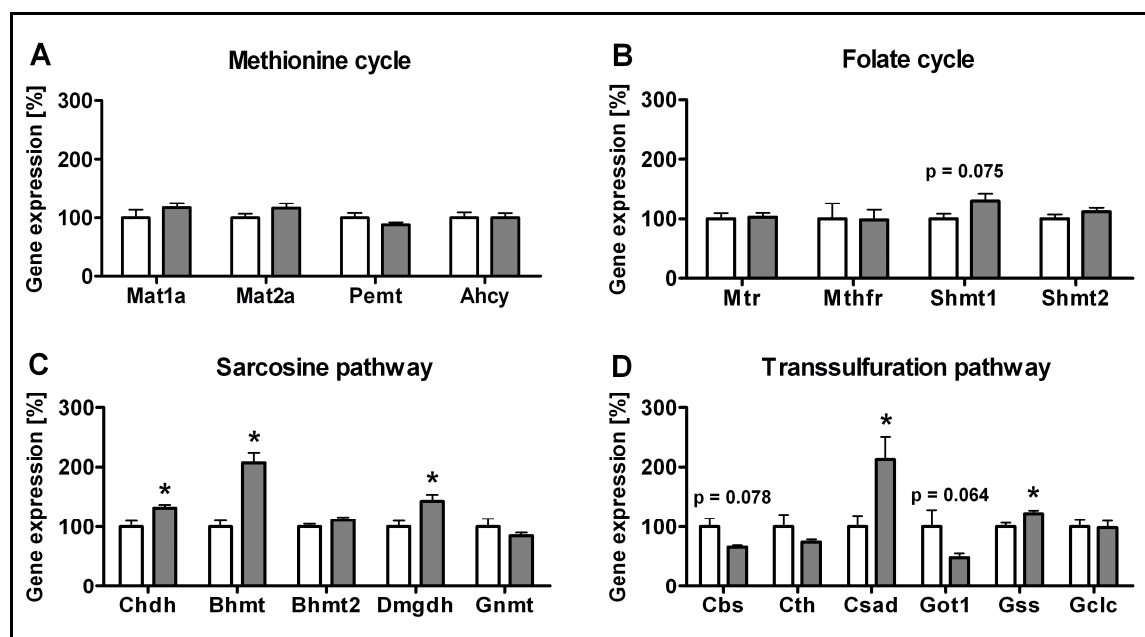


**Figure 12.** Hepatic mRNA expression of genes encoding enzymes in C1-metabolism in mice on C and HF diets. Data are presented for **A** the methionine cycle, **B** the folate cycle, **C** sarcosine pathway, and **D** transsulfuration pathway as mean  $\pm$  SEM ( $n = 5-6$ ). Open and grey columns represent data from control and HF (DIO) animals. Asterisk indicates statistical significance ( $p < 0.05$ ). Abbreviations: Ahcy, S-adenosylhomocysteine hydrolase; Bhmt, Betaine-homocysteine methyltransferase; Bhmt2, Betaine-homocysteine methyltransferase 2; Cbs, Cystathionine  $\beta$ -synthase; Chdh, Choline dehydrogenase; Csad, Cysteine sulfinic acid decarboxylase; Cth, Cystathionase; Dmgdh, Dimethylglycine dehydrogenase precursor; Gclc, Glutamate-cysteine ligase catalytic subunit; Gnmt, Glycine N-methyltransferase; Got1, Glutamate oxaloacetate transaminase 1; Gss, Glutathione synthetase; Mat1a, Methionine adenosyltransferase I alpha; Mat2a, Methionine adenosyltransferase II alpha; Mthfr, 5,10-methylenetetrahydrofolate reductase; Mtr, 5-methyltetrahydrofolate-homocysteine methyltransferase; Pemt, Phosphatidylethanolamine N-methyltransferase; Shmt1, Serine hydroxymethyltransferase 1; Shmt2, Serine hydroxymethyltransferase 2.

### 3.1.2 Hepatic protein levels of BHMT are increased and CBS level are decreased in DIO mice

Gene expression analysis (see 3.1.1) revealed the regulation of the branch-point enzymes Bhmt and Cbs regulating the remethylation or the irreversible degradation of Hcy to L-cysteine in DIO mice (51). In order to examine whether the observed transcriptional changes of Bhmt and Cbs translate into differences on protein level, BHMT and CBS proteins were determined by Western blot analysis. BHMT protein was increased by  $61.9 \pm 8.3 \%$  ( $p < 0.001$ ) whereas CBS protein expression was decreased in HF animals to  $66.6 \pm 6.2 \%$  ( $p = 0.020$ ) compared to C mice (**Figure 13**).

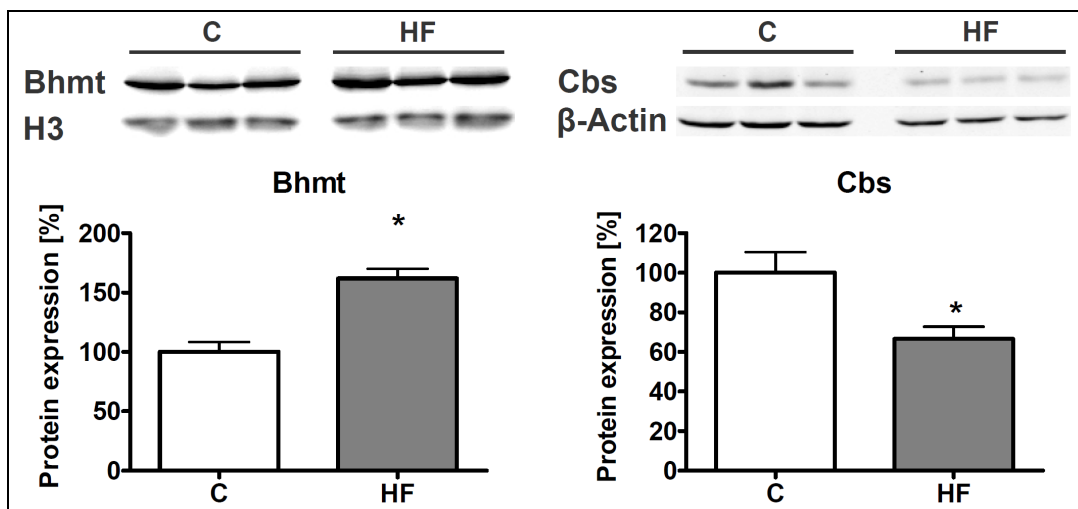


**Figure 13.** Influence of DIO on hepatic BHMT and CBS protein expression after twelve weeks of dietary treatment. Data are presented as mean  $\pm$  SEM ( $n = 6$ ). Open and grey columns represent data from C and HF animals. Asterisk indicates statistical significance ( $p < 0.05$ ). Abbreviations: Bhmt, Betaine-homocysteine methyltransferase; Cbs, Cystathionine  $\beta$ -synthase; H3, Histone H3.

### 3.1.3 Amino acid profiling reveals homeostasis in the methionine cycle, reflects increased BHMT mediated homocysteine remethylation and supports a repression of the transsulfuration pathway

To analyze the influence of DIO induced NAFLD on hepatic amino acid levels the concentrations of a total of 30 amino acids and derivatives were determined by LC-MS / MS analysis in livers of C and HF fed mice (**Figure 14, Table 18**). Taurine and L-glutamine concentrations increased by  $24.7 \pm 5.3 \%$  ( $p = 0.015$ ) and by  $39.9 \pm 9.8 \%$ ; ( $p = 0.034$ ) in HF mice. A decrease in concentration was observed for L- $\alpha$ -amino-n-butyrate to  $49.9 \pm 4.1 \%$  ( $p = 0.015$ ), L-citrulline to  $55.2 \pm 3.6 \%$  ( $p = 0.012$ ), L-ornithine to  $71.4 \pm 5.2 \%$  ( $p = 0.034$ ) and hydroxyproline to  $72.2 \pm 7.2 \%$  ( $p = 0.047$ ) in HF mice compared to C mice. Interestingly, hepatic L-methionine levels were not affected by the dietary treatment (**Figure 14**).

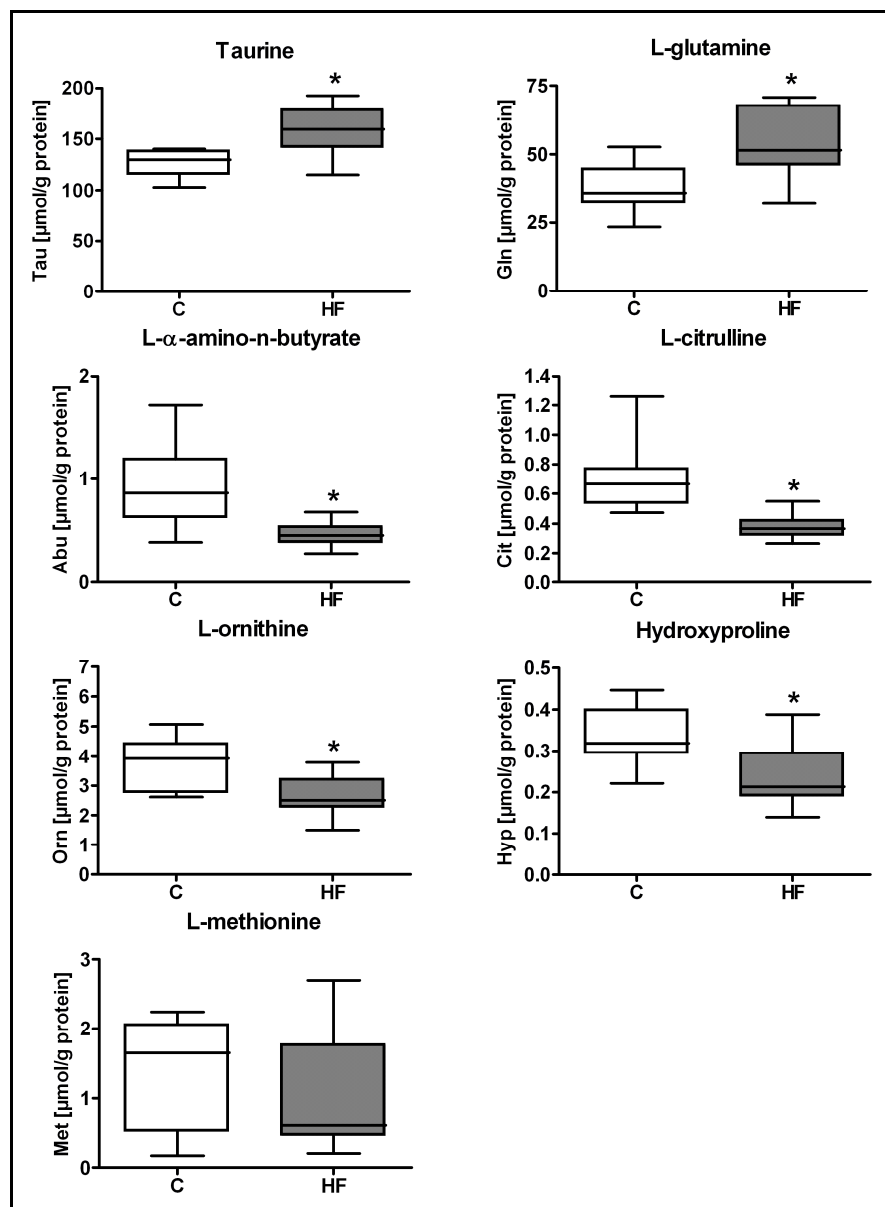


**Figure 14.** Impact of HF diet feeding on selected hepatic metabolites after twelve weeks of dietary treatment. Data are presented as box and whisker plot (n = 9-11). Open and grey boxes represent data from C and HF animals. Asterisk indicates statistical significance ( $p < 0.05$ ). Abbreviations: Abu, L- $\alpha$ -amino-n-butyrate; Cit, L-citrulline; Gln, L-glutamine; Hyp, Hydroxyproline; Met, L-methionine; Orn, L-ornithine; Tau, Taurine.

After the observation that L-methionine levels remained unaffected in DIO mice, the hepatic methionine cycle metabolites SAM, SAH and Hcy and the transsulfuration metabolite cystathionine were analyzed by HPLC-MS / MS and GC-MS / MS. The measurements revealed that neither SAM, SAH or [SAM] / [SAH] ratio nor Hcy levels were altered by the dietary treatment in HF mice (**Figure 15**) suggesting the maintenance of homeostasis in the methionine cycle of DIO mice. However, determination of cystathionine revealed a significant reduction in the liver of HF mice to  $64.0 \pm 7.7 \%$  ( $p = 0.026$ ) compared to C mice (**Figure 15**).

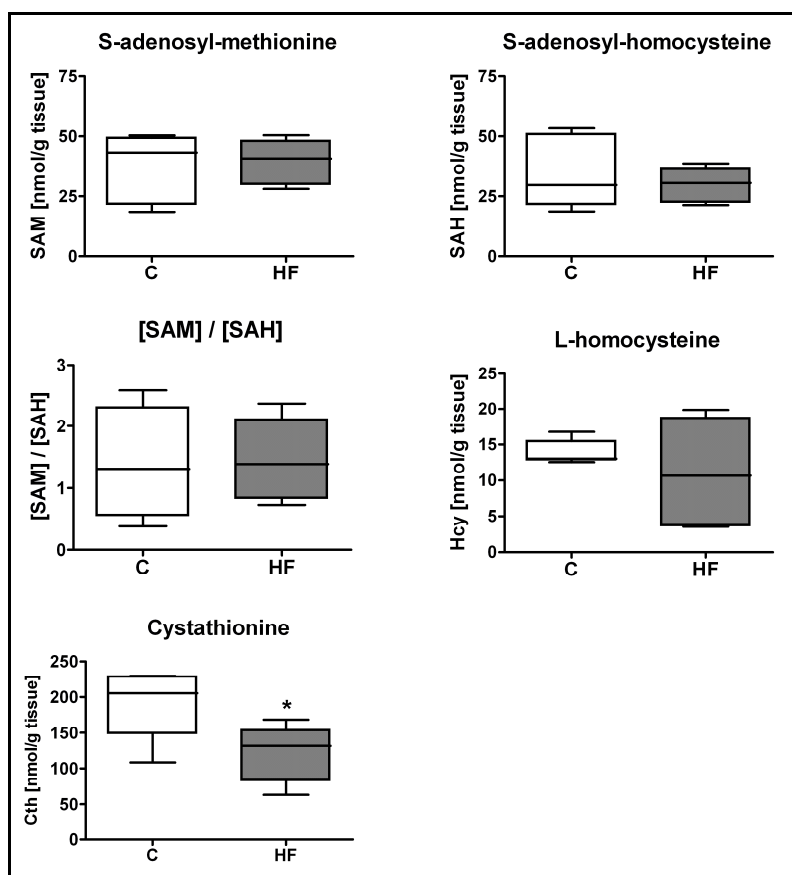


**Figure 15.** Analysis of hepatic SAM, SAH, [SAM]/[SAH] ratio, Hcy and cystathionine in hepatic tissues of C and HF fed mice. Data are presented as box and whisker plot ( $n = 5-6$ ). Open and grey boxes represent data from C and HF animals. Asterisk indicates statistical significance ( $p < 0.05$ ). Abbreviations: Cth, Cystathionine; Hcy, L-homocysteine; SAH, S-adenosyl-homocysteine; SAM, S-adenosyl-methionine.

To assess whether also metabolic alterations in the sarcosine pathway implicated in BHMT mediated Hcy remethylation can be observed in DIO mice, the choline level in liver was determined by an enzymatic fluorimetric analysis. Increased hepatic choline concentrations were detected in HF mice compared to C mice (**Figure 16**), suggesting an increased choline oxidation capacity in DIO mice.



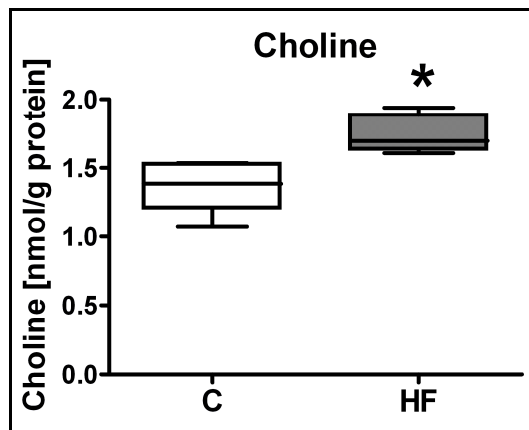


**Figure 16.** The impact of DIO on the choline level in liver tissues of mice fed a C or HF diet. Data are presented as box and whisker plot (n = 6). Open and grey boxes represent data from C and HF animals. Asterisk indicates statistical significance ( $p < 0.05$ ).

#### 3.1.4 PPAR $\alpha$ activity is increased in DIO mice and is implicated in the repression of the transsulfuration pathway

One of the pivotal TFs regulating gene expression in the liver is PPAR $\alpha$ . This TF is known to be involved in the regulation of hepatic lipid metabolism (33). In addition, PPAR $\alpha$  participates in control of gene expression of enzymes in amino acid metabolism and is known to downregulate *Got1* gene expression (156). To assess whether gene expression for the branch-point enzymes *Bhmt* and *Cbs* is regulated by PPAR $\alpha$ , Fao rat hepatoma cells were incubated with the PPAR $\alpha$  agonist WY14,643 for 24 h. *Bhmt* and *Cbs* gene expression was determined by qRT-PCR. Treatment of Fao cells with WY14,643 for 24h indeed augmented the mRNA levels of the PPAR $\alpha$  target gene *Cpt1a* in a dose-dependent manner (25  $\mu$ M,  $169.4 \pm 8.3$  %; 50  $\mu$ M,  $158.4 \pm 7.7$  %; 100  $\mu$ M,  $165.3 \pm 9.4$  %;  $p < 0.001$ ) as expected, and reduced the mRNA of *Cbs* (25  $\mu$ M,  $32.7 \pm 2.6$  %; 50  $\mu$ M,  $37.4 \pm 7.5$  %; 100  $\mu$ M,  $39.1 \pm 11.7$  %;  $p < 0.001$ ) independent of the used agonist concentration. However, PPAR $\alpha$  activation did not change *Bhmt* mRNA expression ( $p = 0.242$ ) in comparison with unstimulated control cells (**Figure 17**)

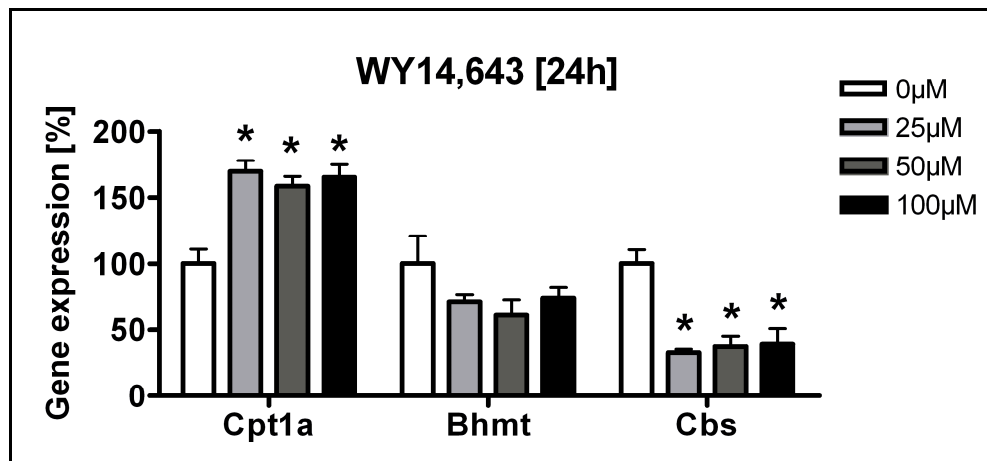


**Figure 17.** Analysis of the effect of WY14,643 on PPAR $\alpha$ -dependent gene expression of Bhmt and Cbs in FaO rat hepatoma cells. Prior to the stimulation, cells were preincubated in DMEM (5.56 mM glucose) supplemented with 0.5 % bovine serum albumin for 48 h followed by stimulation with 25  $\mu$ M, 50  $\mu$ M and 100  $\mu$ M WY14,643. Data are presented as mean  $\pm$  SEM (n = 4). Asterisk indicates statistical significance (p < 0.05). Abbreviations: Bhmt, Betaine-homocysteine methyltransferase; Cbs, Cystathionine  $\beta$ -synthase; Cpt1a, Carnitine palmitoyltransferase 1a.

Furthermore, hepatic gene expression of PPAR $\alpha$  and of the “classical” PPAR $\alpha$  target genes Cpt1a, uncoupling protein 2 (Ucp2) and acyl-coenzyme A oxidase 1 (Acox1) was assessed in C and HF mice by qRT-PCR. Gene expression increased for PPAR $\alpha$  to  $167.4 \pm 17.2$  % (p = 0.022), Cpt1a to  $341.3 \pm 16.1$  % (p = 0.009), Ucp2 to  $193.0 \pm 23.1$  % (p = 0.012) and Acox1 to  $182.6 \pm 12.6$  % (p < 0.001) in HF mice (**Figure 18**), supporting the notion of an increased PPAR $\alpha$  activity in HF mice. This implies that increased PPAR $\alpha$  activity may lead to a repression of the transsulfuration pathway in HF mice.

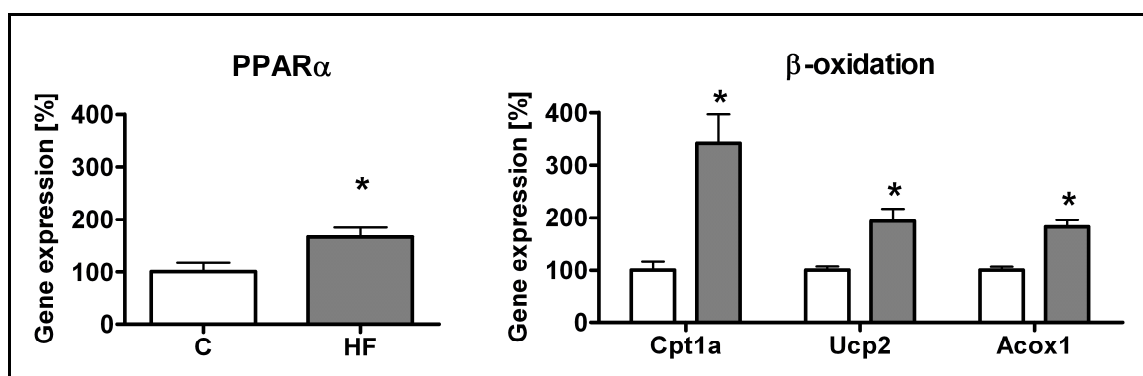


**Figure 18.** Analysis of PPAR $\alpha$  and PPAR $\alpha$  target gene expression in liver of C and HF mice reflecting PPAR $\alpha$  activity. Open and grey columns represent data from C and HF animals. Data are presented as mean  $\pm$  SEM (n = 5-6). Asterisk indicates statistical significance (p < 0.05). Abbreviations: Acox1, Acyl-coenzyme A oxidase 1; Cpt1a, Carnitine palmitoyltransferase 1a; PPAR $\alpha$ , Peroxisome proliferator activated receptor  $\alpha$ ; Ucp2, Uncoupling protein 2.

### 3.2 Influence of HF diet on epigenetic gene regulation and on global and gene-specific DNA methylation

Epigenetic processes are important for genome integrity and the regulation of gene expression by global (whole chromatin) or local (gene promoter specific) DNA methylation. Disturbances of DNA methylation can be implicated in the development of hepatocellular cancer (12) and is associated with short and long-term peroxisome proliferators (PPAR $\alpha$  ligands) mediated PPAR $\alpha$  activation (157-161). For epigenetic processes the principal methyl-group donor SAM is of pivotal importance (162). To investigate whether a HF diet and NAFLD associate with PPAR $\alpha$  activation affects, epigenetic alterations of gene expression of DNA methyltransferases (Dnmts) and global and local genomic DNA methylation of identified target genes were determined.

#### 3.2.1 *De novo* DNA methyltransferase gene expression is reduced in HF mice

Dnmts-pathways are known to be disturbed by certain methyl-group deficiencies (88, 89). To determine whether HF diet induced NAFLD affects Dnmts, gene expression of Dnmt1, Dnmt3a and 3b were determined by qRT-PCR. Animals fed with HF diet showed decreased gene expression levels of Dnmt3b to  $46.5 \pm 3.6$  % ( $p = 0.011$ ) compared to C mice (**Figure 19**), whereas Dnmt1 ( $p = 0.701$ ) and Dnmt3a ( $p = 0.174$ ) were unaffected by dietary treatment.

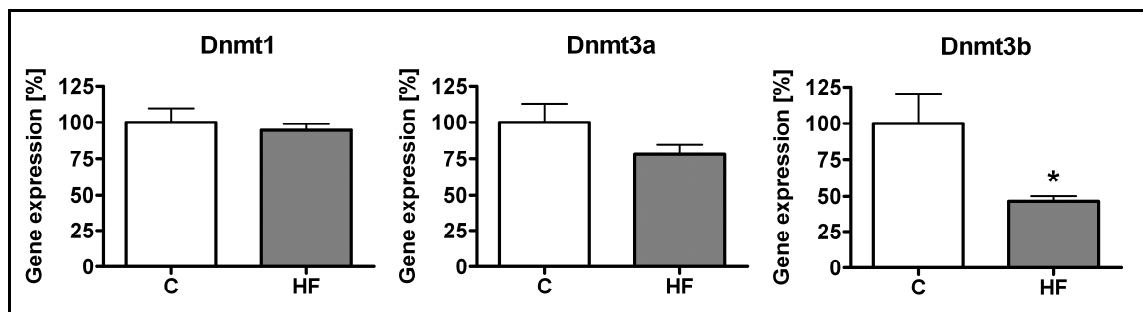


**Figure 19.** Influence of HF diet treatment on hepatic DNA methyltransferase gene expression. Data are presented as mean  $\pm$  SEM ( $n = 5-6$ ). Open and grey columns represent data from C and HF animals. Asterisk indicates statistical significance ( $p < 0.05$ ). Abbreviations: Dnmt1, DNA methyltransferase 1; Dnmt3a, DNA methyltransferase 3a; Dnmt3b, DNA methyltransferase 3b.

#### 3.2.2 Hepatic global DNA methylation is unaffected by a HF diet

The identified downregulation of Dnmt3b gene expression suggests a reduced hepatic expression of *de novo* DNMT in DIO mice which possibly influence global DNA methylation. Therefore, global cytosine DNA methylation levels were determined in C and HF mice by LUMA. The analysis revealed 70 % CpG methylation of restriction

enzyme target CpG-sites and no influence of DIO and NAFLD on global DNA methylation in HF mice (**Figure 20**).

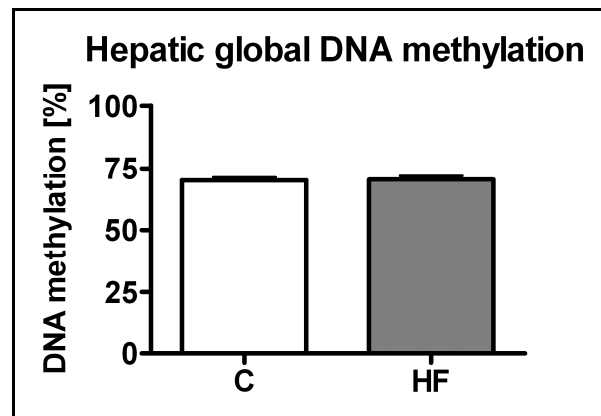


**Figure 20.** Analysis of hepatic global DNA methylation in liver tissue of mice fed C and HF diets. DNA methylation was calculated from the (*HpaII* / *MspI*) ratio. Data are presented as mean  $\pm$  SEM (n = 6). Open and grey columns represent data from C and HF animals. Asterisk indicates statistical significance (p < 0.05).

### 3.2.3 DNA methylation status of CpG-islands in the *Cbs* and *PPAR $\alpha$* gene promoter and CBS intragenic region is unchanged in liver tissue of HF mice

To further assess whether the HF diet induced NAFLD can modulate gene-specific CpG-island DNA methylation in liver tissue, *Cbs* and *PPAR $\alpha$*  CpG-island DNA methylation was determined. Both genes are transcriptional regulated in the DIO model and their promoter CpG-islands are known to be sensitive to DNA methylation changes from studies in rats (163, 164). Analysis of *Cbs* promoter and intragenic CpG-island methylation was performed by MS-qPCR and the experimental design is presented in **Figure 21**.

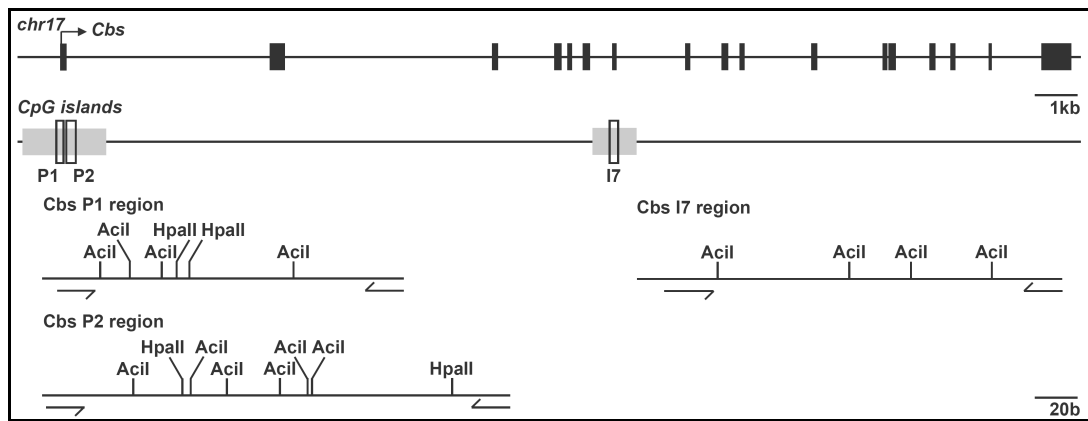


**Figure 21.** Genomic structure of the mouse *Cbs* gene and experimental design of *Cbs* DNA methylation analysis. **Top:** Filled black boxes represent exons interspaced by introns and black arrow indicates transcription start site (ENSMUST00000067801). Filled grey boxes represent *Cbs* CpG-islands and open boxes mark the investigated regions. **Bottom:** Investigated regions and positions of informative restriction sites are depicted. Abbreviations: *Cbs* I7, Cystathionine  $\beta$ -synthase intragenic CpG-island region 7; *Cbs* P1, Cystathionine  $\beta$ -synthase promoter CpG-island region 1; *Cbs* P2, Cystathionine  $\beta$ -synthase promoter CpG-island region 2; chr17, chromosome 17.

For the promoter region, no significant DNA methylation of *Acil* and *HpaII* restriction sites was detected, while the analysis of the intragenic CpG-island revealed 60-70 % DNA methylation of investigated *Acil* restriction sites. No differences in *Cbs* CpG-island DNA methylation however were observed between C and HF mice (**Figure 22**).

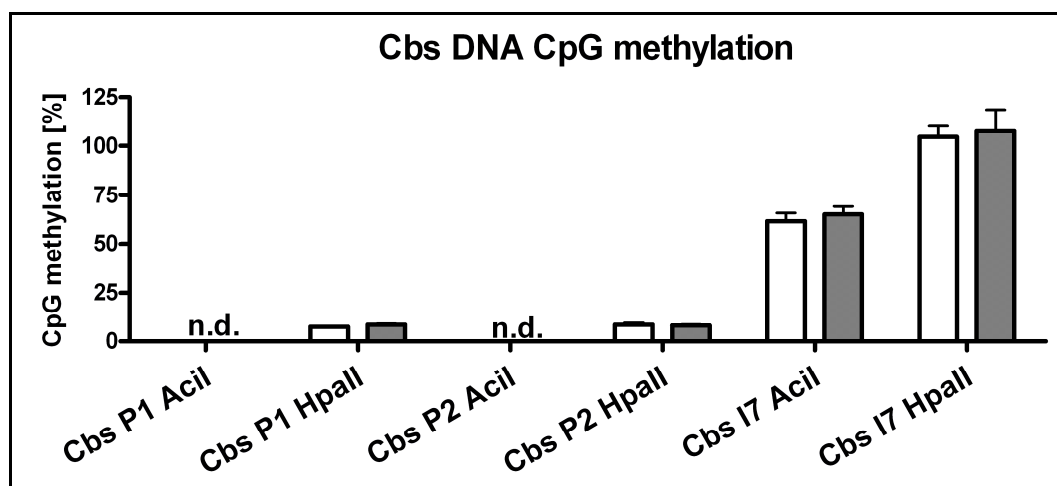


**Figure 22.** Quantitative analysis of CpG restriction sites in promoter and intragenic *Cbs* CpG-islands in liver tissues of C and HF mice. Data are shown for the restriction enzymes *Acil* and *HpaII* in the mentioned regions. Data are presented as mean  $\pm$  SEM (n = 6). Open and grey columns represent data from C and HF animals. Asterisk indicates statistical significance ( $p < 0.05$ ). Abbreviations: *Cbs* I7, Cystathionine  $\beta$ -synthase intragenic CpG-island region 7; *Cbs* P1, Cystathionine  $\beta$ -synthase promoter CpG-island region 1; *Cbs* P2, Cystathionine  $\beta$ -synthase promoter CpG-island region 2; chr17, chromosome 17; n.d., no detection.

The resolution of the MS-qPCR method is only restricted to the CpG methylation of the examined restriction site. To quantify DNA methylation of single CpG-sites in the promoter region, bisulfite genomic pyrosequencing was performed on the forward and reverse strand of *Cbs* promoter CpG-island (**Figure 23**). In total, 6 CpG-sites on the forward and 7 CpG-sites on the reverse strand were analyzed. No differences in DNA methylation between C and HF mice were observed, except for a marginal decrease in methylation of CpG-site 6 on the forward strand ( $p = 0.064$ ) as shown in **Figure 23**.

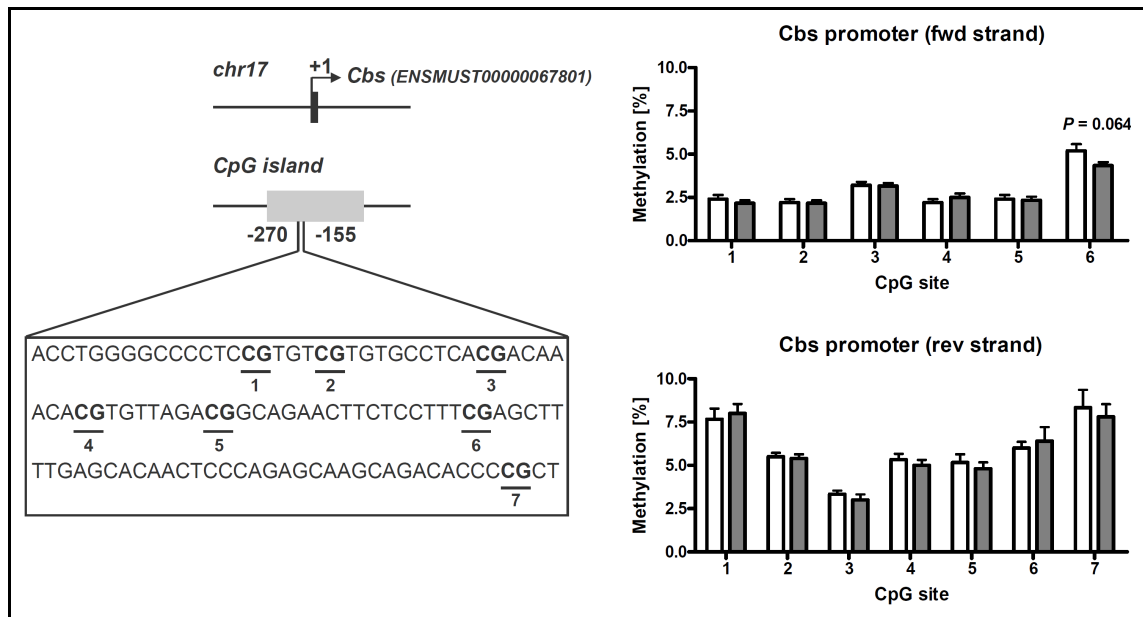


**Figure 23.** Effects of a HF diet on *Cbs* promoter CpG-island DNA methylation assessed by bisulfite genomic pyrosequencing. **Left:** Experimental design is depicted. Filled black box represents exon 1 and black arrow indicates transcription start site (ENSMUST00000067801). Filled grey box represent *Cbs* promoter CpG-islands and open box present the investigated nucleotide sequence. **Right:** Quantification of *Cbs* promoter CpG methylation (forward and reverse strand). Data are presented as mean  $\pm$  SEM ( $n = 5-6$ ). Open and grey columns represent data from C and HF animals. Asterisk indicates statistical significance ( $p < 0.05$ ). Abbreviations: chr17, chromosome 17; fwd, forward; rev, reverse.

Furthermore, CpG-island DNA methylation (forward strand) of the *PPAR $\alpha$*  promoter in C and HF mice was determined by bisulfite genomic pyrosequencing. In total 16 CpG-sites were analyzed, but no CpG-site revealed a significant difference between C and HF mice (**Figure 24**).

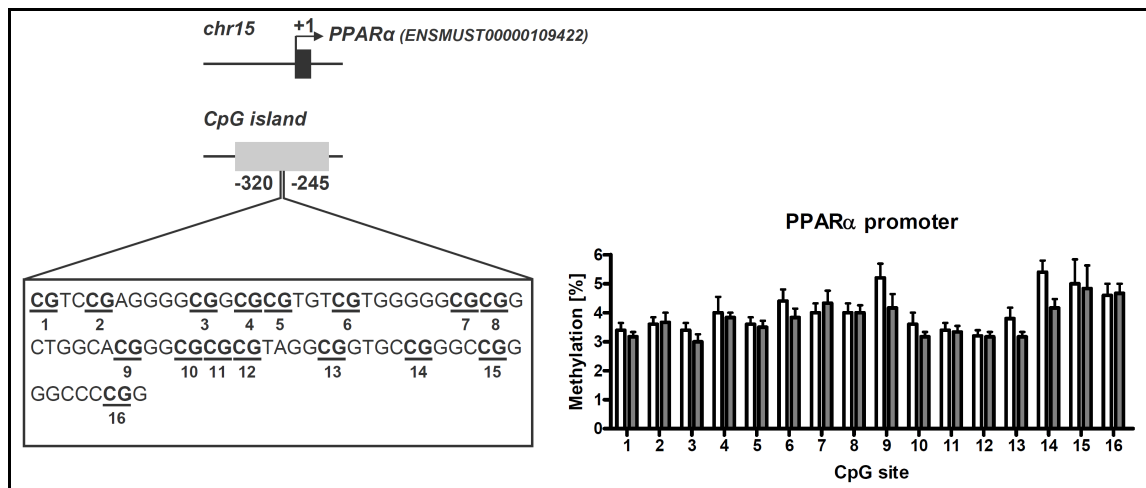


**Figure 24.** Influence of HF diet on PPAR $\alpha$  promoter CpG-island DNA methylation in C and HF mice by bisulfite genomic pyrosequencing. **Left:** Experimental design is depicted. Filled black box represents exon 1 and black arrow indicates transcription start site (ENSMUST00000109422). Filled grey box represent Cbs promoter CpG-islands and open box present the investigated nucleotide sequence. **Right:** Quantification of PPAR $\alpha$  promoter CpG methylation (forward strand). Data are presented as mean  $\pm$  SEM (n = 5-6). Open and grey columns represent data from C and HF animals. Asterisk indicates statistical significance (p < 0.05). Abbreviations: chr15, chromosome 15.

### 3.3 Influence of dietary methyl-group supplementation on the progression of NAFLD in DIO mice

The observed hepatic alterations in PL homeostasis and C1-metabolism in HF mice with NAFLD suggested an altered methyl-group expenditure for PC biosynthesis and increased hepatic PL demand in these animals. Previous studies described an alleviation of hepatic steatosis by permanent betaine supplementation during the trial (91) showing that methyl-group supplementation can alter the development of NAFLD. However, it was so far unknown whether methyl-group supplementation can exert also a therapeutic effect and reverse a NAFLD state. To answer this question, a new feeding trial divided into two phases was performed (**Figure 7**). During the first phase the established DIO model (139) was applied to induce obesity in male C57BL/6N mice by feeding a HF diet for eight weeks (C and HF 8W; n = 23). At the end of this first phase, a part (n = 5) of the HF and C mice (8W) were used for a basic characterization of body and organ weight development, plasma blood glucose, insulin levels and glucose tolerance (see below, **Figure 25**). The remaining mice of the two dietary groups were further used for the supplementation phase of the experiment (**Figure 7**). The basic characterization at the end of first feeding phase showed a significant increase in body weight development by ~35% after eight weeks of dietary feeding in HF mice (p < 0.001). The corresponding food intake during this feeding phase was reduced for HF animals compared to C animals (p < 0.05) shown in **Figure 45**, while the cumulative energy

consumption was significantly increased in HF mice compared to C mice (C:  $3.38 \pm 0.02$  MJ; HF:  $4.21 \pm 0.06$  MJ;  $p < 0.001$ , see 7.4, **Table 24**) after eight weeks of feeding. This was also accompanied by differences in lipotrope and cofactor intake in obese mice (see 7.4, **Table 24**).

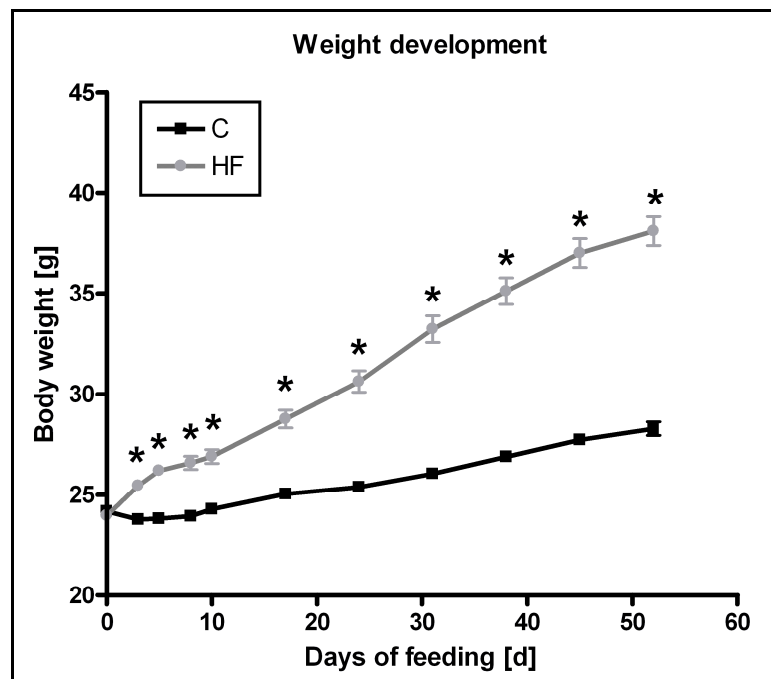


**Figure 25.** Body weight development of animals in C and HF groups during eight weeks before the methyl-group supplementation phase. Data are presented as mean  $\pm$  SEM (n = 8-9). Asterisk indicates statistical significance ( $p < 0.05$ ).

The analysis of liver and visceral adipose tissue (VAT) weight revealed also increased levels by  $\sim 31\%$  ( $p = 0.001$ ) and  $\sim 150\%$  ( $p = 0.002$ ) in HF mice compared to C mice respectively, although when liver weight was related to body weight there were no significant differences (**Table 6**). After eight weeks of HF diet, blood glucose ( $p = 0.012$ ) and plasma insulin level ( $p = 0.161$ ) were increased in HF mice compared to C mice suggesting that DIO animals are hyperglycemic and start to develop hyperinsulinemia (**Table 6**).



**Table 6.** Basal parameters of C and HF C57BL/6N male mice after eight weeks dietary treatment. Data are presented as mean  $\pm$  SEM (n = 5). Different subscript letters indicate statistical significance ( $p < 0.05$ ). VAT was calculated by summing up the weight of epididymal, perirenal and mesenteric adipose tissue. Abbreviations: AUC, area under the curve; ipGTT, intraperitoneal glucose tolerance test; VAT, visceral adipose tissue.

	C	HF
<b>Liver weight [g]</b>	1.24 $\pm$ 0.04 <sup>a</sup>	1.62 $\pm$ 0.04 <sup>b</sup>
<b>% Liver / body weight</b>	4.59 $\pm$ 0.06	4.34 $\pm$ 0.11
<b>VAT weight [g]</b>	1.10 $\pm$ 0.05 <sup>a</sup>	3.86 $\pm$ 0.38 <sup>b</sup>
<b>% VAT / body weight</b>	4.09 $\pm$ 0.11 <sup>a</sup>	10.22 $\pm$ 0.74 <sup>b</sup>
<b>Blood glucose [mg / dl]</b>	123.4 $\pm$ 3.4 <sup>a</sup>	169.4 $\pm$ 10.1 <sup>b</sup>
<b>Plasma insulin [ng / ml]</b>	1.23 $\pm$ 0.25	2.72 $\pm$ 0.77
<b>ipGTT, AUC [mg / dl*min]</b>	15422 $\pm$ 2349	24978 $\pm$ 5070

Analysis of glucose tolerance in HF mice after seven weeks of feeding by an ipGTT revealed a delayed clearance of blood glucose concentrations at time point 60 min ( $p = 0.003$ ) and 120 min ( $p = 0.009$ ) as shown in **Figure 26**. Calculation of the AUC however did not reveal a significant difference (**Table 6**).

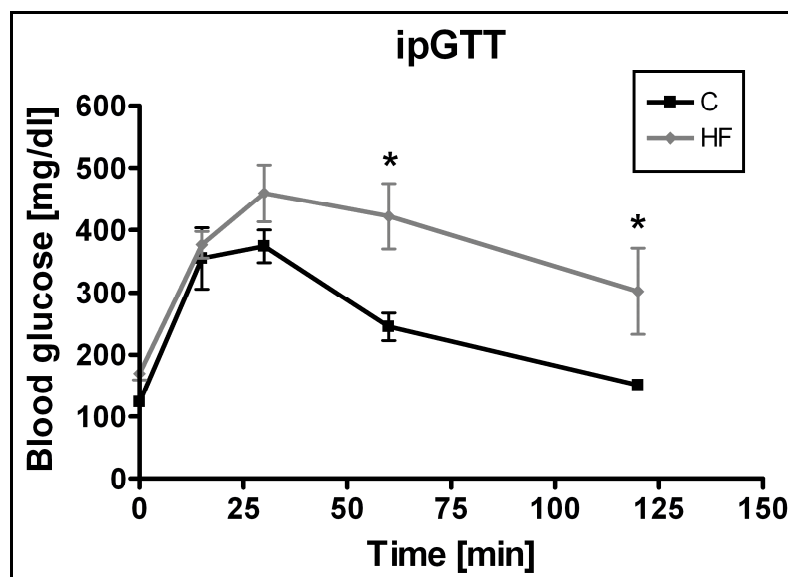


**Figure 26.** Intraperitoneal glucose tolerance test of C and HF mice after seven weeks of C or HF diet treatment is depicted. Data are presented as mean  $\pm$  SEM (n = 5). Asterisk indicates statistical significance ( $p < 0.05$ ).

### 3.3.1 Methyl-group supplementation does not affect body weight development, hyperglycemia, hyperinsulinemia and glucose tolerance

In the supplementation phase, C animals (n=18) were split into two groups and were either fed C (n=9) or CMS (n=9) diets. The remaining HF animals (n=18) were also split into two groups and were either fed HF (n=9) or HFMS (n=9) diet for four weeks as shown in **Figure 7**. CMS and HFMS diets (**Table 1**) were supplemented with choline chloride, betaine, methionine, folic acid, vitamin B<sub>12</sub> and ZnSO<sub>4</sub> according to Wolff *et al.* (97). Measurements of body weight development of mice in the C, CMS, HF and HFMS groups during the therapeutic phase did not show significant body weight differences between the CMS and C or HFMS and HF groups (**Figure 27**). The food intake during the trial was significantly different for C and CMS mice compared to HF and HFMS mice ( $p < 0.05$ ) as reported in **Figure 46**, while the cumulative energy consumption of C and CMS mice was significantly different from that of animals in HF and HFMS groups (C:  $5.16 \pm 0.06$  MJ; CMS:  $5.15 \pm 0.06$  MJ; HF:  $6.06 \pm 0.07$  MJ; HFMS:  $6.05 \pm 0.12$  MJ;  $p < 0.001$ , see 7.4, **Table 25**) after twelve weeks of feeding. In addition, this was again accompanied by differences in lipotrope and cofactor intake in obese mice (see 7.4, **Table 25**).

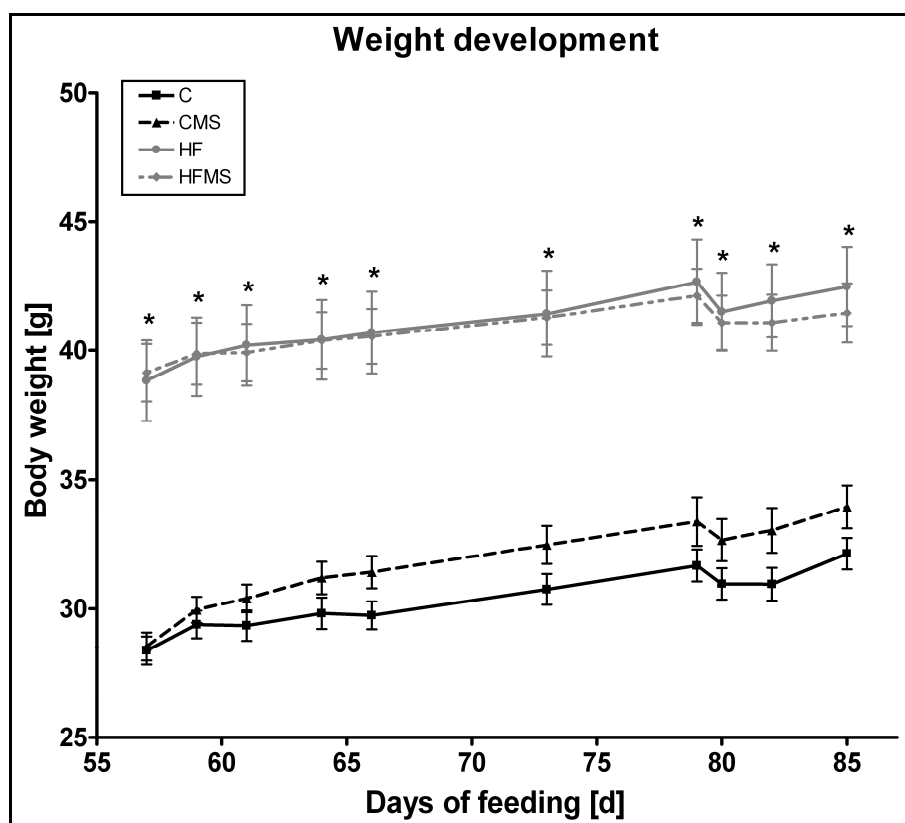


**Figure 27.** Body weight development in mice receiving the C, CMS, HF and HFMS diets for four weeks after the eight weeks pre-treatment. Mice are treated in total for twelve weeks. Data are presented as mean  $\pm$  SEM (n = 8-9). Asterisk indicates statistical significance of HF and HFMS mice compared to C and CMS mice ( $p < 0.05$ ).

Basal phenotypic parameters revealed increased liver ( $p = 0.001$ ) and visceral adipose tissue ( $p < 0.001$ ) weight in HF and HFMS mice after the additional four weeks of dietary treatment (**Table 7**). Liver weight to body weight ratio showed a significant difference ( $p = 0.017$ ) between the CMS and HFMS groups and VAT to body weight ratio reflected the significances in total weight ( $p < 0.001$ ) (**Table 7**). After twelve weeks of dietary treatment blood glucose ( $p < 0.001$ ) and plasma insulin levels ( $p = 0.003$ ) were significantly increased in all HF and HFMS mice suggesting that mice in both groups were hyperglycemic, developed hyperinsulinemia and that methyl-group supplementation did not attenuate these parameters (**Table 7**).

**Table 7.** Basal phenotypic parameters of mice fed the C, CMS, HF and HFMS diets for four weeks. Data are presented as mean  $\pm$  SEM ( $n = 8-9$ ). Different subscript letters indicates statistical significance ( $p < 0.05$ ). VAT was calculated by summing up the weight of epididymal, perirenal and mesenteric adipose tissue. Abbreviations: AUC, area under the curve; ipGTT, intraperitoneal glucose tolerance test; VAT, visceral adipose tissue.

	C	CMS	HF	HFMS
<b>Liver weight [g]</b>	1.40 $\pm$ 0.04 <sup>a</sup>	1.56 $\pm$ 0.04 <sup>ab</sup>	1.83 $\pm$ 0.11 <sup>b</sup>	1.70 $\pm$ 0.08 <sup>b</sup>
<b>% Liver / body weight</b>	4.37 $\pm$ 0.12 <sup>ab</sup>	4.58 $\pm$ 0.07 <sup>a</sup>	4.29 $\pm$ 0.13 <sup>ab</sup>	4.08 $\pm$ 0.10 <sup>b</sup>
<b>VAT weight [g]</b>	1.84 $\pm$ 0.15 <sup>a</sup>	2.15 $\pm$ 0.17 <sup>a</sup>	4.80 $\pm$ 0.37 <sup>b</sup>	4.56 $\pm$ 0.27 <sup>b</sup>
<b>% VAT / body weight</b>	5.67 $\pm$ 0.35 <sup>a</sup>	6.28 $\pm$ 0.36 <sup>a</sup>	11.19 $\pm$ 0.52 <sup>b</sup>	10.94 $\pm$ 0.38 <sup>b</sup>
<b>Blood glucose [mg / dl]</b>	136.9 $\pm$ 4.2 <sup>a</sup>	146.8 $\pm$ 4.2 <sup>a</sup>	171.6 $\pm$ 5.5 <sup>b</sup>	167.7 $\pm$ 1.9 <sup>b</sup>
<b>Serum insulin [ng / ml]</b>	1.42 $\pm$ 0.13 <sup>a</sup>	2.15 $\pm$ 0.48 <sup>ab</sup>	3.68 $\pm$ 0.70 <sup>b</sup>	3.01 $\pm$ 0.57 <sup>b</sup>
<b>ipGTT, AUC [mg / dl*min]</b>	14765 $\pm$ 2179	15053 $\pm$ 1340	19470 $\pm$ 3979	15554 $\pm$ 1808

After three weeks of therapeutic methyl-donor administration, glucose tolerance was assessed by an ipGTT. Data revealed a slightly delayed reduction of blood glucose levels in HF mice compared to C and CMS mice after 30 min ( $p = 0.007$ ) and 60 min ( $p = 0.003$ ) as shown **Figure 28**, but did not reach significance at the basis of the AUC (**Table 7**).

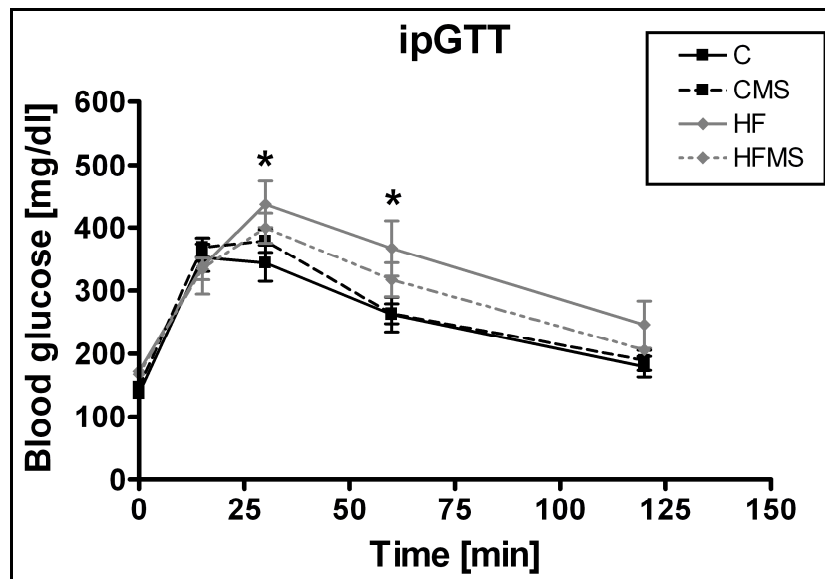


**Figure 28.** Intraperitoneal glucose tolerance test performed in mice receiving the C, CMS, HF and HFMS diets for four weeks. Data are presented as mean  $\pm$  SEM (n = 8-9). Asterisk indicates statistical significance between C and HF mice (time point 30 min) and between C and HF and CMS and HF mice (time point 60 min) ( $p < 0.05$ ).

### 3.3.2 Amino acid analyses reveal a specific plasma and liver metabolic-profile in methyl-group supplemented mice

To determine whether the methyl-group supplementation influences the metabolite-profile of the blood, the plasma concentrations of 31 amino acids and derivatives were analyzed by LC-MS / MS. Selected metabolites are presented in **Figure 29** and **Table 19**. L-serine ( $p = 0.007$ ) and sarcosine ( $p = 0.001$ ) were significantly increased and glycine ( $p < 0.001$ ) was significantly decreased in plasma of methyl-group supplemented CMS and HFMS mice. In addition, L-methionine ( $p = 0.064$ ) was marginally increased in blood of methyl-group supplemented CMS and HFMS mice. L-asparagine ( $p = 0.007$ ), L-citrulline ( $p = 0.013$ ), 3-methyl-histidine ( $p = 0.002$ ) and L-ornithine ( $p = 0.007$ ) were increased in HF or HFMS mice and L- $\alpha$ -amino adipic acid ( $p = 0.028$ ) was decreased in HF mice compared to C mice.

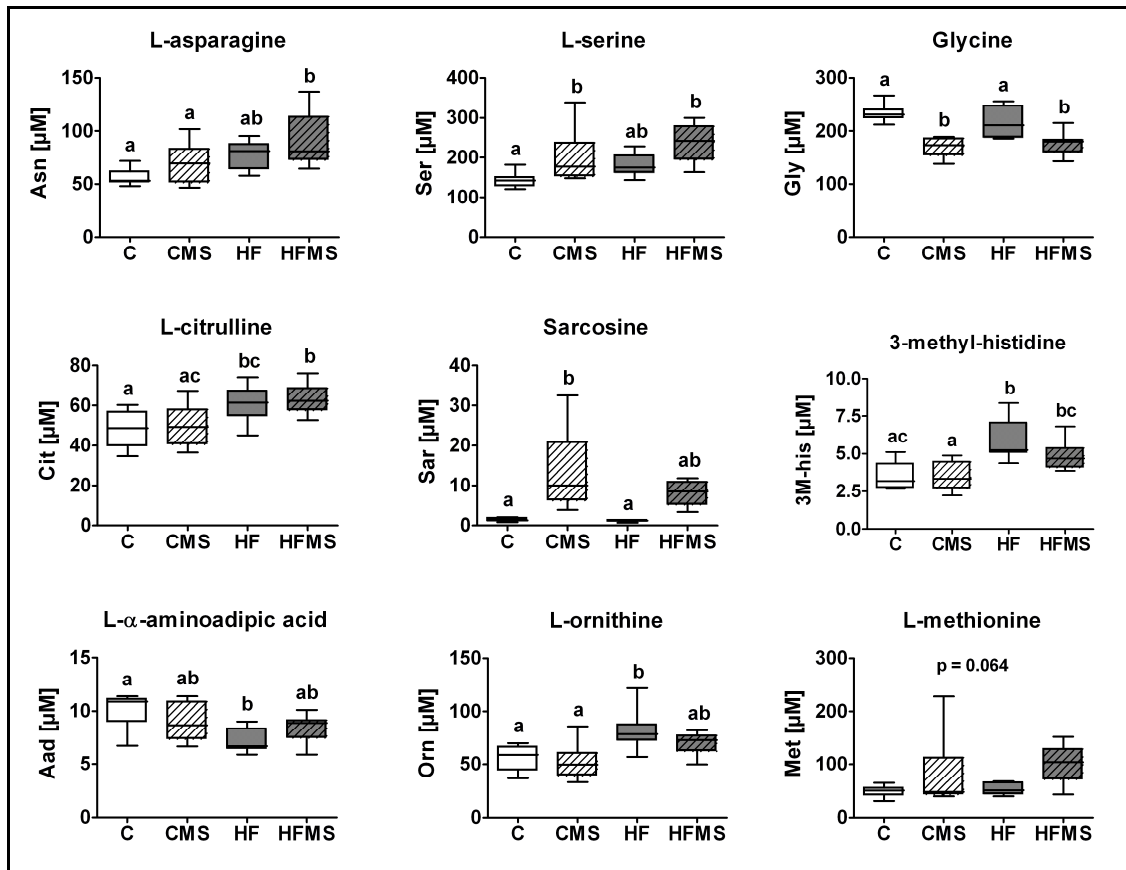


**Figure 29.** Analyses of plasma from animals receiving the C, CMS, HF and HFMS for four weeks. Data are presented as box and whisker plot ( $n = 8-9$ ). Open and grey boxes represent data from C and HF animals and open lined and grey lined boxes represent data from CMS and HFMS animals. Different subscript letters indicate statistical significance ( $p < 0.05$ ). Abbreviations: 3MHis, 3-methyl-histidine; Aad, L- $\alpha$ -aminoadipic acid; Asn, L-asparagine; Cit, L-citrulline; Gly, Glycine; Met, L-methionine; Orn, L-ornithine; Sar, Sarcosine; Ser, L-serine.

Furthermore the influence of dietary treatment and supplementation on blood plasma tHcy levels was determined in C and HF (8W) as well as C, CMS, HF and HFMS (12W) mice by HPLC and fluorescence detection. Interestingly, tHcy level of HF (8W) mice and HF (12W) mice were significantly decreased compared to the corresponding C mice ( $p = 0.001$ ). However, methyl-group supplementation significantly increased plasma tHcy in CMS mice ( $p < 0.001$ ) compared to C mice whereas no increase in tHcy level was observed in HFMS mice (**Figure 30**).

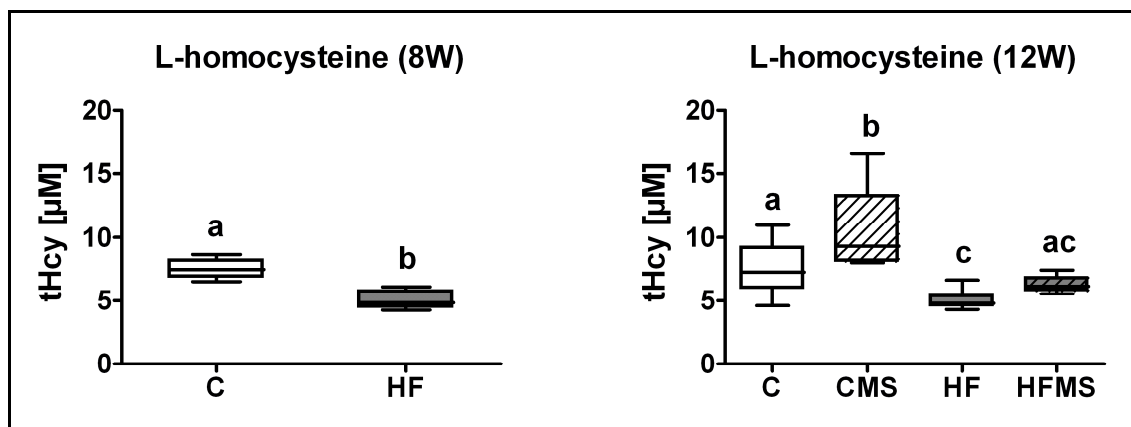


**Figure 30.** Analysis of plasma tHcy in animals on C and HF diets (8W) ( $n = 5$ ) and C, CMS, HF and HFMS diets (12W). Data are presented as box and whisker plot. Open and grey boxes represent data from C and HF animals and open lined and grey lined boxes represent data from CMS and HFMS animals. Different subscript letters indicate statistical significance ( $p < 0.05$ ).

In addition to the plasma metabolic profiling, the influence of methyl-group supplementation on hepatic amino acid metabolite level was determined in the liver of C, CMS, HF and HFMS mice as described before. Increased levels of sarcosine ( $p < 0.001$ ), L-serine ( $p = 0.004$ ), L-aspartate ( $p = 0.007$ ) and ethanolamine ( $p = 0.009$ ) and decreased levels of glycine ( $p < 0.001$ ) and L-citrulline ( $p = 0.002$ ) were observed in methyl-group supplemented mice compared to the corresponding C or HF animals (**Figure 31**). Furthermore, hydroxyproline ( $p = 0.016$ ), D,L- $\beta$ -aminoisobutyrate ( $p = 0.001$ ), L- $\alpha$ -amino-n-butyrate ( $p = 0.029$ ), L-ornithine ( $p = 0.005$ ), L-lysine ( $p = 0.002$ ), L-valine ( $p = 0.008$ ), L-isoleucine ( $p = 0.016$ ) and L-tryptophane ( $p = 0.009$ ) levels were significantly reduced in HF mice compared to C mice. The levels of taurine ( $p = 0.007$ ), L-asparagine ( $p = 0.034$ ), L-threonine ( $p = 0.035$ ), L-tyrosine ( $p = 0.007$ ), L-leucine ( $p = 0.016$ ) and L-phenylalanine ( $p = 0.037$ ) were also altered in the experimental mice by the dietary treatment (**Figure 31**). Interestingly,  $\beta$ -alanine was the only metabolite besides glycine and sarcosine showing significant difference between HF and HFMS livers ( $p = 0.015$ ). Unexpectedly, hepatic L-methionine levels were not affected (**Table 20**) by HF diet treatment or by therapeutic methyl-group supplementation.

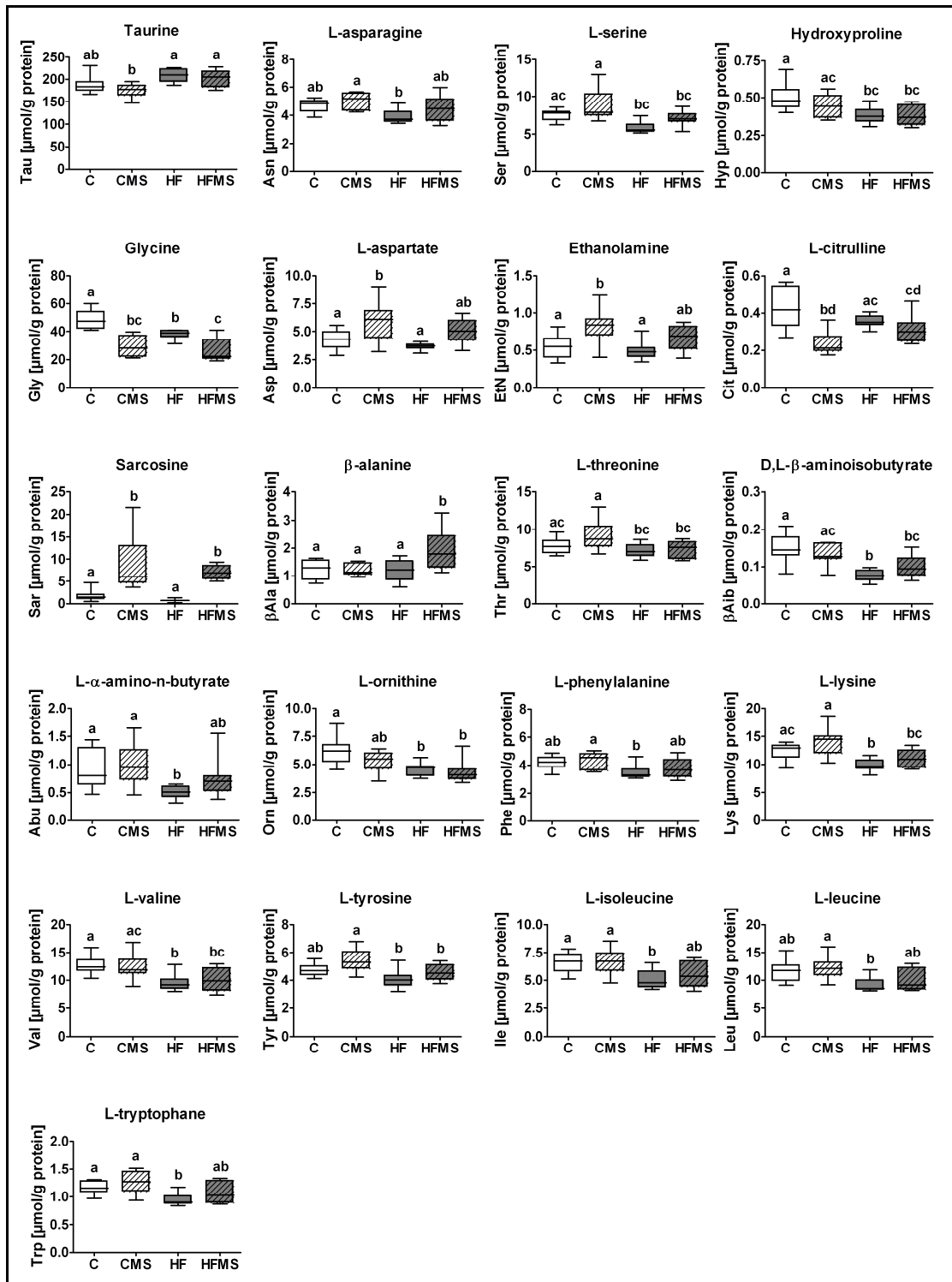


**Figure 31.** Analysis of liver tissue from animals receiving the C, CMS, HF and HFMS for four weeks. Data are presented as box and whisker plot ( $n = 8-9$ ). Open and grey boxes represent data from C and HF animals and open lined and grey lined boxes represent data from CMS and HFMS animals. Different subscript letters indicate statistical significance ( $p < 0.05$ ). Abbreviations: Abu, L- $\alpha$ -amino-n-butyrate;  $\beta\text{Ala}$ ,  $\beta$ -alanine;  $\beta\text{Aib}$ , D,L- $\beta$ -aminoisobutyrate; Asn, L-asparagine; Asp, L-aspartate; Cit, L-citrulline; EtN, Ethanolamine; Gly, Glycine; Hyp, Hydroxyproline; Ile, L-isoleucine; Leu, L-leucine; Lys, L-lysine; Orn, L-ornithine; Phe, L-phenylalanine; Sar, Sarcosine; Ser, L-serine; Tau, Taurine; Thr, L-threonine; Trp, L-tryptophane; Tyr, L-tyrosine; Val, L-valine.

The analyses of hepatic L-methionine levels in the liver of methyl-group supplemented mice were completed by the analysis of hepatic methionine cycle metabolites SAM, SAH, [SAM] / [SAH] ratio, and Hcy, as well as by the analysis of the transsulfuration product cystathionine in C and HF (8W) and C, CMS, HF and HFMS (12W) mice using HPLC-MS / MS and GC-MS / MS methods. The analyses of C and HF (8W) mice after eight weeks of dietary HF treatment revealed no differences (**Figure 32**). Additional four weeks of methyl-group supplementation significantly increased hepatic SAM levels in HFMS mice ( $p = 0.002$ ) but did not influence SAM levels in CMS mice. SAH levels were significantly increased in HFMS mice and decreased in HF mice (12W) ( $p < 0.001$ ). For HF mice, the decrease of hepatic SAH concentrations results also in an increased [SAM] / [SAH] ratio ( $p < 0.001$ ). Furthermore, the data analysis revealed that the supplementation significantly increased hepatic Hcy levels in CMS mice ( $p = 0.009$ ) and marginally in HFMS mice, while significantly increased cystathionine levels in HFMS mice ( $p = 0.001$ ) and marginally in CMS mice could be observed (**Figure 32**).

In addition to the analysis of metabolites in the methionine cycle and transsulfuration pathway, the influence of methyl-group supplementation on polyamine biosynthesis via determination of biogenic amines by LC-MS / MS was performed (**Table 21**). No significant influence on hepatic biogenic amine concentrations was observed in the experimental trial except for sarcosine which was significantly increased in CMS and HFMS mice ( $p < 0.001$ ) and for phenylethylamine (PEA) ( $p < 0.001$ ) which was significantly decreased only in CMS mice ( $p < 0.001$ ), whereas in HF and HFMS mice PEA was below the detection limit.



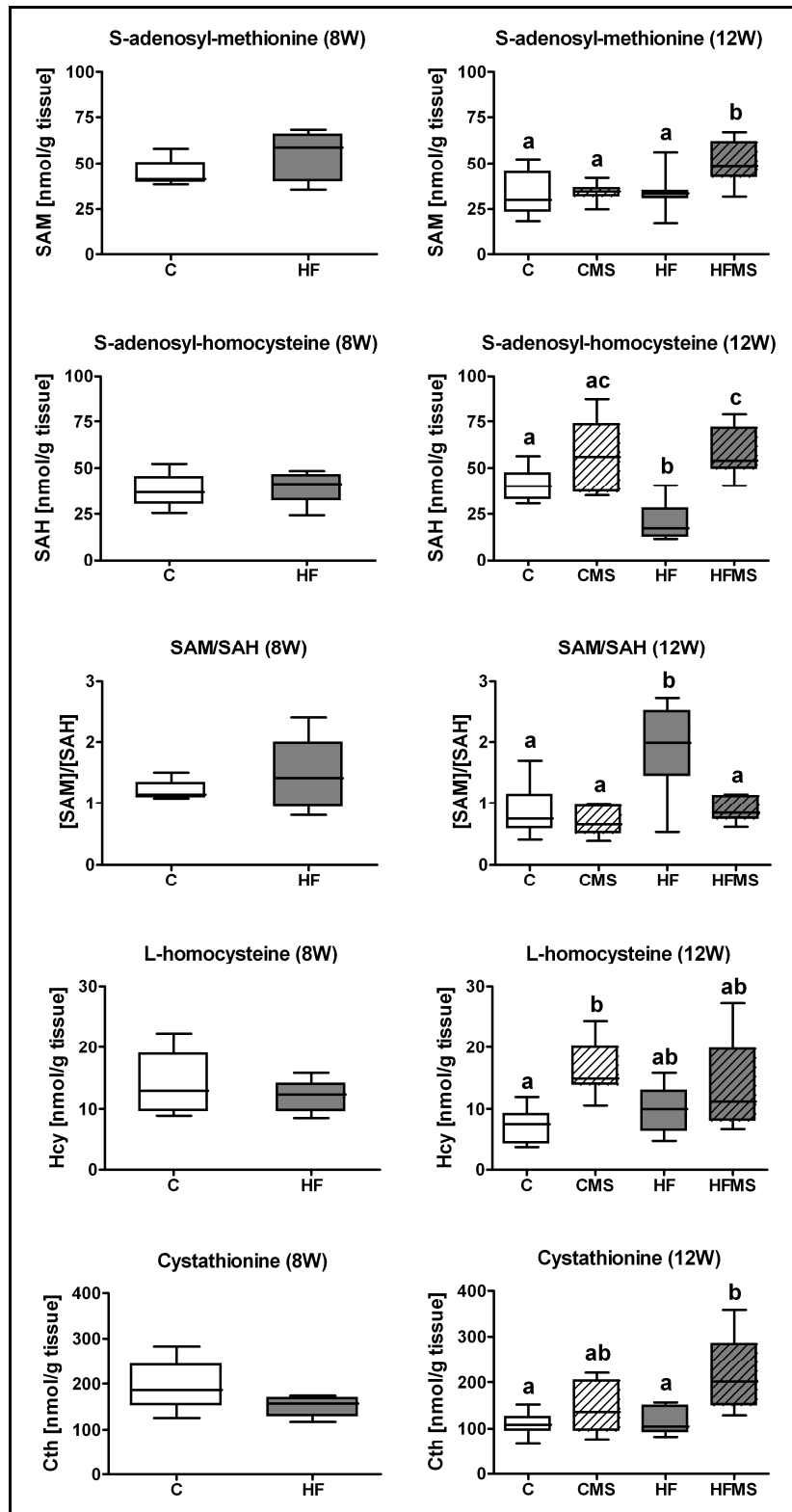


**Figure 32.** Analysis of SAM, SAH, [SAM] / [SAH] ratio, Hcy and cystathionine in the liver of C and HF (8W) mice (n = 4-5) and C, CMS, HF and HFMS mice (n = 7-9) is depicted. Data are presented as box and whisker plot. Open and grey boxes represent data from C and HF animals and open lined and grey lined boxes represent data from CMS and HFMS animals. Different subscript letters indicate statistical significance (p < 0.05). Abbreviations: Cth, Cystathionine; Hcy, Homocysteine; SAH, S-adenosyl-homocysteine; SAM, S-adenosyl-methionine.

### 3.3.3 Hepatic C1-metabolism gene and protein expression are affected by methyl-group supplementation in DIO mice

Data of the HF feeding experiment described here (see 3.1) showed that DIO induced NAFLD led to altered BHMT and CBS gene and protein expression in HF mice compared to C mice after twelve weeks of feeding. To assess whether HF diet induced differences can be changed by an increased methyl-group supply, expression of BHMT and CBS were assessed in C, CMS, HF and HFMS mice by qRT-PCR and Western blot analysis (**Figure 33**, **Figure 34**). HF diet feeding for eight weeks induced an increased gene expression of *Bhmt* by  $61.9 \pm 8.2\%$  ( $p = 0.003$ ) and a decreased gene expression of *Cbs* to  $78.9 \pm 4.5\%$  of control ( $p = 0.047$ ) in HF (8W) mice. The subsequent methyl-group supplementation in CMS and HFMS mice increased the *Bhmt* gene expression by  $129.5 \pm 20.9\%$  in CMS mice and by  $83.9 \pm 14.5\%$  in HFMS mice compared to C mice ( $p < 0.001$ ). Surprisingly, the previously identified increase in *Bhmt* gene expression in HF mice at 8 weeks could not be confirmed in HF mice fed for 12 weeks. The down-regulation of *Cbs* gene expression as observed in HF mice at 8 weeks was however also found in HF mice at 12 weeks ( $p = 0.007$ ), whereas methyl-group supplementation did not reveal a reduced *Cbs* mRNA expression in HFMS mice compared to HF mice. Interestingly, in CMS mice (12W) *Cbs* mRNA expression was reduced upon methyl-group supplementation compared to C mice (12W).

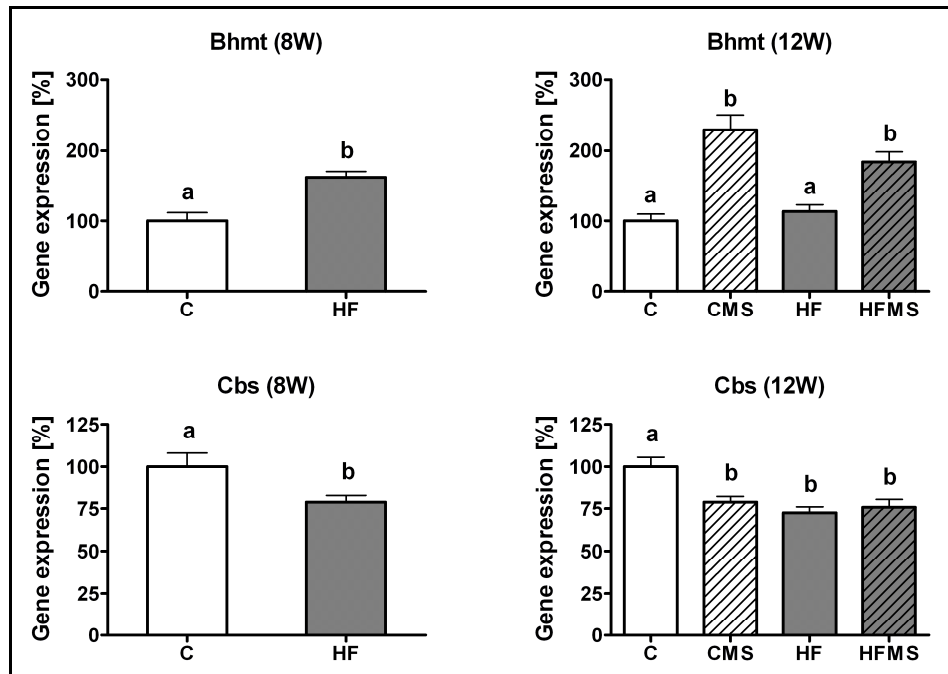


**Figure 33.** Hepatic *Bhmt* and *Cbs* mRNA expression levels in liver of C (8W) and HF mice at week eight ( $n = 5$ ) and C, CMS, HF and HFMS mice at week twelve ( $n = 8-9$ ). Data are presented as mean  $\pm$  SEM. Open and grey columns represent data from C and HF animals and open lined and grey lined columns represent data from CMS and HFMS animals. Different subscript letters indicate statistical significance ( $p < 0.05$ ). Abbreviations: *Bhmt*, Betaine-homocysteine methyltransferase; *Cbs*, Cystathionine  $\beta$ -synthase.

The protein expression analysis, revealed no differences in BHMT or CBS levels after eight weeks of C or HF diet feeding. However, after additional four weeks of HF diet feeding significantly increased BHMT by  $33.8 \pm 8.8\%$  ( $p < 0.001$ ) and decreased CBS protein expression to  $70.1 \pm 6.8\%$  of control ( $p < 0.001$ ) in HF mice compared to C mice was detected. Therapeutic methyl-group supplementation led to a significantly increased BHMT expression by  $70.0 \pm 7.6\%$  and by  $53.5 \pm 4.7\%$  in CMS and HFMS mice ( $p < 0.001$ ). In addition, in CMS and HFMS mice significantly reduced hepatic CBS expression to  $50.6 \pm 4.7\%$  and to  $62.9 \pm 5.4\%$  of control was observed ( $p < 0.001$ ).

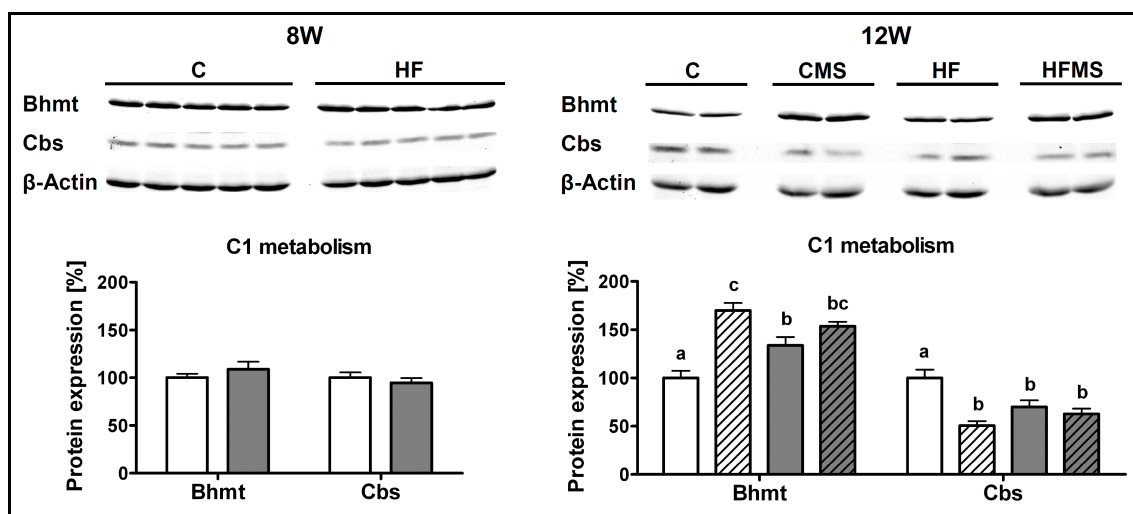


**Figure 34.** Effect of eight weeks (left,  $n = 5$ ) and additional four weeks of dietary treatment (right,  $n = 8-9$ ) on hepatic BHMT and CBS protein expression levels. Data are presented as mean  $\pm$  SEM. Open and grey columns represent data from C and HF animals and open lined and grey lined columns represent data from CMS and HFMS animals. Different subscript letters indicate statistical significance ( $p < 0.05$ ). Abbreviations: Bhmt, Betaine-homocysteine methyltransferase; Cbs, Cystathionine  $\beta$ -synthase.

### 3.3.4 Hepatic steatosis and hepatic free fatty acids are reduced while free fatty acids in blood plasma are unaffected in methyl-group supplemented DIO mice

To assess whether dietary methyl-group supplementation can change NEFA concentrations in blood, plasma NEFA concentrations in C, CMS, HF and HFMS mice were measured by colorimetric analysis. NEFA concentrations were marginally increased in plasma after eight weeks on HF diet compared to C mice (**Figure 35**). However, this effect was not observed anymore after the additional four weeks of dietary treatment (12W) between HF and C mice. Moreover, NEFA concentrations measured for CMS and HFMS mice were in a similar range (**Figure 35**).

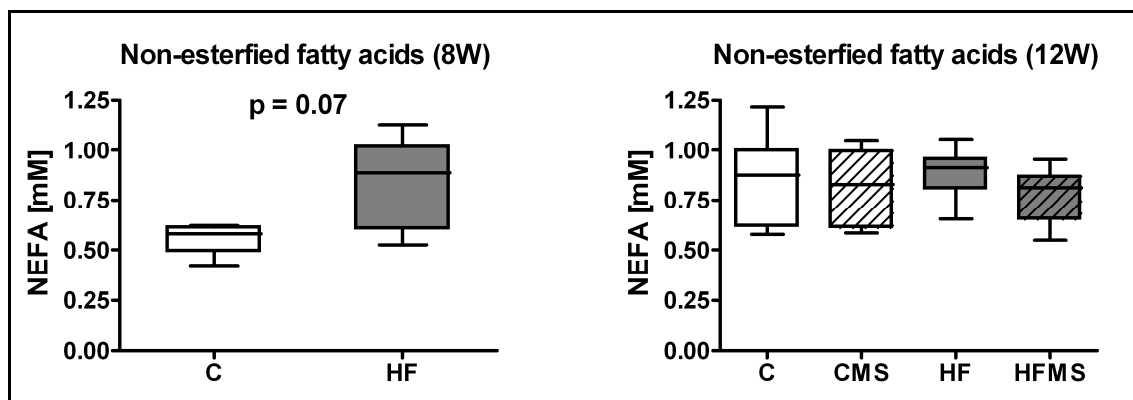


**Figure 35.** Plasma non-esterified fatty acids in C, CMS, HF and HFMS mice after eight weeks ( $n = 5$ ) and twelve weeks ( $n = 8-9$ ) of dietary treatment. Open and grey boxes represent data from C and HF animals and open lined and grey lined boxes represent data from CMS and HFMS animals. Data are presented as box and whisker plot. Different subscript letters indicate statistical significance ( $p < 0.05$ ). Abbreviations: NEFA, non-esterified fatty acids; TG, triacylglycerol.

To analyze whether feeding HF diet for eight weeks induced hepatic steatosis and whether a subsequent methyl-group supplementation for four weeks alleviated the progression of hepatic steatosis in HFMS mice, TG levels were measured in livers of experimental mice by an enzymatic colorimetric assay (**Figure 36**). Furthermore the amount of hepatic NEFA and total PL content were determined (**Figure 36**). TG accumulation was significantly increased in HF (8W) livers to  $497.4 \pm 42.7$  mg / g protein after eight weeks of HF treatment compared to  $204.3 \pm 12.6$  mg / g protein in C mice ( $p = 0.003$ ). After additional four weeks of HF-treatment, HF mice (12W) further increased TG levels to  $708.0 \pm 89.1$  mg / g protein compared to  $221.9 \pm 13.4$  mg / g protein in C mice (12W). The accumulation of TG was alleviated in livers from HFMS mice (12W) to  $463.3 \pm 42.1$  mg / g protein upon methyl-group supplementation ( $p < 0.001$ ) compared to HF. Interestingly, CMS mice at 12 weeks also showed reduced hepatic TG concentrations of  $175.8 \pm 9.6$  mg / g protein as compared to  $221.9 \pm 13.4$  mg / g protein in C mice without reaching significance in the Tukey's Multiple Comparison post hoc test ( $p > 0.05$ ). Hepatic free fatty acids and total PL were not different at 8 weeks. However, NEFA significantly increased during the four weeks of treatment in livers of HF mice, whereas NEFA content did not increase in HFMS mice ( $p < 0.001$ ). Surprisingly total PL were increased in HF and HFMS mice at 12 weeks ( $p = 0.001$ ), which contradicts the decrease in PL content in HF mice described in a previous analysis (138, 139).

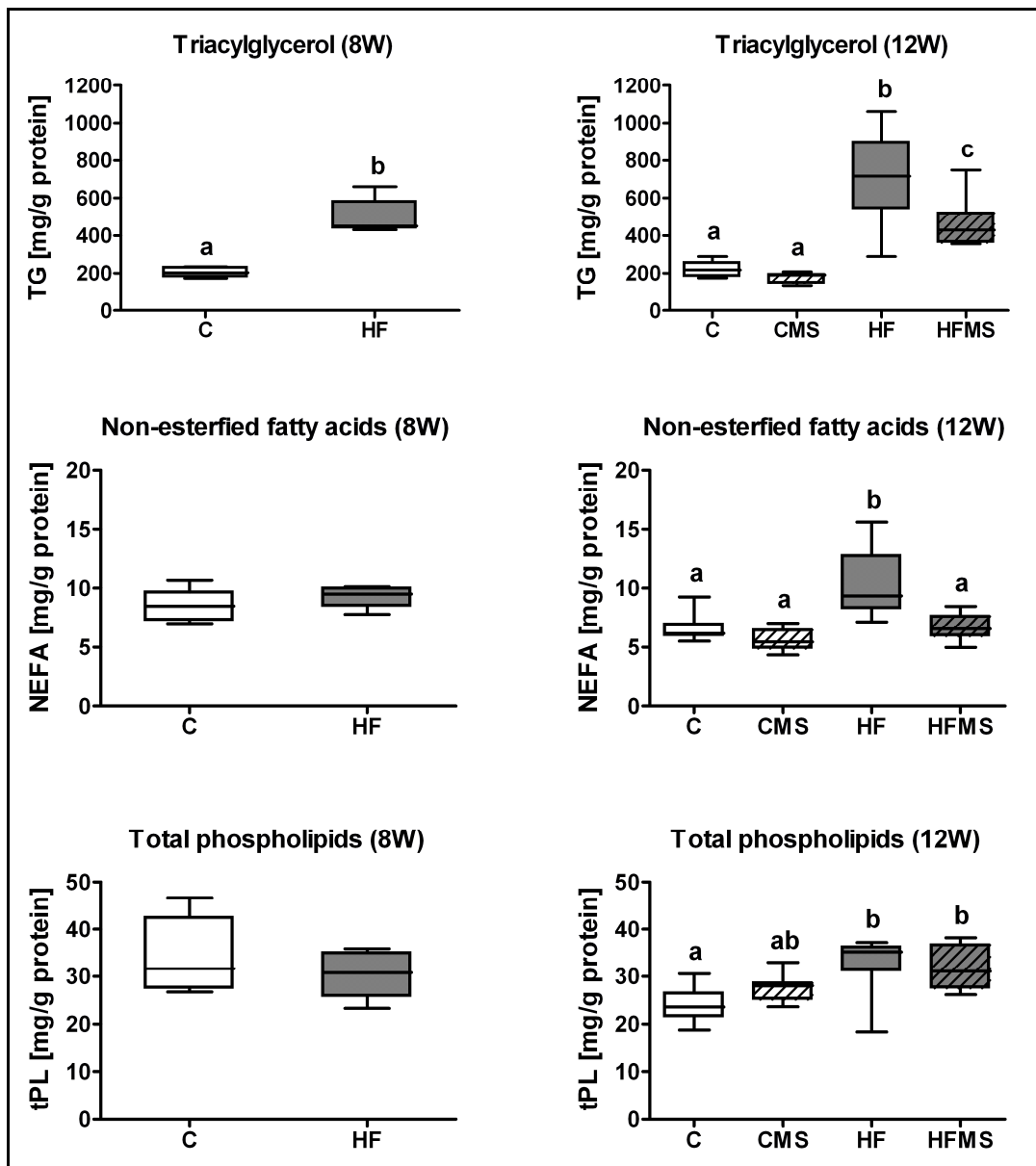


**Figure 36.** Hepatic triacylglycerol, non-esterified fatty acids and total phospholipids in C, CMS, HF and HFMS mice after eight weeks (8W) ( $n = 5$ ) and twelve weeks (12W) ( $n = 8-9$ ) of dietary treatment. Open and grey boxes represent data from C and HF animals and open lined and grey lined boxes represent data from CMS and HFMS animals. Data are presented as box and whisker plot. Different subscript letters indicate statistical significance ( $p < 0.05$ ). Abbreviations: NEFA, non-esterified fatty acids; tPL, total phospholipids; TG, triacylglycerol.

To visualize the alleviation of hepatic TG accumulation by methyl-group supplementation histological analysis of livers from C, CMS, HF and HFMS mice at eight and twelve weeks was performed by Oilred O staining of cryosections (**Figure 37**). The microscopic analysis revealed an apparent increase in hepatic TG staining in HF mice at eight weeks and twelve weeks compared to corresponding C mice whereas in the methyl-group supplemented HFMS mice a reduced TG content by Oilred O staining compared to the HF group was observed.

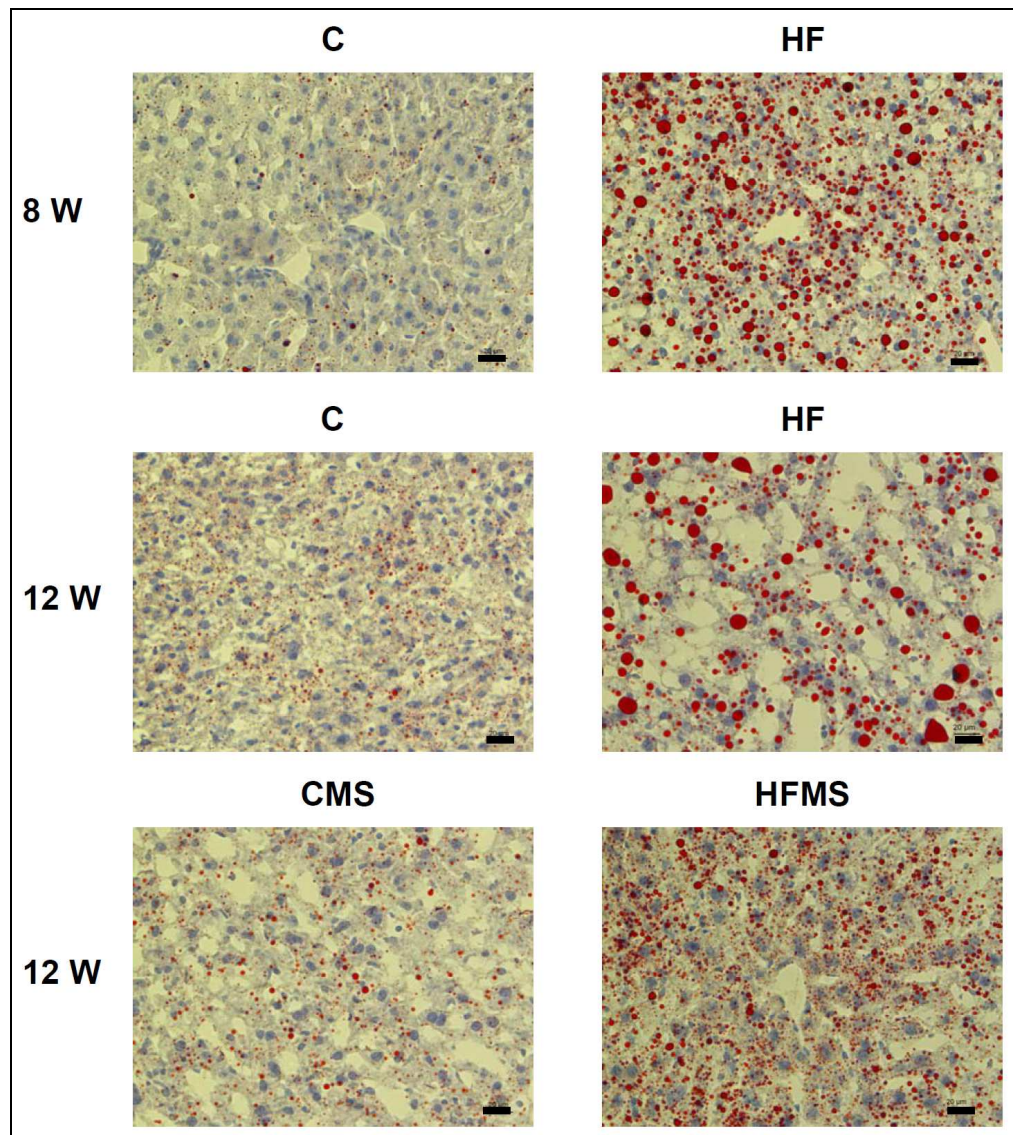


**Figure 37.** Representative histological analysis of livers from C, CMS, HF and HFMS mice after eight weeks and additional four weeks in cryosection with oilred O staining. Scale bar indicates 20  $\mu\text{m}$ . Magnification, 400x.

### 3.3.5 Reduced Fasn mRNA expression and increased PPAR $\alpha$ activity and AMPK $\alpha$ phosphorylation state suggests a reduced *de novo* lipogenesis and increased $\beta$ -oxidation in methyl-group supplemented DIO mice

The reduced TG accumulation in HFMS mice upon methyl-group supplementation could arise from a reduced hepatic fatty acid import, reduced *de novo* fatty acid synthesis or increased fatty acid oxidation or VLDL mediated TG export. Therefore, the hepatic gene expression of Srebp1c and Fasn and SREPB1 activation were analyzed by qRT-PCR and Western blot experiments (**Figure 38**). Analysis of the Srebp1c gene revealed no change in gene expression between the mice after four weeks of methyl-group supplementation (12W), although a tendency for a reduced expression level was observed in methyl-group supplemented mice ( $p = 0.045$ ). Hepatic Fasn gene

expression was significantly decreased in CMS and HFMS mice compared to C mice ( $p = 0.013$ ) and reduced in HF mice without reaching significance. The analysis of SREBP1 activation by Western blot revealed no difference in activated SREBP1 levels suggesting no alterations in proteolytical cleavage or TF activation in the liver of experimental mice.

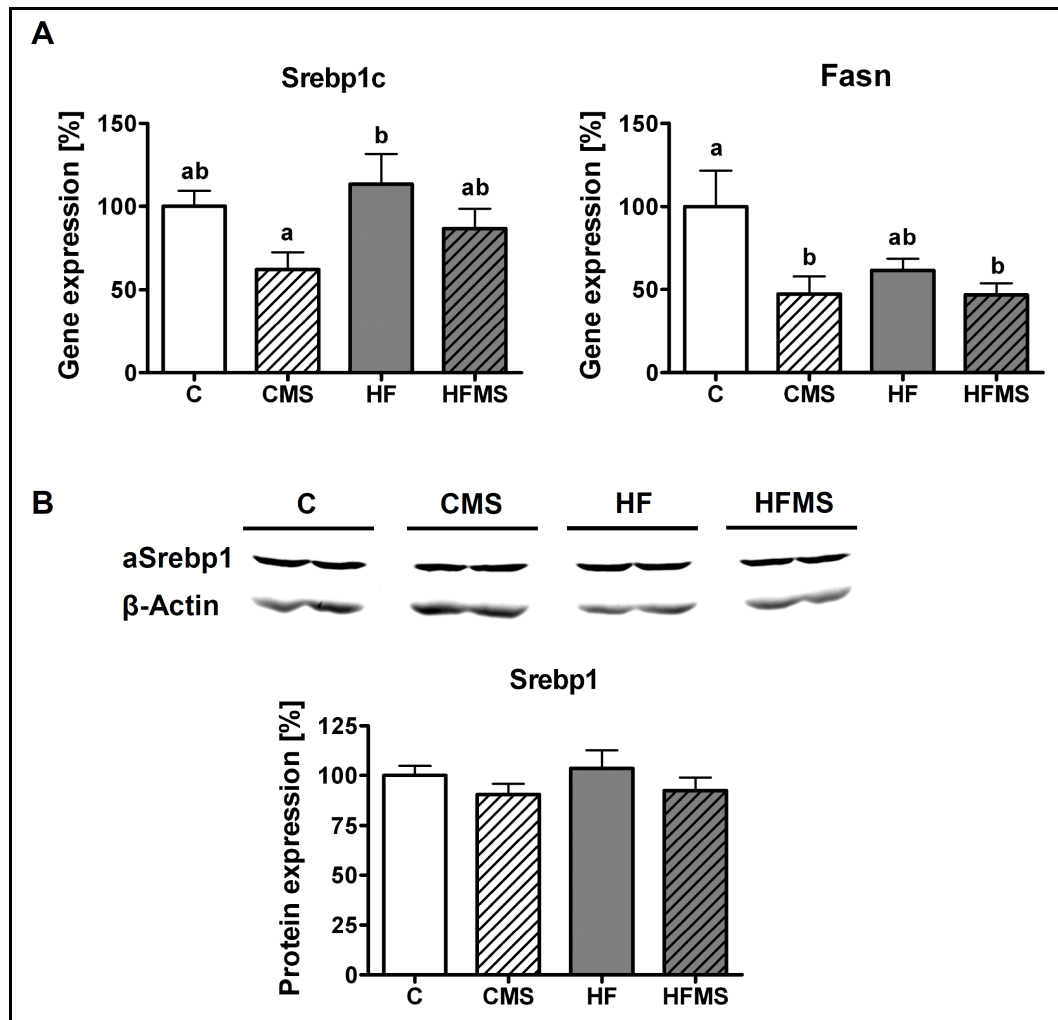


**Figure 38.** Effects of diets on gene and protein expression of marker enzymes implicated in *de novo* lipogenesis. In **A**, *Srebp1c* and *Fasn* mRNA levels and in **B** activation of SREBP1 (aSREBP1) are depicted. Data are presented as mean  $\pm$  SEM ( $n = 8-9$ ). Open and grey columns represent data from C and HF animals and open lined and grey lined columns represent data from CMS and HFMS animals. Different subscript letters indicate statistical significance ( $p < 0.05$ ). Abbreviations: aSrebp1, soluble activated Srebp1; Fasn, Fatty acid synthase.

Hepatic mRNA expression analysis of genes operating in the  $\beta$ -oxidation of fatty acids in HF mice of a previous HF feeding trial reported in this thesis (see 3.1.4) revealed an increased expression of *Cpt1a* and *Acox1* in HF mice. Analyzing the *Cpt1a* gene expression in the methyl-group supplementation experiment showed an increased mRNA level in HF and HFMS mice compared to C and CMS mice ( $p < 0.001$ ) whereas

no enhanced Cpt1a gene expression was observed in HFMS mice compared to HF mice (**Figure 39**).

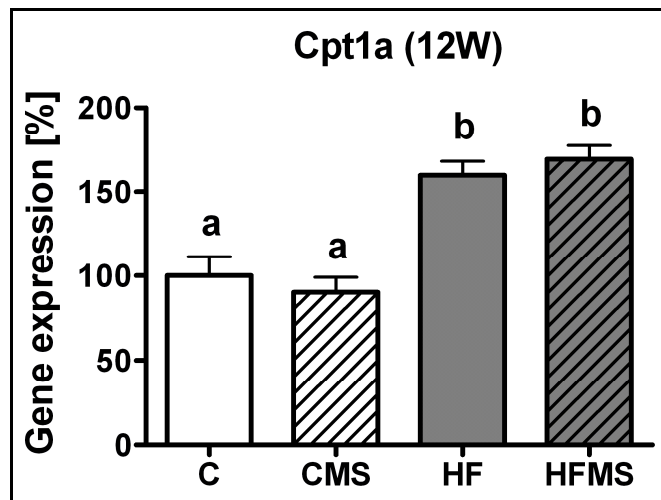


**Figure 39.** Hepatic mRNA expression levels of Cpt1a gene in C, CMS, HF and HFMS mice after 12 weeks (n = 8-9). Data are presented as mean  $\pm$  SEM. Open and grey columns represent data from C and HF animals and open lined and grey lined columns represent data from CMS and HFMS animals. Different subscript letters indicate statistical significance ( $p < 0.05$ ). Abbreviations: Cpt1a, Carnitine palmitoyltransferase 1a.

AMPK is a central metabolic regulator of cellular energy balance and can influence cellular fatty acid oxidation (31). Therefore, changes in the AMPK $\alpha$  phosphorylation status were determined and used as an indication for alterations in hepatic  $\beta$ -oxidation. Analysis of AMPK $\alpha$  protein levels and phosphorylation state in livers from C, CMS, HF and HFMS mice at twelve weeks by Western blot showed that AMPK $\alpha$  protein remained unchanged by the dietary treatment. However, AMPK $\alpha$  activation determined by AMPK $\alpha$  phosphorylation was significantly increased in HF and methyl-group supplemented mice by  $218.5 \pm 39.7\%$  in HF mice,  $273.3 \pm 20.5\%$  in CMS mice and  $416.8 \pm 57.5\%$  in HFMS mice ( $p < 0.001$ ) as compared to C mice (**Figure 40**). Furthermore, HFMS mice showed the highest AMPK $\alpha$  phosphorylation state which was significantly increased compared to HF mice.



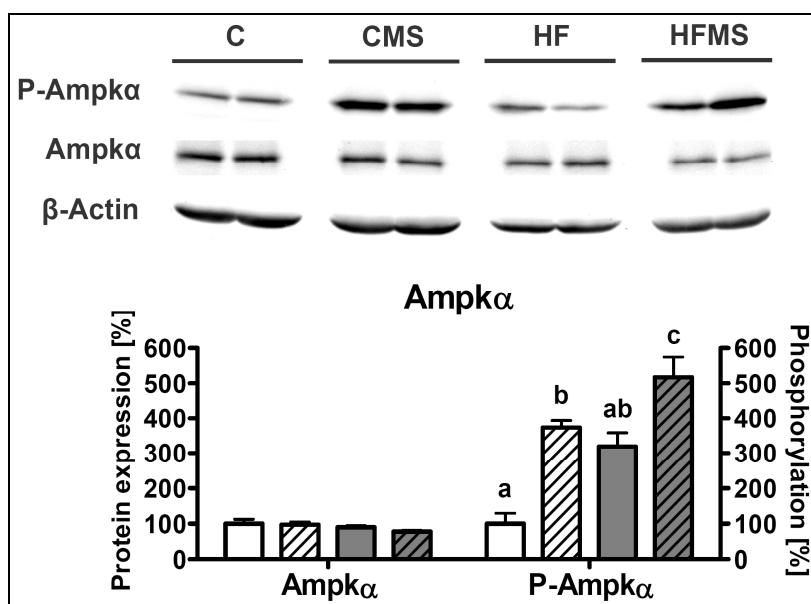


**Figure 40.** Effect of four weeks dietary methyl-group supplementation on hepatic AMPK $\alpha$  expression and phosphorylation state. Data are presented as mean  $\pm$  SEM (n = 7-9). Open and grey columns represent data from C and HF animals and open lined and grey lined columns represent data from CMS and HFMS animals. Different subscript letters indicate statistical significance ( $p < 0.05$ ). Abbreviations: AMPK $\alpha$ , AMP-activated protein kinase  $\alpha$ ; P-AMPK $\alpha$ , Phosphorylated AMP-activated protein kinase  $\alpha$  (Thr172).

### 3.3.6 Methyl-group supplementation leads to reduced hepatic acyl-carnitine concentrations in CMS and HFMS mice, supporting improved $\beta$ -oxidation in methyl-group supplemented mice

The increased phosphorylation of AMPK $\alpha$  in livers from methyl-group supplemented mice suggested an improved hepatic  $\beta$ -oxidation in these mice. To determine whether increased AMPK $\alpha$  phosphorylation leads to altered  $\beta$ -oxidation, hepatic carnitine and acyl-carnitine concentrations were determined in supplemented mice by FIA-MS with data provided in **Figure 41** and **Table 22**. Quantification of free carnitine and long-chain acyl-carnitine concentrations revealed significantly reduced DL-carnitine (C0) ( $p < 0.001$ ), C16 ( $p = 0.002$ ), C16:1 ( $p = 0.013$ ) and C18 ( $p < 0.001$ ) and a tendency for reduced C18:1 long-chain acyl-carnitine concentrations in CMS and HFMS mice compared to their corresponding C and HF mice, respectively. Furthermore, the treatment also decreased the concentrations of C2 ( $p < 0.001$ ), C3 ( $p = 0.002$ ), C3-DC / C4-OH ( $p < 0.001$ ), C4 ( $p < 0.001$ ), C5 ( $p < 0.001$ ), C5-DC / C6-OH ( $p < 0.001$ ), C5-M-DC ( $p < 0.001$ ) and C6 / C4:1-DC ( $p < 0.001$ ) short-chain acyl-carnitines in livers derived from methyl-group supplemented mice. Interestingly, medium-chain acyl-carnitine concentrations like for C7-DC, C8, C9, C10, C10:1, C12 and C12:1 were not significantly reduced by methyl-group supplementation, however C8 ( $p < 0.001$ ), C9 ( $p < 0.001$ ) and C10:1 ( $p < 0.001$ ) medium-chain acyl-carnitines were significantly

increased in HF and HFMS mice compared to C and CMS mice, suggesting an influence of HF diets on medium-chain acyl-carnitine concentrations in the liver.

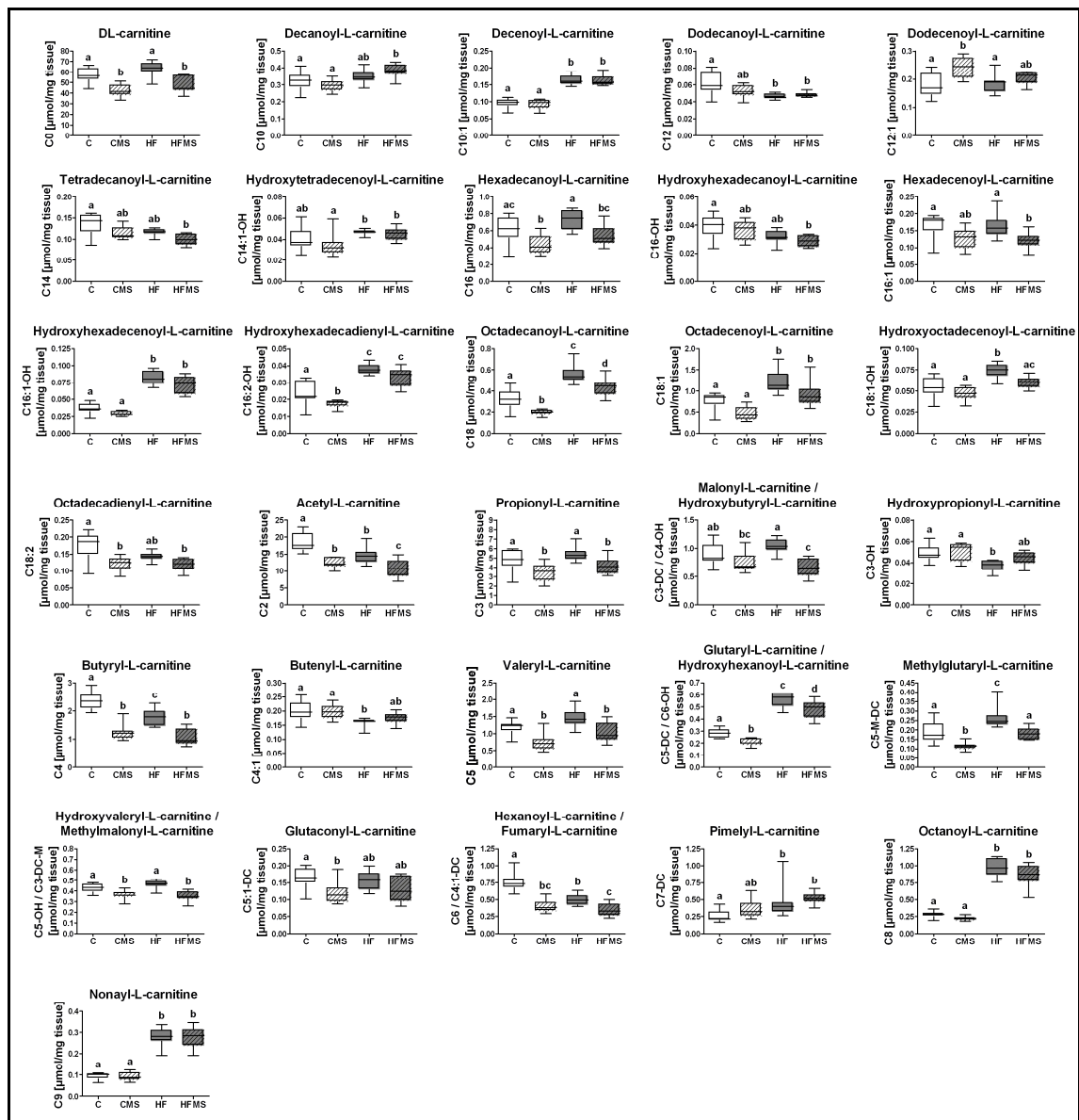


**Figure 41.** Analysis of selected hepatic carnitine and acyl-carnitine concentrations in liver tissues from C, CMS, HF and HFMS mice after four weeks of dietary methyl-group supplementation. Data are presented as box and whisker plot ( $n = 8-9$ ). Open and grey boxes represent data from C and HF animals and open lined and grey lined boxes represent data from CMS and HFMS animals. Different subscript letters indicate statistical significance ( $p < 0.05$ ). Abbreviations: C0, DL-carnitine; C10, Decanoyl-L-carnitine; C10:1 Decenoyl-L-carnitine; C12, Dodecanoyl-L-carnitine; C12:1, Dodecenoyl-L-carnitine; C14, Tetradecanoyl-L-carnitine; C14:1-OH, Hydroxytetradecenoyl-L-carnitine; C16, Hexadecanoyl-L-carnitine; C16-OH, Hydroxyhexadecenoyl-L-carnitine; C16:1, Hexadecenoyl-L-carnitine; C16:1-OH, Hydroxyhexadecenoyl-L-carnitine; C16:2-OH, Hydroxyhexadecadienyl-L-carnitine; C18, Octadecanoyl-L-carnitine; C18:1, Octadecenoyl-L-carnitine; C18:1-OH, Hydroxyoctadecenoyl-L-carnitine; C18:2, Octadecadienyl-L-carnitine; C2, Acetyl-L-carnitine; C3, Propionyl-L-carnitine; C3-DC / C4-OH, Malonyl-L-carnitine / Hydroxybutyryl-L-carnitine; C3-OH, Hydroxypropionyl-L-carnitine; C4,

Butyryl-L-carnitine; C4:1, Butenyl-L-carnitine; C5, Valeryl-L-carnitine; C5-DC / C6-OH, Glutaryl-L-carnitine / Hydroxyhexanoyl-L-carnitine; C5-M-DC, Methylglutaryl-L-carnitine; C5-OH / C3-DC-M, Methylmalonyl-L-carnitine / Hydroxyvaleryl-L-carnitine; C5:1-DC, Glutaconyl-L-carnitine; C6 / C4:1-DC, Fumaryl-L-carnitine / Hexanoyl-L-carnitine; C7-DC, Pimelyl-L-carnitine; C8, Octanoyl-L-carnitine; C9, Nonanyl-L-carnitine.

### 3.3.7 Analysis of hepatic phospholipid signature reveals no significant influence of methyl-group supplementation, but an increase of specific phospholipids by HF diets

The indications for an enhanced fatty acid oxidation in CMS and HFMS mice by gene and protein expression analyses suggested that the methyl-group supplementation also could influence hepatic PL classes due to increased delivery of methyl-groups to the PEMT pathway for PC biosynthesis. Therefore, hepatic PC, ether-PC, lyso-PC, hydroxyl-sphingomyelin (SM-OH) and sphingomyelin (SM) concentrations in livers from C, CMS, HF and HFMS mice were analyzed by FIA-MS. Surprisingly, the analysis revealed that in CMS and HFMS mice none of the determined analytes showed a significant difference compared to their corresponding C or HF mice (**Table 8**). However, 62 out of 105 analytes revealed a significant difference between HF diet (HF, HFMS) and C diet (C, CMS) mice, which was independent of the supplementation. Principally, medium-chain PC (PC aa) concentrations were significantly reduced in HF and HFMS mice (PC aa C30:0  $p = 0.001$ , PC aa C32:0  $p < 0.001$ , PC aa C32:1  $p < 0.001$ , PC aa C32:2  $p < 0.001$ , PC aa C34:3  $p < 0.001$ , PC aa C34:4  $p = 0.002$ ), while long-chain PC (PC aa) concentrations were mainly significantly increased in HF and HFMS mice compared to C and CMS animals, respectively (PC aa C36:1  $p < 0.001$ , PC aa C38:0  $p < 0.001$ , PC aa C38:3  $p < 0.001$ , PC aa C38:4  $p < 0.001$ , PC aa C38:5  $p < 0.001$ , PC aa C40:5  $p < 0.001$ ). Furthermore, 18 out of 23 significantly regulated ether-PC subclasses (PC ae) showed increased concentrations in steatotic livers (HF, HFMS) compared to normal livers (C, CMS) (PC ae C34:0  $p < 0.001$ , PC ae C34:1  $p < 0.001$ , PC ae C36:0  $p = 0.001$ , PC ae C36:1  $p < 0.001$ , PC ae C36:2  $p < 0.001$ , PC ae C36:3  $p < 0.001$ , PC ae C36:4  $p < 0.001$ , PC ae C38:1  $p < 0.001$ , PC ae C38:2  $p < 0.001$ , PC ae C38:3  $p < 0.001$ , PC ae C38:4  $p < 0.001$ , PC ae C38:5  $p < 0.001$ , PC ae C38:6  $p < 0.001$ , PC ae C40:3  $p < 0.001$ , PC ae C40:4  $p < 0.001$ , PC ae C40:5  $p < 0.001$ , PC ae C40:6  $p < 0.001$ , PC ae C42:5  $p < 0.001$ ), suggesting that HF diet induced NAFLD increase hepatic ether phospholipids. The HF diet feeding changed also hepatic lyso-PC concentrations. Mainly, increased levels for lysoPC a C18:0 ( $p < 0.001$ ) and decreased level of lysoPC a C18:2 ( $p < 0.001$ ) were detected in HF and HFMS mice compared to C and CMS mice. In addition, hydroxyl-sphingomyelin concentrations were also affected by the dietary treatment. SM (OH) C14:1 ( $p = 0.006$ ) and SM (OH) C16:1 concentrations were significantly increased in

HF mice ( $p < 0.001$ ), while significantly decreased SM (OH) C24:1 level were measured in CMS mice ( $p = 0.034$ ). Furthermore, sphingomyelin concentrations were significantly increased for SM C18:0, SM C18:1 and significantly decreased for SM C24:0 and SM C24:1 in HF and HFMS animals.

**Table 8.** Concentrations of PC, lyso-PC, hydroxyl- and sphingomyelin metabolites in liver tissues of mice fed C, CMS, HF and HFMS diets for four weeks. Data are presented as mean  $\pm$  SEM ( $n = 8-9$ ). Bold numbers and different subscript letters indicate statistical significance ( $p < 0.05$ ). Abbreviations: PC aa, Phosphatidylcholine diacyl; PC ae, Phosphatidylcholine acyl-alkyl; SM (OH), Hydroxysphingomyeline; SM, Sphingomyeline.

Metabolite [ $\mu\text{mol/mg tissue}$ ]	C	CMS	HF	HFMS
PC aa C24:0	1.37 $\pm$ 0.18	1.13 $\pm$ 0.18	1.39 $\pm$ 0.23	1.66 $\pm$ 0.27
PC aa C26:0	4.59 $\pm$ 0.89	4.66 $\pm$ 0.93	3.05 $\pm$ 0.63	3.92 $\pm$ 0.72
PC aa C28:1	1.50 $\pm$ 0.22	1.37 $\pm$ 0.19	1.29 $\pm$ 0.19	1.48 $\pm$ 0.21
PC aa C30:0	<b>5.63 <math>\pm</math> 0.26<sup>a</sup></b>	<b>5.42 <math>\pm</math> 0.17<sup>a</sup></b>	<b>4.49 <math>\pm</math> 0.21<sup>b</sup></b>	<b>4.51 <math>\pm</math> 0.14<sup>b</sup></b>
PC aa C30:2	0.73 $\pm$ 0.11	0.60 $\pm$ 0.09	0.66 $\pm$ 0.11	0.78 $\pm$ 0.13
PC aa C32:0	<b>233.42 <math>\pm</math> 8.66<sup>a</sup></b>	<b>190.71 <math>\pm</math> 4.84<sup>b</sup></b>	<b>153.70 <math>\pm</math> 9.36<sup>c</sup></b>	<b>147.61 <math>\pm</math> 5.48<sup>c</sup></b>
PC aa C32:1	<b>320.77 <math>\pm</math> 21.63<sup>a</sup></b>	<b>380.67 <math>\pm</math> 19.39<sup>a</sup></b>	<b>199.79 <math>\pm</math> 9.73<sup>b</sup></b>	<b>189.49 <math>\pm</math> 5.64<sup>b</sup></b>
PC aa C32:2	<b>55.15 <math>\pm</math> 2.86<sup>a</sup></b>	<b>67.79 <math>\pm</math> 2.95<sup>b</sup></b>	<b>32.43 <math>\pm</math> 1.58<sup>c</sup></b>	<b>32.10 <math>\pm</math> 1.41<sup>c</sup></b>
PC aa C32:3	3.02 $\pm$ 0.20	3.04 $\pm$ 0.14	2.83 $\pm$ 0.20	3.03 $\pm$ 0.23
PC aa C34:1	964.50 $\pm$ 49.03	910.28 $\pm$ 50.06	860.80 $\pm$ 27.16	988.33 $\pm$ 32.59
PC aa C34:2	<b>797.29 <math>\pm</math> 64.95<sup>ac</sup></b>	<b>635.77 <math>\pm</math> 50.09<sup>a</sup></b>	<b>956.22 <math>\pm</math> 30.77<sup>bc</sup></b>	<b>1064.57 <math>\pm</math> 34.27<sup>c</sup></b>
PC aa C34:3	<b>362.64 <math>\pm</math> 17.52<sup>a</sup></b>	<b>435.95 <math>\pm</math> 9.22<sup>b</sup></b>	<b>212.16 <math>\pm</math> 12.82<sup>c</sup></b>	<b>223.95 <math>\pm</math> 9.71<sup>c</sup></b>
PC aa C34:4	<b>28.90 <math>\pm</math> 1.25<sup>ab</sup></b>	<b>30.69 <math>\pm</math> 0.70<sup>a</sup></b>	<b>24.59 <math>\pm</math> 1.34<sup>b</sup></b>	<b>25.10 <math>\pm</math> 0.87<sup>b</sup></b>
PC aa C36:0	5.62 $\pm$ 0.33	5.22 $\pm$ 0.11	5.76 $\pm$ 0.54	4.91 $\pm$ 0.40
PC aa C36:1	<b>295.24 <math>\pm</math> 10.44<sup>a</sup></b>	<b>272.08 <math>\pm</math> 6.31<sup>a</sup></b>	<b>396.85 <math>\pm</math> 30.12<sup>b</sup></b>	<b>378.45 <math>\pm</math> 8.96<sup>b</sup></b>
PC aa C36:2	925.51 $\pm$ 34.44	882.21 $\pm$ 22.38	898.01 $\pm$ 34.67	965.12 $\pm$ 27.20
PC aa C36:3	<b>788.50 <math>\pm</math> 27.92<sup>ab</sup></b>	<b>743.42 <math>\pm</math> 16.48<sup>a</sup></b>	<b>850.98 <math>\pm</math> 35.66<sup>b</sup></b>	<b>847.81 <math>\pm</math> 21.22<sup>b</sup></b>
PC aa C36:4	1023.12 $\pm$ 58.64	1027.93 $\pm$ 43.71	894.67 $\pm$ 36.13	1033.56 $\pm$ 44.18
PC aa C36:5	<b>223.16 <math>\pm</math> 9.62<sup>a</sup></b>	<b>229.99 <math>\pm</math> 7.53<sup>a</sup></b>	<b>184.63 <math>\pm</math> 10.08<sup>b</sup></b>	<b>188.63 <math>\pm</math> 6.34<sup>b</sup></b>
PC aa C36:6	16.68 $\pm$ 0.92	15.93 $\pm$ 0.67	17.57 $\pm$ 0.95	17.80 $\pm$ 0.53
PC aa C38:0	<b>7.35 <math>\pm</math> 0.26<sup>a</sup></b>	<b>5.88 <math>\pm</math> 0.20<sup>a</sup></b>	<b>12.14 <math>\pm</math> 0.82<sup>b</sup></b>	<b>12.12 <math>\pm</math> 0.47<sup>b</sup></b>
PC aa C38:1	<b>4.51 <math>\pm</math> 0.35<sup>ac</sup></b>	<b>3.13 <math>\pm</math> 0.26<sup>a</sup></b>	<b>5.99 <math>\pm</math> 0.56<sup>b</sup></b>	<b>5.75 <math>\pm</math> 0.22<sup>bc</sup></b>
PC aa C38:3	<b>233.14 <math>\pm</math> 10.07<sup>a</sup></b>	<b>187.56 <math>\pm</math> 7.92<sup>a</sup></b>	<b>396.63 <math>\pm</math> 31.58<sup>b</sup></b>	<b>366.04 <math>\pm</math> 12.92<sup>b</sup></b>
PC aa C38:4	<b>765.00 <math>\pm</math> 22.69<sup>a</sup></b>	<b>673.51 <math>\pm</math> 22.98<sup>a</sup></b>	<b>922.61 <math>\pm</math> 33.06<sup>b</sup></b>	<b>1000.79 <math>\pm</math> 28.57<sup>b</sup></b>
PC aa C38:5	<b>475.33 <math>\pm</math> 21.48<sup>a</sup></b>	<b>412.81 <math>\pm</math> 18.17<sup>a</sup></b>	<b>614.90 <math>\pm</math> 36.32<sup>b</sup></b>	<b>617.23 <math>\pm</math> 19.10<sup>b</sup></b>
PC aa C38:6	<b>1003.86 <math>\pm</math> 41.77<sup>ab</sup></b>	<b>892.95 <math>\pm</math> 23.28<sup>a</sup></b>	<b>995.63 <math>\pm</math> 39.83<sup>ab</sup></b>	<b>1067.03 <math>\pm</math> 26.24<sup>b</sup></b>
PC aa C40:1	<b>1.53 <math>\pm</math> 0.05<sup>ab</sup></b>	<b>1.29 <math>\pm</math> 0.04<sup>a</sup></b>	<b>1.68 <math>\pm</math> 0.10<sup>b</sup></b>	<b>1.68 <math>\pm</math> 0.12<sup>b</sup></b>
PC aa C40:2	2.76 $\pm$ 0.06	2.23 $\pm$ 0.05	2.49 $\pm$ 0.18	2.56 $\pm$ 0.16
PC aa C40:3	<b>4.74 <math>\pm</math> 0.16<sup>a</sup></b>	<b>3.81 <math>\pm</math> 0.09<sup>b</sup></b>	<b>4.29 <math>\pm</math> 0.29<sup>ab</sup></b>	<b>3.97 <math>\pm</math> 0.20<sup>ab</sup></b>
PC aa C40:4	<b>24.01 <math>\pm</math> 0.70<sup>a</sup></b>	<b>18.56 <math>\pm</math> 0.47<sup>b</sup></b>	<b>25.23 <math>\pm</math> 1.94<sup>a</sup></b>	<b>24.15 <math>\pm</math> 0.83<sup>a</sup></b>

PC aa C40:5	42.92 ± 1.70 <sup>ac</sup>	33.73 ± 1.46 <sup>a</sup>	55.00 ± 4.73 <sup>b</sup>	48.44 ± 1.98 <sup>bc</sup>
PC aa C40:6	300.01 ± 8.28 <sup>a</sup>	241.98 ± 10.32 <sup>a</sup>	369.29 ± 26.56 <sup>b</sup>	383.30 ± 8.89 <sup>b</sup>
PC aa C42:0	1.36 ± 0.05	1.29 ± 0.04	1.37 ± 0.09	1.47 ± 0.09
PC aa C42:1	1.25 ± 0.04	1.00 ± 0.06	1.20 ± 0.09	1.19 ± 0.07
PC aa C42:2	1.24 ± 0.04	1.01 ± 0.03	1.08 ± 0.07	1.27 ± 0.11
PC aa C42:4	1.38 ± 0.04	1.13 ± 0.03	1.27 ± 0.10	1.24 ± 0.07
PC aa C42:5	2.11 ± 0.05 <sup>a</sup>	1.69 ± 0.05 <sup>b</sup>	1.71 ± 0.11 <sup>b</sup>	1.72 ± 0.10 <sup>b</sup>
PC aa C42:6	7.20 ± 0.23 <sup>a</sup>	5.36 ± 0.15 <sup>b</sup>	5.22 ± 0.44 <sup>b</sup>	5.23 ± 0.31 <sup>b</sup>
PC ae C30:0	0.50 ± 0.03	0.45 ± 0.02	0.50 ± 0.03	0.56 ± 0.05
PC ae C30:1	1.30 ± 0.30	1.21 ± 0.26	0.74 ± 0.16	0.92 ± 0.18
PC ae C30:2	0.46 ± 0.07	0.40 ± 0.06	0.41 ± 0.06	0.49 ± 0.07
PC ae C32:1	6.93 ± 0.39	6.44 ± 0.24	6.43 ± 0.47	6.76 ± 0.50
PC ae C32:2	2.13 ± 0.27	1.71 ± 0.22	1.78 ± 0.25	2.09 ± 0.28
PC ae C34:0	6.14 ± 0.22 <sup>a</sup>	5.24 ± 0.11 <sup>a</sup>	18.21 ± 1.40 <sup>b</sup>	17.64 ± 0.67 <sup>b</sup>
PC ae C34:1	40.67 ± 1.55 <sup>a</sup>	41.59 ± 1.16 <sup>a</sup>	79.25 ± 4.93 <sup>b</sup>	78.06 ± 2.57 <sup>b</sup>
PC ae C34:2	18.06 ± 1.00 <sup>a</sup>	20.63 ± 0.66 <sup>ac</sup>	24.73 ± 1.77 <sup>bc</sup>	26.91 ± 1.22 <sup>b</sup>
PC ae C34:3	3.43 ± 0.28	3.32 ± 0.19	3.03 ± 0.30	3.42 ± 0.36
PC ae C36:0	2.97 ± 0.23 <sup>a</sup>	3.04 ± 0.10 <sup>a</sup>	4.01 ± 0.23 <sup>b</sup>	4.10 ± 0.23 <sup>b</sup>
PC ae C36:1	28.02 ± 1.24 <sup>a</sup>	30.19 ± 0.55 <sup>a</sup>	76.90 ± 5.91 <sup>b</sup>	75.38 ± 1.88 <sup>b</sup>
PC ae C36:2	39.69 ± 1.63 <sup>a</sup>	42.06 ± 1.15 <sup>a</sup>	104.48 ± 7.32 <sup>b</sup>	106.82 ± 3.13 <sup>b</sup>
PC ae C36:3	15.12 ± 0.59 <sup>a</sup>	16.84 ± 0.34 <sup>a</sup>	26.88 ± 1.66 <sup>b</sup>	26.56 ± 0.93 <sup>b</sup>
PC ae C36:4	21.54 ± 0.89 <sup>a</sup>	18.99 ± 0.58 <sup>a</sup>	28.81 ± 1.89 <sup>b</sup>	29.67 ± 1.54 <sup>b</sup>
PC ae C36:5	7.24 ± 0.23	6.55 ± 0.13	6.99 ± 0.49	6.60 ± 0.31
PC ae C38:0	78.14 ± 5.22	71.24 ± 3.93	74.28 ± 4.79	74.44 ± 3.24
PC ae C38:1	7.19 ± 0.26 <sup>a</sup>	6.18 ± 0.17 <sup>a</sup>	13.85 ± 0.85 <sup>b</sup>	12.97 ± 0.46 <sup>b</sup>
PC ae C38:2	16.30 ± 0.59 <sup>a</sup>	15.25 ± 0.50 <sup>a</sup>	32.31 ± 2.49 <sup>b</sup>	29.76 ± 1.35 <sup>b</sup>
PC ae C38:3	15.69 ± 0.44 <sup>a</sup>	13.89 ± 0.50 <sup>a</sup>	40.75 ± 2.66 <sup>b</sup>	38.81 ± 1.19 <sup>b</sup>
PC ae C38:4	31.11 ± 0.91 <sup>a</sup>	28.31 ± 1.26 <sup>a</sup>	115.84 ± 8.61 <sup>b</sup>	118.50 ± 3.77 <sup>b</sup>
PC ae C38:5	25.44 ± 0.90 <sup>a</sup>	22.29 ± 0.63 <sup>a</sup>	38.46 ± 2.51 <sup>b</sup>	38.22 ± 1.63 <sup>b</sup>
PC ae C38:6	11.70 ± 0.38 <sup>a</sup>	10.34 ± 0.32 <sup>a</sup>	16.96 ± 1.26 <sup>b</sup>	17.66 ± 0.77 <sup>b</sup>
PC ae C40:1	61.06 ± 4.11 <sup>a</sup>	42.70 ± 2.39 <sup>b</sup>	49.49 ± 3.38 <sup>ab</sup>	45.95 ± 2.01 <sup>b</sup>
PC ae C40:2	7.03 ± 0.34	6.00 ± 0.27	6.96 ± 0.49	6.67 ± 0.32
PC ae C40:3	6.26 ± 0.17 <sup>a</sup>	5.60 ± 0.13 <sup>a</sup>	11.47 ± 0.68 <sup>b</sup>	10.46 ± 0.37 <sup>b</sup>
PC ae C40:4	12.01 ± 0.32 <sup>a</sup>	10.86 ± 0.48 <sup>a</sup>	31.02 ± 2.37 <sup>b</sup>	28.56 ± 1.19 <sup>b</sup>
PC ae C40:5	9.96 ± 0.36 <sup>a</sup>	7.67 ± 0.27 <sup>a</sup>	15.05 ± 0.93 <sup>b</sup>	14.38 ± 0.68 <sup>b</sup>
PC ae C40:6	14.49 ± 0.54 <sup>a</sup>	11.83 ± 0.58 <sup>a</sup>	51.51 ± 4.03 <sup>b</sup>	53.17 ± 1.36 <sup>b</sup>
PC ae C42:0	6.14 ± 0.32 <sup>a</sup>	4.86 ± 0.23 <sup>b</sup>	4.95 ± 0.32 <sup>b</sup>	4.78 ± 0.28 <sup>b</sup>
PC ae C42:1	5.54 ± 0.40	4.22 ± 0.38	4.93 ± 0.55	5.41 ± 0.60
PC ae C42:2	5.37 ± 0.36 <sup>a</sup>	3.46 ± 0.26 <sup>b</sup>	4.86 ± 0.37 <sup>a</sup>	4.41 ± 0.36 <sup>ab</sup>
PC ae C42:3	19.21 ± 1.32 <sup>a</sup>	10.71 ± 0.75 <sup>b</sup>	13.83 ± 1.16 <sup>b</sup>	12.82 ± 0.87 <sup>b</sup>
PC ae C42:4	2.42 ± 0.08 <sup>a</sup>	1.89 ± 0.09 <sup>b</sup>	2.60 ± 0.18 <sup>a</sup>	2.64 ± 0.11 <sup>a</sup>
PC ae C42:5	3.02 ± 0.09 <sup>a</sup>	2.46 ± 0.07 <sup>a</sup>	3.99 ± 0.25 <sup>b</sup>	3.72 ± 0.15 <sup>b</sup>
PC ae C44:3	1.46 ± 0.13	1.21 ± 0.11	1.29 ± 0.15	1.54 ± 0.19
PC ae C44:4	1.11 ± 0.11	0.83 ± 0.10	0.97 ± 0.11	1.08 ± 0.15
PC ae C44:5	1.93 ± 0.12	1.39 ± 0.10	1.52 ± 0.12	1.61 ± 0.14
PC ae C44:6	1.32 ± 0.04	1.49 ± 0.09	1.49 ± 0.09	1.61 ± 0.07

lysoPC a C14:0	3.64 ± 0.21	3.33 ± 0.17	2.98 ± 0.10	3.42 ± 0.13
lysoPC a C16:0	<b>113.28 ± 5.33<sup>ab</sup></b>	<b>120.38 ± 2.40<sup>a</sup></b>	<b>102.26 ± 2.63<sup>b</sup></b>	<b>101.40 ± 4.01<sup>b</sup></b>
lysoPC a C16:1	<b>5.74 ± 0.42<sup>a</sup></b>	<b>6.67 ± 0.18<sup>a</sup></b>	<b>4.51 ± 0.18<sup>b</sup></b>	<b>4.20 ± 0.25<sup>b</sup></b>
lysoPC a C17:0	<b>1.43 ± 0.05<sup>a</sup></b>	<b>1.44 ± 0.05<sup>a</sup></b>	<b>4.54 ± 0.16<sup>b</sup></b>	<b>4.63 ± 0.14<sup>b</sup></b>
lysoPC a C18:0	<b>59.88 ± 1.95<sup>a</sup></b>	<b>54.78 ± 1.23<sup>a</sup></b>	<b>71.60 ± 1.76<sup>b</sup></b>	<b>73.72 ± 2.12<sup>b</sup></b>
lysoPC a C18:1	33.29 ± 2.49	32.95 ± 1.15	37.93 ± 1.03	34.63 ± 1.27
lysoPC a C18:2	<b>39.65 ± 2.20<sup>a</sup></b>	<b>37.73 ± 1.03<sup>a</sup></b>	<b>29.50 ± 1.14<sup>b</sup></b>	<b>27.36 ± 0.85<sup>b</sup></b>
lysoPC a C20:3	<b>5.95 ± 0.50<sup>ab</sup></b>	<b>4.71 ± 0.18<sup>a</sup></b>	<b>7.41 ± 0.38<sup>b</sup></b>	<b>6.33 ± 0.29<sup>b</sup></b>
lysoPC a C20:4	<b>26.12 ± 1.95<sup>ab</sup></b>	<b>22.23 ± 0.86<sup>a</sup></b>	<b>29.05 ± 1.24<sup>b</sup></b>	<b>27.89 ± 1.31<sup>b</sup></b>
lysoPC a C24:0	1.53 ± 0.15	1.30 ± 0.14	1.37 ± 0.18	1.71 ± 0.23
lysoPC a C26:0	1.62 ± 0.19	1.44 ± 0.19	1.59 ± 0.23	2.01 ± 0.29
lysoPC a C26:1	4.01 ± 0.46	3.50 ± 0.36	3.27 ± 0.44	4.07 ± 0.46
lysoPC a C28:0	0.97 ± 0.10	0.85 ± 0.10	1.16 ± 0.16	1.38 ± 0.19
lysoPC a C28:1	1.86 ± 0.29	1.58 ± 0.25	1.69 ± 0.35	2.12 ± 0.38
SM (OH) C14:1	<b>1.44 ± 0.08<sup>a</sup></b>	<b>1.45 ± 0.06<sup>ac</sup></b>	<b>1.83 ± 0.11<sup>b</sup></b>	<b>1.77 ± 0.07<sup>bc</sup></b>
SM (OH) C16:1	<b>0.38 ± 0.02<sup>a</sup></b>	<b>0.37 ± 0.01<sup>a</sup></b>	<b>1.52 ± 0.09<sup>b</sup></b>	<b>1.63 ± 0.07<sup>b</sup></b>
SM (OH) C22:1	6.14 ± 0.32	6.41 ± 0.27	8.39 ± 1.03	8.31 ± 0.50
SM (OH) C22:2	1.41 ± 0.09	1.58 ± 0.07	1.69 ± 0.19	1.62 ± 0.11
SM (OH) C24:1	<b>2.18 ± 0.13<sup>a</sup></b>	<b>1.58 ± 0.09<sup>b</sup></b>	<b>1.90 ± 0.16<sup>ab</sup></b>	<b>1.87 ± 0.10<sup>ab</sup></b>
SM C16:0	35.92 ± 1.35	37.16 ± 1.21	40.11 ± 2.07	41.25 ± 1.38
SM C16:1	1.68 ± 0.11	1.67 ± 0.09	1.67 ± 0.11	1.78 ± 0.11
SM C18:0	<b>4.10 ± 0.15<sup>a</sup></b>	<b>3.83 ± 0.11<sup>a</sup></b>	<b>10.05 ± 0.77<sup>b</sup></b>	<b>10.64 ± 0.42<sup>b</sup></b>
SM C18:1	<b>0.38 ± 0.02<sup>a</sup></b>	<b>0.36 ± 0.01<sup>a</sup></b>	<b>0.86 ± 0.06<sup>b</sup></b>	<b>0.93 ± 0.03<sup>b</sup></b>
SM C20:2	0.20 ± 0.03	0.28 ± 0.02	0.02 ± 0.01	0.04 ± 0.01
SM C22:3	2.74 ± 0.15	2.30 ± 0.25	3.07 ± 0.26	2.88 ± 0.20
SM C24:0	<b>18.86 ± 0.53<sup>a</sup></b>	<b>19.64 ± 0.60<sup>a</sup></b>	<b>13.53 ± 1.37<sup>b</sup></b>	<b>13.56 ± 0.74<sup>b</sup></b>
SM C24:1	<b>9.76 ± 0.73<sup>a</sup></b>	<b>15.12 ± 0.95<sup>b</sup></b>	<b>2.21 ± 0.64<sup>c</sup></b>	<b>2.66 ± 0.66<sup>c</sup></b>
SM C26:0	0.05 ± 0.01	0.06 ± 0.01	0.06 ± 0.01	0.06 ± 0.01
SM C26:1	0.13 ± 0.01	0.11 ± 0.01	0.15 ± 0.01	0.15 ± 0.02

## 4 Discussion

NAFLD is frequently associated with obesity and the metabolic syndrome and impairments in metabolism or in genetics are implicated in the etiology. The diet induced obese mouse model is often used to mimic the human condition that leads to or promotes also NAFLD which results from alterations in hepatic lipid handling. C1-metabolism in liver provides a causal link of methyl-group turn-over and lipid homeostasis. The methyl-group dependent PC biosynthesis via the PEMT pathway is a mechanism with a very high demand for methyl-groups in hepatocytes. Hepatic steatosis in the HF DIO mouse is coupled to increased intestinal absorption and hepatic processing of dietary fat, which is dependent on hepatic PC and bile acids. Associated disturbances of hepatic fatty acid uptake, TG synthesis, fatty acid oxidation and lipoprotein dependent lipid export cause NAFLD (1, 35, 64, 100). This leads to the consideration that the enhanced fat processing in the mice fed HF diets may affect hepatic PC metabolism as PC represents a core phospholipid essential for intestinal fat absorption and hepatic VLDL assembly. Data from previous nutritional, biochemical and genetic studies led to the following working hypothesis and key questions of this thesis:

Does a HF diet and NAFLD affects

- 1) hepatic C1-metabolism which is linked to PC metabolism via SAM-dependent methylation of phosphatidylethanolamine to synthesize PC
- 2) hepatic nuclear epigenetic processes by dissipating intracellular activated methyl-groups (SAM)

and, can therapeutic methyl-group supplementation influence

- 3) a HF diet induced NAFLD progression by attenuating hepatic TG deposition and phospholipid homeostasis

### 4.1 High-fat diet induced NAFLD in phospholipid homeostasis and regulation of C1-metabolism

In a previous study performed by Desmarchelier *et al.* using the same DIO mouse model it was shown that HF diet feeding of C57BL/6N mice resulted in obesity, hyperglycemia, hyperinsulinemia, altered glucose tolerance and increased hepatic TG accumulation (138, 139). This project also provided evidence that the hepatic PC signature changed by increased levels of long-chain polyunsaturated PC subclasses in the HF mice (139), which could arise from the PE methylation pathway (107). This

would be associated with an increased expenditure of hepatic SAM due to an increase of PC.aa.38:4, PC.ae.38:4, PC.ae.40:5 and PC.ae.40:6 concentrations. PC is one of the most prominent PL classes, important for cellular plasma membrane integrity as shown in *Pemt*<sup>-/-</sup> mice (101). Furthermore, the PE methylation pathway contributes to hepatic VLDL particle secretion (35, 118) and the occurrence of PEMT in the canalicular membrane of hepatocytes suggests also a contribution of the PE methylation pathway in the production of biliary PC (121). Interestingly, mice fed a HF / high cholesterol diet secreted more PC derived from PEMT synthesis into bile (122), while PEMT derived PC seems not to be quantitatively essential for biliary PC secretion during acute and chronic metabolic stress induced by either tauroursodeoxycholate infusion or dietary taurocholate administration (115). But recently, Zhang *et al.* provided evidence for the induction of hyperhomocysteinemia and C1-metabolism counter-regulations in inbred mice on a cholesterol / cholic acid lithogenic diet (165). Altogether, the contribution of PEMT mediated PC biosynthesis in biliary PC production seems especially important in the context of HF administration. The observed alterations of PEMT associated PC subclasses in the liver from HF mice reported by Desmarchelier *et al.* (139) supported the assumption of an enhanced PEMT activity resulting in C1-metabolism metabolic adaptations, as observed by others for mice on a lithogenic diet (165).

#### **4.1.1 The influence of HF diet on NAFLD and the hepatic C1-metabolism**

To investigate the influence and interactions of altered PEMT-derived PC biosynthesis and C1-metabolism in the context of an obesogenic and steatotic HF diet in mice, the analysis of the first feeding trial (see 3.1) comprised the determination of gene expression, protein and metabolite levels of hepatic C1-metabolism. The data from the experiments *in vivo* and analyses of hepatoma cells *in vitro* provided evidence for a PPAR $\alpha$ -mediated downregulation of the transsulfuration pathway, an enhanced sarcosine pathway associated Hcy remethylation capacity and evidence for elevated taurine synthesis accompanied by reduced sulfate release in obese mice. Interestingly, no disturbances of the hepatic methionine cycle or methionine homeostasis could be observed in the context of HF diet induced NAFLD.

#### **4.1.2 Regulation of the Hcy branch-point in HF diet-dependent NAFLD**

One of the most interesting findings regarding the hepatic C1-metabolism represents the regulation of the branch-point enzymes BHMT and CBS (see 3.1.1 and 3.1.2) operating in the homeostasis of methionine and Hcy degradation in HF diet induced NAFLD. A metabolic regulation of increased BHMT activity and decreased CBS activity was found in rats fed a low methionine diet (0.25 %) provided with extra dietary cystine (166, 167). The reduced methionine supply combined with cystine supplementation resulted in a downregulation of CBS and an upregulation of BHMT activity. But this cystine



based methionine-sparing effect based on the downregulation of CBS could only be observed in combination with low dietary methionine supply (166). Whether the altered enzymatic activities of BHMT and CBS are based on difference in the protein levels remains unknown. The findings gained from HF diet fed C57BL/6N mice with sufficient dietary methionine (0.86 %) and extra dietary cystine (0.35 %) used here suggests that despite an adequate methionine supply, a reduced hepatic transsulfuration of Hcy is a consequence, supported by decreased gene and protein expression levels of CBS and by reduced metabolite levels of cystathionine and L- $\alpha$ -amino-n-butyrate. The principal mechanism of the methionine-associated downregulation of hepatic transsulfuration and enhanced Hcy remethylation via BHMT has also been identified in methionine-deprived C57BL/6 mice (168). Tang *et al.* described that methionine-deprivation resulted in a posttranslational downregulation of CBS and increased BHMT activity associated with a transient increase in plasma Hcy levels (168).

#### 4.1.3 Homeostasis of the hepatic methionine cycle in DIO mice

Interestingly, despite clear evidence for reduced transsulfuration and enhanced BHMT mediated Hcy remethylation in HF animals no differences in metabolite levels in the methionine cycle between C and HF livers were detected. This strongly suggests that conserving methionine homeostasis is most important for the cell or organ system which as an essential amino acid is also of crucial importance for large scale hepatic protein synthesis. This is also supported by the regulations found for enzymes of C1-metabolism with methionine as precursor of intracellular SAM. Homeostasis in the methionine cycle is based on a balance between the abundance of the methyl-group carrier-backbone Hcy in the cycle and on the influx of methyl-groups from the folate cycle or sarcosine pathway or on the dietary intake of L-methionine, as well as on the efflux of methyl-groups mediated by SAM-dependent methyltransferases. The observed increase in long-chain polyunsaturated PC levels in HF mice (139) point to an enhanced PEMT activity and expenditure of activated methyl-groups. This is potentially counterbalanced via enhanced methyl-group influx from folate independent Hcy remethylation (BHMT) and via Hcy conservation mediated by CBS downregulation in the methionine cycle. The net transmethylation flux of methyl-groups may therefore result in methionine cycle homeostasis in HF mice.

#### 4.1.4 Choline availability in DIO mice

The identified increase in BHMT gene and protein expression suggests a higher methyl-group influx in HF mice. In addition, the indication for this higher influx is supported by increased hepatic free choline levels measured in the present study (see 3.1.3) suggesting an enhanced choline oxidation potential in obese mice. Interestingly, *in vivo* BHMT expression is influenced by dietary changes of choline and betaine (169) and the

magnitude of BHMT induction is associated with methionine restriction (170). Furthermore, expression of BHMT is associated with increased hepatic VLDL and apolipoprotein B production in McArdle RH-7777 cells which was confirmed *in vivo* by feeding rats a L-methionine restricted but betaine containing diet (171, 172). This suggests that enhanced choline availability increased BHMT expression and subsequently enhanced TG secretion in HF mice. In addition, the availability of choline is important in the coordination of hepatic PC biosynthesis from the CDP-choline and PEMT pathway. Choline is the central link of both pathways since choline is a metabolic precursor of betaine, the essential substrate and methyl-group source for BHMT mediated Hcy methylation, and is implicated in direct CDP-choline PC biosynthesis (64). Furthermore, PEMT activity coupled with phospholipase catabolism of PC constitutes a *de novo* choline biosynthesis pathway based on PE methylation (64). Hepatic choline homeostasis is mainly influenced by two choline acquisition pathways - dietary intake and PEMT pathway - and two crucial choline depletion pathways - choline oxidation and biliary PC secretion (64). In addition, the importance of choline balance in lipid homeostasis was recently revealed in *Pemt*<sup>-/-</sup> mice. Jacobs *et al.* provided evidence for a link between hepatic PC biosynthesis and DIO. *Pemt*<sup>-/-</sup> mice on a HF diet were protected from DIO, insulin resistance and displayed increased energy expenditure, while mice with disturbed CDP-choline pathway were not protected from DIO. However, the HF diet resulted in hepatomegaly and steatosis in *Pemt*<sup>-/-</sup> mice. Dietary choline supplementation reversed the DIO protection, suggesting that choline homeostasis and *de novo* choline biosynthesis via the PE methylation pathway have an important role in whole body energy metabolism (173). In this context, the increased hepatic free choline content in HF mice identified here suggests an enhanced choline oxidation potential influencing lipid metabolism in mice on HF diets.

#### 4.1.5 Transcriptional regulation of the Hcy branch-point in the C1-metabolism

One feature of HF DIO models is the development of hyperglycemia and hyperinsulinemia that was also established in the present study (138). Therefore it is reasonable to assess the association of altered insulin sensitivity with C1-metabolism in HF mice. Evidence for the influence of insulin signaling on the C1-metabolism has been shown in streptozotocin induced diabetes mellitus (type 1) and in Zucker diabetic fatty rats (type 2). Impairments of insulin secretion or insulin signaling were shown to increase hepatic gene expression of the branch-point enzymes CBS and BHMT (174), suggesting that the identified regulatory mechanism for Hcy remethylation in DIO mice could also originate from a disturbed insulin signaling that translates into changes of *Bhmt* gene expression. However, the downregulation of *Cbs* gene expression described in this thesis is contradictory to the disturbed insulin signaling in the regulation of this transsulfuration pathway entry enzyme in HF mice. Similar reduced hepatic CBS gene

expression and enzyme activity has been previously reported in rats fed a HF diet (175, 176), supporting evolutionary conservation in murine animal models. The prominent role of the transsulfuration pathway and CBS in the development of a fatty liver has been also discovered in studies of *Cbs*<sup>-/-</sup> mice. CBS deficiency in these mice not only results in severe hyperhomocysteinemia, but is also associated with hepatic lipid metabolic dysfunction and liver injury, likely derived from altered fatty acid oxidation, lipoprotein particle secretion and oxidative stress (62, 63, 177). Interestingly, the study by Sheikh *et al.* described a reduced gene expression of *Cbs* only in rats fed a HF diet when treated with the PPAR $\alpha$  agonist WY14,643 (178). This suggested that PPAR $\alpha$  signaling is implicated in regulation of *Cbs* gene expression. In this context, the data from *in vitro* and *in vivo* experiments of the present thesis demonstrate for the following reasons that increased hepatic PPAR $\alpha$  activity is most likely involved in the downregulation of the transsulfuration pathway in DIO mice. Firstly, the treatment of Fao rat hepatoma cells with WY14,643 to enhance PPAR $\alpha$  activity resulted in the expected increased gene expression of the “classical” PPAR $\alpha$  target gene *Cpt1a* and in a reduced *Cbs* gene expression demonstrating that PPAR $\alpha$  activity influences *Cbs* gene expression at least in this *in vitro* model (see 3.1.4). Secondly, the identified increased mRNA expression of *Ppar $\alpha$*  and its prototypical target genes *Cpt1a*, *Ucp2*, *Acox1* in HF treated mice suggest that DIO enhanced the hepatic PPAR $\alpha$  activity in HF mice which induced the downregulation of the transsulfuration pathway (see 3.1.4). Interestingly, numerous short-term and long-term epidemiological studies revealed that fibrate drug treatment (e.g. fenofibrate, bezafibrate) is associated with a 40-50 % elevation of serum Hcy levels in humans (179-183). Furthermore, in rodents it was shown that the Hcy increasing effect of fibrates is related to the activation of PPAR $\alpha$  (184, 185). In addition to PPAR $\alpha$  associated elevation of Hcy, *in vitro* experiments by Mikael *et al.* revealed that increasing Hcy concentrations resulted in decreased expression of PPAR $\alpha$  in HepG2 cells (186) suggesting a Hcy based negative feedback-loop on PPAR $\alpha$  expression levels that has to be confirmed *in vivo*.

#### **4.1.6 HF diet and NAFLD effects on the hepatic C1-metabolism associated with the synthesis of taurine, glutathione, ophthalmic acid and sulfate**

PPAR $\alpha$  is classically considered as a prime regulator of fatty acid oxidation and other lipid metabolism related genes in the liver (187). PPAR $\alpha$  is however also involved in the regulation of hepatic amino acid metabolism (33). In the study by Kersten *et al.* the association of PPAR $\alpha$  signaling and amino acid metabolism was shown in PPAR $\alpha$ <sup>-/-</sup> mice demonstrating that PPAR $\alpha$  activation causes a downregulation of *Got1* gene expression (156). GOT1 is therefore another example for an enzyme of the transsulfuration pathway that is regulated on expression level by PPAR $\alpha$ . In the present DIO model, HF treatment resulted in a marginal significant downregulation of *Got1* and

in increased gene expression of *Csad* (see 3.1.1) which may translate into a reduced sulfate production from cysteine and a concomitant enhanced taurine synthesis. This is also evident by enhanced hepatic taurine levels found in HF mice (see 3.1.3). The reduced expression of *Got1* suggests also the influence of PPAR $\alpha$  signaling triggering reduced cysteine sulfinic acid transamination. However, the transcriptional effector of *Csad* favoring cysteine sulfinic acid decarboxylation and taurine synthesis in the liver is so far unknown.

Regarding the regulation of CSAD activity, Jerkins and Steele described that dietary sulfur amino acid supplementation with cystine, homocysteine, methionine and ethionine resulted in a downregulation of CSAD activity in male rats (188). In addition, Jerkins *et al.* reported that *Csad* mRNA abundance and CSAD activity were reduced in rats fed a high-protein diet (189), suggesting that CSAD activity and protein expression is regulated by mRNA abundance. In the feeding trial presented here, cystine supplementation (0.35 %) by the HF diet was not sufficient to observe a reduction of *Csad* gene expression. The dietary protein dependent CSAD regulation mentioned above reflects that under high dietary protein taurine biosynthesis is limited and synthesis of pyruvate and sulfate is favored. Data analysis of the presented HF feeding trial suggests that enhanced HF treatment of C57BL/6N mice results in reciprocal regulation preferring taurine synthesis (see 3.1.1 and 3.1.3). Interestingly, increased CSAD protein and mRNA abundance was also detected in rats during hepatocarcinogenesis and maintained in hepatocellular carcinoma (190) with enhanced *Csad* expression proposed as a biomarker for carcinogenesis. However, the increased *Csad* gene expression identified in DIO mice here could also represent an adaptation of the steatotic liver for an increased demand of the osmoregulatory, cytoprotective and antioxidant features of taurine (191, 192). Increased fat accumulation with increased lipid droplets in NAFLD may cause as well osmotic adaptation and taurine is a prime osmolyte.

In addition to a favored taurine synthesis in HF mice, the identified reduced transsulfuration of Hcy shown here is supported by decreased hepatic cystathionine concentrations in obese mice. This could also result in a reduced  $\alpha$ -ketobutyrate production from cystathionine and subsequently causes the observed reduction of L- $\alpha$ -amino-n-butyrate levels. This in consequence could also affect the levels of ophthalmic acid and indirectly influence glutathione synthesis. It has been shown that decreased levels of L- $\alpha$ -amino-n-butyrate can lead to a reduced synthesis of the alternative non-thiol product ophthalmic acid produced by glutathione synthetase (193). Therefore, decreased levels of L- $\alpha$ -amino-n-butyrate could also favor enhanced glutathione synthesis in the liver of DIO mice.

## 4.2 DIO induced NAFLD in nuclear epigenetic processes

The influence of HF diet induced NAFLD on PL metabolism and hepatic C1-metabolism homeostasis affecting mainly the transsulfuration pathway as demonstrated here, suggested that a downregulation of the transsulfuration is mediated by enhanced PPAR $\alpha$  activity in HF mice. For enhanced PPAR $\alpha$  activity, epigenetic processes and hepatic liver diseases there exists also interesting links. One end-stage liver disease of NAFLD is hepatocellular carcinoma that can be induced by aberrant DNA methylation and histone modification mechanisms while during hepatocarcinogenesis aberrant methylation of tumor related genes is frequent and can be an early event (12). Interestingly, non-genotoxic carcinogens like peroxisome proliferators induce neoplastic cell transformation without directly damaging the DNA (157), whereby the molecular target is PPAR $\alpha$  in the liver (158, 159). Short-term treatment results in DNA hypomethylation in mouse livers (160) and Pogribny *et al.* provided evidence that WY14,643 mediated prolonged activation of PPAR $\alpha$  leads to global DNA and histone hypomethylation (161). This effect can be attributed to constitutive PPAR $\alpha$  activity, because PPAR $\alpha$ <sup>-/-</sup> mice did not respond with altered DNA or histone methylation. The DNA hypomethylation affects especially DNA repetitive elements like LINE and LTR IAP of which DNA methylation is important to maintain somatic genome integrity (194). Furthermore, hepatic DNA hypomethylation in a streptozotocin rat model revealed an association of type 1 diabetes, altered C1-metabolism regulation and nuclear epigenetic processes (195).

### 4.2.1 Hepatic DNA methylation in HF diet induced NAFLD

The identified alterations of the C1-metabolism and the enhanced intrinsic activation of PPAR $\alpha$  in livers from hyperinsulinemic and hyperglycemic HF mice described here (see 3.1) led to the suggestion that the dietary treatment also modifies nuclear epigenetic processes. Analysis revealed a reduced gene expression of Dnmt3b, but global DNA methylation and gene specific CpG methylation of Cbs and PPAR $\alpha$  were not affected in HF mice (see 3.2), although it has been shown that the promoters of these murine genes are sensitive to DNA methylation changes (163, 164). The previously published association of DNA hypomethylation with prolonged PPAR $\alpha$  activation by a synthetic agonist or with the synthetic induction of type I diabetes could not be confirmed in the HF diet induced NAFLD mouse model described here. However, an aberrant DNA methylation of tumor suppressor genes or proto-oncogenes can not be excluded *a priori*. It would be necessary to further investigate DNA methylation of known carcinogenesis markers to determine if aberrant methylation can occur at an early stage of NAFLD programming neoplastic cell transformation.

### 4.3 Methyl-group supplementation and the effects on progression of DIO induced NAFLD

HF diets caused hepatic steatosis is one hallmark of mice DIO models. The linkage of obesity associated hepatic fat infiltration to metabolic disturbances in C1-metabolism affecting mainly the transsulfuration pathway suggests reciprocal interactions between lipotropic compounds and C1-metabolism in the progression of NAFLD. The influence of C1-metabolism lipotropes ameliorating the hepatic fat deposition was reported for alcoholic and non-alcoholic fatty liver animal models (90-92, 196). Interestingly, betaine supplementation was reported to attenuate steatosis by restoring ethanol mediated repression of PC biosynthesis via the PEMT pathway in an alcoholic steatosis model (197). This indicated a functional relation and disturbance of PEMT associated PC biosynthesis in the progression of hepatic steatosis. The observed alterations of PL homeostasis and C1-metabolism in HF diet induced NAFLD in the present thesis (see 3.1) suggested also alterations in PC biosynthesis in DIO mice, which could be possibly attenuated by methyl-group supplementation. The effectiveness of lipotropic substances in improving the degree of hepatic steatosis was shown by intervention studies in attenuating NAFLD development (90, 91, 198). So far however, the question whether a dietary methyl-group supplementation with lipotropes can have a “therapeutic effect” on NAFLD and reverse the pathophysiology has been rather poorly investigated. Only recently, Kathirvel *et al.* described an improvement in the degree of hepatic fat deposition in a murine DIO model by betaine supplementation for the last 6 weeks of the trial (199).

#### 4.3.1 Obesity related changes in basal clinical parameters in DIO mice

In the present thesis the therapeutic effect of methyl-group supplementation on NAFLD disease progression was investigated by feeding additional lipotropic nutrients to obese C57BL/6N mice, which had developed a HF diet induced hepatic steatosis / NAFLD. As anticipated, mice fed the HF diets developed increased body weight, total liver and VAT weight as compared to C mice (see 3.3). Furthermore, eight weeks of HF diet treatment was sufficient to induce a hyperglycemia, increased plasma insulin levels and altered plasma glucose tolerance in HF mice as compared to the controls. The preceding HF treatment was sufficient to develop DIO and appeared as adequate model to study the influence of four weeks of a methyl-group supplementation on the progression of NAFLD in DIO mice.

### 4.3.2 Influence of methyl-group supplementation on changes in basal clinical parameters

The analysis after four weeks of methyl-group supplementation in CMS and HFMS mice revealed no significant differences in body weight development, liver weight, VAT weight, blood glucose, serum insulin and glucose tolerance compared to the corresponding C or HF animals (see 3.3.1). These data contradict the study from Kathirvel *et al.* reporting that consecutive betaine supplementation during eight month HF diet feeding reduced fasting glucose and fasting insulin level as well as visceral fat weight in this trial (199). In addition, the authors reported that betaine reversed hepatic insulin resistance which was induced by HF diet feeding. Furthermore, Kathirvel *et al.* observed effects on blood glucose, blood insulin and visceral fat also by six weeks of a therapeutic betaine supplementation at the end of the eight month HF feeding trial (199). A possible explanation for the contradicting data between the report of Kathirvel *et al.* and the analyses of the present thesis can be the difference in the duration of the trials leading to more pronounced effects in the study from Kathirvel *et al.* Furthermore, the statistical analysis in the study by Kathirvel *et al.* was performed with unpaired student's *t*-test analyzing three experimental groups. This incorrect statistical analysis may leads to false positive significant results.

### 4.3.3 Specific blood plasma metabolite profile in methyl-group supplemented mice

Although there were no obvious differences in basal clinical parameters detectable in mice of the supplementation trial analysis of blood and liver metabolic profiles identified methyl-group specific effects (see 3.3.2). Plasma analysis revealed specific effects on L-serine, sarcosine and glycine in CMS and HFMS mice, which possibly can be attributed to betaine supplementation (200). Furthermore, a marginally significant increased L-methionine concentration was observed in CMS and HFMS blood, which likely resulted from the 0.75 % increase in dietary L-methionine content of CMS and HFMS diet. Especially the identified markedly increase of plasma sarcosine levels in CMS and HFMS mice could be the result of an enhanced betaine oxidation in the sarcosine pathway or an enhanced glycine methylation via GNMT, regulating SAM homeostasis (201). In addition, the methyl-group supplementation induced an increase in plasma L-serine and a decrease in glycine concentrations which is in line with data from Kim *et al.* implying serine hydroxymethyltransferase to convert glycine to serine by using the methyl-group from THF in betaine treated mice (200). The unexpected decrease of blood L- $\alpha$ -amino adipic acid in the present study may arise from differences in L-lysine metabolism in HF mice (202) and the increase of urea cycle metabolite concentrations of L-ornithine and L-citrulline in blood of HF and HFMS mice likely reflects an influence of dietary fat on the urea cycle.

Interestingly, the analysis of plasma tHcy concentrations in C and HF mice after eight weeks of dietary treatment and in C, CMS, HF and HFMS mice after twelve weeks of treatment revealed significantly decreased plasma tHcy concentration in HF mice compared to C mice. This surprising result contradicts the data from a recently published work by Bravo *et al.* reporting that a HF diet induced NAFLD in rats is associated with increased plasma Hcy concentrations caused by downregulation of the hepatic transsulfuration pathway (176). In addition, Gulsen *et al.* also described that plasma Hcy levels were significantly higher in NAFLD patients as compared to healthy subjects and predicted the progression to NASH (203), while Hirsch *et al.* failed to observe significant difference in plasma Hcy concentrations between obese subjects with or without NAFLD (204). These contradicting data show that the regulation of systemic plasma Hcy levels is more complex and can not only be attributed to the suppression of hepatic transsulfuration in HF diet fed animal models or obesity associated NAFLD in patients.

The suppression of hepatic transsulfuration in HF diet induced NAFLD reported by Bravo *et al.* (176) is in line with the results reported here (see 3.1 and 3.3.3), but the association to enhanced plasma Hcy concentrations in HF diet treated animals were not detected in the feeding trials of the present thesis (see 3.3.2). It is known that Hcy levels are not only controlled by the transsulfuration pathway but also by cellular Hcy remethylation pathways (folate or hepatic betaine dependent Hcy remethylation) in different tissues or by renal plasma Hcy clearance. The pivotal role of the renal function in the regulation of plasma Hcy levels have been observed in Type 1 and Type 2 diabetes mellitus and in patients with end-stage renal disease (205-207), suggesting that decreasing renal function can result in plasma Hcy elevation in these diseases (208). This demonstrates that more physiological parameters are involved in plasma Hcy homeostasis. The causative link proposed by Bravo *et al.* between the suppression of transsulfuration and enhanced plasma Hcy concentrations by HF diet induced NAFLD is not experimentally proven and therefore not conclusive. In the present study, the decreased plasma tHcy concentrations observed in HF animals in the methyl-group supplementation feeding trial suggest i) an enhanced systemic Hcy remethylation potential or ii) an altered renal Hcy clearance in obese animals. This is further supported by the plasma tHcy concentrations of CMS and HFMS animals. Methyl-group supplementation induced a significant increase of plasma tHcy in CMS mice, possibly due to enhanced dietary L-methionine intake, while HFMS animals almost maintained the tHcy levels found in HF mice. This supports the notion of either an enhanced systemic Hcy remethylation or altered renal Hcy clearance in methyl-group supplemented obese animals.



#### 4.3.4 Specific hepatic metabolite profile in methyl-group supplemented mice

Hepatic analysis of amino acids and their derivatives in C, CMS, HF and HFMS mice resulted in similar regulations of some amino acids in CMS and HFMS mice as described for blood analysis (see 3.3.2). Sarcosine, L-serine showed increased and glycine revealed decreased hepatic concentrations in methyl-group supplemented animals. Therefore it is likely, that the hepatic alterations influence the systemic plasma concentrations of sarcosine, L-serine and glycine in these mice. The differences of glycine and L-serine again correspond to the findings of Kim *et al.*, who analyzed the effect of betaine supplementation on hepatic amino acids in mice (200). Additionally, 18 amino acids were altered in the analyzed liver samples, whereby for some amino acids such as L- $\alpha$ -amino-n-butyrate, L-ornithine and hydroxyproline data from the first described HF diet study were confirmed (see 3.1). Significant differences between C and HF animals in L-lysine, L-valine, L-isoleucine and L-tryptophane levels reveal differences in hepatic amino acid metabolism in these animals beyond C1-metabolism. This can be extended by amino acids or derivatives that differ between CMS and HF mice like L-aspartate, ethanolamine and L-leucine. Further altered amino acids were identified, which are associated with DNA and RNA metabolism. L- $\beta$ -aminoisobutyrate and  $\beta$ -alanine are metabolites of thymine and uracil metabolism (209), while L- $\beta$ -aminoisobutyrate is a catabolic product of thymine and  $\beta$ -alanine of uracil. The urinary excretion of L- $\beta$ -aminoisobutyrate was shown to diminish in animals with a rapidly growing hepatoma (Novikoff hepatoma) probably due to the enhanced incorporation of thymine into DNA and reduced degradation of thymine in tumorous tissue (210, 211). The significant reduction of hepatic L- $\beta$ -aminoisobutyrate identified in HF fed mice (HF, HFMS) of the present trial suggests that the progression of NAFLD is associated with reduced thymine degradation and may probably provide a hint for tumorous degeneration of the liver. However, no significant effect of folate supplementation in CMS and HFMS mice could be observed on L- $\beta$ -aminoisobutyrate concentrations compared to the corresponding C and HF animals. This suggests no influence on thymine synthesis and degradation in the methyl-group supplemented mice. In addition, L- $\beta$ -aminoisobutyrate administration in partial leptin deficient (*ob/+*) mice is also described to prevent DIO and to increase fatty acid oxidation in the liver (212) showing that increased L- $\beta$ -aminoisobutyrate levels have a protective effect on obesity associated diseases. Furthermore, the uracil degradation product  $\beta$ -alanine is a precursor for the synthesis of carnosine, which was also recently reported to alleviate hepatic steatosis in DIO mice (213). The significant increase of  $\beta$ -alanine in HFMS mice may be taken as a measure of an enhanced capacity for carnosine synthesis. However hepatic carnosine measurements did not show any significant difference in mice of the methyl-group supplementation (see 7.2) suggesting that elevated  $\beta$ -alanine concentrations did not translate into increased carnosine level in HFMS mice.

Amino acid analysis revealed a metabolic fingerprint of methyl-group supplementation in blood and liver tissue of CMS and HFMS mice – mainly for sarcosine, L-serine and glycine that link to C1-metabolism. Analysis of intermediates of the methionine cycle and transsulfuration pathway revealed that the increased dietary methionine supply within the methyl-group supplementation resulted in marginally, yet significant increased blood concentrations of L-methionine in CMS and HFMS mice but not in liver tissues. This finding confirms data from Finkelstein and Martin by analyzing the effect of increasing dietary methionine on the C1-metabolism in rats (214). They demonstrated that hepatic methionine concentrations remain constant in the range from 1.0 % - 3.0 % of dietary methionine, while SAH increased significantly at 1.5 % and SAM at 3.0 % dietary methionine. In the present studies, hepatic L-methionine levels remained unaffected even under conditions of an excess of dietary methionine (see 3.3.2). The amount of dietary methionine fed to C and HF and CMS and HFMS mice constituted ~0.75 % or ~1.5 % methionine respectively, which did not result in a raise of hepatic L-methionine as described by Finkelstein and Martin (214). Analysis of hepatic SAH levels in CMS and HFMS mice revealed an increase in SAH concentrations compared to C or HF mice (see 3.3.2), which also confirms similar data reported with a ~1.5 % dietary methionine supply (214). Unexpectedly, the concentration of SAH was significantly reduced in HF mice compared to the remaining groups. This is also consistent with the plasma Hcy concentrations in these HF mice (see 3.3.2). The decreased hepatic SAH and plasma tHcy concentrations support an increased Hcy remethylation potential in HF mice.

The observation that methyl-group supplementation resulted in significantly increased hepatic SAM concentration in HFMS mice matches with data from other trials in which betaine was provided in HF or high-sucrose diet fed animals and in animal models of alcoholic liver disease supplemented with betaine or a complex methyl-donor diet (91, 196-199). The absence of increased SAM concentrations in CMS mice suggests that enhanced SAM catabolism via the GNMT reaction prevents increased hepatic SAM levels in these mice (see 1.2.1). This is also supported by hepatic and blood sarcosine concentrations showing a higher variability in CMS mice in contrast to HFMS mice.

The analysis of the [SAM] / [SAH] ratio did not reveal any significant difference in mice of the dietary groups except for HF mice. Due to the reduced hepatic SAH concentrations in HF mice, it reflects a reinforced transmethylation potential in these animals. In general, the ratio is more a generalization of the possible transmethylation flux dependent on enzyme velocity (67). Finkelstein revealed that product formation and the [SAM] / [SAH] ratio has no linear relationship and is dependent on enzyme specific properties (67). Therefore, the ratio can be no indicator for specific enzymatic methyl-group fluxes. The lack of an increase of the ratio in CMS and HFMS mice can likely be attributed to the increased methionine content of the methyl-group enriched

diets. L-methionine not only provides methyl-groups for SAM synthesis, it also provides Hcy the backbone-carrier of the methyl-group. This could lead to an increase in cellular SAH concentrations as observed in CMS and HFMS mice, due to a thermodynamically favoured SAH synthesis (55).

The increased supply of methionine in CMS and HFMS mice possibly also explains the altered hepatic Hcy levels, which were significantly increased in CMS mice and also modestly in plasma. Interestingly, these responses in CMS mice were not detected in HFMS mice, which is likely due to i) increased SAM levels suggesting enhanced Hcy remethylation and / or ii) increased Hcy transsulfuration in HFMS mice. Differences in Hcy transsulfuration in HFMS mice compared to the other groups were accompanied by increased hepatic cystathionine concentrations as compared to C and HF mice. Surprisingly, no significant decrease of cystathionine in HF animals could be detected after twelve weeks of dietary treatment compared to C animals, while at eight weeks of HF diet feeding a trend for reduced cystathionine levels was observed. It suggests that maintenance of the metabolite levels in the methionine cycle results in reduced hepatic Hcy transsulfuration due to downregulation of CBS expression as observed in the first HF feeding trial (see 3.1). However, the basal downregulation of CBS does not exclude an increased enzymatic CBS activity as the enzyme is regulated for example by SAM or SAH as described by Finkelstein *et al.* (74, 75), resulting in enhanced cystathionine levels accompanied by reduced SAH levels. The latter was observed in HF mice of the methyl-group supplementation feeding trial.

#### **4.3.5 Influence of methyl-group supplementation on the Hcy branch-point of the C1-metabolism**

The regulation of the hepatic CBS and BHMT gene and protein levels in the methyl-supplementation trail (see 3.3.3) confirms the findings on increased expression of BHMT and reduced expression CBS in HF mice (see 3.1). That leads to the conclusion that the reduced expression of CBS reflects a basal downregulation of the transsulfuration pathway in HF mice. The methyl-group supplementation in CMS and HFMS mice also significantly increased hepatic BHMT and reduced CBS expression revealing an increased Hcy remethylation potential in these mice. However, despite reduced CBS expression levels in HFMS mice, increased hepatic cystathionine levels were found suggesting an enhanced hepatic transsulfuration capacity. This is possibly a consequence of elevated SAM concentrations leading to an increased allosteric activation of CBS activity (74). Unexpectedly, CMS mice showed a significant reduction of CBS expression in the liver. Whether this is mediated by PPAR $\alpha$  activity or other regulatory factors remains to be determined.

The increased expression of BHMT in CMS and HFMS mice can likely be attributed to the methyl-group supplementation and especially to the provision of choline and betaine

in this diet. Various publications describe betaine or choline based induction of enhanced BHMT activity and mRNA expression on the background of methionine deficient or adequate diets (169, 170, 215). The increased expression of BHMT in CMS mice proves that hepatic BHMT expression is dependent on the supply of methyl-donors in the diet. The importance of BHMT in balancing the Hcy homeostasis and its association to NAFLD was recently shown in a *Bhmt*<sup>-/-</sup> mouse model published by Teng *et al.* The authors observed increased hepatic and plasma Hcy concentrations, decreased SAM and increased SAH levels, as well as altered choline and phosphatidylcholine concentrations in the BHMT deficient mice (216). Furthermore the lack of BHMT resulted in hepatic steatosis associated with a reduced secretion of VLDL particles and a progression to hepatocellular carcinoma (216). These data demonstrate the central importance of BHMT in C1-metabolism and hepatic lipid handling.

#### 4.3.6 Progression of NAFLD in methyl-group supplemented mice

Methyl-group supplementation resulted in changes in amino acid metabolism especially of those associated with C1-metabolism (e.g. amino acids like sarcosine, glycine, L-serine and SAM and enzymes like BHMT and CBS). These changes were associated with a less pronounced progression in hepatic lipid accumulation in animals receiving the extra methyl-donors (see 3.3.4). The plasma NEFA concentrations did not reveal any significant changes suggesting that plasma free fatty acids as derived from lipolysis in visceral adipose tissue (see 1.1.1) may play a minor role in this described diet induced NAFLD model. It also suggests that HF and HFMS animals did not have an altered hepatic fatty acid uptake from the blood (see 1.1.1). However hepatic TG levels increased in all HF mice suggesting that plasma TG clearance of chylomicron remnants may contribute to hepatic TG accumulation. This is supported by apolipoprotein E deficiency in mice shown to have a protective effect in diet induced NAFLD (217). The comparison of hepatic TG deposition between eight and twelve weeks of feeding a HF diet demonstrates that during the four weeks TG accumulation and hepatic steatosis progressed. This was also observed by histological lipid staining in these mice (see 3.3.4). The dietary methyl-group supplementation however could completely prevent this progressive accumulation of hepatic TG in HFMS mice (see 3.3.4). This is in line with studies (91, 198, 199) describing that enduring supplementation attenuates hepatic steatosis in murine NAFLD models. However, hepatic TG levels did not decrease below the values observed after eight weeks (see 3.3.4) leading to the conclusion that the NAFLD can not be reversed during this period. Methyl-group supplementation also prevented the increase of hepatic free fatty acids in HFMS mice as compared to HF mice that showed further increase in NEFA levels between eight and twelve weeks. This suggests either a reduced DNL or increased fatty acid oxidation in HFMS mice. Since an accumulation of NEFA is considered by their lipotoxicity to impair further

insulin sensitivity of the organ this finding is of prime importance. HF diets also resulted in significantly increased total PL concentrations in HF and HFMS mice those did not further increase in HFMS mice. However, the data demonstrate that the hepatic phospholipid signature is altered in such HF diet induced NAFLD mouse models.

#### **4.3.7 Possible causes of the alleviation of NAFLD progression in methyl-group supplemented mice**

The observed phenotypic difference of TG deposition and free fatty acids in the liver of HF and HFMS mice raises the question of whether hepatic DNL and / or fatty acid utilisation are affected in the HFMS mice leading to the alleviation of NAFLD progression. A pivotal transcription factor regulating *de novo* fatty acid synthesis is SREBP-1c (1.1.1). However, Srebp-1c mRNA levels remained unchanged in methyl-group supplemented mice. In addition the mature aSREBP-1 protein did not show increased activation (see 3.3.5). Analysis of downstream targets such as of the lipogenic enzyme FASN in liver revealed that its mRNA expression is repressed in the livers of methyl-group supplemented mice in relation to C mice. In addition, HF feeding resulted also in reduction of hepatic Fasn expression of HF mice, suggesting that repression of DNL plays a minor role in contribution to reduced TG deposition in HFMS mice. However, Song *et al.* and Ji and Kaplowitz described that a betaine supplementation resulted in suppression of Srebp-1c and Fasn expression in high-sucrose diet induced hepatic steatosis model and in an alcoholic fatty liver disease model (92, 198). The effects may therefore be dependent on the fatty liver model.

As an enhanced activity of PPAR $\alpha$  in HF mice is supported by the present findings (see 3.1.4) it was important to ask whether an increased mitochondrial  $\beta$ -oxidation as a dominant oxidative pathway (11), – which is regulated with key enzymes by PPAR $\alpha$  – contributes to the reduced TG and NEFA levels in HFMS livers (see 3.3.6). The rate limiting step in mitochondrial  $\beta$ -oxidation is the acylation of the carnitine carrier catalyzed by CPT-1 (see 1.1.1). Analysis of Cpt1a transcripts revealed significantly elevated expression in HF animals confirming similar data of the first feeding trial (see 3.1.4), but the methyl-group supplementation failed to alter Cpt1a mRNA levels. However, CPT-1 activity is controlled by malonyl-CoA concentrations and its synthesis at the outer mitochondrial membrane (1.1.1). A high malonyl-CoA level reduces CPT-1 activity and thus reduces fatty acid import into mitochondria (31). Acetyl-CoA-carboxylase 2 (ACC2) is phosphorylated by AMPK which acts as an AMP / ATP sensor and integrator of the energy state with mitochondrial  $\beta$ -oxidation and cytosolic fatty acid synthesis (31). The analysis of the subunit AMPK $\alpha$  revealed an enhanced hepatic threonine 172 (Thr172) phosphorylation state in all livers from methyl-group supplemented mice as compared to their corresponding controls. AMPK $\alpha$  phosphorylation mediated by upstream kinases is a prerequisite for AMPK activation

(218, 219) and therefore the increased phosphorylation state reflects an enhanced activation of AMPK in methyl-group supplemented mice. These data confirm previous findings from Song *et al.* demonstrating *in vitro* and *in vivo* that a betaine supplementation in HepG2 cells and in high sucrose diet induced hepatic steatosis resulted in increased AMPK $\alpha$  Thr172 phosphorylation (198). Song *et al.* also demonstrated an increased phosphorylation of ACC causing the inhibition of ACC activity (198, 220). Enhanced AMPK $\alpha$  phosphorylation in livers of CMS and HFMS mice therefore strongly suggests a reduced malonyl-CoA synthesis by ACC phosphorylation and in turn increased CPT-1 activity. The prime importance of CPT-1 in limiting fatty acid oxidation was elegantly shown by adenovirus mediated long-term hepatic gene transfer of Cpt1a or its constitutive active mutant Cpt1a-AM in mice on HF diets or in genetically obese mice (221). Transfection increased CPT-1 activity in the liver substantially and protected the mice against diet induced obesity, hepatic steatosis and insulin resistance (221). Furthermore, the increased activity of AMPK suggests that besides mitochondrial fatty acid oxidation also mitochondrial biogenesis could be affected via the transcriptional coactivator peroxisome proliferative activated receptor  $\gamma$  coactivator 1  $\alpha$  (PGC-1 $\alpha$ ). This could occur either by direct PGC-1 $\alpha$  phosphorylation or by a sirtuin 1 mediated deacetylation of PGC-1 $\alpha$  (31). In addition, PGC-1 $\alpha$  activity seems to be enhanced by its methylation dependent on protein arginine methyltransferase 1 (222), while dietary methyl-donor deficiency was recently described to impair fatty acid oxidation through PGC-1 $\alpha$  hypomethylation (223). Interestingly, PGC-1 $\alpha$  is also known to influence homocysteine homeostasis, likely via hepatic nuclear factor 4 $\alpha$  mediated expression control of BHMT (224). This suggests that besides AMPK, PGC-1 $\alpha$  may also be implicated in the alleviation of TG accumulation in the livers of methyl-group supplemented mice and that the increased BHMT expression observed in these mice (see 3.3.3) may be indicates enhanced PGC-1 $\alpha$  activity. However, whether methyl-donor supplementation leads to enhanced PGC-1 $\alpha$  methylation and activity remains to be determined.

Most interestingly, the methyl-group supplementation changed also hepatic L-carnitine and more specific acyl-carnitine concentrations significantly (see 3.3.6). This became obvious for all short and all long-chain acylcarnitines that revealed reduced levels in liver tissues of CMS and HFMS mice. Since AMPK mediated stimulation of L-carnitine acylation by CPT-1 as the rate limiting enzyme in mitochondrial  $\beta$ -oxidation (225), has to be assumed, a more effective entry of long-chain fatty acids into mitochondria and more effective fatty acid oxidation would lead to reduced acyl-carnitine levels. Corresponding NEFA levels should also decline and this was observed which in turn would prevent also the TG levels to rise in HFMS mice. Surprisingly, concentrations of hepatic DL-carnitine (C0) were also reduced by methyl-group supplementation. As this is needed for the Carnitine-acylcarnitine translocase (CACT)-mediated transfer of the

fatty acids across the inner mitochondrial it may indicate a limited availability of carnitine when CPT-1 operates at highest activity level. Carnitine is known to be synthesized from the amino acids L-lysine and L-methionine, whereby trimethyl-lysine (TML) is the ultimately source for carnitine biosynthesis (226). TML is a posttranslational modification of lysine occurring in various proteins like calmodulin, myosin, actin, cytochrome c or histones and therefore TML abundance is dependent on lysine methyltransferases, the supply of SAM and on protein degradation (226, 227) to release TML. Therefore, enhanced dietary supply of lipotropes should lead to an increased biosynthesis of carnitine by enhanced availability of TML, especially on the background of NAFLD. However, the lower carnitine levels found do not support this hypothesis.

Whereas free carnitine, short-chain and long-chain acylcarnitines all declined by methyl-group supplementation, medium-chain acyl-carnitines did not change in concentration. Although their levels all increased in the HF fed animals, they did not respond to methyl-group input. This is most likely explained by the fact that the import of medium-chain fatty acids into mitochondria occurs by diffusion and independent of CPT-1 and only requires a mitochondrial medium-chain acyl-dehydrogenase for metabolism (228)

One of the key question of course is, what increases the phosphorylation state of AMPK when methyl-groups are supplemented? Different hypothesis are conceivable here. AMPK is heterotrimeric consisting of the catalytic  $\alpha$  subunit and regulatory  $\beta$  and  $\gamma$  subunits, whereby the  $\gamma$  subunit contains four tandem repeats of evolutionary conserved CBS domains. These CBS domains are known to bind the regulatory nucleotides AMP or ATP (31). In the enzyme CBS, the corresponding CBS domain is known to bind SAM resulting in an allosteric activation (229). This led Finkelstein to the proposal that SAM may exert its metabolic regulatory properties by binding to CBS domains also in the  $\gamma$  subunit in AMPK causing its activation (67). Although SAM concentrations in liver from CMS mice did not change, while AMPK showed increased phosphorylation state in CMS and HFMS mice, the highest SAM levels seemed to be associated with the highest AMPK-activation states observed in HFMS mice.

An alterantive explanation may be based on the cross-talk between adipose tissue and liver. Wang *et al.* reported an improved adipose tissue function by betaine supplementation in DIO mice with improved insulin signalling and prevention of endoplasmatic reticulum stress in adipose tissue (230). Furthermore, the supplementation normalized the DIO induced decrease of plasma adiponectin concentrations (230). This adipokine is known to activate AMPK by an unknown mechanism (231). Betaine supplementation could thereby indirectly lead to a hepatoprotective effect by AMPK activation by improved adipose tissue function and adiponectin secretion. *In vitro* experiments of betaine supplementation in HepG2 cells

(198) demonstrated that the activation of AMPK by betaine is an intrinsic mechanism in hepatocytes and does not require adiponectin or adipose tissue.

AMPK measures the cellular energy state due to its AMP-dependent activation, which is antagonized by ATP (31). Therefore, the AMP / ATP ratio is determining AMPK activity state and its coordinative functions in anabolic and catabolic processes. AMP binding to the  $\gamma$  subunit allosterically promotes AMPK activation (31, 232) and furthermore protects AMPK against dephosphorylation by protein phosphatases (233). This dual effect of AMP multiplies the activation of AMPK and in combination with generally low cellular AMP concentrations leads to a system that records and amplifies minimal changes in the AMP / ATP ratio. As the enhanced supply of methyl-donors increases the biosynthesis of SAM (e.g. by MAT), SAM synthesis consumes ATP and turn-over delivers SAH and hence Hcy and adenosine. As previously reported, the reversible hydrolysis of SAH thermodynamically favours SAH synthesis and therefore Hcy and adenosine have to be constantly metabolized (51, 55). Adenosine is primarily converted by adenosine kinase in the liver in to AMP (50, 234) and it is therefore conceivable that enhanced SAM synthesis and turnover in methyl-group supplemented mice increased cellular AMP concentrations and the AMP / ATP ratio resulting in AMPK activation. This constitutes a third hypothesis for how methyl-groups could cause an activation of AMPK.

#### **4.3.8 Hepatic phospholipid synthesis in HF diet induced NAFLD and methyl-group supplementation**

Hepatic PL synthesis is an important biosynthesis pathway for the maintenance of hepatocyte membrane integrity due to its secretory function of PL. Especially for PC, it is dependent on the disposability of diacylglycerol and CDP-choline. Furthermore, the availability of activated methyl-groups also contributes to the biosynthesis of PC by the PEMT pathway (see 1.3). Using the HF diet model it was previously reported that NAFLD was associated with a specific increase of selected PC subclasses (see 3.1) possibly derived from the PEMT pathway. Surprisingly, phospholipid profiling of liver tissues here revealed no significant difference between C and CMS or the HF and HFMS mice – although the effects of HF diets could be demonstrated (see 3.3.7). This finding supports the notion a reduced transsulfuration accompanied by enhanced Hcy remethylation described in the first feeding trial (see 3.1) is sufficient to balance methyl-group supply for the PEMT-mediated PC biosynthesis in HF diet induced NAFLD conditions. Additional methyl-group supplementation could obviously not further increase PL biosynthesis. This is in line with recently published results from HF diet fed mice carrying a liver-specific  $CT\alpha^{-/-}$  deficiency ( $LCT\alpha^{-/-}$ ). Phenotypically, the impairment of the CDP-choline pathway in the liver simply resulted in a decreased VLDL secretion and reduced lipid efflux and a mild steatosis when animals were fed a



chow diet (235).  $LCT\alpha^{-/-}$  mice fed a HF diet however developed NASH within one week and showed 20 % reduction of hepatic PC content (235). To prevent NASH,  $LCT\alpha^{-/-}$  mice on a HF diet received injections of CDP-choline or were supplemented with betaine. CDP-choline injection increased hepatic PC concentrations, while betaine supplementation attenuated hepatic TG accumulation without influencing the PC levels (235). These data by Niebergall *et al.* demonstrate, like the methyl-group supplementation trial described here (see 3.3), that methyl-group supplementation (by betaine feeding) can not increase hepatic PC content in a HF diet induced NAFLD model while the betaine supplementation in  $LCT\alpha^{-/-}$  mice produced a reduced hepatic TG content, most likely due to enhanced fatty acid oxidation associated with AMPK activation.

The observed differences in hepatic PC, lysoPC and SM subclasses only distinguish C and HF diets in the mice with a characteristic molecular signature in the NAFLD state. This may mainly come from the increased dietary fatty acid intake (see 2.1). The overall increase of long-chain PCaa, the simultaneous decrease of medium-chain PCaa and the modulation of SM subclasses in HF diet treated mice suggest alterations also in membrane fluidity of hepatocytes (236-238) and demonstrate that dietary lipids change the fatty acid composition and the organization of biomembranes (238). It is also conceivable that PL modification results in modulation of hepatic gene expression by i) direct ligand activation of transcription factors (34, 239) or ii) indirectly by influencing membrane associated intracellular signalling cascades (237). Furthermore, the main increase of ether-PC concentrations support a modulation of peroxisomal ether-PL biosynthesis likely by influencing the first two enzymes dihydroxyacetonephosphate (DHAP) acyltransferase and alkyl-DHAP synthase of this biosynthesis pathway (240). In total, the majority of determined PL subclasses increased due to feeding the HF diets which is shown in an increase of total PL in HF and HFMS mice (see 3.3.4).

#### 4.4 Concluding remarks and perspectives

Taken together, in this thesis it is demonstrated that a complex metabolic networks links lipid and C1-metabolism in liver that leads to NAFLD or prevents the development of NAFLD. HF diet induced NAFLD accompanied by an increased requirement of phospholipids, induce a  $PPAR\alpha$ -mediated suppression of key enzymes of the transsulfuration pathway in favour of a betaine-dependent Hcy-remethylation to conserve hepatic L-methionine levels and to maintain a proper supply of labile methyl-groups. The primacy of methionine homeostasis becomes the critical control point as this essential amino acid ensures the maintenance of basic liver functions (i.e. large scale protein synthesis) even under pathophysiologic conditions as of NAFLD.

The protection from NAFLD by supply of additional methyl-donors proved to work in the mice and this seems to be mediated primarily by the energy sensor AMPK with its effects on enhancing mitochondrial  $\beta$ -oxidation associated with a decline in hepatic acyl-carnitine level. The supplementation however also resulted in a specific amino acid profile that likely contributes to the activation of  $\beta$ -oxidation to prevent NAFLD progression and TG accumulation.

Applying a methionine loading test (241) to mice with NAFLD with or without additional betaine as a methyl-group source could help to dissect the role of Hcy-branch-point regulation in C1-metabolism in obese mice in favour of a betaine-dependent Hcy remethylation. Furthermore, specific inhibition of Bhmt by administration of S-( $\Delta$ -carboxybutyl)-D,L-Hcy (242) in HF fed mice could enable to define the role of the betaine-dependent maintenance of L-methionine homeostasis in NAFLD. Using stable isotope tracing studies (243) with L-methionine-(methyl- $^{13}\text{C}$ ) would allow to trace the fate of methyl-groups and to determine the specific methyl-group flux towards the PEMT pathway in PC synthesis in liver pathologies caused by HF diets. In addition, it will be necessary to study the molecular mechanism of methyl-group dependent AMPK activation by focusing on hepatic AMP / ATP ratio in relation to transmethylation dependent methyl-group flux as revealed by stable isotope tracing studies. Analysis of methyl-group supplementation on AMPK activation could be studied in RNA interference approaches to adenosine kinase and the AMP / ATP ratio. The contribution of PPAR $\alpha$  in regulating C1-metabolism could be assessed by chromatin immunoprecipitation asking also whether C1-metabolism is implicated in PPAR $\alpha$  mediated aberrant DNA and histone methylation. Furthermore, it is conceivable to titrate methyl-group consumption by nicotinamide supplementation (80) to understand the kinetics of the onset of aberrant DNA or histone methylation in relation to disposable labile methyl-group source.

Altogether, this study contributed to a better understanding of the interrelationship between C1-metabolism and lipid metabolism in relation to adaptation mechanisms in the etiology of NAFLD and demonstrated the potential of methyl-group supplementation to prevent NAFLD and its related liver pathologies.

## 5 Summary

Non-alcoholic fatty liver disease (NAFLD) reflects a lipid metabolic dysfunction of the liver that is generally associated with obesity and the metabolic syndrome in humans. Increased lipid accumulation characterises the onset and progression of NAFLD and impairments of hepatic phosphatidylcholine (PC) metabolism may be central to the pathogenesis. Diet induced mouse models of obesity (DIO) using high-fat (HF) diets challenge the metabolic system with increasing dietary fat absorption and lipid transport by providing sufficient phosphatidylcholine (PC) as an essential constituent of lipid handling. This needs increased *de novo* biosynthesis and PC turnover. PC biosynthesis involves activated methyl-groups provided by the one-carbon (C1) metabolism in the phosphatidylethanolamine methyltransferase (PEMT) pathway. In rodents, continuous supplementation of methyl-group donors during HF feeding reduces NAFLD but whether this also reverses a NAFLD state has not been studied.

The overall aim of the present work was to elucidate metabolic and molecular interactions between lipid and C1-metabolism in the context of a HF diet induced NAFLD and to assess whether a therapeutic methyl-group supplementation can reverse a pre-existing NAFLD state. In addition to exploring the metabolic links between C1- and lipid metabolism, methyl-group effects on nuclear epigenetic regulations were analyzed by DNA methylation analysis.

As prime findings, a PPAR $\alpha$ -mediated downregulation of the hepatic transsulfuration pathway enzyme cystathionine  $\beta$ -synthase (CBS) and an increase in betaine-homocysteine methyltransferase (BHMT) expression was observed. Hepatic metabolite profiles also identified decreased concentrations of cystathionine and L- $\alpha$ -amino-n-butyrate in NAFLD livers confirming a CBS downregulation on metabolite level of the transsulfuration pathway while no changes in the methionine cycle were observed. The identified decreased DNA methyltransferase 3b gene expression however did not affect nuclear epigenetic processes of global and gene specific DNA methylation of Cbs and PPAR $\alpha$  target genes measured by luminometric methylation analysis or bisulfite genomic pyrosequencing.

Additional methyl-donors in the diet prevented a further fat accumulation in liver of animals on HF diets but failed to reverse NAFLD. The supplementation however resulted in specific plasma and hepatic metabolic profiles accompanied by an increased activation of AMP-activated protein kinase (AMPK). AMPK can increase fatty acid import and oxidation in mitochondria and thereby reduce fatty acid and TG levels in liver. This was also indicated by markedly reduced acyl-carnitine concentrations in liver of methyl-group supplemented mice. Analysis of hepatic phospholipid classes revealed

a HF diet change in the phospholipid signature while no supplementation effects on specific hepatic phospholipid classes could be observed.

Altogether, this study shows that NAFLD induced by HF diets can cause a PPAR $\alpha$  mediated suppression of a key enzyme operating in the transsulfuration pathway and favouring betaine-dependent Hcy remethylation. This preserves hepatic L-methionine levels and maintains the supply of labile methyl-groups without altering nuclear epigenetic processes. This is also accompanied by increased fatty acid oxidation dependent on labile methyl-group supply and regulated via AMPK leading to reduced lipid toxicity for liver and preventing NAFLD progression.

## 6 References

1. Musso G, Gambino R, Cassader M. Recent insights into hepatic lipid metabolism in non-alcoholic fatty liver disease (NAFLD). *Prog Lipid Res.* 2009 Jan;48:1-26.
2. Starley BQ, Calcagno CJ, Harrison SA. Nonalcoholic fatty liver disease and hepatocellular carcinoma: a weighty connection. *Hepatology.* 2010 May;51:1820-32.
3. Westwater JO, Fainer D. Liver impairment in the obese. *Gastroenterology.* 1958 Apr;34:686-93.
4. Adler M, Schaffner F. Fatty liver hepatitis and cirrhosis in obese patients. *Am J Med.* 1979 Nov;67:811-6.
5. Ludwig J, Viggiano TR, McGill DB, Oh BJ. Nonalcoholic steatohepatitis: Mayo Clinic experiences with a hitherto unnamed disease. *Mayo Clin Proc.* 1980 Jul;55:434-8.
6. Cave M, Deaciuc I, Mendez C, Song Z, Joshi-Barve S, Barve S, McClain C. Nonalcoholic fatty liver disease: predisposing factors and the role of nutrition. *J Nutr Biochem.* 2007 Mar;18:184-95.
7. Angulo P. Nonalcoholic fatty liver disease. *N Engl J Med.* 2002 Apr 18;346:1221-31.
8. Varela-Rey M, Embade N, Ariz U, Lu SC, Mato JM, Martinez-Chantar ML. Non-alcoholic steatohepatitis and animal models: understanding the human disease. *Int J Biochem Cell Biol.* 2009 May;41:969-76.
9. Alfire ME, Treem WR. Nonalcoholic fatty liver disease. *Pediatr Ann.* 2006 Apr;35:290-4, 7-9.
10. Tannapfel A, Denk H, Dienes HP, Langner C, Schirmacher P, Trauner M, Flott-Rahmel B. Histopathological diagnosis of non-alcoholic and alcoholic fatty liver disease. *Virchows Arch.* 2011 Mar 26.
11. Browning JD, Horton JD. Molecular mediators of hepatic steatosis and liver injury. *J Clin Invest.* 2004 Jul;114:147-52.
12. Tischoff I, Tannapfe A. DNA methylation in hepatocellular carcinoma. *World J Gastroenterol.* 2008 Mar 21;14:1741-8.
13. Lazo M, Clark JM. The epidemiology of nonalcoholic fatty liver disease: a global perspective. *Semin Liver Dis.* 2008 Nov;28:339-50.
14. Wree A, Kahraman A, Gerken G, Canbay A. Obesity affects the liver - the link between adipocytes and hepatocytes. *Digestion.* 2011;83:124-33.
15. Anstee QM, Goldin RD. Mouse models in non-alcoholic fatty liver disease and steatohepatitis research. *Int J Exp Pathol.* 2006 Feb;87:1-16.
16. Ruderman N, Prentki M. AMP kinase and malonyl-CoA: targets for therapy of the metabolic syndrome. *Nat Rev Drug Discov.* 2004 Apr;3:340-51.
17. Faergeman NJ, Knudsen J. Role of long-chain fatty acyl-CoA esters in the regulation of metabolism and in cell signalling. *Biochem J.* 1997 Apr 1;323 ( Pt 1):1-12.

18. Shimomura I, Bashmakov Y, Ikemoto S, Horton JD, Brown MS, Goldstein JL. Insulin selectively increases SREBP-1c mRNA in the livers of rats with streptozotocin-induced diabetes. *Proc Natl Acad Sci U S A*. 1999 Nov 23;96:13656-61.
19. Azzout-Marniche D, Becard D, Guichard C, Foretz M, Ferre P, Foufelle F. Insulin effects on sterol regulatory-element-binding protein-1c (SREBP-1c) transcriptional activity in rat hepatocytes. *Biochem J*. 2000 Sep 1;350 Pt 2:389-93.
20. Sewter C, Berger D, Considine RV, Medina G, Rochford J, Ciaraldi T, Henry R, Dohm L, Flier JS, et al. Human obesity and type 2 diabetes are associated with alterations in SREBP1 isoform expression that are reproduced ex vivo by tumor necrosis factor-alpha. *Diabetes*. 2002 Apr;51:1035-41.
21. Ducluzeau PH, Perretti N, Laville M, Andreelli F, Vega N, Riou JP, Vidal H. Regulation by insulin of gene expression in human skeletal muscle and adipose tissue. Evidence for specific defects in type 2 diabetes. *Diabetes*. 2001 May;50:1134-42.
22. Fleischmann M, Iynedjian PB. Regulation of sterol regulatory-element binding protein 1 gene expression in liver: role of insulin and protein kinase B/cAkt. *Biochem J*. 2000 Jul 1;349:13-7.
23. Horton JD, Shah NA, Warrington JA, Anderson NN, Park SW, Brown MS, Goldstein JL. Combined analysis of oligonucleotide microarray data from transgenic and knockout mice identifies direct SREBP target genes. *Proc Natl Acad Sci U S A*. 2003 Oct 14;100:12027-32.
24. Raghov R, Yellaturu C, Deng X, Park EA, Elam MB. SREBPs: the crossroads of physiological and pathological lipid homeostasis. *Trends Endocrinol Metab*. 2008 Mar;19:65-73.
25. Horton JD, Goldstein JL, Brown MS. SREBPs: activators of the complete program of cholesterol and fatty acid synthesis in the liver. *J Clin Invest*. 2002 May;109:1125-31.
26. Shimano H, Horton JD, Shimomura I, Hammer RE, Brown MS, Goldstein JL. Isoform 1c of sterol regulatory element binding protein is less active than isoform 1a in livers of transgenic mice and in cultured cells. *J Clin Invest*. 1997 Mar 1;99:846-54.
27. Shimomura I, Bashmakov Y, Horton JD. Increased levels of nuclear SREBP-1c associated with fatty livers in two mouse models of diabetes mellitus. *J Biol Chem*. 1999 Oct 15;274:30028-32.
28. Martin RJ. In vivo lipogenesis and enzyme levels in adipose and liver tissues from pair-fed genetically obese and lean rats. *Life Sci*. 1974 Apr 16;14:1447-53.
29. Memon RA, Grunfeld C, Moser AH, Feingold KR. Fatty acid synthesis in obese insulin resistant diabetic mice. *Horm Metab Res*. 1994 Feb;26:85-7.
30. Abu-Elheiga L, Brinkley WR, Zhong L, Chirala SS, Woldegiorgis G, Wakil SJ. The subcellular localization of acetyl-CoA carboxylase 2. *Proc Natl Acad Sci U S A*. 2000 Feb 15;97:1444-9.
31. Hardie DG. AMP-activated protein kinase: a cellular energy sensor with a key role in metabolic disorders and in cancer. *Biochemical Society Transactions*. 2011;39:1-13.
32. Merrill GM, Kurth E, Hardie DG, Winder WW. AICAR decreases malonyl-CoA and increases fatty acid oxidation in skeletal muscle of the rat. *Am J Physiol*. 1997;273:E1107-E12.

33. Rakhshandehroo M, Knoch B, Muller M, Kersten S. Peroxisome proliferator-activated receptor alpha target genes. *PPAR Res.* 2010;2010.
34. Chakravarthy MV, Lodhi IJ, Yin L, Malapaka RR, Xu HE, Turk J, Semenkovich CF. Identification of a physiologically relevant endogenous ligand for PPARalpha in liver. *Cell.* 2009 Aug 7;138:476-88.
35. Yao ZM, Vance DE. The active synthesis of phosphatidylcholine is required for very low density lipoprotein secretion from rat hepatocytes. *J Biol Chem.* 1988 Feb 25;263:2998-3004.
36. Letteron P, Sutton A, Mansouri A, Fromenty B, Pessayre D. Inhibition of microsomal triglyceride transfer protein: another mechanism for drug-induced steatosis in mice. *Hepatology.* 2003 Jul;38:133-40.
37. Raabe M, Veniant MM, Sullivan MA, Zlot CH, Bjorkegren J, Nielsen LB, Wong JS, Hamilton RL, Young SG. Analysis of the role of microsomal triglyceride transfer protein in the liver of tissue-specific knockout mice. *J Clin Invest.* 1999 May;103:1287-98.
38. Charlton M, Sreekumar R, Rasmussen D, Lindor K, Nair KS. Apolipoprotein synthesis in nonalcoholic steatohepatitis. *Hepatology.* 2002 Apr;35:898-904.
39. Day CP, James OF. Steatohepatitis: a tale of two "hits"? *Gastroenterology.* 1998 Apr;114:842-5.
40. Schattenberg JM, Galle PR. Animal models of non-alcoholic steatohepatitis: of mice and man. *Dig Dis.* 2010;28:247-54.
41. Rinella ME, Elias MS, Smolak RR, Fu T, Borensztajn J, Green RM. Mechanisms of hepatic steatosis in mice fed a lipogenic methionine choline-deficient diet. *J Lipid Res.* 2008 May;49:1068-76.
42. Gao D, Wei C, Chen L, Huang J, Yang S, Diehl AM. Oxidative DNA damage and DNA repair enzyme expression are inversely related in murine models of fatty liver disease. *Am J Physiol Gastrointest Liver Physiol.* 2004 Nov;287:G1070-7.
43. Mu YP, Ogawa T, Kawada N. Reversibility of fibrosis, inflammation, and endoplasmic reticulum stress in the liver of rats fed a methionine-choline-deficient diet. *Lab Invest.* 2010 Feb;90:245-56.
44. Caballero F, Fernandez A, Matias N, Martinez L, Fucho R, Elena M, Caballeria J, Morales A, Fernandez-Checa JC, Garcia-Ruiz C. Specific contribution of methionine and choline in nutritional nonalcoholic steatohepatitis: impact on mitochondrial S-adenosyl-L-methionine and glutathione. *J Biol Chem.* 2010 Jun 11;285:18528-36.
45. Buettner R, Scholmerich J, Bollheimer LC. High-fat diets: modeling the metabolic disorders of human obesity in rodents. *Obesity (Silver Spring).* 2007 Apr;15:798-808.
46. Kang SS, Wong PW, Malinow MR. Hyperhomocyst(e)inemia as a risk factor for occlusive vascular disease. *Annu Rev Nutr.* 1992;12:279-98.
47. Newberne PM, Rogers AE. Labile methyl groups and the promotion of cancer. *Annu Rev Nutr.* 1986;6:407-32.
48. Mattson MP, Shea TB. Folate and homocysteine metabolism in neural plasticity and neurodegenerative disorders. *Trends Neurosci.* 2003 Mar;26:137-46.
49. Scott JM, Kirke PN, Weir DG. The role of nutrition in neural tube defects. *Annu Rev Nutr.* 1990;10:277-95.

50. Mato JM, Martinez-Chantar ML, Lu SC. Methionine metabolism and liver disease. *Annu Rev Nutr.* 2008;28:273-93.
51. Finkelstein JD. Methionine metabolism in mammals. *J Nutr Biochem.* 1990 May;1:228-37.
52. Williams KT, Schalinske KL. Homocysteine metabolism and its relation to health and disease. *Biofactors.* 2010 Jan-Feb;36:19-24.
53. Farooqui JZ, Lee HW, Kim S, Paik WK. Studies on compartmentation of S-adenosyl-L-methionine in *Saccharomyces cerevisiae* and isolated rat hepatocytes. *Biochim Biophys Acta.* 1983 Jun 9;757:342-51.
54. Agrimi G, Di Noia MA, Marobbio CM, Fiermonte G, Lasorsa FM, Palmieri F. Identification of the human mitochondrial S-adenosylmethionine transporter: bacterial expression, reconstitution, functional characterization and tissue distribution. *Biochem J.* 2004 Apr 1;379:183-90.
55. De La Haba G, Cantoni GL. The enzymatic synthesis of S-adenosyl-L-homocysteine from adenosine and homocysteine. *J Biol Chem.* 1959 Mar;234:603-8.
56. Refsum H, Ueland PM, Nygard O, Vollset SE. Homocysteine and cardiovascular disease. *Annu Rev Med.* 1998;49:31-62.
57. Boushey CJ, Beresford SA, Omenn GS, Motulsky AG. A quantitative assessment of plasma homocysteine as a risk factor for vascular disease. Probable benefits of increasing folic acid intakes. *Jama.* 1995 Oct 4;274:1049-57.
58. Frosst P, Blom HJ, Milos R, Goyette P, Sheppard CA, Matthews RG, Boers GJ, den Heijer M, Kluijtmans LA, et al. A candidate genetic risk factor for vascular disease: a common mutation in methylenetetrahydrofolate reductase. *Nat Genet.* 1995 May;10:111-3.
59. Jacques PF, Bostom AG, Williams RR, Ellison RC, Eckfeldt JH, Rosenberg IH, Selhub J, Rozen R. Relation between folate status, a common mutation in methylenetetrahydrofolate reductase, and plasma homocysteine concentrations. *Circulation.* 1996 Jan 1;93:7-9.
60. Nelen WL, Blom HJ, Thomas CM, Steegers EA, Boers GH, Eskes TK. Methylenetetrahydrofolate reductase polymorphism affects the change in homocysteine and folate concentrations resulting from low dose folic acid supplementation in women with unexplained recurrent miscarriages. *J Nutr.* 1998 Aug;128:1336-41.
61. Collinsova M, Strakova J, Jiracek J, Garrow TA. Inhibition of betaine-homocysteine S-methyltransferase causes hyperhomocysteinemia in mice. *J Nutr.* 2006 Jun;136:1493-7.
62. Namekata K, Enokido Y, Ishii I, Nagai Y, Harada T, Kimura H. Abnormal lipid metabolism in cystathionine beta-synthase-deficient mice, an animal model for hyperhomocysteinemia. *J Biol Chem.* 2004 Dec 17;279:52961-9.
63. Watanabe M, Osada J, Aratani Y, Kluckman K, Reddick R, Malinow MR, Maeda N. Mice deficient in cystathionine beta-synthase: animal models for mild and severe homocyst(e)inemia. *Proc Natl Acad Sci U S A.* 1995 Feb 28;92:1585-9.
64. Li Z, Vance DE. Phosphatidylcholine and choline homeostasis. *J Lipid Res.* 2008 Jun;49:1187-94.
65. Igarashi K, Kashiwagi K. Modulation of cellular function by polyamines. *Int J Biochem Cell Biol.* 2010 Jan;42:39-51.



66. Pirkov I, Norbeck J, Gustafsson L, Albers E. A complete inventory of all enzymes in the eukaryotic methionine salvage pathway. *FEBS J.* 2008 Aug;275:4111-20.
67. Finkelstein JD. Metabolic regulatory properties of S-adenosylmethionine and S-adenosylhomocysteine. *Clin Chem Lab Med.* 2007;45:1694-9.
68. Cabrero C, Puerta J, Alemany S. Purification and comparison of two forms of S-adenosyl-L-methionine synthetase from rat liver. *Eur J Biochem.* 1987 Dec 30;170:299-304.
69. Sullivan DM, Hoffman JL. Fractionation and kinetic properties of rat liver and kidney methionine adenosyltransferase isozymes. *Biochemistry.* 1983 Mar 29;22:1636-41.
70. Jencks DA, Mathews RG. Allosteric inhibition of methylenetetrahydrofolate reductase by adenosylmethionine. Effects of adenosylmethionine and NADPH on the equilibrium between active and inactive forms of the enzyme and on the kinetics of approach to equilibrium. *J Biol Chem.* 1987 Feb 25;262:2485-93.
71. Wagner C, Briggs WT, Cook RJ. Inhibition of glycine N-methyltransferase activity by folate derivatives: implications for regulation of methyl group metabolism. *Biochem Biophys Res Commun.* 1985 Mar 29;127:746-52.
72. Ogawa H, Fujioka M. Purification and properties of glycine N-methyltransferase from rat liver. *J Biol Chem.* 1982 Apr 10;257:3447-52.
73. Sreekumar A, Poisson LM, Rajendiran TM, Khan AP, Cao Q, Yu J, Laxman B, Mehra R, Lonigro RJ, et al. Metabolomic profiles delineate potential role for sarcosine in prostate cancer progression. *Nature.* 2009 Feb 12;457:910-4.
74. Finkelstein JD, Kyle WE, Martin JL, Pick AM. Activation of cystathionine synthase by adenosylmethionine and adenosylethionine. *Biochem Biophys Res Commun.* 1975 Sep 2;66:81-7.
75. Finkelstein JD, Kyle WE, Harris BJ. Methionine metabolism in mammals: regulatory effects of S-adenosylhomocysteine. *Arch Biochem Biophys.* 1974 Dec;165:774-9.
76. Williams KT, Schalinske KL. New insights into the regulation of methyl group and homocysteine metabolism. *J Nutr.* 2007 Feb;137:311-4.
77. Lu SC, Alvarez L, Huang ZZ, Chen L, An W, Corrales FJ, Avila MA, Kanel G, Mato JM. Methionine adenosyltransferase 1A knockout mice are predisposed to liver injury and exhibit increased expression of genes involved in proliferation. *Proc Natl Acad Sci U S A.* 2001 May 8;98:5560-5.
78. Luka Z, Capdevila A, Mato JM, Wagner C. A glycine N-methyltransferase knockout mouse model for humans with deficiency of this enzyme. *Transgenic Res.* 2006 Jun;15:393-7.
79. Martinez-Chantar ML, Vazquez-Chantada M, Ariz U, Martinez N, Varela M, Luka Z, Capdevila A, Rodriguez J, Aransay AM, et al. Loss of the glycine N-methyltransferase gene leads to steatosis and hepatocellular carcinoma in mice. *Hepatology.* 2008 Apr;47:1191-9.
80. Varela-Rey M, Martinez-Lopez N, Fernandez-Ramos D, Embade N, Calvisi DF, Woodhoo A, Rodriguez J, Fraga MF, Julve J, et al. Fatty liver and fibrosis in glycine N-methyltransferase knockout mice is prevented by nicotinamide. *Hepatology.* 2010 Jul;52:105-14.

81. Chen Z, Karaplis AC, Ackerman SL, Pogribny IP, Melnyk S, Lussier-Cacan S, Chen MF, Pai A, John SW, et al. Mice deficient in methylenetetrahydrofolate reductase exhibit hyperhomocysteinemia and decreased methylation capacity, with neuropathology and aortic lipid deposition. *Hum Mol Genet.* 2001 Mar 1;10:433-43.
82. Ghandour H, Chen Z, Selhub J, Rozen R. Mice deficient in methylenetetrahydrofolate reductase exhibit tissue-specific distribution of folates. *J Nutr.* 2004 Nov;134:2975-8.
83. Sächwahn BC, Chen Z, Laryea MD, Wendel U, Lussier-Cacan S, Genest J, Jr., Mar MH, Zeisel SH, Castro C, et al. Homocysteine-betaine interactions in a murine model of 5,10-methylenetetrahydrofolate reductase deficiency. *FASEB J.* 2003 Mar;17:512-4.
84. Selhub J. Homocysteine metabolism. *Annu Rev Nutr.* 1999;19:217-46.
85. Miller JW, Nadeau MR, Smith J, Smith D, Selhub J. Folate-deficiency-induced homocysteinaemia in rats: disruption of S-adenosylmethionine's co-ordinate regulation of homocysteine metabolism. *Biochem J.* 1994 Mar 1;298 ( Pt 2):415-9.
86. Miller JW, Ribaya-Mercado JD, Russell RM, Shepard DC, Morrow FD, Cochary EF, Sadowski JA, Gershoff SN, Selhub J. Effect of vitamin B-6 deficiency on fasting plasma homocysteine concentrations. *Am J Clin Nutr.* 1992 Jun;55:1154-60.
87. Miller JW, Nadeau MR, Smith D, Selhub J. Vitamin B-6 deficiency vs folate deficiency: comparison of responses to methionine loading in rats. *Am J Clin Nutr.* 1994 May;59:1033-9.
88. Ghoshal K, Li X, Datta J, Bai S, Pogribny I, Pogribny M, Huang Y, Young D, Jacob ST. A folate- and methyl-deficient diet alters the expression of DNA methyltransferases and methyl CpG binding proteins involved in epigenetic gene silencing in livers of F344 rats. *J Nutr.* 2006 Jun;136:1522-7.
89. Pogribny IP, Tryndyak VP, Bagnyukova TV, Melnyk S, Montgomery B, Ross SA, Latendresse JR, Rusyn I, Beland FA. Hepatic epigenetic phenotype predetermines individual susceptibility to hepatic steatosis in mice fed a lipogenic methyl-deficient diet. *J Hepatol.* 2009 Jul;51:176-86.
90. Ball CR. Actions of Betaine, Carnitine and Choline on the Pattern of Hepatic Liposis in Mice Fed a High-Fat, Low-Protein Diet. *Anat Rec.* 1964 Aug;149:677-89.
91. Kwon DY, Jung YS, Kim SJ, Park HK, Park JH, Kim YC. Impaired Sulfur-Amino Acid Metabolism and Oxidative Stress in Nonalcoholic Fatty Liver Are Alleviated by Betaine Supplementation in Rats. *Journal of Nutrition.* 2009;139:63-8.
92. Ji C, Kaplowitz N. Betaine decreases hyperhomocysteinemia, endoplasmic reticulum stress, and liver injury in alcohol-fed mice. *Gastroenterology.* 2003 May;124:1488-99.
93. Strnad P, Zatloukal K, Stumptner C, Kulaksiz H, Denk H. Mallory-Denk-bodies: lessons from keratin-containing hepatic inclusion bodies. *Biochim Biophys Acta.* 2008 Dec;1782:764-74.
94. Bardag-Gorce F, Dedes J, French BA, Oliva JV, Li J, French SW. Mallory body formation is associated with epigenetic phenotypic change in hepatocytes in vivo. *Exp Mol Pathol.* 2007 Oct;83:160-8.
95. Li J, Bardag-Gorce F, Dedes J, French BA, Amidi F, Oliva J, French SW. S-adenosylmethionine prevents Mallory Denk body formation in drug-primed mice by inhibiting the epigenetic memory. *Hepatology.* 2008 Feb;47:613-24.

96. Oliva J, Bardag-Gorce F, Li J, French BA, Nguyen SK, Lu SC, French SW. Betaine prevents Mallory-Denk body formation in drug-primed mice by epigenetic mechanisms. *Exp Mol Pathol*. 2009 Apr;86:77-86.
97. Wolff GL, Kodell RL, Moore SR, Cooney CA. Maternal epigenetics and methyl supplements affect agouti gene expression in Avy/a mice. *FASEB J*. 1998 Aug;12:949-57.
98. Cooney CA, Dave AA, Wolff GL. Maternal methyl supplements in mice affect epigenetic variation and DNA methylation of offspring. *J Nutr*. 2002 Aug;132:2393S-400S.
99. Devaux PF. Static and dynamic lipid asymmetry in cell membranes. *Biochemistry*. 1991 Feb 5;30:1163-73.
100. Wang DQ, Cohen DE, Carey MC. Biliary lipids and cholesterol gallstone disease. *J Lipid Res*. 2009 Apr;50 Suppl:S406-11.
101. Li Z, Agellon LB, Allen TM, Umeda M, Jewell L, Mason A, Vance DE. The ratio of phosphatidylcholine to phosphatidylethanolamine influences membrane integrity and steatohepatitis. *Cell Metab*. 2006 May;3:321-31.
102. Sundler R, Akesson B. Regulation of phospholipid biosynthesis in isolated rat hepatocytes. Effect of different substrates. *J Biol Chem*. 1975 May 10;250:3359-67.
103. Vance DE, Choy PC. How is phosphatidylcholine biosynthesis regulated? *Trends Biochem Sci*. 1979;4:145-8.
104. Cornell R, Vance DE. Translocation of CTP: phosphocholine cytidyltransferase from cytosol to membranes in HeLa cells: stimulation by fatty acid, fatty alcohol, mono- and diacylglycerol. *Biochim Biophys Acta*. 1987 May 13;919:26-36.
105. Kuksis A, Mookerjee S. Choline. *Nutr Rev*. 1978 Jul;36:201-7.
106. Alberts W, Johnson A, Lewis J, Raff M, Roberts K, Walter P. *Molekularbiologie der Zelle*. 4th ed; 2004.
107. DeLong CJ, Shen YJ, Thomas MJ, Cui Z. Molecular distinction of phosphatidylcholine synthesis between the CDP-choline pathway and phosphatidylethanolamine methylation pathway. *J Biol Chem*. 1999 Oct 15;274:29683-8.
108. Vance DE, Ridgway ND. The methylation of phosphatidylethanolamine. *Prog Lipid Res*. 1988;27:61-79.
109. Cui Z, Vance JE, Chen MH, Voelker DR, Vance DE. Cloning and expression of a novel phosphatidylethanolamine N-methyltransferase. A specific biochemical and cytological marker for a unique membrane fraction in rat liver. *J Biol Chem*. 1993 Aug 5;268:16655-63.
110. Vance DE, Walkey CJ, Cui Z. Phosphatidylethanolamine N-methyltransferase from liver. *Biochim Biophys Acta*. 1997 Sep 4;1348:142-50.
111. Schneider WJ, Vance DE. Effect of choline deficiency on the enzymes that synthesize phosphatidylcholine and phosphatidylethanolamine in rat liver. *Eur J Biochem*. 1978 Apr;85:181-7.

112. Ridgway ND, Yao Z, Vance DE. Phosphatidylethanolamine levels and regulation of phosphatidylethanolamine N-methyltransferase. *J Biol Chem.* 1989 Jan 15;264:1203-7.
113. Walkey CJ, Donohue LR, Bronson R, Agellon LB, Vance DE. Disruption of the murine gene encoding phosphatidylethanolamine N-methyltransferase. *Proc Natl Acad Sci U S A.* 1997 Nov 25;94:12880-5.
114. Agellon LB, Walkey CJ, Vance DE, Kuipers F, Verkade HJ. The unique acyl chain specificity of biliary phosphatidylcholines in mice is independent of their biosynthetic origin in the liver. *Hepatology.* 1999 Sep;30:725-9.
115. Verkade HJ, Havinga R, Shields DJ, Wolters H, Bloks VW, Kuipers F, Vance DE, Agellon LB. The phosphatidylethanolamine N-methyltransferase pathway is quantitatively not essential for biliary phosphatidylcholine secretion. *J Lipid Res.* 2007 Sep;48:2058-64.
116. Walkey CJ, Yu L, Agellon LB, Vance DE. Biochemical and evolutionary significance of phospholipid methylation. *J Biol Chem.* 1998 Oct 16;273:27043-6.
117. Song J, da Costa KA, Fischer LM, Kohlmeier M, Kwock L, Wang S, Zeisel SH. Polymorphism of the PEMT gene and susceptibility to nonalcoholic fatty liver disease (NAFLD). *Faseb J.* 2005 Aug;19:1266-71.
118. Noga AA, Zhao Y, Vance DE. An unexpected requirement for phosphatidylethanolamine N-methyltransferase in the secretion of very low density lipoproteins. *J Biol Chem.* 2002 Nov 1;277:42358-65.
119. Noga AA, Vance DE. A gender-specific role for phosphatidylethanolamine N-methyltransferase-derived phosphatidylcholine in the regulation of plasma high density and very low density lipoproteins in mice. *J Biol Chem.* 2003 Jun 13;278:21851-9.
120. Zhao Y, Su B, Jacobs RL, Kennedy B, Francis GA, Waddington E, Brosnan JT, Vance JE, Vance DE. Lack of phosphatidylethanolamine N-methyltransferase alters plasma VLDL phospholipids and attenuates atherosclerosis in mice. *Arterioscler Thromb Vasc Biol.* 2009 Sep;29:1349-55.
121. Sehayek E, Wang R, Ono JG, Zinchuk VS, Duncan EM, Shefer S, Vance DE, Ananthanarayanan M, Chait BT, Breslow JL. Localization of the PE methylation pathway and SR-BI to the canalicular membrane: evidence for apical PC biosynthesis that may promote biliary excretion of phospholipid and cholesterol. *J Lipid Res.* 2003 Sep;44:1605-13.
122. Noga AA, Vance DE. Insights into the requirement of phosphatidylcholine synthesis for liver function in mice. *J Lipid Res.* 2003 Oct;44:1998-2005.
123. Noga AA, Stead LM, Zhao Y, Brosnan ME, Brosnan JT, Vance DE. Plasma homocysteine is regulated by phospholipid methylation. *J Biol Chem.* 2003 Feb 21;278:5952-5.
124. Jacobs RL, Stead LM, Devlin C, Tabas I, Brosnan ME, Brosnan JT, Vance DE. Physiological regulation of phospholipid methylation alters plasma homocysteine in mice. *J Biol Chem.* 2005 Aug 5;280:28299-305.
125. Esteller M. Cancer epigenomics: DNA methylomes and histone-modification maps. *Nat Rev Genet.* 2007 Apr;8:286-98.
126. Jirtle RL, Skinner MK. Environmental epigenomics and disease susceptibility. *Nat Rev Genet.* 2007 Apr;8:253-62.

127. Gluckman PD, Hanson MA, Pinal C. The developmental origins of adult disease. *Matern Child Nutr.* 2005 Jul;1:130-41.
128. Johnson CN, Adkins NL, Georgel P. Chromatin remodeling complexes: ATP-dependent machines in action. *Biochem Cell Biol.* 2005 Aug;83:405-17.
129. Misteli T. Beyond the sequence: cellular organization of genome function. *Cell.* 2007 Feb 23;128:787-800.
130. Grewal SI, Moazed D. Heterochromatin and epigenetic control of gene expression. *Science.* 2003 Aug 8;301:798-802.
131. Kouzarides T. Chromatin modifications and their function. *Cell.* 2007 Feb 23;128:693-705.
132. Bernstein BE, Meissner A, Lander ES. The mammalian epigenome. *Cell.* 2007 Feb 23;128:669-81.
133. Grewal SI, Elgin SC. Transcription and RNA interference in the formation of heterochromatin. *Nature.* 2007 May 24;447:399-406.
134. Jaenisch R, Bird A. Epigenetic regulation of gene expression: how the genome integrates intrinsic and environmental signals. *Nat Genet.* 2003 Mar;33 Suppl:245-54.
135. Gardiner-Garden M, Frommer M. CpG islands in vertebrate genomes. *J Mol Biol.* 1987 Jul 20;196:261-82.
136. Dahlhoff C, Fürst RW, Ruhlig K, Sedlmeier EM, Bader BL. Epigenetik und Ernährung. *Ernährung.* 2008;2:116-24.
137. Turner BM. Histone acetylation and an epigenetic code. *Bioessays.* 2000 Sep;22:836-45.
138. Desmarchelier C. Effect of high fat and cafeteria diets on obesity development and associated metabolic disturbances in mice. 85350 Freising-Weihenstephan: Technische Universität München; 2010.
139. Desmarchelier C, Dahlhoff C, Keller S, Sailer M, Jahreis G, Daniel H. C57Bl/6N mice on a Western diet display reduced intestinal and hepatic cholesterol levels despite a plasma hypercholesterolemia. *BMC Genomics.* 2012 Mar 6;13:84.
140. Kirsch SH, Knapp JP, Geisel J, Herrmann W, Obeid R. Simultaneous quantification of S-adenosyl methionine and S-adenosyl homocysteine in human plasma by stable-isotope dilution ultra performance liquid chromatography tandem mass spectrometry. *J Chromatogr B Analyt Technol Biomed Life Sci.* 2009 Nov 15;877:3865-70.
141. Stabler SP, Lindenbaum J, Savage DG, Allen RH. Elevation of serum cystathionine levels in patients with cobalamin and folate deficiency. *Blood.* 1993 Jun 15;81:3404-13.
142. Römisch-Margl W, Prehn C, Bogumil R, Röhring C, Suhre C, Adamski J. Procedure for tissue sample preparation and metabolite extraction for high-throughput targeted metabolomics. *Metabolomics.* 2011.
143. Bustin SA. *Real-Time PCR.* New York; 2005.
144. Livak KJ, Schmittgen TD. Analysis of relative gene expression data using real-time quantitative PCR and the 2<sup>-</sup>(Delta Delta C(T)) Method. *Methods.* 2001 Dec;25:402-8.

145. Pfaffl MW, Tichopad A, Prgomet C, Neuvians TP. Determination of stable housekeeping genes, differentially regulated target genes and sample integrity: BestKeeper--Excel-based tool using pair-wise correlations. *Biotechnol Lett.* 2004 Mar;26:509-15.
146. Towbin H, Staehelin T, Gordon J. Electrophoretic transfer of proteins from polyacrylamide gels to nitrocellulose sheets: procedure and some applications. *Proc Natl Acad Sci U S A.* 1979 Sep;76:4350-4.
147. Karimi M, Johansson S, Ekstrom TJ. Using LUMA: a Luminometric-based assay for global DNA-methylation. *Epigenetics.* 2006 Jan-Mar;1:45-8.
148. Karimi M, Johansson S, Stach D, Corcoran M, Grandner D, Schalling M, Bakalkin G, Lyko F, Larsson C, Ekstrom TJ. LUMA (LUMInometric Methylation Assay)--a high throughput method to the analysis of genomic DNA methylation. *Exp Cell Res.* 2006 Jul 1;312:1989-95.
149. Oakes CC, La Salle S, Robaire B, Trasler JM. Evaluation of a quantitative DNA methylation analysis technique using methylation-sensitive/dependent restriction enzymes and real-time PCR. *Epigenetics.* 2006 Jul-Sep;1:146-52.
150. Oakes CC, La Salle S, Trasler JM, Robaire B. Restriction digestion and real-time PCR (qAMP). *Methods Mol Biol.* 2009;507:271-80.
151. Hayatsu H. Discovery of bisulfite-mediated cytosine conversion to uracil, the key reaction for DNA methylation analysis--a personal account. *Proc Jpn Acad Ser B Phys Biol Sci.* 2008;84:321-30.
152. Ronaghi M. Pyrosequencing sheds light on DNA sequencing. *Genome Res.* 2001 Jan;11:3-11.
153. Tost J, Gut IG. DNA methylation analysis by pyrosequencing. *Nat Protoc.* 2007;2:2265-75.
154. R-Development-Core-Team. R: A language and environment for statistical computing. Vienna Austria: R Foundation for Statistical Computing. 2009.
155. Smyth GK. Limma: linear models for microarray data. In: *Bioinformatics and Computational Biology Solutions using R and Bioconductor.* 2005:397-420.
156. Kersten S, Mandard S, Escher P, Gonzalez FJ, Tafuri S, Desvergne B, Wahli W. The peroxisome proliferator-activated receptor alpha regulates amino acid metabolism. *Faseb J.* 2001 Sep;15:1971-8.
157. Silva Lima B, Van der Laan JW. Mechanisms of nongenotoxic carcinogenesis and assessment of the human hazard. *Regul Toxicol Pharmacol.* 2000 Oct;32:135-43.
158. Peters JM, Cattley RC, Gonzalez FJ. Role of PPAR alpha in the mechanism of action of the nongenotoxic carcinogen and peroxisome proliferator Wy-14,643. *Carcinogenesis.* 1997 Nov;18:2029-33.
159. Peters JM, Cheung C, Gonzalez FJ. Peroxisome proliferator-activated receptor-alpha and liver cancer: where do we stand? *J Mol Med.* 2005 Oct;83:774-85.
160. Ge R, Wang W, Kramer PM, Yang S, Tao L, Pereira MA. Wy-14,643-induced hypomethylation of the c-myc gene in mouse liver. *Toxicol Sci.* 2001 Jul;62:28-35.
161. Pogribny IP, Tryndyak VP, Woods CG, Witt SE, Rusyn I. Epigenetic effects of the continuous exposure to peroxisome proliferator WY-14,643 in mouse liver are

dependent upon peroxisome proliferator activated receptor alpha. *Mutat Res.* 2007 Dec 1;625:62-71.

162. Niculescu MD, Zeisel SH. Diet, methyl donors and DNA methylation: interactions between dietary folate, methionine and choline. *J Nutr.* 2002 Aug;132:2333S-5S.

163. Uekawa A, Katsushima K, Ogata A, Kawata T, Maeda N, Kobayashi K, Maekawa A, Tadokoro T, Yamamoto Y. Change of epigenetic control of cystathionine beta-synthase gene expression through dietary vitamin B12 is not recovered by methionine supplementation. *J Nutrigenet Nutrigenomics.* 2009;2:29-36.

164. Lillycrop KA, Phillips ES, Torrens C, Hanson MA, Jackson AA, Burdge GC. Feeding pregnant rats a protein-restricted diet persistently alters the methylation of specific cytosines in the hepatic PPAR alpha promoter of the offspring. *Br J Nutr.* 2008 Aug;100:278-82.

165. Zhang J, Handy DE, Wang Y, Bouchard G, Selhub J, Loscalzo J, Carey MC. Hyperhomocysteinemia from trimethylation of hepatic phosphatidylethanolamine during cholesterol cholelithogenesis in inbred mice. *Hepatology.* 2011 May 12.

166. Finkelstein JD, Martin JJ, Harris BJ. Effect of dietary cystine on methionine metabolism in rat liver. *J Nutr.* 1986 Jun;116:985-90.

167. Finkelstein JD, Martin JJ, Harris BJ. Methionine metabolism in mammals. The methionine-sparing effect of cystine. *J Biol Chem.* 1988 Aug 25;263:11750-4.

168. Tang B, Mustafa A, Gupta S, Melnyk S, James SJ, Kruger WD. Methionine-deficient diet induces post-transcriptional downregulation of cystathionine beta-synthase. *Nutrition.* 2009 Dec 24.

169. Finkelstein JD, Martin JJ, Harris BJ, Kyle WE. Regulation of hepatic betaine-homocysteine methyltransferase by dietary betaine. *J Nutr.* 1983 Mar;113:519-21.

170. Park EI, Garrow TA. Interaction between dietary methionine and methyl donor intake on rat liver betaine-homocysteine methyltransferase gene expression and organization of the human gene. *J Biol Chem.* 1999 Mar 19;274:7816-24.

171. Sowden MP, Collins HL, Smith HC, Garrow TA, Sparks JD, Sparks CE. Apolipoprotein B mRNA and lipoprotein secretion are increased in McArdle RH-7777 cells by expression of betaine-homocysteine S-methyltransferase. *Biochem J.* 1999 Aug 1;341 ( Pt 3):639-45.

172. Sparks JD, Collins HL, Chirieac DV, Cianci J, Jokinen J, Sowden MP, Galloway CA, Sparks CE. Hepatic very-low-density lipoprotein and apolipoprotein B production are increased following in vivo induction of betaine-homocysteine S-methyltransferase. *Biochem J.* 2006 Apr 15;395:363-71.

173. Jacobs RL, Zhao Y, Koonen DP, Sletten T, Su B, Lingrell S, Cao G, Peake DA, Kuo MS, et al. Impaired de novo choline synthesis explains why phosphatidylethanolamine N-methyltransferase-deficient mice are protected from diet-induced obesity. *J Biol Chem.* 2010 Jul 16;285:22403-13.

174. Jacobs RL, House JD, Brosnan ME, Brosnan JT. Effects of streptozotocin-induced diabetes and of insulin treatment on homocysteine metabolism in the rat. *Diabetes.* 1998 Dec;47:1967-70.

175. Fonseca V, Dicker-Brown A, Ranganathan S, Song W, Barnard RJ, Fink L, Kern PA. Effects of a high-fat-sucrose diet on enzymes in homocysteine metabolism in the rat. *Metabolism*. 2000 Jun;49:736-41.
176. Bravo E, Palleschi S, Aspichueta P, Buque X, Rossi B, Cano A, Napolitano M, Ochoa B, Botham KM. High fat diet-induced non alcoholic fatty liver disease in rats is associated with hyperhomocysteinemia caused by down regulation of the transsulphuration pathway. *Lipids Health Dis*. 2011 Apr 19;10:60.
177. Robert K, Nehme J, Bourdon E, Pivert G, Friguet B, Delcayre C, Delabar JM, Janel N. Cystathionine beta synthase deficiency promotes oxidative stress, fibrosis, and steatosis in mice liver. *Gastroenterology*. 2005 May;128:1405-15.
178. Sheikh K, Camejo G, Lanne B, Halvarsson T, Landergren MR, Oakes ND. Beyond lipids, pharmacological PPARalpha activation has important effects on amino acid metabolism as studied in the rat. *Am J Physiol Endocrinol Metab*. 2007 Apr;292:E1157-65.
179. Dierkes J, Westphal S, Luley C. Serum homocysteine increases after therapy with fenofibrate or bezafibrate. *Lancet*. 1999 Jul 17;354:219-20.
180. Landray MJ, Townend JN, Martin S, Martin U, Wheeler DC. Lipid-lowering drugs and homocysteine. *Lancet*. 1999 Jun 5;353:1974-5.
181. Giral P, Bruckert E, Jacob N, Chapman MJ, Foglietti MJ, Turpin G. Homocysteine and lipid lowering agents. A comparison between atorvastatin and fenofibrate in patients with mixed hyperlipidemia. *Atherosclerosis*. 2001 Feb 1;154:421-7.
182. Bissonnette R, Treacy E, Rozen R, Boucher B, Cohn JS, Genest J, Jr. Fenofibrate raises plasma homocysteine levels in the fasted and fed states. *Atherosclerosis*. 2001 Apr;155:455-62.
183. Dierkes J, Luley C, Westphal S. Effect of lipid-lowering and anti-hypertensive drugs on plasma homocysteine levels. *Vasc Health Risk Manag*. 2007;3:99-108.
184. Legendre C, Causse E, Chaput E, Salvayre R, Pineau T, Edgar AD. Fenofibrate induces a selective increase of protein-bound homocysteine in rodents: a PPARalpha-mediated effect. *Biochem Biophys Res Commun*. 2002 Aug 2;295:1052-6.
185. Luc G, Jacob N, Bouly M, Fruchart JC, Staels B, Giral P. Fenofibrate increases homocystinemia through a PPARalpha-mediated mechanism. *J Cardiovasc Pharmacol*. 2004 Mar;43:452-3.
186. Mikael LG, Genest J, Jr., Rozen R. Elevated homocysteine reduces apolipoprotein A-I expression in hyperhomocysteinemic mice and in males with coronary artery disease. *Circ Res*. 2006 Mar 3;98:564-71.
187. Rakhshandehroo M, Sanderson LM, Matilainen M, Stienstra R, Carlberg C, de Groot PJ, Muller M, Kersten S. Comprehensive analysis of PPARalpha-dependent regulation of hepatic lipid metabolism by expression profiling. *PPAR Res*. 2007;2007:26839.
188. Jerkins AA, Steele RD. Dietary sulfur amino acid modulation of cysteine sulfinic acid decarboxylase. *Am J Physiol*. 1991 Nov;261:E551-5.
189. Jerkins AA, Jones DD, Kohlhepp EA. Cysteine sulfinic acid decarboxylase mRNA abundance decreases in rats fed a high-protein diet. *J Nutr*. 1998 Nov;128:1890-5.



190. Kishimoto T, Kokura K, Nakadai T, Miyazawa Y, Wakamatsu T, Makino Y, Nakamura T, Hara E, Oda K, et al. Overexpression of cysteine sulfinic acid decarboxylase stimulated by hepatocarcinogenesis results in autoantibody production in rats. *Cancer Res.* 1996 Nov 15;56:5230-7.
191. Nakashima T, Takino T, Kuriyama K. Therapeutic and prophylactic effects of taurine administration on experimental liver injury. *Prog Clin Biol Res.* 1983;125:449-59.
192. Schaffer SW, Azuma J, Mozaffari M. Role of antioxidant activity of taurine in diabetes. *Can J Physiol Pharmacol.* 2009 Feb;87:91-9.
193. Soga T, Baran R, Suematsu M, Ueno Y, Ikeda S, Sakurakawa T, Kakazu Y, Ishikawa T, Robert M, et al. Differential metabolomics reveals ophthalmic acid as an oxidative stress biomarker indicating hepatic glutathione consumption. *J Biol Chem.* 2006 Jun 16;281:16768-76.
194. Schulz WA, Steinhoff C, Florl AR. Methylation of endogenous human retroelements in health and disease. *Curr Top Microbiol Immunol.* 2006;310:211-50.
195. Williams KT, Garrow TA, Schalinske KL. Type I diabetes leads to tissue-specific DNA hypomethylation in male rats. *J Nutr.* 2008 Nov;138:2064-9.
196. Powell CL, Bradford BU, Craig CP, Tsuchiya M, Uehara T, O'Connell TM, Pogribny IP, Melnyk S, Koop DR, et al. Mechanism for prevention of alcohol-induced liver injury by dietary methyl donors. *Toxicol Sci.* 2010 May;115:131-9.
197. Kharbanda KK, Mailliard ME, Baldwin CR, Beckenhauer HC, Sorrell MF, Tuma DJ. Betaine attenuates alcoholic steatosis by restoring phosphatidylcholine generation via the phosphatidylethanolamine methyltransferase pathway. *J Hepatol.* 2007 Feb;46:314-21.
198. Song Z, Deaciuc I, Zhou Z, Song M, Chen T, Hill D, McClain CJ. Involvement of AMP-activated protein kinase in beneficial effects of betaine on high-sucrose diet-induced hepatic steatosis. *Am J Physiol Gastrointest Liver Physiol.* 2007 Oct;293:G894-902.
199. Kathirvel E, Morgan K, Nandgiri G, Sandoval BC, Caudill MA, Bottiglieri T, French SW, Morgan TR. Betaine improves nonalcoholic fatty liver and associated hepatic insulin resistance: a potential mechanism for hepatoprotection by betaine. *Am J Physiol Gastrointest Liver Physiol.* 2010 Nov;299:G1068-77.
200. Kim SK, Kim YC. Effects of betaine supplementation on hepatic metabolism of sulfur-containing amino acids in mice. *J Hepatol.* 2005 Jun;42:907-13.
201. Luka Z, Mudd SH, Wagner C. Glycine N-methyltransferase and regulation of S-adenosylmethionine levels. *J Biol Chem.* 2009 Aug 21;284:22507-11.
202. Higashino K, Fujioka M, Yamamura Y. The conversion of L-lysine to saccharopine and alpha-amino adipate in mouse. *Arch Biochem Biophys.* 1971 Feb;142:606-14.
203. Gulsen M, Yesilova Z, Bagci S, Uygun A, Ozcan A, Ercin CN, Erdil A, Sanisoglu SY, Cakir E, et al. Elevated plasma homocysteine concentrations as a predictor of steatohepatitis in patients with non-alcoholic fatty liver disease. *J Gastroenterol Hepatol.* 2005 Sep;20:1448-55.

204. Hirsch S, Poniachick J, Avendano M, Csendes A, Burdiles P, Smok G, Diaz JC, de la Maza MP. Serum folate and homocysteine levels in obese females with non-alcoholic fatty liver. *Nutrition*. 2005 Feb;21:137-41.
205. Chico A, Perez A, Cordoba A, Arcelus R, Carreras G, de Leiva A, Gonzalez-Sastre F, Blanco-Vaca F. Plasma homocysteine is related to albumin excretion rate in patients with diabetes mellitus: a new link between diabetic nephropathy and cardiovascular disease? *Diabetologia*. 1998 Jun;41:684-93.
206. Hultberg B, Agardh E, Andersson A, Brattstrom L, Isaksson A, Israelsson B, Agardh CD. Increased levels of plasma homocysteine are associated with nephropathy, but not severe retinopathy in type 1 diabetes mellitus. *Scand J Clin Lab Invest*. 1991 May;51:277-82.
207. Bostom A, Brosnan JT, Hall B, Nadeau MR, Selhub J. Net uptake of plasma homocysteine by the rat kidney in vivo. *Atherosclerosis*. 1995 Jul;116:59-62.
208. Wijekoon EP, Brosnan ME, Brosnan JT. Homocysteine metabolism in diabetes. *Biochem Soc Trans*. 2007 Nov;35:1175-9.
209. Yasumitsu T, Takao T, Kakimoto Y. Inhibition of metabolism of beta-alanine and D-beta-aminoisobutyric acid by D-cycloserine. *Biochem Pharmacol*. 1976 Feb 1;25:253-8.
210. Nielsen HR, Sjolín KE, Nyholm K, Baliga BS, Wong R, Borek E. Beta-aminoisobutyric acid, a new probe for the metabolism of DNA and RNA in normal and tumorous tissue. *Cancer Res*. 1974 Jun;34:1381-4.
211. Baliga BS, Borek E. Metabolism of thymine in tumor tissue: the origins of beta-aminoisobutyric acid. *Adv Enzyme Regul*. 1975;13:27-36.
212. Begriche K, Massart J, Abbey-Toby A, Igoudjil A, Letteron P, Fromenty B. Beta-aminoisobutyric acid prevents diet-induced obesity in mice with partial leptin deficiency. *Obesity (Silver Spring)*. 2008 Sep;16:2053-67.
213. Mong MC, Chao CY, Yin MC. Histidine and carnosine alleviated hepatic steatosis in mice consumed high saturated fat diet. *Eur J Pharmacol*. 2011 Feb 25;653:82-8.
214. Finkelstein JD, Martin JJ. Methionine metabolism in mammals. Adaptation to methionine excess. *J Biol Chem*. 1986 Feb 5;261:1582-7.
215. Park E, Renduchintala MS, Garrow T. Diet-induced changes in hepatic betaine-homocysteine methyltransferase activity are mediated by changes in the steady-state level of its mRNA. *Nutritional Biochemistry*. 1997;8:541-5.
216. Teng YW, Mehedint MG, Garrow TA, Zeisel SH. Deletion of betaine-homocysteine s-methyltransferase in mice perturbs choline and 1-carbon metabolism, resulting in Fatty liver and hepatocellular carcinomas. *J Biol Chem*. 2011 Oct 21;286:36258-67.
217. Karavia EA, Papachristou DJ, Kotsikogianni I, Giopanou I, Kypreos KE. Deficiency in apolipoprotein E has a protective effect on diet-induced nonalcoholic fatty liver disease in mice. *FEBS J*. 2011 Sep;278:3119-29.
218. Ingebritsen TS, Lee HS, Parker RA, Gibson DM. Reversible modulation of the activities of both liver microsomal hydroxymethylglutaryl coenzyme A reductase and its inactivating enzyme. Evidence for regulation by phosphorylation-dephosphorylation. *Biochem Biophys Res Commun*. 1978 Apr 28;81:1268-77.

219. Hawley SA, Davison M, Woods A, Davies SP, Beri RK, Carling D, Hardie DG. Characterization of the AMP-activated protein kinase kinase from rat liver and identification of threonine 172 as the major site at which it phosphorylates AMP-activated protein kinase. *J Biol Chem*. 1996 Nov 1;271:27879-87.
220. Saggerson D. Malonyl-CoA, a key signaling molecule in mammalian cells. *Annu Rev Nutr*. 2008;28:253-72.
221. Orellana-Gavalda JM, Herrero L, Malandrino MI, Paneda A, Sol Rodriguez-Pena M, Petry H, Asins G, Van Deventer S, Hegardt FG, Serra D. Molecular therapy for obesity and diabetes based on a long-term increase in hepatic fatty-acid oxidation. *Hepatology*. 2011 Mar;53:821-32.
222. Teyssier C, Ma H, Emter R, Kralli A, Stallcup MR. Activation of nuclear receptor coactivator PGC-1alpha by arginine methylation. *Genes Dev*. 2005 Jun 15;19:1466-73.
223. Pooya S, Blaise S, Moreno Garcia M, Giudicelli J, Alberto JM, Gueant-Rodriguez RM, Jeannesson E, Gueguen N, Bressenot A, et al. Methyl donor deficiency impairs fatty acid oxidation through PGC-1alpha hypomethylation and decreased ER-alpha, ERR-alpha, and HNF-4alpha in the rat liver. *J Hepatol*. 2012 Apr 17.
224. Li S, Arning E, Liu C, Vitvitsky V, Hernandez C, Banerjee R, Bottiglieri T, Lin JD. Regulation of homocysteine homeostasis through the transcriptional coactivator PGC-1alpha. *Am J Physiol Endocrinol Metab*. 2009 Mar;296:E543-8.
225. Bartlett K, Eaton S. Mitochondrial beta-oxidation. *Eur J Biochem*. 2004 Feb;271:462-9.
226. Vaz FM, Wanders RJ. Carnitine biosynthesis in mammals. *Biochem J*. 2002 Feb 1;361:417-29.
227. Paik WK, Kim S. Protein methylation. *Science*. 1971 Oct 8;174:114-9.
228. Gulick T, Cresci S, Caira T, Moore DD, Kelly DP. The peroxisome proliferator-activated receptor regulates mitochondrial fatty acid oxidative enzyme gene expression. *Proc Natl Acad Sci U S A*. 1994 Nov 8;91:11012-6.
229. Ignoul S, Eggermont J. CBS domains: structure, function, and pathology in human proteins. *Am J Physiol Cell Physiol*. 2005 Dec;289:C1369-78.
230. Wang Z, Yao T, Pini M, Zhou Z, Fantuzzi G, Song Z. Betaine improved adipose tissue function in mice fed a high-fat diet: a mechanism for hepatoprotective effect of betaine in nonalcoholic fatty liver disease. *Am J Physiol Gastrointest Liver Physiol*. 2010 May;298:G634-42.
231. Yamauchi T, Kamon J, Minokoshi Y, Ito Y, Waki H, Uchida S, Yamashita S, Noda M, Kita S, et al. Adiponectin stimulates glucose utilization and fatty-acid oxidation by activating AMP-activated protein kinase. *Nat Med*. 2002 Nov;8:1288-95.
232. Weekes J, Hawley SA, Corton J, Shugar D, Hardie DG. Activation of rat liver AMP-activated protein kinase by kinase kinase in a purified, reconstituted system. Effects of AMP and AMP analogues. *Eur J Biochem*. 1994 Feb 1;219:751-7.
233. Davies SP, Helps NR, Cohen PT, Hardie DG. 5'-AMP inhibits dephosphorylation, as well as promoting phosphorylation, of the AMP-activated protein kinase. Studies using bacterially expressed human protein phosphatase-2C alpha and native bovine protein phosphatase-2AC. *FEBS Lett*. 1995 Dec 27;377:421-5.

234. Boison D, Scheurer L, Zumsteg V, Rulicke T, Litynski P, Fowler B, Brandner S, Mohler H. Neonatal hepatic steatosis by disruption of the adenosine kinase gene. *Proc Natl Acad Sci U S A*. 2002 May 14;99:6985-90.
235. Niebergall LJ, Jacobs RL, Chaba T, Vance DE. Phosphatidylcholine protects against steatosis in mice but not non-alcoholic steatohepatitis. *Biochim Biophys Acta*. 2011 Dec;1811:1177-85.
236. Wahle KW. Fatty acid modification and membrane lipids. *Proc Nutr Soc*. 1983 Jun;42:273-87.
237. Spector AA, Yorek MA. Membrane lipid composition and cellular function. *J Lipid Res*. 1985 Sep;26:1015-35.
238. Clamp AG, Ladha S, Clark DC, Grimble RF, Lund EK. The influence of dietary lipids on the composition and membrane fluidity of rat hepatocyte plasma membrane. *Lipids*. 1997 Feb;32:179-84.
239. Lee JM, Lee YK, Mamrosh JL, Busby SA, Griffin PR, Pathak MC, Ortlund EA, Moore DD. A nuclear-receptor-dependent phosphatidylcholine pathway with antidiabetic effects. *Nature*. 2011 Jun 23;474:506-10.
240. de Vet EC, van den Bosch H. Alkyl-dihydroxyacetonephosphate synthase. *Cell Biochem Biophys*. 2000;32 Spring:117-21.
241. da Costa KA, Gaffney CE, Fischer LM, Zeisel SH. Choline deficiency in mice and humans is associated with increased plasma homocysteine concentration after a methionine load. *Am J Clin Nutr*. 2005 Feb;81:440-4.
242. Strakova J, Gupta S, Kruger WD, Dilger RN, Tryon K, Li L, Garrow TA. Inhibition of betaine-homocysteine S-methyltransferase in rats causes hyperhomocysteinemia and reduces liver cystathionine beta-synthase activity and methylation capacity. *Nutr Res*. 2011 Jul;31:563-71.
243. Walczyk T, Coward A, Schoeller DA, Preston T, Dainty J, Turnlund JR, Iyengar V. Stable isotope techniques in human nutrition research: concerted action is needed. *Food Nutr Bull*. 2002 Sep;23:69-75.

## 7 Appendix

### 7.1 qRT-PCR

**Table 9.** Analysis of HF diet induced NAFLD on hepatic gene expression.  $C_q$ -values of invariant house keeping genes are listed for C and HF group. Abbreviations: Actb,  $\beta$ -Actin; Gapdh, Glyceraldehyde-3-phosphate dehydrogenase; Hprt, Hypoxanthine guanine phosphoribosyl transferase.

	<b>Gapdh</b>	<b>Actb</b>	<b>Hprt</b>
<b>C</b>	19.47	21.23	26.38
	19.91	20.63	26.35
	19.99	19.81	26.36
	19.78	21	26.42
	20.26	20.69	26.87
<b>HF</b>	19.84	21.18	25.89
	19.6	20.66	26.16
	19.18	20.7	25.96
	19.36	20.82	25.81
	19.81	21.26	26.11
	19.96	20.28	26.2

**Table 10.** Analysis of HF diet induced NAFLD on hepatic gene expression.  $C_q$ -values of genes operating in the methionine cycle are listed for C and HF group. Abbreviations: Ahcy, S-adenosylhomocysteine hydrolase; Mat1a, Methionine adenosyltransferase I alpha; Mat2a, Methionine adenosyltransferase II alpha; Pemt, Phosphatidylethanolamine N-methyltransferase.

	<b>Mat1a</b>	<b>Mat2a</b>	<b>Pemt</b>	<b>Ahcy</b>
<b>C</b>	20.76	25.79	24.02	20.67
	20.11	26.04	23.96	20.21
	21.27	25.7	24.24	20.76
	20.94	26.29	23.89	20.75
	21.17	-	24.13	20.87
<b>HF</b>	20.26	25.62	24.12	20.33
	20.28	25.63	24.22	20.47
	20.33	25.19	23.83	20.61
	19.73	25.29	23.67	20.05
	20.5	25.97	24.24	20.98
	20.39	26.16	24.22	20.44

**Table 11.** Analysis of HF diet induced NAFLD on hepatic gene expression.  $C_q$ -values of genes operating in the folate cycle are listed for C and HF group. Abbreviations: Mthfr, 5,10-methylenetetrahydrofolate reductase; Mtr, 5-methyltetrahydrofolate-homocysteine methyltransferase; Shmt1, Serine hydroxymethyltransferase 1; Shmt2, Serine hydroxymethyltransferase 2.

	<b>Mtr</b>	<b>Mthfr</b>	<b>Shmt1</b>	<b>Shmt2</b>
<b>C</b>	28.43	30.34	24.57	24.11
	28.74	29.13	24.91	24.28
	28.82	29.92	25.03	24.4
	28.42	30.49	24.95	24.19
	28.78	28.91	25.03	24.45
<b>HF</b>	28.37	30.27	24.31	23.89
	28.18	30.09	24.58	24.11
	28.08	28.87	24.08	23.88
	28.55	30	23.7	23.55
	28.58	29.07	24.81	24.1
	28.75	28.96	24.6	24.22

**Table 12.** Analysis of HF diet induced NAFLD on hepatic gene expression.  $C_q$ -values of genes operating in the sarcosine pathway are listed for C and HF group. Abbreviations: Bhmt, Betaine-homocysteine methyltransferase; Bhmt2, Betaine-homocysteine methyltransferase 2; Chdh, Choline dehydrogenase; Dmgdh, Dimethylglycine dehydrogenase precursor; Gnmmt, Glycine N-methyltransferase.

	<b>Chdh</b>	<b>Bhmt</b>	<b>Bhmt2</b>	<b>Dmgdh</b>	<b>Gnmmt</b>
<b>C</b>	26.11	20.71	27.86	23.02	20.28
	26.1	20.99	27.78	23.45	19.84
	26.25	21.12	27.64	23.43	20.54
	25.77	21.09	27.71	23.18	20.82
	25.99	20.75	27.79	23.19	20.99
<b>HF</b>	25.53	19.42	27.47	22.35	20.37
	25.71	20.11	27.64	22.98	20.59
	25.2	19.61	27.28	22.36	20.63
	25.14	19.4	27.05	22.27	20.43
	25.72	19.96	27.66	22.77	20.8
	25.38	19.7	27.49	22.59	20.36

**Table 13.** Analysis of HF diet induced NAFLD on hepatic gene expression.  $C_q$ -values of genes operating in the transsulfuration pathway are listed for C and HF group. Abbreviations: Cbs, Cystathionine  $\beta$ -synthase; Csad, Cysteine sulfinic acid decarboxylase; Cth, Cystathionase; Gclc, Glutamate-cysteine ligase catalytic subunit; Got1, Glutamate oxaloacetate transaminase 1; Gss, Glutathione synthetase.

	<b>Cbs</b>	<b>Cth</b>	<b>Csad</b>	<b>Got1</b>	<b>Gss</b>	<b>Gclc</b>
<b>C</b>	23.54	22.31	26.22	22.85	26.65	23.52
	22.86	21.23	24.84	21.5	26.59	22.74
	23.67	22.67	25.97	23.73	26.88	23.37
	23.88	22.47	25.79	22.94	26.71	23.5
	23.41	22.34	25.85	23.08	26.97	23.47
<b>HF</b>	23.93	22.5	24.58	23.25	26.49	23.49
	23.83	22.75	25.62	23.39	26.15	23.18
	23.4	22.28	23.5	23.93	25.82	22.58
	23.9	21.86	24.9	22.73	26.32	23.73
	24.14	22.55	24.11	23.95	26.52	22.89
	23.86	22.29	24.43	24.01	26.45	23.29

**Table 14.** Analysis of HF diet induced NAFLD on hepatic gene expression.  $C_q$ -values of PPAR $\alpha$  and PPAR $\alpha$  target genes are listed for C and HF group. Abbreviations: Acox1, Acyl-coenzyme A oxidase 1; Cpt1a, Carnitine palmitoyltransferase 1a; Ppara, Peroxisome proliferator activated receptor  $\alpha$ ; Ucp2, Uncoupling protein 2.

	<b>Ppara</b>	<b>Cpt1a</b>	<b>Acox1</b>	<b>Ucp2</b>
<b>C</b>	24.5	27.31	20.63	29.06
	24.93	26.77	20.57	28.64
	24.53	27.18	20.83	28.94
	23.75	26.26	20.65	28.81
	24.57	26.89	20.94	29.08
<b>HF</b>	23.44	25.31	19.78	28.09
	23.59	25.72	19.77	28.04
	23.17	25.24	19.37	27.42
	22.83	24.63	19.17	27.2
	24.09	24.48	19.99	27.66
	23.91	24.41	20.05	28.57

**Table 15.** Analysis of HF diet induced NAFLD on hepatic gene expression.  $C_q$ -values of DNA methyltransferase genes are listed for C and HF group. Abbreviations: Dnmt1, DNA methyltransferase 1; Dnmt3a, DNA methyltransferase 3a; Dnmt3b, DNA methyltransferase 3b.

	<b>Dnmt1</b>	<b>Dnmt3a</b>	<b>Dnmt3b</b>
<b>C</b>	25.18	28.24	31.21
	25.19	27.9	29.81
	25.32	28.38	30.27
	24.94	27.62	31.34
	25.06	28.38	30.1
<b>HF</b>	25.4	28.23	31.69
	25.11	28.2	31.85
	24.79	27.86	31.17
	24.63	27.82	31.07
	25.16	28.61	31.41
	25.07	28.97	31.05

**Table 16.** Influence of WY14,643 mediated PPAR $\alpha$  activation on gene expression of invariant housekeeping gene (Gus), PPAR $\alpha$  target gene (Cpt1a) and genes operating in the C1-metabolism (Cbs, Bhmt) in rat hepatoma FAO cells.  $C_q$ -values are listed for 0 – 100  $\mu$ M WY14,643 treatment for 24 h. Abbreviations: Bhmt, Betaine-homocysteine methyltransferase; Cbs, Cystathionine  $\beta$ -synthase; Cpt1a, Carnitine palmitoyltransferase 1a; Gus,  $\beta$ -Glucuronidase.

	<b>Gus</b>	<b>Cpt1a</b>	<b>Cbs</b>	<b>Bhmt</b>
<b>0 <math>\mu</math>M</b>	24.96	23.45	24.56	21.63
	24.47	23.53	24.16	21.14
	25.02	24.03	24.94	20.72
	24.51	23.66	23.72	21.43
<b>25 <math>\mu</math>M</b>	24.85	23.01	26.16	22.03
	25.05	23.05	26.03	21.96
	24.74	22.83	26.23	21.38
	24.84	23.18	25.89	21.74
<b>50 <math>\mu</math>M</b>	24.75	23	26.1	22.13
	24.75	23.03	25.1	22.31
	25.08	23.14	26.68	21.53
	24.74	23.13	25.76	22.18
<b>100 <math>\mu</math>M</b>	24.86	23.02	25.91	21.8
	24.64	22.96	24.69	21.97
	24.79	23.08	26.84	21.47
	25.03	23	26.35	21.57



**Table 17.** Analysis of hepatic gene expression in animals of the methyl-group supplementation feeding trial.  $C_q$ -values of invariant housekeeping genes (Gapdh, Hprt), genes operating in the C1-metabolism (Bhmt, Cbs), genes implicated in DNL (Srebp1c, Fasn) as well as  $C_q$ -values of a PPAR $\alpha$  target gene (Cpt1a) are listed for C, CMS, HF and HFMS mice. Abbreviations: Bhmt, Betaine-homocysteine methyltransferase; Cbs, Cystathionine  $\beta$ -synthase; Cpt1a, Carnitine palmitoyltransferase 1a; Fasn, Fatty acid synthase; Gapdh, Glyceraldehyde-3-phosphate dehydrogenase; Hprt, Hypoxanthine guanine phosphoribosyl transferase; Srebp1c, Sterol regulatory element binding transcription factor 1c.

	<b>Gapdh</b>	<b>Hprt</b>	<b>Bhmt</b>	<b>Cbs</b>	<b>Srebp1c</b>	<b>Fasn</b>	<b>Cpt1a</b>
<b>C</b>	19.69	26.84	20.35	23.11	25.36	22.56	23.47
	19.89	26.71	21.06	22.97	25.06	23.47	23.32
	19.6	27.01	20.26	23	25.01	22.81	22.38
	19.22	26.88	20.08	23	24.18	20.5	23.06
	19.76	26.82	20.8	22.68	24.71	21.38	23.66
	19.61	26.94	20.66	23.48	25.73	22.37	22.88
	19.8	26.78	19.8	23.34	24.52	22.03	23.8
	19.87	26.94	19.94	23.24	25.44	23.05	23.53
	19.66	26.83	20.1	22.91	24.85	22.3	23.24
<b>CMS</b>	19.81	27.02	19.13	23.4	25.51	22.78	23.59
	19.89	26.83	19.43	23.16	26.75	24.1	23.12
	19.59	26.81	19.39	23.24	26.29	23.86	22.68
	19.42	26.22	18.72	23.23	24.62	21.31	23.53
	19.64	26.33	18.89	23.29	25.97	23.86	23.61
	20.2	26.58	19.56	23.53	24.85	23.43	23.34
	20.24	26.8	18.69	23.77	25.93	23.36	23.86
	19.75	26.76	18.84	23.41	25.36	23.57	23.76
	19.75	26.52	19.38	23.61	26.58	23.79	23.01
<b>HF</b>	19.51	26.02	19.98	23.34	24.55	22.31	22.36
	19.54	26.07	19.61	23.21	24.31	23.5	22.19
	20.3	26.48	20.04	23.56	23.91	22.88	22.48
	19.87	26.22	19.85	23.16	24.97	22.28	22.14
	19.88	26.29	20.06	23.48	24.66	23.08	22.52
	19.77	26.1	20.52	23.55	24.57	21.89	22.01
	20.07	26.27	19.62	23.37	25.69	22.49	22.63
	20.05	26.13	20.05	23.24	24.78	22.89	22.6
<b>HFMS</b>	20	26.1	18.68	22.89	25.32	24.45	22.65
	20.05	26.3	19.5	23.33	24.48	22.37	22.43
	19.57	25.82	19.06	23.29	24.01	22.3	21.71
	19.61	25.88	19.1	22.9	25.21	22.28	22.18
	20.45	26.09	19.45	23.54	25.35	23.41	22.62
	19.91	26.55	19.84	23.75	25.38	22.68	22.21
	20.03	26.44	19.09	23.33	-	24.25	22.66
	20.34	26.52	19.87	23.72	26.45	23.76	22.57
	20.03	26.23	19.51	23.74	24.82	23.36	22.2

## 7.2 Metabolites

**Table 18.** Effect of dietary HF treatment on hepatic metabolite level is listed. Data are presented as mean  $\pm$  SEM [ $\mu\text{mol/g}$  protein] ( $n = 9-11$ ). Bold numbers indicate statistical significance ( $P < 0.05$ ). Abbreviations: 1MHis, 1-methyl-L-histidine; Aad, L- $\alpha$ -amino adipic acid; Abu, L- $\alpha$ -amino-n-butyrate; Ala, L-alanine; Asn, L-asparagine; Asp, L-asparic acid; bAib, D,L- $\beta$ -aminoisobutyrate; Cit, L-citrulline; Cth, Cystathionine; EtN, Ethanolamine; GABA,  $\gamma$ -amino-n-butyrate; Gln, L-glutamine; Glu, L-glutamate; Gly, Glycine; His, L-histidine; Hyp, Hydroxyproline; Ile, L-isoleucine; Leu, L-leucine; Lys, L-lysine; Met, L-methionine; Orn, L-ornithine; PEtN, O-phosphoethanolamine; Phe, L-phenylalanine; Pro, L-proline; Sar, Sarcosine; Ser, L-serine; Tau, Taurine; Thr, L-threonine; Trp, L-tryptophane; Tyr, L-tyrosine; Val, L-valine.

Metabolite [ $\mu\text{mol/g}$ protein]	C	HF
1MHis	0.36 $\pm$ 0.02	0.47 $\pm$ 0.05
Aad	0.52 $\pm$ 0.07	0.56 $\pm$ 0.08
Abu	<b>0.96 <math>\pm</math> 0.14</b>	<b>0.47 <math>\pm</math> 0.04</b>
Ala	70.30 $\pm$ 3.48	77.87 $\pm$ 4.21
Asn	2.39 $\pm$ 0.16	2.72 $\pm$ 0.18
Asp	3.20 $\pm$ 0.27	2.71 $\pm$ 0.30
bAib	0.13 $\pm$ 0.01	0.10 $\pm$ 0.01
Cit	<b>0.71 <math>\pm</math> 0.08</b>	<b>0.38 <math>\pm</math> 0.03</b>
EtN	0.35 $\pm$ 0.02	0.33 $\pm$ 0.03
GABA	0.22 $\pm$ 0.01	0.23 $\pm$ 0.02
Gln	<b>38.43 <math>\pm</math> 2.95</b>	<b>53.07 <math>\pm</math> 3.71</b>
Glu	13.96 $\pm$ 0.77	18.19 $\pm$ 1.91
Gly	32.00 $\pm$ 1.16	28.75 $\pm$ 1.23
His	7.99 $\pm$ 0.57	7.91 $\pm$ 0.61
Hyp	<b>0.34 <math>\pm</math> 0.02</b>	<b>0.24 <math>\pm</math> 0.02</b>
Ile	4.13 $\pm$ 0.32	3.80 $\pm$ 0.29
Leu	7.03 $\pm$ 0.55	6.53 $\pm$ 0.48
Lys	9.04 $\pm$ 0.71	7.69 $\pm$ 0.51
Met	1.37 $\pm$ 0.26	0.96 $\pm$ 0.24
Orn	<b>3.65 <math>\pm</math> 0.31</b>	<b>2.64 <math>\pm</math> 0.19</b>
PEtN	3.60 $\pm$ 0.23	3.98 $\pm$ 0.36
Phe	2.18 $\pm$ 0.19	2.41 $\pm$ 0.21
Pro	5.69 $\pm$ 0.80	5.57 $\pm$ 0.52
Sar	0.88 $\pm$ 0.15	0.83 $\pm$ 0.03
Ser	3.48 $\pm$ 0.33	3.57 $\pm$ 0.27
Tau	<b>125.56 <math>\pm</math> 4.31</b>	<b>158.38 <math>\pm</math> 6.68</b>
Thr	4.43 $\pm$ 0.49	4.40 $\pm$ 0.34
Trp	0.66 $\pm$ 0.05	0.65 $\pm$ 0.05
Tyr	2.51 $\pm$ 0.13	2.22 $\pm$ 0.19
Val	7.84 $\pm$ 0.56	6.95 $\pm$ 0.54

**Table 19.** Analysis of C, CMS, HF and HFMS blood plasma metabolite level after four weeks of dietary methyl-group supplementation is listed. Data are presented as mean  $\pm$  SEM (n = 8-9). Bold numbers indicate statistical significance ( $p < 0.05$ ). Abbreviations: 3MHis, 3-methyl-L-histidine; Aad, L- $\alpha$ -aminoadipic acid; Abu, L- $\alpha$ -amino-n-butyrate; Ala, L-alanine; Arg, L-arginine; Asn, L-asparagine; Asp, L-aspartic acid; Cit, L-citrulline; Cys, L-cystine; EtN, Ethanolamine; Gln, L-glutamine; Glu, L-glutamate; Gly, Glycine; His, L-histidine; Hyp, Hydroxyproline; Ile, L-isoleucine; Leu, L-leucine; Lys, L-lysine; Met, L-methionine; Orn, L-ornithine; PEtN, O-phosphoethanolamine; Phe, L-phenylalanine; Pro, L-proline; Sar, Sarcosine; Ser, L-serine; Tau, Taurine; Thr, L-threonine; Trp, L-tryptophane; Tyr, L-tyrosine; Val, L-valine.

Metabolite [ $\mu$ M]	C	CMS	HF	HFMS
<b>3MHis</b>	<b>3.58 <math>\pm</math> 0.29</b>	<b>3.51 <math>\pm</math> 0.30</b>	<b>5.80 <math>\pm</math> 0.49</b>	<b>4.86 <math>\pm</math> 0.30</b>
<b>Aad</b>	<b>10.04 <math>\pm</math> 0.49</b>	<b>8.93 <math>\pm</math> 0.56</b>	<b>7.30 <math>\pm</math> 0.42</b>	<b>8.31 <math>\pm</math> 0.40</b>
Abu	8.12 $\pm$ 0.68	8.83 $\pm$ 0.84	6.46 $\pm$ 0.32	8.73 $\pm$ 0.55
Ala	559.00 $\pm$ 27.16	641.11 $\pm$ 42.98	661.43 $\pm$ 45.84	765.22 $\pm$ 79.53
Arg	93.22 $\pm$ 3.89	100.60 $\pm$ 6.93	87.10 $\pm$ 6.07	101.97 $\pm$ 6.20
<b>Asn</b>	<b>56.41 <math>\pm</math> 2.38</b>	<b>68.93 <math>\pm</math> 5.97</b>	<b>77.70 <math>\pm</math> 4.76</b>	<b>92.31 <math>\pm</math> 7.79</b>
Asp	9.61 $\pm$ 0.60	9.81 $\pm$ 1.03	7.88 $\pm$ 0.56	8.10 $\pm$ 0.50
<b>Cit</b>	<b>48.41 <math>\pm</math> 2.88</b>	<b>50.18 <math>\pm</math> 3.24</b>	<b>61.31 <math>\pm</math> 3.36</b>	<b>63.01 <math>\pm</math> 2.34</b>
Cys	15.99 $\pm$ 2.69	24.66 $\pm$ 2.63	21.24 $\pm$ 4.22	32.36 $\pm$ 6.26
EtN	13.12 $\pm$ 0.70	13.47 $\pm$ 0.70	13.50 $\pm$ 0.85	12.27 $\pm$ 0.44
Gln	707.44 $\pm$ 18.49	775.89 $\pm$ 18.63	793.86 $\pm$ 38.77	812.56 $\pm$ 27.98
Glu	63.79 $\pm$ 4.66	61.28 $\pm$ 3.37	51.57 $\pm$ 3.56	61.19 $\pm$ 3.68
<b>Gly</b>	<b>233.56 <math>\pm</math> 5.09</b>	<b>169.56 <math>\pm</math> 5.83</b>	<b>218.43 <math>\pm</math> 9.95</b>	<b>174.67 <math>\pm</math> 6.59</b>
His	74.67 $\pm$ 2.54	71.24 $\pm$ 5.27	74.63 $\pm$ 2.33	85.48 $\pm$ 3.05
Hyp	16.18 $\pm$ 0.70	16.17 $\pm$ 0.55	16.71 $\pm$ 0.91	16.01 $\pm$ 0.49
Ile	138.00 $\pm$ 7.41	155.01 $\pm$ 16.82	130.57 $\pm$ 6.86	151.56 $\pm$ 9.03
Leu	222.44 $\pm$ 11.95	249.00 $\pm$ 28.86	203.43 $\pm$ 11.61	234.22 $\pm$ 12.69
Lys	329.11 $\pm$ 12.50	331.11 $\pm$ 36.25	349.00 $\pm$ 17.98	345.11 $\pm$ 30.40
Met	48.60 $\pm$ 3.30	86.68 $\pm$ 19.73	53.10 $\pm$ 3.93	101.07 $\pm$ 11.58
<b>Orn</b>	<b>55.20 <math>\pm</math> 3.79</b>	<b>52.04 <math>\pm</math> 5.18</b>	<b>82.53 <math>\pm</math> 7.09</b>	<b>69.70 <math>\pm</math> 3.38</b>
PEtN	4.94 $\pm$ 0.63	6.67 $\pm$ 0.72	6.15 $\pm$ 0.91	6.88 $\pm$ 0.71
Phe	71.97 $\pm$ 3.68	75.58 $\pm$ 5.65	69.04 $\pm$ 4.08	80.79 $\pm$ 3.57
Pro	128.72 $\pm$ 10.92	157.10 $\pm$ 33.78	160.27 $\pm$ 15.85	191.23 $\pm$ 19.21
<b>Sar</b>	<b>1.43 <math>\pm</math> 0.15</b>	<b>13.34 <math>\pm</math> 3.04</b>	<b>1.13 <math>\pm</math> 0.09</b>	<b>8.03 <math>\pm</math> 0.95</b>
<b>Ser</b>	<b>143.22 <math>\pm</math> 5.83</b>	<b>203.56 <math>\pm</math> 19.71</b>	<b>182.71 <math>\pm</math> 10.15</b>	<b>235.00 <math>\pm</math> 15.39</b>
Tau	310.78 $\pm$ 20.69	370.67 $\pm$ 35.22	386.86 $\pm$ 34.04	425.11 $\pm$ 32.00
Thr	191.67 $\pm$ 11.45	197.56 $\pm$ 24.32	228.71 $\pm$ 13.00	232.33 $\pm$ 13.78
Trp	74.01 $\pm$ 4.15	86.22 $\pm$ 5.94	70.53 $\pm$ 3.40	79.93 $\pm$ 3.20
Tyr	92.47 $\pm$ 4.79	106.26 $\pm$ 9.39	97.84 $\pm$ 7.32	118.34 $\pm$ 7.00
Val	346.00 $\pm$ 17.98	342.11 $\pm$ 35.50	312.86 $\pm$ 13.21	345.67 $\pm$ 15.98

**Table 20.** Analysis of C, CMS, HF and HFMS liver tissue for selected hepatic metabolite level after four weeks of dietary methyl-group supplementation is listed. Data are presented as mean  $\pm$  SEM [ $\mu\text{mol/g}$  protein] ( $n = 8-9$ ). Bold numbers indicate statistical significance ( $p < 0.05$ ). Abbreviations: 1MHis, 1-methyl-L-histidine; Aad, L- $\alpha$ -amino adipic acid; Abu, L- $\alpha$ -amino-n-butyrate; Ala, L-alanine; Asn, L-asparagine; Asp, L-asparic acid; bAib, D,L- $\beta$ -aminoisobutyrate; bAla,  $\beta$ -alanine; Cit, L-citrulline; Cth, Cystathionine; EtN, Ethanolamine; GABA,  $\gamma$ -amino-n-butyrate; Gln, L-glutamine; Glu, L-glutamate; Gly, Glycine; His, L-histidine; Hyp, Hydroxyproline; Ile, L-isoleucine; Leu, L-leucine; Lys, L-lysine; Met, L-methionine; Orn, L-ornithine; PEtN, O-phosphoethanolamine; Phe, L-phenylalanine; Pro, L-proline; Sar, Sarcosine; Ser, L-serine; Tau, Taurine; Thr, L-threonine; Trp, L-tryptophane; Tyr, L-tyrosine; Val, L-valine.

Metabolite [ $\mu\text{mol/g}$ protein]	C	CMS	HF	HFMS
1MHis	0.43 $\pm$ 0.03	0.41 $\pm$ 0.02	0.46 $\pm$ 0.02	0.45 $\pm$ 0.04
Aad	1.15 $\pm$ 0.23	0.91 $\pm$ 0.19	0.56 $\pm$ 0.05	0.87 $\pm$ 0.13
Abu	<b>0.96 <math>\pm</math> 0.12</b>	<b>0.97 <math>\pm</math> 0.12</b>	<b>0.50 <math>\pm</math> 0.04</b>	<b>0.74 <math>\pm</math> 0.11</b>
Ala	99.31 $\pm$ 5.10	106.94 $\pm$ 4.30	104.34 $\pm$ 5.76	101.60 $\pm$ 4.32
Asn	<b>4.65 <math>\pm</math> 0.15</b>	<b>4.96 <math>\pm</math> 0.20</b>	<b>3.91 <math>\pm</math> 0.17</b>	<b>4.43 <math>\pm</math> 0.29</b>
Asp	<b>4.23 <math>\pm</math> 0.27</b>	<b>5.86 <math>\pm</math> 0.55</b>	<b>3.66 <math>\pm</math> 0.11</b>	<b>5.12 <math>\pm</math> 0.34</b>
bAib	<b>0.15 <math>\pm</math> 0.01</b>	<b>0.14 <math>\pm</math> 0.01</b>	<b>0.08 <math>\pm</math> 0.01</b>	<b>0.10 <math>\pm</math> 0.01</b>
bAla	<b>1.22 <math>\pm</math> 0.11</b>	<b>1.22 <math>\pm</math> 0.07</b>	<b>1.19 <math>\pm</math> 0.14</b>	<b>1.90 <math>\pm</math> 0.22</b>
Cit	<b>0.42 <math>\pm</math> 0.04</b>	<b>0.24 <math>\pm</math> 0.02</b>	<b>0.36 <math>\pm</math> 0.01</b>	<b>0.31 <math>\pm</math> 0.02</b>
EtN	<b>0.55 <math>\pm</math> 0.05</b>	<b>0.82 <math>\pm</math> 0.07</b>	<b>0.49 <math>\pm</math> 0.04</b>	<b>0.67 <math>\pm</math> 0.05</b>
GABA	0.52 $\pm$ 0.06	0.54 $\pm$ 0.04	0.44 $\pm$ 0.03	0.45 $\pm$ 0.03
Gln	73.93 $\pm$ 4.62	88.54 $\pm$ 3.54	86.57 $\pm$ 4.35	85.77 $\pm$ 4.80
Glu	28.89 $\pm$ 3.20	23.89 $\pm$ 1.56	27.96 $\pm$ 0.66	29.19 $\pm$ 2.05
Gly	<b>48.20 <math>\pm</math> 2.19</b>	<b>29.49 <math>\pm</math> 2.51</b>	<b>37.94 <math>\pm</math> 1.14</b>	<b>26.38 <math>\pm</math> 2.53</b>
His	10.65 $\pm$ 0.59	10.66 $\pm$ 0.47	10.07 $\pm$ 0.40	10.61 $\pm$ 0.45
Hyp	<b>0.50 <math>\pm</math> 0.03</b>	<b>0.44 <math>\pm</math> 0.02</b>	<b>0.38 <math>\pm</math> 0.02</b>	<b>0.38 <math>\pm</math> 0.02</b>
Ile	<b>6.55 <math>\pm</math> 0.29</b>	<b>6.68 <math>\pm</math> 0.36</b>	<b>5.08 <math>\pm</math> 0.31</b>	<b>5.52 <math>\pm</math> 0.37</b>
Leu	<b>11.63 <math>\pm</math> 0.61</b>	<b>12.22 <math>\pm</math> 0.61</b>	<b>9.22 <math>\pm</math> 0.49</b>	<b>10.10 <math>\pm</math> 0.64</b>
Lys	<b>12.32 <math>\pm</math> 0.48</b>	<b>13.94 <math>\pm</math> 0.77</b>	<b>9.90 <math>\pm</math> 0.39</b>	<b>11.06 <math>\pm</math> 0.49</b>
Met	0.64 $\pm$ 0.05	0.70 $\pm$ 0.09	0.55 $\pm$ 0.03	0.73 $\pm$ 0.05
Orn	<b>6.18 <math>\pm</math> 0.38</b>	<b>5.30 <math>\pm</math> 0.29</b>	<b>4.55 <math>\pm</math> 0.21</b>	<b>4.28 <math>\pm</math> 0.31</b>
PEtN	4.58 $\pm$ 0.37	4.77 $\pm$ 0.19	4.49 $\pm$ 0.13	4.68 $\pm$ 0.33
Phe	<b>4.21 <math>\pm</math> 0.15</b>	<b>4.33 <math>\pm</math> 0.19</b>	<b>3.52 <math>\pm</math> 0.19</b>	<b>3.76 <math>\pm</math> 0.22</b>
Pro	8.19 $\pm$ 0.63	8.68 $\pm$ 0.90	6.50 $\pm$ 0.35	8.08 $\pm$ 0.55
Sar	<b>1.76 <math>\pm</math> 0.40</b>	<b>9.22 <math>\pm</math> 1.89</b>	<b>0.75 <math>\pm</math> 0.10</b>	<b>6.90 <math>\pm</math> 0.52</b>
Ser	<b>7.53 <math>\pm</math> 0.25</b>	<b>8.78 <math>\pm</math> 0.65</b>	<b>5.85 <math>\pm</math> 0.28</b>	<b>7.08 <math>\pm</math> 0.30</b>
Tau	<b>187.45 <math>\pm</math> 6.09</b>	<b>174.97 <math>\pm</math> 4.81</b>	<b>208.79 <math>\pm</math> 5.18</b>	<b>202.04 <math>\pm</math> 6.10</b>
Thr	<b>7.78 <math>\pm</math> 0.34</b>	<b>9.09 <math>\pm</math> 0.63</b>	<b>7.16 <math>\pm</math> 0.32</b>	<b>7.25 <math>\pm</math> 0.37</b>
Trp	<b>1.16 <math>\pm</math> 0.04</b>	<b>1.26 <math>\pm</math> 0.06</b>	<b>0.95 <math>\pm</math> 0.04</b>	<b>1.08 <math>\pm</math> 0.06</b>
Tyr	<b>4.70 <math>\pm</math> 0.14</b>	<b>5.41 <math>\pm</math> 0.25</b>	<b>4.08 <math>\pm</math> 0.23</b>	<b>4.54 <math>\pm</math> 0.19</b>
Val	<b>12.72 <math>\pm</math> 0.51</b>	<b>12.47 <math>\pm</math> 0.71</b>	<b>9.56 <math>\pm</math> 0.52</b>	<b>10.20 <math>\pm</math> 0.65</b>

**Table 21.** Analysis of C, CMS, HF and HFMS liver tissue for hepatic biogenic amine concentrations after four weeks of dietary methyl-group supplementation is listed. Data are presented as mean  $\pm$  SEM [ $\mu\text{mol}/\text{mg}$  tissue] ( $n = 8-9$ ). Bold numbers and different subscript letters indicate statistical significance ( $p < 0.05$ ), - indicates below detection limit. Abbreviations: ADMA, asymmetric dimethylarginine; Ac-Orn, acetylmethionine; DOPA, dihydroxy-phenylalanine; Met-SO, methioninesulfoxide; Nitro-Tyr, nitrotyrosine; OH-Pro, Hydroxyproline; PEA, phenylethylamine; SDMA, symmetric dimethylarginine; alpha-AAA,  $\alpha$ -aminoadipic acid; total DMA, total dimethylarginine.

Metabolite [ $\mu\text{mol}/\text{mg}$ tissue]	C	CMS	HF	HFMS
ADMA	1,16 $\pm$ 0,13	0,48 $\pm$ 0,10	0,40 $\pm$ 0,14	0,27 $\pm$ 0,09
Ac-Orn	2,07 $\pm$ 0,45	0,94 $\pm$ 0,15	1,29 $\pm$ 0,23	0,52 $\pm$ 0,13
Carnosine	0,57 $\pm$ 0,16	0,37 $\pm$ 0,02	0,37 $\pm$ 0,02	0,41 $\pm$ 0,02
Creatinine	5,88 $\pm$ 2,43	3,20 $\pm$ 0,10	3,11 $\pm$ 0,08	3,14 $\pm$ 0,20
DOPA	0,73 $\pm$ 0,24	0,53 $\pm$ 0,03	0,38 $\pm$ 0,05	0,43 $\pm$ 0,05
Dopamine	0,89 $\pm$ 0,33	0,51 $\pm$ 0,03	0,47 $\pm$ 0,02	0,51 $\pm$ 0,02
Histamine	1,76 $\pm$ 0,38	1,27 $\pm$ 0,08	1,07 $\pm$ 0,10	1,16 $\pm$ 0,12
Kynurenine	1,23 $\pm$ 0,30	0,80 $\pm$ 0,06	0,59 $\pm$ 0,03	0,65 $\pm$ 0,06
Met-SO	2,50 $\pm$ 0,26	2,14 $\pm$ 0,29	1,43 $\pm$ 0,18	1,89 $\pm$ 0,14
Nitro-Tyr	-	-	-	-
OH-Pro	-	-	-	-
PEA	<b>0,12 <math>\pm</math> 0,02</b>	<b>0,07 <math>\pm</math> 0,01</b>	-	-
Putrescine	-	-	-	-
SDMA	-	-	-	-
Sarcosine	<b>110,43 <math>\pm</math> 11,07<sup>a</sup></b>	<b>294,99 <math>\pm</math> 37,73<sup>b</sup></b>	<b>100,38 <math>\pm</math> 7,88<sup>a</sup></b>	<b>257,66 <math>\pm</math> 13,40<sup>b</sup></b>
Serotonin	1,57 $\pm$ 0,06	1,49 $\pm$ 0,11	1,73 $\pm$ 0,21	1,27 $\pm$ 0,04
Spermidine	8,10 $\pm$ 1,07	9,33 $\pm$ 1,85	7,51 $\pm$ 0,62	10,02 $\pm$ 1,91
Spermine	5,16 $\pm$ 1,29	3,42 $\pm$ 1,38	2,13 $\pm$ 0,51	5,15 $\pm$ 2,35
Taurine	50,02 $\pm$ 12,12	19,79 $\pm$ 5,81	25,59 $\pm$ 8,49	25,00 $\pm$ 5,81
alpha-AAA	108,82 $\pm$ 16,45	97,94 $\pm$ 14,50	81,22 $\pm$ 5,54	105,68 $\pm$ 9,68
total DMA	2,26 $\pm$ 0,69	1,41 $\pm$ 0,08	1,23 $\pm$ 0,06	1,11 $\pm$ 0,09

**Table 22.** Analysis of C, CMS, HF and HFMS liver tissue for hepatic acyl-carnitine concentrations after four weeks of dietary methyl-group supplementation is listed. Data are presented as mean  $\pm$  SEM [ $\mu\text{mol}/\text{mg}$  tissue] ( $n = 8-9$ ). Bold numbers indicate statistical significance ( $p < 0.05$ ). Abbreviations: C0, DL-carnitine; C10, Decanoyl-L-carnitine; C10:1 Decenoyl-L-carnitine; C10:2, Decadienyl-L-carnitine; C12, Dodecanoyl-L-carnitine; C12-DC, Dodecanedioyl-L-carnitine; C12:1, Dodecenoyl-L-carnitine; C14, Tetradecanoyl-L-carnitine; C14:1, Tetradecenoyl-L-carnitine; C14:1-OH, Hydroxytetradecenoyl-L-carnitine; C14:2, Tetradecadienyl-L-carnitine; C14:2-OH, Hydroxytetradecadienyl-L-carnitine; C16, Hexadecanoyl-L-carnitine; C16-OH, Hydroxyhexadecanoyl-L-carnitine; c16:1, Hexadecenoyl-L-carnitine; C16:1-OH, Hydroxyhexadecenoyl-L-carnitine; C16:2, Hexadecadienyl-L-carnitine; C16:2-OH, Hydroxyhexadecadienyl-L-carnitine; C18, Octadecanoyl-L-carnitine; C18:1, Octadecenoyl-L-carnitine; C18:1-OH, Hydroxyoctadecenoyl-L-carnitine; C18:2, Octadecadienyl-L-carnitine; C2, Acetyl-L-carnitine; C3, Propionyl-L-carnitine; C3-

DC / C4-OH, Malonyl-L-carnitine / Hydroxybutyryl-L-carnitine; C3-OH, C3:1, Propenyl-L-carnitine; Hydroxypropionyl-L-carnitine; C4, Butyryl-L-carnitine; C4:1, Butenyl-L-carnitine; C5, Valeryl-L-carnitine; C5-DC / C6-OH, Glutaryl-L-carnitine / Hydroxyhexanoyl-L-carnitine; C5-M-DC, Methylglutaryl-L-carnitine; C5-OH / C3-DC-M, Methylmalonyl-L-carnitine / Hydroxyvaleryl-L-carnitine; C5:1, Tiglyl-L-carnitine; C5:1-DC, Glutaconyl-L-carnitine; C6 / C4:1-DC, Fumaryl-L-carnitine / Hexanoyl-L-carnitine; C6:1, Hexenoyl-L-carnitine; C7-DC, Pimelyl-L-carnitine; C8, Octanoyl-L-carnitine; C9, Nonayl-L-carnitine

Metabolite [ $\mu\text{mol}/\text{mg}$ tissue]	C	CMS	HF	HFMS
C0	57.561 $\pm$ 2.219	42.271 $\pm$ 1.819	63.116 $\pm$ 2.457	47.757 $\pm$ 2.405
C10	0.318 $\pm$ 0.017	0.294 $\pm$ 0.010	0.347 $\pm$ 0.014	0.385 $\pm$ 0.012
C10:1	0.095 $\pm$ 0.004	0.093 $\pm$ 0.004	0.164 $\pm$ 0.005	0.162 $\pm$ 0.005
C10:2	0.079 $\pm$ 0.005	0.082 $\pm$ 0.004	0.084 $\pm$ 0.002	0.085 $\pm$ 0.003
C12	0.062 $\pm$ 0.004	0.052 $\pm$ 0.002	0.046 $\pm$ 0.001	0.048 $\pm$ 0.001
C12-DC	0.159 $\pm$ 0.010	0.149 $\pm$ 0.008	0.128 $\pm$ 0.004	0.154 $\pm$ 0.007
C12:1	0.177 $\pm$ 0.013	0.240 $\pm$ 0.011	0.183 $\pm$ 0.011	0.202 $\pm$ 0.007
C14	0.135 $\pm$ 0.008	0.114 $\pm$ 0.005	0.117 $\pm$ 0.003	0.099 $\pm$ 0.004
C14:1	0.051 $\pm$ 0.003	0.048 $\pm$ 0.002	0.054 $\pm$ 0.003	0.049 $\pm$ 0.002
C14:1-OH	0.040 $\pm$ 0.003	0.034 $\pm$ 0.003	0.046 $\pm$ 0.001	0.045 $\pm$ 0.002
C14:2	0.025 $\pm$ 0.002	0.021 $\pm$ 0.001	0.022 $\pm$ 0.001	0.023 $\pm$ 0.001
C14:2-OH	0.041 $\pm$ 0.003	0.038 $\pm$ 0.001	0.039 $\pm$ 0.001	0.040 $\pm$ 0.002
C16	0.614 $\pm$ 0.050	0.438 $\pm$ 0.036	0.726 $\pm$ 0.040	0.545 $\pm$ 0.037
C16-OH	0.039 $\pm$ 0.003	0.036 $\pm$ 0.002	0.032 $\pm$ 0.002	0.029 $\pm$ 0.001
C16:1	0.164 $\pm$ 0.011	0.125 $\pm$ 0.010	0.164 $\pm$ 0.013	0.120 $\pm$ 0.007
C16:1-OH	0.037 $\pm$ 0.002	0.029 $\pm$ 0.001	0.082 $\pm$ 0.004	0.071 $\pm$ 0.004
C16:2	0.019 $\pm$ 0.001	0.018 $\pm$ 0.001	0.018 $\pm$ 0.001	0.016 $\pm$ 0.001
C16:2-OH	0.024 $\pm$ 0.002	0.017 $\pm$ 0.001	0.038 $\pm$ 0.001	0.033 $\pm$ 0.002
C18	0.322 $\pm$ 0.029	0.197 $\pm$ 0.008	0.561 $\pm$ 0.030	0.441 $\pm$ 0.027
C18:1	0.756 $\pm$ 0.061	0.469 $\pm$ 0.050	1.217 $\pm$ 0.097	0.913 $\pm$ 0.092
C18:1-OH	0.055 $\pm$ 0.004	0.046 $\pm$ 0.002	0.074 $\pm$ 0.003	0.060 $\pm$ 0.002
C18:2	0.174 $\pm$ 0.013	0.122 $\pm$ 0.006	0.143 $\pm$ 0.005	0.119 $\pm$ 0.006
C2	18.413 $\pm$ 0.858	12.340 $\pm$ 0.474	14.566 $\pm$ 0.841	10.685 $\pm$ 0.827
C3	4.772 $\pm$ 0.362	3.363 $\pm$ 0.302	5.396 $\pm$ 0.264	4.129 $\pm$ 0.272
C3-DC (C4-OH)	0.907 $\pm$ 0.062	0.759 $\pm$ 0.053	1.042 $\pm$ 0.045	0.666 $\pm$ 0.052
C3-OH	0.049 $\pm$ 0.003	0.050 $\pm$ 0.003	0.037 $\pm$ 0.002	0.044 $\pm$ 0.002
C3:1	0.017 $\pm$ 0.001	0.016 $\pm$ 0.001	0.014 $\pm$ 0.001	0.016 $\pm$ 0.001
C4	2.344 $\pm$ 0.100	1.238 $\pm$ 0.088	1.773 $\pm$ 0.105	1.078 $\pm$ 0.088
C4:1	0.198 $\pm$ 0.011	0.196 $\pm$ 0.008	0.160 $\pm$ 0.005	0.174 $\pm$ 0.006
C5	1.179 $\pm$ 0.064	0.733 $\pm$ 0.080	1.453 $\pm$ 0.095	1.033 $\pm$ 0.089
C5-DC (C6-OH)	0.281 $\pm$ 0.012	0.207 $\pm$ 0.009	0.557 $\pm$ 0.021	0.482 $\pm$ 0.023
C5-M-DC	0.188 $\pm$ 0.018	0.112 $\pm$ 0.006	0.264 $\pm$ 0.021	0.181 $\pm$ 0.010
C5-OH (C3-DC-M)	0.426 $\pm$ 0.013	0.362 $\pm$ 0.013	0.464 $\pm$ 0.014	0.350 $\pm$ 0.015
C5:1	0.044 $\pm$ 0.004	0.039 $\pm$ 0.003	0.033 $\pm$ 0.001	0.036 $\pm$ 0.001
C5:1-DC	0.164 $\pm$ 0.010	0.119 $\pm$ 0.010	0.156 $\pm$ 0.010	0.129 $\pm$ 0.011

<b>C6 (C4:1-DC)</b>	<b>0.749 ± 0.041</b>	<b>0.399 ± 0.028</b>	<b>0.497 ± 0.028</b>	<b>0.341 ± 0.030</b>
<b>C6:1</b>	0.047 ± 0.004	0.043 ± 0.003	0.037 ± 0.002	0.042 ± 0.002
<b>C7-DC</b>	<b>0.255 ± 0.027</b>	<b>0.354 ± 0.043</b>	<b>0.459 ± 0.085</b>	<b>0.519 ± 0.025</b>
<b>C8</b>	<b>0.276 ± 0.014</b>	<b>0.217 ± 0.009</b>	<b>0.973 ± 0.047</b>	<b>0.862 ± 0.050</b>
<b>C9</b>	<b>0.094 ± 0.005</b>	<b>0.091 ± 0.007</b>	<b>0.279 ± 0.015</b>	<b>0.277 ± 0.015</b>

### 7.3 Methylation-sensitive qPCR

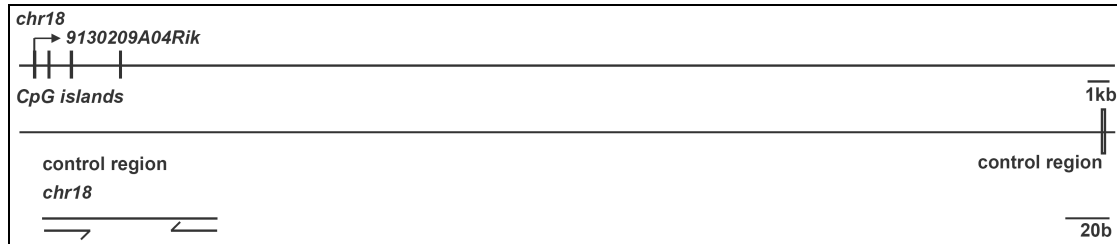


**Figure 42.** Restriction map of informative restriction sites for MS-qPCR in the normalisation region on chromosome 18. No *Acil* or *HpaII* restriction sites can be detected.

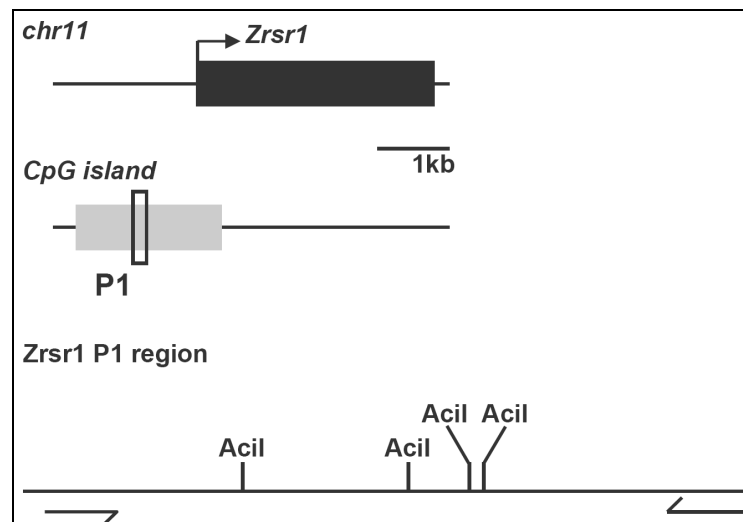


**Figure 43.** Zrsr1 CpG-island restriction map of informative restriction sites for MS-qPCR. **Top:** Filled black box represents the first exon and black arrow indicates transcription start site (ENSMUST00000049506). Filled grey box represents Zrsr1 CpG-island and open box mark the investigated region. **Down:** Investigated regions and position of informative restriction sites are depicted. Abbreviations: Zrsr1, Zinc finger (CCCH type), RNA binding motif and serine/arginine rich 1

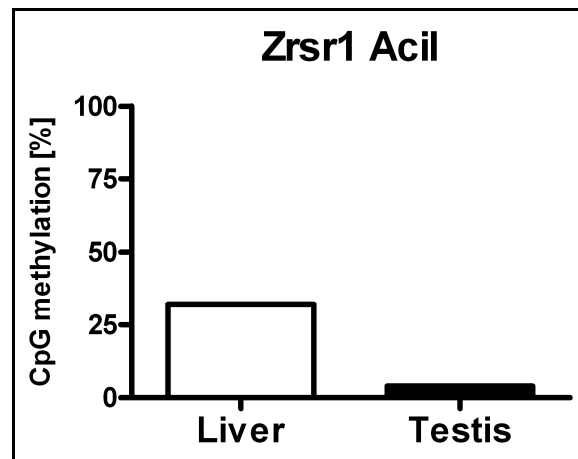


**Figure 44.** Quantitative analysis of CpG restriction sites in promoter *Zrsr1* CpG-island in liver and testis of C57BL/6N mouse. Data are shown for the restriction enzymes *Acil* a in the previously mentioned region. Data are presented as mean  $\pm$  SEM (n = 1). Open and black bar represents liver and testis. Abbreviations: *Zrsr1*, Zinc finger (CCCH type), RNA binding motif and serine/arginine rich 1

#### 7.4 Food intake

**Table 23.** Effect of HF diet feeding on nutrient and energy intake of C and HF mice of the first feeding trial. Data are presented as mean  $\pm$  SEM (n = 9-11). Bold numbers and asterisk indicates statistical significance (p < 0.05).

	C	HF
<b>Food intake [g]</b>	<b>306.6 <math>\pm</math> 2.4</b>	<b>262.5 <math>\pm</math> 2.3*</b>
<b>Energy intake [MJ]</b>	<b>5.52 <math>\pm</math> 0.04</b>	<b>6.61 <math>\pm</math> 0.06*</b>
<b>Methionine intake [g]</b>	<b>2.33 <math>\pm</math> 0.02</b>	<b>2.26 <math>\pm</math> 0.02*</b>
<b>Cystine intake [g]</b>	<b>0.28 <math>\pm</math> 0.002</b>	<b>1.21 <math>\pm</math> 0.01*</b>
<b>Choline chloride intake [g]</b>	<b>0.319 <math>\pm</math> 0.003</b>	<b>0.604 <math>\pm</math> 0.005*</b>
<b>Folate intake [mg]</b>	<b>6.13 <math>\pm</math> 0.05</b>	<b>5.25 <math>\pm</math> 0.05*</b>
<b>Vitamin B<sub>12</sub> intake [<math>\mu</math>g]</b>	<b>9.20 <math>\pm</math> 0.07</b>	<b>7.88 <math>\pm</math> 0.07*</b>
<b>Vitamin B<sub>6</sub> intake [mg]</b>	<b>5.52 <math>\pm</math> 0.04</b>	<b>4.73 <math>\pm</math> 0.14*</b>



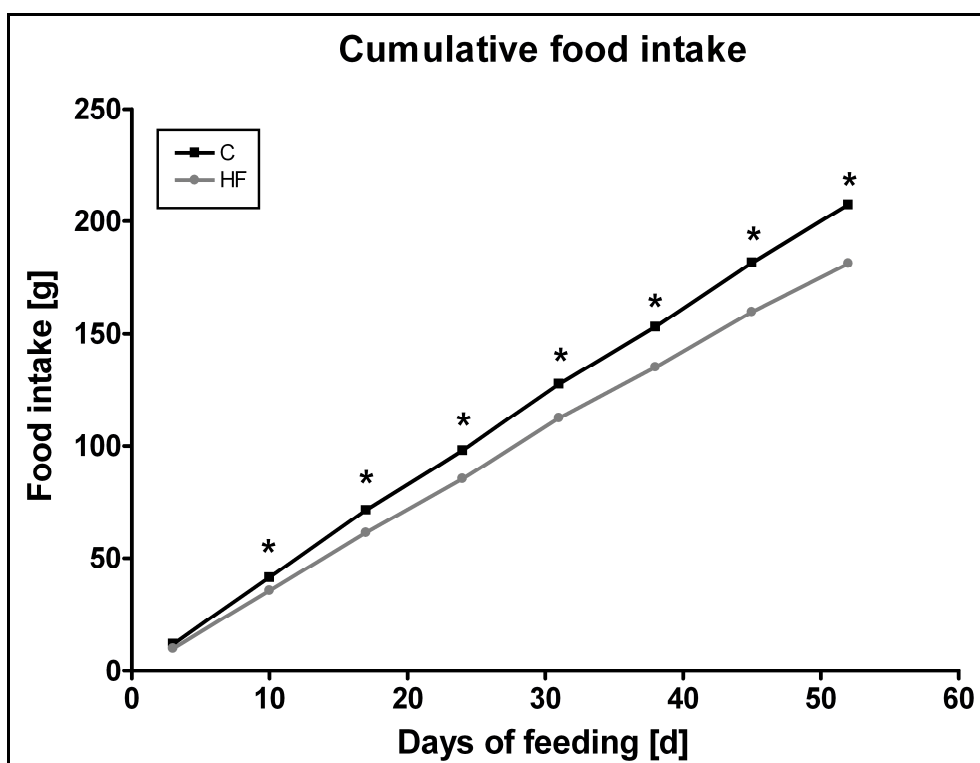


**Figure 45.** Food intake of C, HF group during the first eight weeks of dietary treatment is depicted. Data are presented as mean  $\pm$  SEM (n = 8-9). Asterisk indicates statistical significance ( $p < 0.05$ ).

**Table 24.** Effect of HF diet feeding on nutrient and energy intake of C and HF mice of the methyl-group supplementation feeding trial after eight weeks. Data are presented as mean  $\pm$  SEM (n = 8-9). Bold numbers and asterisk indicates statistical significance ( $p < 0.05$ ).

	<b>C</b>	<b>HF</b>
<b>Energy intake [MJ]</b>	<b>3.38 <math>\pm</math> 0.02</b>	<b>4.21 <math>\pm</math> 0.06*</b>
<b>Methionine intake [g]</b>	1.65 $\pm$ 0.01	1.62 $\pm$ 0.03
<b>Cystine intake [g]</b>	<b>0.20 <math>\pm</math> 0.001</b>	<b>0.90 <math>\pm</math> 0.001*</b>
<b>Choline chloride intake [g]</b>	<b>0.23 <math>\pm</math> 0.002</b>	<b>0.45 <math>\pm</math> 0.007*</b>
<b>Folate intake [mg]</b>	<b>4.28 <math>\pm</math> 0.03</b>	<b>3.74 <math>\pm</math> 0.05*</b>
<b>Vitamin B<sub>12</sub> intake [<math>\mu</math>g]</b>	<b>6.76 <math>\pm</math> 0.05</b>	<b>5.90 <math>\pm</math> 0.09*</b>
<b>Vitamin B<sub>6</sub> intake [mg]</b>	<b>4.06 <math>\pm</math> 0.03</b>	<b>3.54 <math>\pm</math> 0.05*</b>

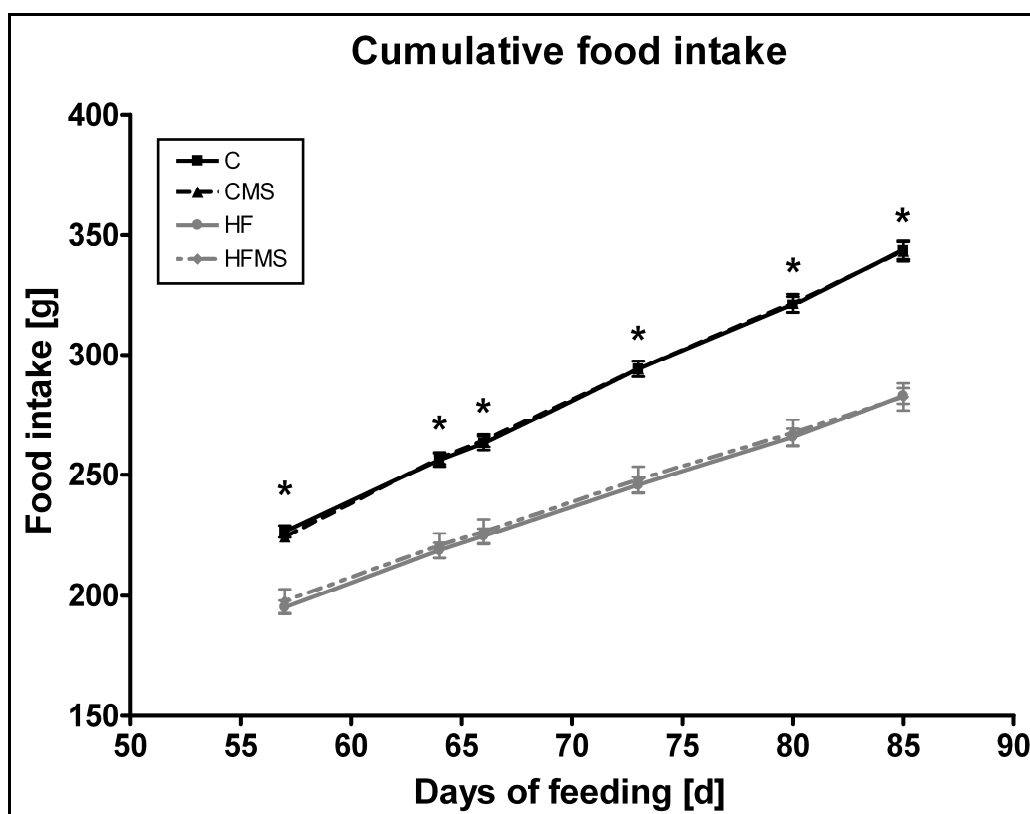


**Figure 46.** Cumulative food intake of C, CMS, HF and HFMS group during the last four weeks of the twelve weeks of dietary treatment is depicted. Vertical line indicates start of therapeutic intervention by methyl-group supplementation in CMS and HFMS mice. Data are presented as mean  $\pm$  SEM (n = 8-9). Asterisk indicates statistical significance of C and HF, C and HFMS, CMS and HF, CMS and HFMS groups at the depicted time points ( $p < 0.05$ ).

**Table 25.** Effect of HF diet feeding on nutrient and energy intake of C, CMS, HF and HFMS mice of the methyl-group supplementation feeding trial after twelve weeks. Data are presented as mean  $\pm$  SEM (n = 8-9). Bold numbers and different subscript letters indicate statistical significance ( $p < 0.05$ ).

	C	CMS	HF	HFMS
<b>Energy intake [MJ]</b>	<b>5.16 <math>\pm</math> 0.06<sup>a</sup></b>	<b>5.15 <math>\pm</math> 0.06<sup>a</sup></b>	<b>6.06 <math>\pm</math> 0.07<sup>b</sup></b>	<b>6.05 <math>\pm</math> 0.12<sup>b</sup></b>
<b>Methionine intake [g]</b>	<b>2.51 <math>\pm</math> 0.03<sup>a</sup></b>	<b>5.08 <math>\pm</math> 0.06<sup>b</sup></b>	<b>2.35 <math>\pm</math> 0.03<sup>c</sup></b>	<b>4.47 <math>\pm</math> 0.09<sup>d</sup></b>
<b>Cystine intake [g]</b>	<b>0.31 <math>\pm</math> 0.004<sup>a</sup></b>	<b>0.31 <math>\pm</math> 0.004<sup>a</sup></b>	<b>1.30 <math>\pm</math> 0.01<sup>b</sup></b>	<b>1.30 <math>\pm</math> 0.03<sup>b</sup></b>
<b>Choline chloride intake [g]</b>	<b>0.36 <math>\pm</math> 0.004<sup>a</sup></b>	<b>5.50 <math>\pm</math> 0.07<sup>b</sup></b>	<b>0.65 <math>\pm</math> 0.01<sup>c</sup></b>	<b>4.89 <math>\pm</math> 0.10<sup>d</sup></b>
<b>Folate intake [mg]</b>	<b>6.53 <math>\pm</math> 0.08<sup>a</sup></b>	<b>11.66 <math>\pm</math> 0.14<sup>b</sup></b>	<b>5.38 <math>\pm</math> 0.06<sup>c</sup></b>	<b>9.61 <math>\pm</math> 0.19<sup>d</sup></b>
<b>Vitamin B<sub>12</sub> intake [<math>\mu</math>g]</b>	<b>10.31 <math>\pm</math> 0.12<sup>a</sup></b>	<b>524.90 <math>\pm</math> 6.33<sup>b</sup></b>	<b>8.49 <math>\pm</math> 0.10<sup>c</sup></b>	<b>432.40 <math>\pm</math> 8.55<sup>d</sup></b>
<b>Vitamin B<sub>6</sub> intake [mg]</b>	<b>6.19 <math>\pm</math> 0.07<sup>a</sup></b>	<b>6.18 <math>\pm</math> 0.07<sup>a</sup></b>	<b>5.09 <math>\pm</math> 0.06<sup>b</sup></b>	<b>5.09 <math>\pm</math> 0.10<sup>b</sup></b>

## 7.5 Chemicals

Chemicals	Company
20 % glucose solution	B.Braun Melsung AG, Berlin, Germany
Acetic acid	Roth, Karlsruhe, Germany
Agarose	Sigma-Aldrich, Munich, Germany
$\epsilon$ -amino-n-caproic acid	Merck KGaA, Darmstadt, Germany
Ammonium acetate	Sigma-Aldrich, Munich, Germany
Aquatex	Merck KGaA, Darmstadt, Germany
Boric acid	Merck KGaA, Darmstadt, Germany
Bovine serum albumin	Sigma-Aldrich, Munich, Germany
Bromphenol blue	Merck KGaA, Darmstadt, Germany
Chloroform	Roth, Karlsruhe, Germany
Dimethylsulfoxide (DMSO)	Sigma-Aldrich, Munich, Germany
Dithiothreitol (DTT)	Omni Life Science gmbH & Co. KG, Bremen, Germany
DMEM (high glucose)	Invitrogen, Karlsruhe, Germany
DMEM (low glucose)	Invitrogen, Karlsruhe, Germany
Ethidium bromide	Sigma-Aldrich, Munich, Germany
Ethylenediaminetetraacetate (EDTA)	Merck KGaA, Darmstadt, Germany
Fetal calf serum	PAA Laboratories GmbH, Cölbe, Germany
Formalin	Roth, Karlsruhe, Germany
Glycerol	Merck KGaA, Darmstadt, Germany
Glycine	Merck KGaA, Darmstadt, Germany
H <sub>3</sub> PO <sub>4</sub>	Serva Electrophoresis GmbH, Heidelberg, Germany
Hematoxylin	Medite GmbH, Burgdorf, Germany
Hydrochloric acid	Roth, Karlsruhe, Germany
Isopropanol	Roth, Karlsruhe, Germany
Isopropanol	Roth, Karlsruhe, Germany
KOH	Sigma-Aldrich, Munich, Germany
Methanol	Roth, Karlsruhe, Germany
NaCl	Sigma-Aldrich, Munich, Germany
Nonidet P40	Sigma-Aldrich, Munich, Germany
Orange G	Sigma-Aldrich, Munich, Germany
Penicillin/Streptomycin	PAA Laboratories GmbH, Cölbe, Germany
Phosphatase Inhibitor cocktail II	Sigma-Aldrich, Munich, Germany
Protease Inhibitor cocktail	Sigma-Aldrich, Munich, Germany
Sodium deoxycholate	Sigma-Aldrich, Munich, Germany
Sodium dodecyl sulfate (SDS)	Sigma-Aldrich, Munich, Germany
Sucrose	Sigma-Aldrich, Munich, Germany
Trishydroxymethyl aminomethan hydrochlorid (Tris)	Roche, Penzberg, Germany
Trizol	Invitrogen, Karlsruhe, Germany
WY14,643	Sigma-Aldrich, Munich, Germany

## Acknowledgements

I'd like to thank the following people for their assistance in completing this thesis:

Prof. Dr. Hannelore Daniel for giving me the opportunity and the freedom to study and to work in this scientific field. Also, for the guidance, for providing the resources and for the discussions during the practical and written part of this thesis.

Dr. Bernhard L. Bader for the supervision, patience, reliability, foresight and valuable scientific and personal discussions during this thesis.

Prof. Dr. Martin Klingenspor, Prof. Dr. Dirk Haller, Prof Dr. Heinrich H.D. Meyer and Prof. Dr. Hans Hauner for use of facilities at the departments and for the scientific discussions and support.

Dr. Charles Desmarchelier for corporation and kind donation of liver samples.

Manuela Sailer and Dr. Christian Scherling for corporation, discussion and valuable support during the thesis.

Prof. Dr. Jürgen Geisel, Dr. Björn Hummel and Dr. Rima Obeid for corporation and analysis of methionine cycle metabolites.

Rainer W. Fürst, Eva-Maria Sedlmeier, Katharina Heller, Dr. Susanne E. Ulbrich and Dr. Ingrid Schmöller for corporation, technical advice, fruitful discussions, motivation and support.

Dr. Isabelle Mack and Tobias Ludwig for technical advice and support, valuable discussions and motivation during the thesis.

Kerstin Geillinger for the support, valuable and fruitful discussions, technical advice and mindfulness.

Simone Matthä and Dr. Thomas Skurk for the kind donation of FAO cells and technical support.

Dr. Florian Lipsmeier for statistical support.

Ronny Scheundel, Johanna Welzhofer, Alexander Haag, Dr. Britta Spanier, Dr. Tobias Fromme, Dr. Florian Bolze, Nadine Rink and Kirsten Uebel for discussion and support.

Sabine Mocek, Manuela Hubersberger, Nico Gebhardt, Elmar Jocham, Katrin Lasch and Liese Baller for support.

Sylvia Heinrich, Brigitte Asafu and Cordula Hertwig for assistance with administrative work.

Finally, I'd like to thank my family for their personal advice and support and especially my companion Katja for her unlimited thoughtfulness, understanding, motivation and love.

The ZIEL - Research Center for Nutrition and Food Science for funding me and the project.

## Curriculum Vitae

**Dipl.-Biol. (Univ.) Christoph Dahlhoff**

**Persönliche Angaben:**

- Familienstand: ledig
- Nationalität: deutsch
- Geburtsdatum: 31.05.1981
- Geburtsort: Lippstadt, Deutschland

---

**Berufliches Arbeitsverhältnis:**

**Seit 06.03.2011:**

**Amgen Research (Munich) GmbH**

**Senior Associate Scientist, BiTE Technology**

**01.05.2011 – 05.03.2012:**

**Micromet GmbH**

**Scientist, Immunotherapy**

**Universitäre Ausbildung:**

**01.02.2007 – 28.02.2011:**

**Technische Universität München**

**Promotion / Wissenschaftlicher Mitarbeiter:**

Murine one-carbon metabolism in non-alcoholic fatty liver disease.

Wissenschaftszentrum-Weihenstephan, Zentralinstitut für Ernährungs- und Lebensmittelforschung (ZIEL), Nachwuchsforschergruppe PhD-Kolleg „Epigenetik, Imprinting und Ernährung“ und Abteilung Biochemie Univ.-Prof. Dr. Hannelore Daniel

**28.12.2006:**

**Westfälische Wilhelms-Universität Münster**

Erlangung des akademischen Grads Diplom-Biologe  
(Dipl.-Biol. (Univ.)) mit Auszeichnung (Note: 1,0)

**01.02.2006 - 31.12.2006:**

**Westfälische Wilhelms-Universität Münster**

**Diplomarbeit:** Expressionsanalyse des humanen epithelialen Natriumkanals (ENaC) im Nasenepithel von Patienten mit und ohne Mukoviszidose (Note: 1,0).

Institut für Tierphysiologie, Univ.-Prof. Dr. Wolf-Michael Weber

**15.10.2001 - 31.12.2006:**

**Westfälische Wilhelms-Universität Münster**

**Studium der Biologie**

#### **Schulische Ausbildung und Wehrdienst:**

**01.07.2000 - 30.04.2001:**

**Grundwehrdienst,** Transportbataillon 801  
Lippstadt, Deutschland

**01.07.1997 - 30.06.2000:**

**Abitur,** Evangelisches Gymnasium Lippstadt,  
Deutschland

#### **Publikationen:**

Teile dieser Arbeit gingen in folgende Publikationen ein (published, submitted oder in preparation)

1. Desmarchelier C, **Dahlhoff C**, Keller S, Sailer M, Jahreis G, Daniel H. C57Bl/6N mice on a Western diet display reduced intestinal and hepatic cholesterol levels despite a plasma hypercholesterolemia. BMC Genomics. 2012 Mar 6;13:84
2. **Dahlhoff C**, Fürst RW, Ruhlig K, Sedlmeier EM, Bader BL. Epigenetik und Ernährung. Ernährung. 2008;2:116-24
3. **Dahlhoff C**, Desmarchelier C, Sailer M, Fürst RW, Ulbrich SE, Hummel H, Obeid R, Geisel J, Bader BL, Daniel H. Hepatic methionine homeostasis is conserved in C57BL/6 mice on high-fat diet despite major changes in hepatic one-carbon metabolism. PLoS ONE 2012, submitted

4. **Dahlhoff C**, Sailer M, Hummel B, Obeid R, Scherling C, Geisel J, Bader BL, Daniel H. Methyl-donor supplementation prevents the progression of NAFLD in diet induced obese mice and is associated with AMPK activation and decreased acyl-carnitine levels. JBC 2012, submitted
5. Sailer M, **Dahlhoff C**, Giesbertz P, Marth M, deWit N, Rubio-Aliaga I, Boekschoten M, Müller M, Daniel H. Increased plasma citrulline may as a marker of diet induced obesity in mice predict the development of the metabolic syndrome. 2012, in preparation

**Weitere Publikationen:**

6. Bangel N, **Dahlhoff C**, Sobczak K, Weber WM, Kusche-Vihrog K. Upregulated expression of ENaC in human CF nasal epithelium. J Cyst Fibros. 2008 May;7:197-205

**Kongresse:**

1. **qPCR Symposium 2009** – Diagnostics & Molecular Markers (09.-13.03.2009)
2. **Mosbacher Kolloquium 2008** – Epigenetics – Molecular Principles and Mechanisms (26.-29.03.2008)
3. **99. Jahrestagung der Deutschen Zoologischen Gesellschaft**. Mitglied des Organisationskomitees (Münster, DZG 2006)